REGULATION OF THE ARABIDOPSIS AGC KINASE PINOID BY PDK1 AND THE MICROTUBULE CYTOSKELETON

Mickel Elisabeth Johannes Habets

ISBN: 978-94-6375-361-6

Cover design and layout: Myckel Habets

Printing: Ridderprint BV, the Netherlands

REGULATION OF THE ARABIDOPSIS AGC KINASE PINOID BY PDK1 AND THE MICROTUBULE CYTOSKELETON

Proefschrift

Ter verkrijging van
de graad van Doctor aan de Universiteit Leiden,
op gezag van Rector Magnificus prof. mr. C.J.J.M. Stolker,
volgens besluit van het College voor Promoties
te verdedigen op donderdag 25 april 2019
klokke 13:45 uur

door

Mickel Elisabeth Johannes Habets

Geboren te Heerlen,
25 October 1982

Promotiecommissie

Promotor:	Prof. dr. R. Offringa
Overige leden:	Prof. dr. P.J.J. Hooykaas
	Dr. ir. M.J. Ketelaar, Wageningen UR
	Prof. dr. J. Memelink
	Prof. dr. C.S. Testerink, Wageningen UR
	Prof. dr. G.P. van Wezel

CONTENTS

ONE

PIN-DRIVEN POLAR AUXIN TRANSPORT IN PLANT DEVELOPMENTAL PLASTICITY: A KEY TARGET FOR ENVIRONMENTAL AND ENDOGENOUS SIGNALS

Myckel E.J. Habets[1] and Remko Offringa[1]

[1] Institute of Biology Leiden / Leiden University, Sylviusweg 72, 2333 BE Leiden, The Netherlands

Modified from New Phytologist 203: 362-377, 2014, doi:10.1111/nph.12831

Summary

Plants master the art of coping with environmental challenges in two ways: on the one hand, through their extensive defense systems, and on the other, by their developmental plasticity. The plant hormone auxin plays an important role in a plant's adaptations to its surroundings, as it specifies organ orientation and positioning by regulating cell growth and division in response to internal and external signals. Important in auxin action is the family of PIN-FORMED (PIN) auxin transport proteins that generate auxin maxima and minima by driving polar cell-to-cell transport of auxin through their asymmetric subcellular distribution. Here, we review how regulatory proteins, the cytoskeleton, and membrane trafficking affect PIN expression and localization. Transcriptional regulation of *PIN* genes alters protein abundance, provides tissue-specific expression, and enables feedback based on auxin concentrations and crosstalk with other hormones. Post-transcriptional modification, for example by PIN phosphorylation or ubiquitination, provides regulation through protein trafficking and degradation, changing the direction and quantity of the auxin flow. Several plant hormones affect PIN abundance, resulting in another means of crosstalk between auxin and these hormones. In conclusion, PIN proteins are instrumental in directing plant developmental responses to environmental and endogenous signals.

Introduction

Plant development is flexible and indeterminate in nature. This is in contrast to animal development, where at birth the young animal has acquired most, if not all, of the organs and limbs, and thus resembles the adult organism. During plant embryogenesis, only the basic body plan is laid down, and the shape of the adult plant differs considerably from that of the embryo. As sessile organisms, plants have acquired two important features that allow them to adapt and optimize their architecture to (changes in) their environment. The first comprises groups of stem cells organized in meristems in the root and the shoot apex that continuously produce new cell files and organs, respectively. The second is a plethora of signaling pathways that allow plants to accurately monitor their environment and to adapt their growth in response to external stimuli.
Based on observations on the bending of oat coleoptiles in response to directional light, Charles Darwin and his son concluded that something in the coleoptile tip was acted upon by light, resulting in bending of the coleoptile (Darwin & Darwin, 1880). These initial observations led to the identification of the responsible compound in this process, the plant hormone IAA, which was named auxin after the Greek word *auxein* for 'to grow' (Went, 1926; Kögl & Haagen-Smit, 1931). Intensive research on this plant hormone has revealed that auxin instructs plant development by regulating very basic processes such as cell division, growth, and differentiation in a concentration-dependent manner. This research has also unraveled a unique characteristic of auxin, its polar cell-to-cell transport, which acts in concert with auxin biosynthesis and metabolism to generate dynamic auxin maxima and minima that direct plant development and growth. The differential auxin concentrations are subsequently sensed and translated into a cellular response by complex signaling networks (Perrot-Rechenmann, 2010; Vernoux *et al.*, 2010; Ruiz Rosquete *et al.*, 2012). In this review, we will briefly summarize what is known about auxin signaling and transport, and then focus on the PIN-FORMED (PIN) proteins that mediate and direct polar auxin transport (PAT), and how endogenous and external signals act on transcriptional and post-transcriptional mechanisms to regulate their activity.

Auxin action

Auxin is sensed at different subcellular locations

The response of a cell to a hormone is determined, on the one hand, by its concentration, and on the other, by the sensitivity of the cell to the hormone. The initial search for auxin receptors identified three auxin binding sites: in the nucleus, the endoplasmatic reticulum (ER) and at the plasmamembrane (PM). Auxin binding in the ER and at the PM appeared to be mediated by the same protein, the AUXIN BINDING PROTEIN1 (ABP1; Hertel *et al.*, 1972; Ray, 1977; Feldwisch *et al.*, 1992; Jones & Herman, 1993). The PM localization suggested that ABP1 mediates rapid cellular responses to auxin (Rück *et al.*, 1993), such as the induction of cell division and cell expansion (Steffens *et al.*, 2001; David *et al.*, 2007; Braun *et al.*, 2008; Dahlke *et al.*, 2010). Despite its early identification, the function of ABP1 as auxin receptor has remained unclear for many years. Although it is likely that ABP1 activates multiple signaling pathways, the most well established effect of ABP1 is its stimulatory role in clathrin-mediated endocytosis (Robert *et al.*, 2010) via the Rho of Plants (ROP) family of GTPases (Xu *et al.*, 2010, 2014; Chen *et al.*, 2012). Disruption of the ABP1-ROP signaling pathway results in different developmental defects depending on the strength of the knockdown, ranging from arrest of embryo development (Chen *et al.*, 2001) to defects in pavement cell (PC) interdigitation (Xu *et al.*, 2010), leaf venation patterning, and gravitropic responses (Wang *et al.*, 2013).
A second receptor was initially identified through a mutation in the Arabidopsis *TRANSPORT INHIBITOR RESISTANT 1* (*TIR1*) gene (Ruegger *et al.*, 1998), but its function as auxin co-receptor acting in the nucleus to regulate auxin-responsive gene expression was uncovered much later (Dharmasiri *et al.*, 2005a; Kepinski & Leyser, 2005). TIR1 was found to act redundantly with five homologous AUXIN-RESPONSIVE F-BOX (AFB) proteins (Dharmasiri *et al.*, 2005b). Auxin-responsive gene expression is mediated by two classes of proteins: the DNA-binding auxin response factors (ARFs) that either activate or repress transcription, and the Aux/IAA family of transcriptional repressors (Fig. 1). In Arabidopsis, the ARFs comprise a family of 23 proteins, most of which have four conserved domains (Remington *et al.*, 2004; Okushima *et al.*, 2005). The DNA-binding domain at the N-terminus allows the ARFs to bind to the TGTCxC core sequence containing auxin response elements (AuxREs) in

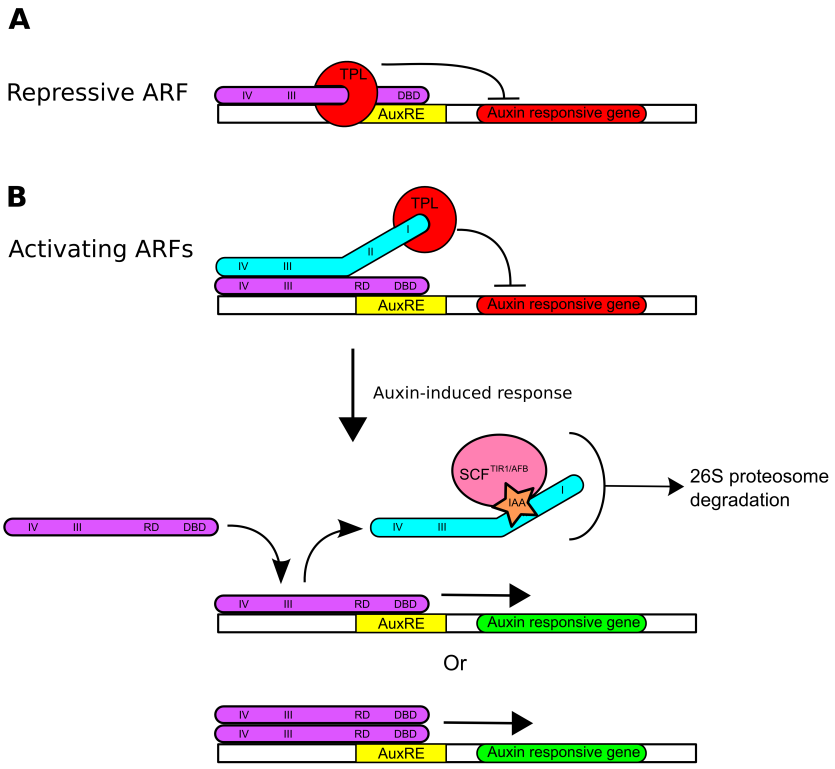

Figure 1: Model of the regulation of auxin responsive gene expression by the auxin response factor (ARF) transcription factors and Aux/IAA repressor proteins. Two types of ARFs exist: repressive (a) and activating (b). (a) Repressive ARFs are thought to block gene expression when bound to auxin-responsive elements (AuxREs) through their interaction with TOPLESS (TPL). (b) Activating ARFs block gene expression while forming a dimer with an Aux/IAA protein in complex with TPL. In the presence of auxin, the TRANSPORT INHIBITOR RESISTANT 1 (TIR1) receptor and the Aux/IAA coreceptor form a complex, leading to Aux/IAA ubiquitination and its targeting for degradation by the 26S proteasome. The ARFs remaining at the AuxRE can then promote auxin-responsive gene transcription as monomer or dimer. DBD, DNA-binding domain; RD, regulatory domain; SCF, SKP1-LIKE CULLIN1 AND F-BOX protein complex; AFB, AUXIN-RESPONSIVE F-BOX PROTEIN; IAA, auxin.

the promoters of auxin-responsive genes (Ulmasov *et al.*, 1995, 1997). The middle domain is involved in either activating or repressing gene expression, depending on the amino acid residues present (Ulmasov *et al.*, 1999a). At the C-terminus, the conserved domains III and IV are located, which are found in both ARFs and Aux/IAA proteins and are involved in dimerization with other ARFs or with Aux/IAA proteins (Ulmasov *et al.*, 1999b; Tiwari *et al.*, 2003). Aux/IAA proteins are encoded by a family of 29 genes in Arabidopsis (Liscum & Reed, 2002). Apart from

the conserved C-terminal domains III and IV involved in protein–protein dimerization, the N-terminal domain I in most Aux/IAA proteins contains an ERF-associated Amphiphilic Repression (EAR) motif (LxLxL) that is required for binding of the transcriptional corepressors TOPLESS or the four TOPLESS RELATED proteins (TPL/TPRs). Aux/IAAs need TPL binding for their repressing function (Tiwari *et al.*, 2004; Szemenyei *et al.*, 2008).
The middle domain II of Aux/IAA proteins is involved in protein stability and is the binding target for the TIR1/AFB F-box proteins. Together with an SKP1-like protein and CULLIN1, the TIR1/AFB proteins form the E3 ubiquitin protein ligase $SCF^{TIR1/AFB}$. Auxin promotes the interaction between TIR1/AFBs and domain II of the Aux/IAA coreceptors (Tan *et al.*, 2007; Calderón Villalobos *et al.*, 2012), thereby recruiting the Aux/IAA proteins for ubiquitination and subsequent degradation by the 26S proteasome (Dos Santos Maraschin *et al.*, 2009). After Aux/IAA degradation, the ARF remaining at the AuxRE in a promoter region can then activate the downstream gene either as a monomer or as a dimer with another ARF protein (Ulmasov *et al.*, 1999b; Tiwari *et al.*, 2003). Recently, TPL/TPR proteins were shown to interact with several repressive ARFs, suggesting that TPL/TPR proteins act in both Aux/IAA- and ARF-mediated transcriptional repression (Causier *et al.*, 2012).

Polar auxin transport-generated auxin maxima and minima

As described earlier, the response of a cell to auxin is, for the most part, determined by the concentration of the hormone in the cell, which, in addition to auxin biosynthesis and metabolism, is determined by polar cell-to-cell transport of auxin. PAT is a complex process that is mediated by at least three types of transporters. In line with the chemiosmotic hypothesis proposed for PAT (Rubery & Sheldrake, 1974; Raven, 1975), in the relatively acidic environment of the apoplast *c.* 15% of the auxin molecules are in the protonated state (IAAH), which allows auxin to pass the PM by diffusion. However, the majority of auxin is in the deprotonated form (IAA^-) and requires active uptake by the AUXIN1/LIKE-AUX1 (AUX/LAX) import carriers (Bennett *et al.*, 1996; Swarup & Péret, 2012). In the more alkaline cytosol, auxin molecules are deprotonated and the resulting anions can only pass the PM with the help of auxin efflux carriers. Polar placement of such carriers in the PM at the same side of a row of cells thus leads to polar cell-to-cell transport.

To date, two classes of auxin efflux carriers have been identified: the family of PIN proteins, consisting of eight members in Arabidopsis (Friml *et al.*, 2003); and the ABC-B/MULTI-DRUG RESISTANT/P-GLYCOPROTEIN (ABCB/MDR/PGP) transporters that belong to a subfamily of 20 proteins in Arabidopsis (Kaneda *et al.*, 2011).

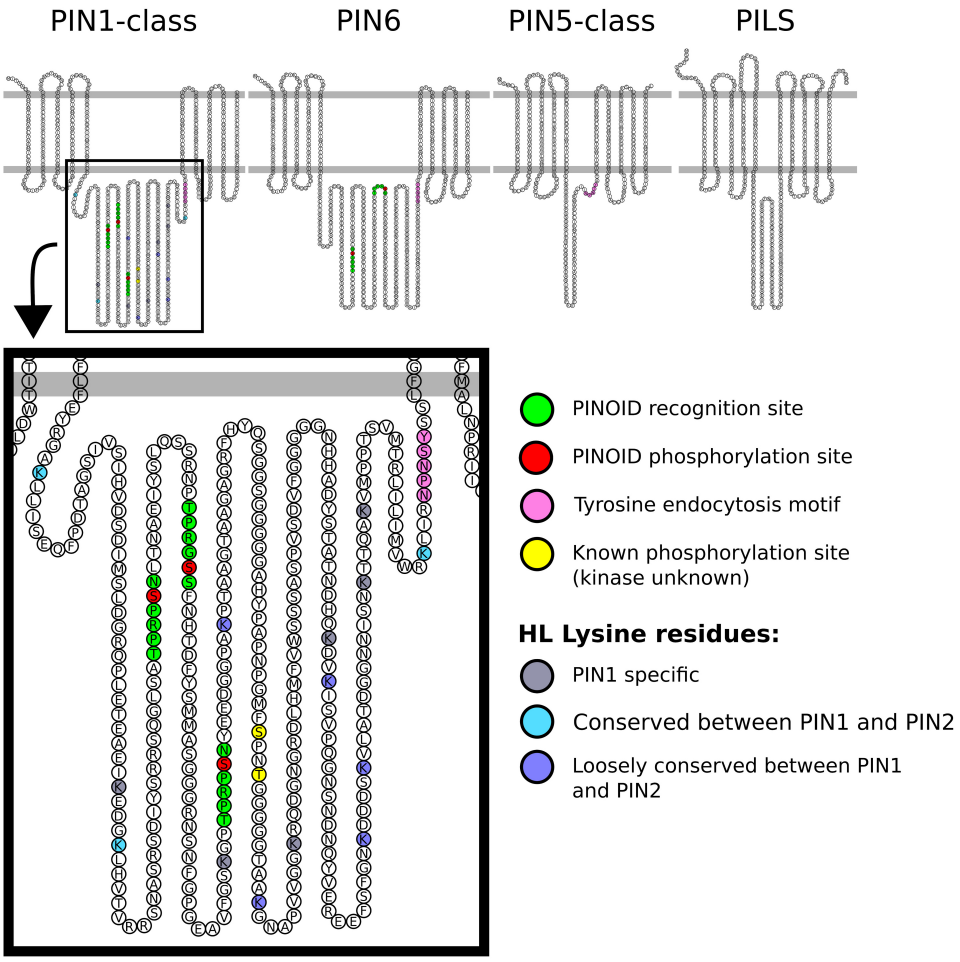

Figure 2: Schematic representation of the protein structures of PIN1 (representing the PIN1-class), PIN6, PIN5 (representing the PIN5-class), and PILS2 (representing the PILS family). Important amino acids in the PIN1 hydrophilic loop (HL) are color-coded, including the lysines and the five serine/threonine residues whose phosphorylation by PINOID, WAG1 or WAG2 (red) or other unknown kinases (yellow) has been shown to direct PIN polarity. HL, hydrophilic loop.

Arabidopsis ABCB family members were identified as auxin transporters because loss-of-function mutants showed auxin-related developmental

defects and reduced auxin transport, and the proteins were found to bind to the PAT inhibitor 1-naphthylphthalamic acid (NPA; Noh *et al.*, 2001; Geisler *et al.*, 2005). For ABCB1 and -19 the role of nonpolar auxin efflux carriers has now been well established, and they are thought to act in auxin transport channels to regulate the intracellular auxin available for the polar transport pathway (Petrášek *et al.*, 2006; Mravec *et al.*, 2008). More recent data suggest that ABCB14 and ABCB15 act as auxin efflux carriers in this pathway as well (Kaneda *et al.*, 2011), whereas ABCB4 seems to act as both an auxin influx carrier and an auxin efflux carrier, depending on the intracellular auxin concentrations (Kubeš *et al.*, 2012).
In contrast to the nonpolarly localized ABCB proteins, five of the Arabidopsis PIN proteins do show asymmetric localization at the PM (Gälweiler *et al.*, 1998; Müller *et al.*, 1998; Friml *et al.*, 2002a,b, 2003). Because the action of these PIN proteins appeared to be rate-limiting (Petrášek *et al.*, 2006), and their subcellular distribution at the PM correlated well with the direction of PAT (Benková *et al.*, 2003; Wiśniewska *et al.*, 2006), these PIN proteins are now considered to be the auxin efflux carriers proposed in the chemiosmotic model, driving and channeling polar cell-to-cell auxin transport. PIN proteins typically consist of two hydrophobic, transmembrane regions, interrupted by a short or long hydrophilic loop (HL, Fig. 2). All PM localized PINs have a long HL, and are referred to as PIN1-type or long PIN proteins (Viaene *et al.*, 2013). The importance of these long PIN proteins in their contribution to PAT is shown by loss-of-function mutants. Of the single mutant alleles, only those of the founding *PIN-FORMED/PIN1* gene show strong defects in development, with needle-like inflorescences that lack lateral organs (Gälweiler *et al.*, 1998), whereas mutations in *PIN2* and *PIN3* only reduce the ability of plants to respond to external signals, such as gravity and light (Luschnig *et al.*, 1998; Friml *et al.*, 2002b). By combining mutations in three to four *PIN* genes, very severe defects in early embryogenesis are obtained, on the one hand indicating strong functional redundancy between *PIN* genes and, on the other, corroborating the crucial role of PIN-mediated PAT in plant development (Friml *et al.*, 2003; Blilou *et al.*, 2005). The long PINs are often asymmetrically distributed over the PM (PIN1, PIN2, PIN4 and PIN7) or are able to polarize after external stimulation (PIN3; Tanaka *et al.*, 2006).

An ancient role for the endoplasmatic reticulum in controlling auxin action

The other three members of the PIN family in Arabidopsis, PIN5, PIN6 and PIN8, localize to the ER and, in some cell-types to the PM (Mravec *et al.*, 2009; Ganguly *et al.*, 2010, 2014; Dal Bosco *et al.*, 2012; Ding *et al.*, 2012; Sawchuk *et al.*, 2013). PIN5 and PIN8 are classified as short PINs, based on the length of their HLs (Viaene *et al.*, 2013), and their predominant ER localization suggests that PM localization of the long PINs is promoted by sequences in their long HL. A conserved tyrosine motif (NPXXY) present at the C-terminal end of the HL has been suggested as a possible interaction site for adapter proteins during clathrin-mediated endocytosis (Zažímalová *et al.*, 2007). That this motif is also conserved in the HL of PIN5 and PIN8 (Fig. 2), is in line with the recently observed clathin-mediated endocytosis of these short PINs in young root epidermis cells, where they localize to the PM (Ganguly *et al.*, 2014).

An *in silico* screen for proteins with homology and a similar topology to the PIN family members in Arabidopsis has identified seven ER-localized PIN-LIKES (PILS) proteins (Barbez *et al.*, 2012; Fig. 2). Despite the limited sequence similarity with PINs, PILS proteins contain the InterPro auxin carrier domain that is also present in PINs, and for PILS2 and PILS5, evidence of auxin transport activity has been obtained. The fact that they, and not the PIN proteins, occur in unicellular algae, suggests that PILS are evolutionarily older than PINs (Feraru *et al.*, 2012).

In contrast to the obvious function of the PM-localized PINs as drivers of PAT, the role of the ER-localized auxin transporters (PINs and PILS) is not yet clear. Several auxin-conjugating enzymes have been reported to localize in the ER (Bartel & Fink, 1995; Woodward & Bartel, 2005), and both phenotypic analysis and IAA metabolic profiling of lines overexpressing the ER-localized auxin transporters have indicated that they seem to act antagonistically (PIN6 and PIN8, efflux; PIN5 and PILS, influx) in controlling auxin homeostasis, and thus the amount of free auxin available in the cytosol for PAT, or in the nucleus for auxin response (Mravec *et al.*, 2009; Barbez *et al.*, 2012; Ding *et al.*, 2012; Sawchuk *et al.*, 2013). Two mechanisms have been proposed for a possible feedback on the action of ER-localized PINs in controlling auxin homeostasis and signaling. The first mechanism relates to the observation that the majority of the ABP1 protein pool is located in the ER and could potentially

regulate the activity or trafficking of the ER-localized PINs. However, at a pH of 7, ABP1 has been reported to bind auxin inefficiently, making it unlikely that auxin triggers ABP1 signaling in the ER (Ray, 1977; Jones & Herman, 1993; Tian *et al.*, 1995). Another possibility is that direct transport of auxin from the ER into the nucleus via PIN6/8 (Sawchuk *et al.*, 2013) could possibly provide feedback control on auxin homeostasis through TIR1/AFB signaling.

For the PILS in unicellular algae, the most obvious function would be regulation of auxin homeostasis. For multicellular systems, however, mathematical modeling of ER-localized auxin influx and efflux carriers, together with the feedback systems described earlier, has predicted that intracellular auxin retention in the ER, combined with controlled release in the cytosol/nucleus, could lead to canalization of auxin transport, giving rise to localized auxin maxima (Wabnik *et al.*, 2011). Interestingly, this model is supported by recent data suggesting that ER-localized PINs generate tissue-specific context and enhance PAT during vein patterning in leaves (Sawchuk *et al.*, 2013). Whether the observed partial PM localization of PIN5, PIN6 and PIN8 is important for their role in vein patterning, is currently unclear (Ganguly *et al.*, 2010, 2014).

PIN regulation by a complex network of feedback loops

Transcriptional regulation of PIN abundance: a matter of redundancy

Detailed expression studies have shown that each of the individual Arabidopsis *PIN* genes shows a specific expression pattern and that, in developmental processes such as embryogenesis or root growth, multiple PINs act in concert to generate and maintain dynamic auxin maxima that steer development and growth (reviewed in Tanaka *et al.*, 2006; Křeček *et al.*, 2009). For most *PIN* genes their expression pattern only partially correlates with the developmental defects observed in corresponding loss-of-function mutants (Gälweiler *et al.*, 1998; Friml *et al.*, 2003; Scarpella *et al.*, 2006).

In various single and multiple *pin* loss-of-function mutants, PIN proteins were found to be ectopically expressed, most likely because of the imbalance in auxin homeostasis (Blilou *et al.*, 2005; Vieten *et al.*, 2005; Rigas *et al.*, 2013). Pronounced embryo defects were only observed in quadruple *pin* mutant combinations that included *pin4* and *pin7* (Friml

et al., 2003; Blilou *et al.*, 2005). This shows that there is a molecular mechanism that uses the redundancy of the PIN proteins to overcome the effects of these mutations to some extent.

An important part of this redundancy is mediated by the auxin responsiveness of *PIN* expression. Vieten *et al.* (2005) used heat shock promoter-driven dominant *axr3/iaa17* or *solitary-root-1*(*slr-1*)/*iaa14* mutant genes to suppress auxin-responsive expression of the five 'long' *PIN* genes. This confirmed that these *PIN* genes are regulated through the Aux/IAA and ARF system (Vieten *et al.*, 2005). In addition, *PIN1* expression was found to be regulated by MONOPTEROS(MP)/ARF5 (Wenzel *et al.*, 2007), which interacts with and is repressed by BODENLOS (BDL)/IAA12 (Hamann *et al.*, 2002). A recently described dominant mutant allele of *MP autobahn*, of which the encoded protein (MP^{abn}) no longer interacts with BDL, suggests that the MP–BDL interaction not only restricts *PIN1* expression, but also determines PIN1 asymmetric localization to canalize PAT during vascular development (Garrett *et al.*, 2012). Although the authors do not rule out the possibility that PIN apolarity is a result of its enhanced expression, the proposed second regulatory role of the MP–BDL complex might correspond to the observed canalization of PAT by ARF-Aux/IAA-dependent feedback on PIN polarity (Sauer *et al.*, 2006).

We used known Arabidopsis *PIN* promoter sequences to detect putative AuxREs (Fig. 3). Surprisingly we did not find a clear correlation between the number of AuxREs in an upstream region and the reported auxin responsiveness of the corresponding gene. For example, *PIN1*, *PIN3*, and *PIN7* all react strongly to auxin application (Vieten *et al.*, 2005), whereas the *PIN3* and *PIN7* promoters contain much more known AuxREs compared with the *PIN1* promoter (Fig. 3). A possible explanation might lie in the presence of as yet uncharacterized AuxREs in the *PIN1* promoter, and also possibly in the recent finding that efficient DNA binding and dimerization of ARFs depend on the distance between two AuxREs (Boer *et al.*, 2014). Remarkably, in the shoot apical meristem of the *pin1* mutant, the expression of other *PIN* genes was not found to be elevated (Guenot *et al.*, 2012), suggesting that feedback regulation of auxin on *PIN* transcription does not work in every tissue.

Another group of transcription factors that is known to regulate *PIN* expression are the BABY BOOM (BBM)/PLETHORA (PLT) AP-2 domain transcription factors (Boutilier *et al.*, 2002; Blilou *et al.*, 2005;

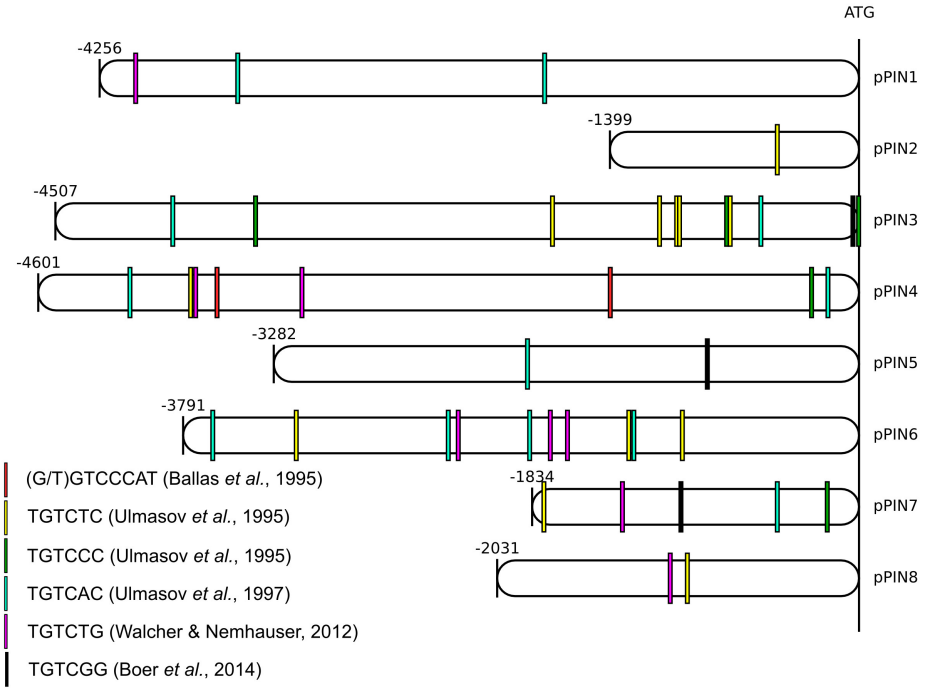

Figure 3: Schematic representation of the *Arabidopsis thaliana PIN* upstream regions, indicating the positions of putative auxin-responsive elements (AuxREs). The selected upstream regions are from the stop codon of the upstream gene until the *AtPIN* ATG start codon.

Galinha *et al.*, 2007). These transcription factors play an important role in maintaining the stem cell niche and in tissue patterning. In the embryo and the root meristem, PIN proteins restrict ARF-mediated *PLT* gene expression, and in turn PLTs act in concert with the SCARECROW (SCR) and SHORT ROOT (SHR) transcription factors to determine which *PIN* genes are expressed, thereby providing reciprocal regulatory loops between auxin and the PLTs (Blilou *et al.*, 2005; Xu *et al.*, 2006). Initial observations suggested that PLT3, PLT5, and PLT7 are involved in phyllotactic patterning in the shoot apical and inflorescence meristems by enhancing *PIN1* gene expression (Prasad *et al.*, 2011). More recently, evidence was obtained that PLTs are required for phyllotactic patterning by activating auxin biosynthesis in the center of the inflorescence meristem, suggesting that PLTs do not necessarily directly regulate *PIN* gene expression (Pinon *et al.*, 2013). It will be important to determine whether

BBM/PLTs directly bind the promoters of *PIN* genes.

Regulation of PIN abundance and polarity by membrane trafficking

After the *PIN* genes are transcribed, the newly synthesized short PINs (including PIN6) are retained in the ER, and the long PINs traffic via the trans-Golgi network/early endosomes (TGN/EE) to the PM in a nonpolar fashion. At this point, the PIN proteins start to undergo continuous endocytosis and recycling back to the PM, a process that can coincide with transcytosis, and which is required for the establishment and maintenance of PIN polarity (Geldner *et al.*, 2001; Dhonukshe *et al.*, 2008, 2010; Fig. 4). PIN endocytosis occurs via clathrin-coated vesicles, and disrupting the clathrin machinery reduces endocytosis, which causes changes in auxin distribution and leads to developmental defects (Dhonukshe *et al.*, 2007; Kitakura *et al.*, 2011). Auxin was shown to interfere with PIN endocytosis and, as a result, to stabilize PINs at the PM, thereby enhancing auxin efflux (Paciorek *et al.*, 2005). This was shown to be mediated by the apoplastic ABP1: ABP1 normally stimulates endocytosis, and binding of auxin inhibits this activity. In this way, ABP1 provides a positive feedback loop by which exported auxin induces local stabilization of PINs at the PM, thereby enhancing auxin efflux at that same position (Robert *et al.*, 2010; Čovanová *et al.*, 2013).

PIN endocytosis, transcytosis, and recycling require the actin cytoskeleton and the action of specific ADP-ribosylation factor-(ARF)-type GTPases and the corresponding ARF-GTP exchange factors (ARF-GEFs). In general, recycling of PIN proteins to the basal (rootward) PM in root cells is dependent on the ARF-GEF GNOM, which is sensitive to the fungal toxin brefeldin A (BFA; Geldner *et al.*, 2001, 2003; Kleine-Vehn *et al.*, 2008a). Exposure of roots to high BFA concentrations results in accumulation of PIN proteins in large intracellular structures called 'BFA compartments'. PIN-loaded BFA compartments are readily formed in cells that show basal PIN localization, whereas only limited PIN cargo accumulates in BFA compartments in cells where PINs show apical (shootward) localization. Moreover, long-term exposure to intermediate BFA concentrations leads to transcytosis of basal PIN proteins to the apical PM of root cells, suggesting that transcytosis and apical recycling are mediated by BFA-insensitive ARF-GEFs (Kleine-Vehn *et al.*, 2008a).

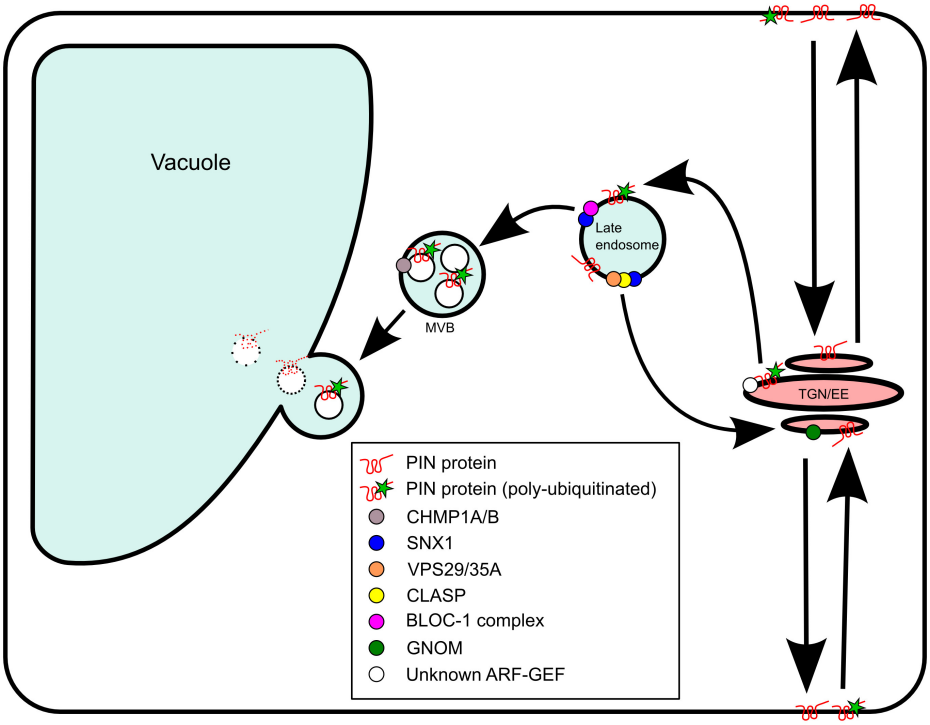

Figure 4: Regulation of PIN protein trafficking by phosphorylation and ubiquitination. Following their biosynthetic delivery via the trans-Golgi endosomes (TGN/EE) to the plasma membrane (PM), PIN proteins undergo continuous recycling between the PM and the TGN/EE. Unphosphorylated PINs, or those dephosphorylated by PP2A/PP6 phosphatase, are recycled to the PM by the brefeldin A (BFA)-sensitive ADP-ribosylation factor-guanine nucleotide exchange factors (ARF-GEF) GNOM, whereas phosphorylation of PIN proteins by PINOID (PID) results in their GNOM-independent recycling to the opposite PM. Monoubiquitination and subsequent polyubiquitination of PIN proteins induce their endocytosis, followed by trafficking from the TGN/EE to late endosomes, from where the SNX1/BLOC-1 complex mediates transfer to multivesicular bodies (MVBs) for vacuolar degradation. Alternatively, the SNX1/CLASP/VPS29/ retromer complex recruits PIN proteins from the late endosomes back to the TGN/EE. CHMP1A/B, CHARGED MULTIVESICULAR BODY PROTEIN/CHROMATIN MODIFYING PROTEIN 1A/B; SNX1, SORTING NEXIN 1; VPS29/35A, VACUOLAR PROTEIN SORTING 29/35A; CLASP, CLIP-ASSOCIATED PROTEIN; BLOC-1, BIOGENESIS OF LYSOSOME-RELATED ORGANELLES COMPLEX 1.

Reversible phosphorylation of PINs signals their polar subcellular distribution

Based on pharmacological experiments with suspension-cultured tobacco cells, it was concluded that protein phosphorylation is important

to sustain auxin efflux activity (Delbarre *et al.*, 1998). Support for this hypothesis was provided by the identification of the protein kinase PINOID (PID) as a positive regulator of PAT (Benjamins *et al.*, 2001). PID belongs to the plant-specific AGCVIII subfamily of the large family of AGC protein kinases (Christensen *et al.*, 2000; Benjamins *et al.*, 2001). The *PID* gene was named after the main phenotype of loss-of-function mutants, which develop pin-like inflorescences just like the *pin1* mutant. Other mutant phenotypes are seedlings with three instead of two cotyledons, defects in leaf venation, the altered floral phyllotaxis and the trumpet-shaped pistil in the few flowers that are formed (Christensen *et al.*, 2000; Benjamins *et al.*, 2001; Kleine-Vehn *et al.*, 2009). These defects were found to be caused by a shift in PIN1 polarity from the apical to the basal side of the cells. By contrast, *PID* overexpression resulted in a switch of basally localized PINs (PIN1, PIN2 and PIN4) to the apical PM of root cells, implying that PID activity is involved in apical PIN polarity establishment (Friml *et al.*, 2004). Serine residues in three conserved TPRXS(N/S) motives in the PIN hydrophilic loop have been identified as the targets for PID phosphorylation (Fig. 2), and expression of loss-of-phosphorylation or phosphomimic versions of PIN1-GFP or PIN2-VENUS in their respective mutant background demonstrated that PIN phosphorylation is essential and sufficient to direct PIN polarity (Dhonukshe *et al.*, 2010; Huang *et al.*, 2010).

Phylogenetic analysis of the kinase domains of the Arabidopsis AGCVIII kinases showed that PID clusters in the AGC3 clade together with three other protein kinases, these being WAVING AGRAVITROPIC ROOT1 (WAG1), WAG2, and an as yet uncharacterized kinase named AGC3-4 (Galván-Ampudia & Offringa, 2007). WAG1 and WAG2 were found to be involved in root waving (Santner & Watson, 2006) and to act redundantly with PID in apical polarity establishment of PIN2 in the root epidermis and lateral root cap to regulate (gravitropic) root growth, and of PIN1 in the protoderm of the embryo during cotyledon initiation. In line with their redundant action, WAG1 and WAG2 were found to phosphorylate the same serine residues in the PIN HL as PID (Dhonukshe *et al.*, 2010). While these three kinases show functional redundancy and have overlapping expression domains, they are also differentially expressed (Santner & Watson, 2006; Cheng *et al.*, 2008; Dhonukshe *et al.*, 2010) and a differential role for PID and WAG2 has been suggested in valve margin specification during Arabidopsis fruit development (Sorefan *et al.*, 2009).

Mass spectrometry analysis has identified several other amino acid residues in the PIN HL that are targets for phosphorylation (reviewed in Offringa & Huang, 2013), of which Ser337 and/or Thr340 in the PIN1 HL were shown to be important for PIN1 polarity establishment. As these residues are clearly not phosphorylated by PID, WAG1, or WAG2 (Dhonukshe *et al.*, 2010; Huang *et al.*, 2010; Zhang *et al.*, 2010), it is likely that they are targets of other kinases. A member of the Ca^{2+}/calmodulin-dependent kinase-related family CRK5 was able to phosphorylate the PIN2 HL, and the *crk5-1* mutant showed reduced PIN2 exocytosis, suggesting that phosphorylation of the CRK5 phosphorylation site enhances PIN2 exocytosis (Rigó *et al.*, 2013). Also the four D6 PROTEIN KINASES (D6PKs), which are members of the AGC1 subfamily of AGCVIII kinases, were found to phosphorylate the PIN HL *in vitro* (Galván-Ampudia & Offringa, 2007; Zourelidou *et al.*, 2009). Because the D6PKs do not affect PIN protein localization (Dhonukshe *et al.*, 2010), these kinases most likely target a different, possibly overlapping, set of serine/threonine residues than the AGC3 kinases. The fact that *d6pk* loss-of-function mutants show reduced auxin transport suggests that these kinases might be involved in regulating PIN auxin transport activity rather than polarity.

AGC3 kinases label PIN proteins following their nonpolar biosynthetic secretion to the PM, and this then leads to their asymmetric distribution through clathrin-dependent endocytosis, transcytosis, and recycling (Dhonukshe *et al.*, 2008, 2010). How the phosphorylation status of PIN cargo is perceived by the endomembrane trafficking system is currently unclear. The fact that D6 kinases are able to phosphorylate PIN proteins, most likely at different residues, but do not alter PIN polarity suggests that the PIN phosphorylation status is monitored by specific adaptor proteins that are able to distinguish which residues in cargo proteins are phosphorylated.

Apart from the AGC3 kinases, trimeric phosphatases were found to act antagonistically in determining the phosphorylation status of the PIN HL (Michniewicz *et al.*, 2007). Earlier research had shown that a mutation in a gene encoding a regulatory A subunit of a PP2A type phosphatase ROOTS CURL IN NAPHTHYLPHTHALAMIC ACID1 (RCN1/PP2A-A1) resulted in PAT-related root growth defects (Garbers *et al.*, 1996). Loss-of-function mutants in two of the three *PP2A-A* genes phenocopied some of the seedling phenotypes observed in *PID* overexpression lines and resulted in the same basal to apical shift of PIN polarity in the root (Michniewicz

et al., 2007). Initially, the PP2A-A subunits were shown not to be part of a typical PP2A holoenzyme, but rather to form a PP6-type heterotrimeric complex together with a PP6 catalytic (C) subunit (FyPP1 or FyPP3), and a SAPS domain-Like protein (SAL1-4) as a B subunit. Interestingly, yeast two-hybrid analysis suggested that SAL1 binding to the PIN HL was enhanced by phosphorylation (Dai *et al.*, 2012). More recent data, however, suggest that the PP2A-A subunits are promiscuous and that the PP2A holoenzyme might be specifically active during embryogenesis (Ballesteros *et al.*, 2013).

PIN trafficking regulated by environmental signals

AGC3 kinase and PIN polarity regulation by external signals

The amazing flexibility of plant development and growth is exemplified by the growth responses to external signals, such as light and gravity, through which a plant can optimize the position and orientation of its organs to its environment. AGC3 kinase-mediated PIN phosphorylation not only leads to apical targeting of PIN proteins for organ initiation in the embryo or in the inflorescence meristem, but is also required for proper root growth. *wag1 wag2* double mutant roots grow hyper-wavy on tilted agar plates, and *pid wag1 wag2* triple mutant roots are agravitropic (Santner & Watson, 2006; Dhonukshe *et al.*, 2010). The latter phenotype can be mimicked by expressing a nonphosphorylatable PIN2 S>A-YFP in the *pin2* loss-of-function mutant background, indicating that regulation of PIN2 polarity through phosphorylation by these kinases is important for gravitropic root growth. In addition, PID was also shown to play a role in phototropic response of the hypocotyl. In the dark, PIN3 was shown to be apolarly localized in the endodermis, and PHOT1-mediated signaling of unilateral blue light triggered a reduction in *PID* expression, resulting in a GNOM-dependent switch in PIN3 polarity to the inner-lateral PM, which initiates polar transport of auxin to the dark side (Ding *et al.*, 2011).
In the phototropism example, PID activity is regulated through its expression. Another way the activity of these kinases might be changed in response to internal and external signals is through their interacting regulatory proteins. For PID, several binding proteins have been identified, of which the calcium-regulated interaction with two calcium-binding proteins is very likely to link with signaling pathways that trigger calcium responses in the cell (Benjamins *et al.*, 2003). In addition, PID was found

to bind to, and to be phosphorylated by, the 3-phosphoinositide-dependent kinase 1 (PDK1), resulting in its hyperactivation (Zegzouti *et al.*, 2006a). PDK1 is an upstream regulator of several AGC kinases and involved in many developmental and stress-related processes (Bögre *et al.*, 2003; Zegzouti *et al.*, 2006b), making it difficult to deduce the *in vivo* significance of its interaction with PID.

Regulation of PIN PM abundance by gravity and light

When a seedling or plant is turned on its side, the shoot will bend up against the gravity vector (negative gravitropism), whereas the root will bend down with the gravity vector (positive gravitropism). In both cases, the growth response is the result of asymmetric auxin distribution, with elevated concentrations at the lower side of the tissue and reduced concentrations at the upper side. The mechanism behind gravity-induced asymmetric auxin distribution has been studied in most detail in roots. In a vertically oriented Arabidopsis root tip, apolar PIN3 and PIN7 redistribute auxin from the maximum in the collumella initials to the epidermis and lateral root cap, from where PIN2 drives the symmetric shootward-directed flow of auxin through the epidermis. Gravity stimulation of roots induces rapid polarization of PIN3 and PIN7 toward the lateral PM, resulting in enhanced auxin transport to the lower side of the root (Friml *et al.*, 2002b; Tanaka *et al.*, 2006; Kleine-Vehn *et al.*, 2010). This initial asymmetry in auxin distribution can already be observed a few minutes after gravity stimulation (Band *et al.*, 2012), and is significantly enhanced by strong post-translational regulation of PIN2 PM abundance. The reduced auxin concentrations destabilize PIN2 in the upper epidermis of the root, whereas the enhanced auxin concentrations in the lower epidermis cells stabilize PIN2 at the apical PM in an ABP1-dependent manner, resulting in canalization of auxin transport through the lower epidermis (Paciorek *et al.*, 2005; Abas *et al.*, 2006; Robert *et al.*, 2010). About 2h after gravity stimulation, when root bending has reached the 40° 'tipping point', the elevated auxin concentrations at the lower side now destabilize PIN2 in a $SCF^{TIR1/AFB}$-dependent way, thereby allowing auxin distribution to normalize again (Abas *et al.*, 2006; Band *et al.*, 2012; Baster *et al.*, 2013). It is well established that the turnover of PM proteins requires their ubiquitination, which triggers endocytosis and trafficking to the lytic vacuole for degradation (reviewed in Korbei & Luschnig, 2013). PIN2 is lysine-63-chain-ubiquitinated at multiple lysine residues in its hydrophilic

loop. Only when the majority of the lysines in the hydrophilic loop are substituted for arginines is PIN2 ubiquitination severely reduced, meaning that the mutant protein can no longer complement the *pin2* mutant, corroborating the idea that ubiquitination and vacuolar trafficking are relevant for PIN2 functionality. PIN2 alleles mimicking constitutive monoubiquitination were endocytosed, whereas vacuolar targeting was found to coincide with the formation of K63-linked polyubiquitin chains (Leitner *et al.*, 2012). When using Arabidopsis seedlings expressing a PIN2-GFP fusion, the turnover and vacuolar accumulation of this fusion protein can be nicely visualized by incubation in the dark, as the GFP moiety is stabilized in the vacuole under these conditions (Tamura *et al.*, 2003). At the same time, light stabilizes PIN2 at the PM, and by introducing the *PIN2:GFP* construct in different mutant backgrounds, it was shown that PIN2 turnover most likely involves the COP9 signalosome (CSN), the light-regulated COP1 ubiquitin E3 ligase and the basic helix–loop–helix transcription factor HY5. Dark-grown *PIN2:GFP* seedlings accumulate GFP in the vacuoles, and *cop9* mutants show reduced vacuolar GFP signal when grown in the dark, whereas *hy5* mutants show reduced PM-localized PIN2:GFP when grown in the light (Laxmi *et al.*, 2008). The involvement of the COP1 E3 ubiquitin ligase in PIN turnover was supported by the fact that *cop1* mutants show increased PIN1 and PIN2 PM localization and display a reduced gravitropic response (Sassi *et al.*, 2012).

The post-translational regulation of PIN2 is essential for the generation of a sufficiently strong asymmetric auxin distribution required for a full gravitropic growth response. This is demonstrated by the *pin2* mutant, where PIN1 is ectopically expressed in the root epidermis and cortex. Even though PIN1 in the *pin2* mutant is expressed in the PIN2 domain, where it shows the correct apical and basal polarity in the epidermis and cortex, respectively (Vieten *et al.*, 2005; Rigas *et al.*, 2013), it fails to restore the gravitropic root growth (Luschnig *et al.*, 1998). Moreover, ectopic PIN1 expression in the epidermis and cortex in *35S::PIN1* seedlings also leads to root agravitropic growth (Petrášek *et al.*, 2006). The reason that PIN2 is more sensitive to turnover than PIN1 could lie in the number of lysines in the HL (13 in PIN1 and 20 in PIN2) or in the entire protein (22 for PIN1 and 28 for PIN2). The fact that multiple lysine-to-arginine substitutions in PIN2 HL are necessary to obtain noncomplementing versions corroborates this hypothesis (Leitner *et al.*, 2012).

Recently, the small GOLVEN (GLV) peptides were identified to regulate PIN2 subcellular localization and influence root gravitropism (Whitford *et al.*, 2012). Arabidopsis contains 11 genes encoding GLV peptides, which are expressed in various domains throughout the plant (Fernandez *et al.*, 2013). After application of GLV peptides to roots, increased PIN2 PM membrane localization can be observed, while other GLV peptides cause PIN2 to accumulate in internal vesicles (Fernandez *et al.*, 2013). How these GLV peptides regulate PIN2 trafficking and what their function is in the gravitropic response remains to be shown. As for the GLV peptides, which are specifically expressed in the shoot, it would be interesting to see if these peptides could be linked to other external responses where auxin is involved, for example, phototropism.

PIN turnover: ubiquitination-driven sorting or anchoring

As described earlier, PIN ubiquitination has a dual role. Mono-ubiquitination triggers PIN endocytosis, and subsequent poly-ubiquitination labels PIN proteins for trafficking to and degradation in the lytic vacuole (Leitner *et al.*, 2012). Whether PINs labeled for degradation use the same endocytosis route as PINs that enter the recycling pathway is currently not clear.

For endocytosed PINs, the endosomal trafficking to the vacuole is at least partially separate from the normal recycling pathway (Jaillais *et al.*, 2007), and occurs GNOM-independently by another BFA-sensitive ARF-GEF (Kleine-Vehn *et al.*, 2008b) from the EEs via late endosomes (LEs) and multivesicular bodies (MVBs) to the vacuole (Fig. 4). LEs are labeled with the associated proteins SORTING NEXIN 1 (SNX1), VACUOLAR PROTEIN SORTING 29 (VPS29) and CLIP-ASSOCIATED PROTEIN (CLASP; Jaillais *et al.*, 2006, 2007; Ambrose *et al.*, 2013). VPS29 was found to interact with VPS35A and loss-of-function mutants show enhanced internal PIN accumulation, suggesting that VPS29 and VPS35A work in a complex in PIN vacuolar trafficking (Nodzyński *et al.*, 2013). Loss-of-function mutants in any of the corresponding genes show reduced PIN2 at the PM, indicating that SNX1, VPS29, and CLASP are part of the retromer that rescues PIN2 from degradation, thereby regulating its PM abundance (Kleine-Vehn *et al.*, 2008b; Ambrose *et al.*, 2013).

CLASP is a microtubule (MT)-associated protein involved in MT rescue and stabilization (Al-Bassam & Chang, 2011), but was also found to interact with SNX1 (Ambrose *et al.*, 2013). This suggests that the MT

cytoskeleton is important in preventing PIN degradation. PIN2-GFP seedlings treated with the MT-destabilizing drug oryzalin indeed show enhanced vacuolar GFP signal (Ambrose *et al.*, 2013), suggesting that CLASP and MT are important in retromer-mediated recycling of PIN proteins from the LEs via the TGN/EE back to the PM.

The mammalian BLOC-1 complex is involved in endosome trafficking from EE to lysosome-related organelles (Setty *et al.*, 2007). Two components of this complex, BLOS1 and BLOS2, were identified in Arabidopsis as interacting partners of SNX1. RNAi-mediated knockdown of BLOS1 resulted in increased PIN1 and PIN2 PM abundance (Cui *et al.*, 2010). These results suggest that the Arabidopsis BLOC-1 complex is involved in sorting the LEs to MVBs to enhance PIN degradation. At the same time, the results imply a dual function for SNX1, both in recycling PIN vesicles from the LE to the TGN/EE as part of the retromer complex, and in trafficking of PIN vesicles from the LE to the MVBs. Merging of MVBs with the vacuole exposes the PIN proteins to the lytic environment of the vacuole and causes their degradation (Fig. 4). However, if LEs were to merge directly with the vacuole, the PIN proteins would localize to the tonoplast instead of being degraded. This can be observed in double mutants in the *CHARGED MULTIVESICULAR BODY PROTEIN/CHROMATIN MODIFYING PROTEIN 1A* and *1B* (*CHMP1A* and *CHMP1B*) genes that fail to accumulate PIN LEs as lumenal vesicles of MVBs (Spitzer *et al.*, 2009).

Recent detailed analysis and modeling of PIN dynamics suggest that some PIN pools are in immobilized membrane fractions, and that PIN polarity is established by reducing diffusion and localizing endocytosis rather than through polar exocytosis (Kleine-Vehn *et al.*, 2011). One way in which PINs seem to be immobilized is by direct interaction with the cell wall, as genetic and pharmacological disruption of the cellulose matrix in the cell walls results in increased PIN diffusion and PIN polarity defects (Feraru *et al.*, 2011). In addition, some PIN-binding proteins have been identified that could reduce PIN turnover by enhancing PIN stability at the PM. For example, the interaction between ABCB19 and PIN1 (Blakeslee *et al.*, 2007; Titapiwatanakun *et al.*, 2009) was suggested to keep PIN1 in immobilized membrane fractions.

Other proteins that might keep PINs in nonmobile PM domains are the *MACCHI-BOU 4*/ENHANCER OF PINOID-Like (MEL)/NAKED PINS IN YUC MUTANTS (NPY) proteins. MEL/NPYs are typical scaffold

proteins that colocalize with the polarly localized PIN proteins in the epidermis of the embryo and root, and stabilize PIN polarity by reducing their internalization (Furutani *et al.*, 2011).

Regulation of PIN proteins by internal signals

Auxin-regulated PIN trafficking: the ABP1, AGC3 kinase, cytoskeleton module

Research into the influence of auxin on interdigitation of PCs yielded a pathway that involves ABP1, Rho GTPases and both the actin and microtubule cytoskeleton. Various mutants within known auxin-related genes show reduced interdigitation of PCs. External auxin application only rescues a subset of these mutants (Xu *et al.*, 2010).

After sensing auxin, the apoplastic ABP1 signals to the RhoGTP-ases ROP2 and ROP6 through its interaction with the PM-localized receptor-like transmembrane kinases (TMKs; Xu *et al.*, 2014). In leaf PCs, ROP2 and ROP6 activate ROP interactive CRIB motif-containing proteins RIC4 and RIC1, respectively (Xu *et al.*, 2010). ROP2/RIC4 stabilizes the actin cytoskeleton in the lobes (Fu *et al.*, 2002), reducing PIN1 endocytosis and thereby promoting PIN1 PM localization in the lobes (Nagawa *et al.*, 2012). ROP6 loads RIC1 onto the MT, causing it to promote MT ordering, and inhibiting exocytosis, thereby generating the indentations. By contrast, ROP2 removes RIC1 from the MT, possibly to enhance local outgrowth during lobe formation (Fu *et al.*, 2005).

With PIN1 being stabilized in the lobes, the exported auxin is sensed by ABP1, which again acts on ROP6 in the indentation of the opposite cell and back again on the ROP2 in the lobe. In roots, ROP6 seems to fulfill the role of ROP2, preventing PIN2 endocytosis by promoting actin stabilization (Chen *et al.*, 2012; Lin *et al.*, 2012). This is surprising, and suggests that the function of these ROPs can vary depending on the tissue, possibly by tissue-specific modulators of ROP function.

PIN regulation by ABP1, the ROPs, and the cytoskeleton during interdigitated patterning of PC seems to be integrated with the PIN polar targeting pathway of the AGC3 kinases and the PP2A phosphatases (Li *et al.*, 2011). In the PP2A phosphatase mutant *fypp1* and the *35S::PID* overexpression plants, PIN1 localization was shifted from the lobes to the indentations, resulting in PCs with a reduced number of lobes (Li *et al.*, 2011). This confirms that placement of PIN1 at the lobe tips is

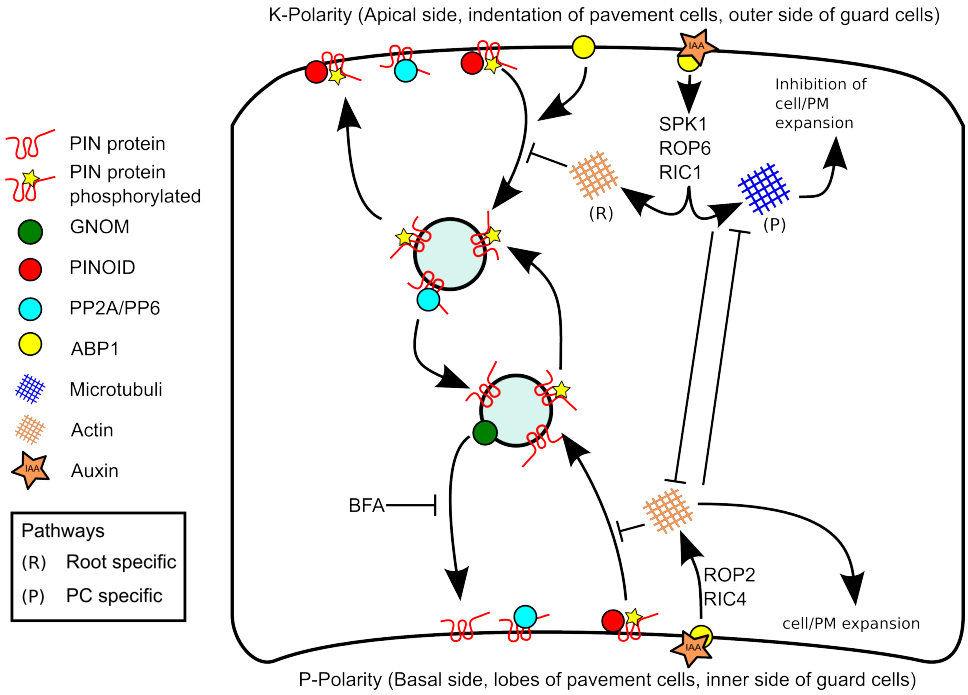

Figure 5: Combined model on the regulation of PIN trafficking by phosphorylation and the auxin binding protein 1/transmembrane kinase/Rho of Plants/ROP interactive CRIB-motif containing protein (ABP1/TMK/ROP/RIC) pathway. PIN proteins recycle continuously between the plasma membrane (PM) and trans-Golgi network/early endosomes (TGN/EE). Based on their phosphorylation status, which is determined by the antagonistic action of the PINOID kinase and PP2A/PP6 phosphatases, PIN proteins move either to the kinase (K)-polarity pole or the phosphatase (P)-polarity pole, respectively, through transcytosis and exocytosis. ABP1 acts on PIN endocytosis, dependent on the presence of auxin. Without auxin, ABP1 enhances PIN endocytosis. In the presence of auxin, ABP1 acts through TMK/ROP6/RIC1 or TMK/ROP2/RIC4 signaling to the actin cytoskeleton to inhibit PIN endocytosis. PP2A, PROTEIN PHOSPHATASE 2A; PP6, PROTEIN PHOSPHATASE 6; BFA, brefeldin A; PC, pavement cell.

important for proper indentation of PCs. Moreover, this suggests that there is a conserved mechanism where the AGC3 kinases and PP2A phosphatases regulate PIN polarity in all plant cells, but that the effect of PIN phosphorylation depends on the polarity field(s) in the cell (Fig. 5).

Regulation of PIN proteins by hormonal crosstalk

Apart from auxin, eight other plant hormones have been discovered, some of which are important in plant defense (salicylic acid and jasmonic acid), and others that have either a central (cytokinin

(CK), brassinosteroids (BRs)) or a more specific role (ABA, GA, strigolactones (SLs), ethylene) in directing plant development. Besides their well-established functions, a complex network of crosstalk has been uncovered between the signaling pathways of these hormones, and as part of this crosstalk, several hormones affect PIN action at either the transcriptional or the post-transcriptional level (Vanstraelen & Benková, 2012).

Strigolactones were initially identified as signaling molecules in symbiotic interaction between plants and arbuscular mycorrhizal fungi or parasitic weeds (Cook *et al.*, 1966; Akiyama *et al.*, 2005; Matusova *et al.*, 2005). Later, it was discovered that the same molecules are present in plants and that their amounts were reduced in the pea *ramosus* (*rms*), rice *dwarf* (*d*) and Arabidopsis *more axillary branching* (*max*) shoot branching mutants (Gomez-Roldan *et al.*, 2008; Umehara *et al.*, 2008). Over the years, two models emerged to explain the action of SLs. The first model proposes that a second messenger is produced in the main stem vasculature and transported upward into the bud, where it represses outgrowth. The second model involves the auxin canalization theory, where SLs reduce PIN abundance and basipetal PAT in the inflorescence stem, thereby inhibiting auxin efflux from the lateral buds (Bennett *et al.*, 2006). Various publications support the first model (Brewer *et al.*, 2009), including the discovery of an SL- and CK-responsive transcription factor that inhibits bud outgrowth (Braun *et al.*, 2012; Dun *et al.*, 2013). In favor of the second model, it was recently shown that SL application reduces PM levels of PIN1 by enhancing clathrin-mediated endocytosis (Crawford *et al.*, 2010; Shinohara *et al.*, 2013). This in turn would suppress the induction of canalized auxin transport from the buds, thereby maintaining their dormant state (Bennett *et al.*, 2006; Crawford *et al.*, 2010). In addition, it was shown that SLs promote root branching under phosphate-limiting conditions, by reducing PIN PM abundance in the root (Ruyter-Spira *et al.*, 2011).

Similar to SLs, CK application also resulted in a rapid reduction of PIN1:GFP abundance at the PM in lateral root primordia. In this case, an enhanced GFP signal could be observed in the vacuoles, when seedlings were incubated in the dark, suggesting that CK enhances PIN1 degradation. This regulation of PIN1 is mediated through the CK-responsive ARABIDOPSIS HISTIDINE KINASE 4 (AHK4), but not AHK2 and AHK3, and by B-type Arabidopsis response regulator (ARR)

components ARR2 and ARR12. Other PINs, such as PIN2 and PIN7, are not sensitive to CK, suggesting that this type of regulation is specific for PIN1 (Marhavý *et al.*, 2011). CK also represses *PIN* gene transcription. Upon CK detection, the AHK3 receptor relays the signal to ARR1 and ARR12, which activate SHY2/IAA3 and cause suppression of *PIN* expression (Dello Ioio *et al.*, 2008). Both *PIN1* and *PIN4* are down-regulated and *PIN7* is up-regulated by CK application (Růžička *et al.*, 2009). In line with these CK application experiments, genetic evidence was obtained by the analysis of the *auxin up-regulated f-box protein1* (*auf1*) mutant. The *AUF1* gene was found to be regulated by auxin, and AUF1 was found to act on ARR1, thereby forming a feedback loop between auxin and CK on PIN-mediated auxin transport (Zheng *et al.*, 2011). The analysis of the influence of CK is tricky, because ethylene is formed after CK application and ethylene is another hormone that influences *PIN* expression. An earlier publication reported that *PIN1*, *PIN2* and *PIN4* were found to be up-regulated by ethylene and that *PIN7* did not respond to the treatment (Růžička *et al.*, 2007). This is in strong contrast with the report of (Žádníková *et al.*, 2010) Žádníková *et al.* (2010), in which *PIN1* and *PIN4* were found to be down-regulated by ethylene and *PIN2* did not change expression. This discrepancy in observations could possibly be explained by the different tissues that were observed, in these cases being the root vs the apical hook.

Two other hormone families that show crosstalk with auxin by affecting PIN stability are GAs and BRs. Auxin is known to promote the GA-mediated degradation of DELLA proteins, thereby enhancing the cellular response to GA (Fu & Harberd, 2003), and in turn GA promotes the PM localization of PIN proteins. In various GA mutants, reduced amounts of PIN proteins are observed at the PM and the vacuolar targeting of PIN2:GFP is increased, whereas asymmetric GA distribution during root gravitropism is involved in decreasing PIN2 vacuolar targeting in the lower root epidermis (Willige *et al.*, 2011; Löfke *et al.*, 2013). BRs provide a delicate modulation to PIN abundance. Reduction of endogenous BRs by inhibiting BR synthesis increases *PIN2* and *PIN4* transcription, while supplying exogenous BRs causes a decrease in the expression of these *PIN* genes. In the BR receptor mutant *bri1*, however, a large reduction of both PIN2 and PIN4 can be observed, suggesting that BR signaling is required to prevent PIN turnover (Hacham *et al.*, 2012). This shows that BRs regulate PIN2 and PIN4 in the root at both the

transcriptional and post-transcriptional level.

Conclusions/future perspectives

As the initial identification of auxin is based on phototropic growth experiments of plant coleoptiles, it was clear from the start that this plant hormone plays an important role in adaptations of a plant's growth and development to environmental signals. In view of the central role of the polar transport-driven asymmetric distribution of auxin, it is not surprising that the PM-localized PIN auxin efflux carriers, and especially their post-translational regulation, are important targets for such signaling pathways. Several signaling pathways interfere with the post-translational modification of these PINs by phosphorylation or ubiquitination, thereby altering their PM abundance or polarity (Abas *et al.*, 2006; Michniewicz *et al.*, 2007; Dhonukshe *et al.*, 2008). Recently, ABP1-mediated PIN regulation through ROPs and the actin and microtubule cytoskeleton revealed another pathway that seems independent of PIN modification (Xu *et al.*, 2010; Chen *et al.*, 2012; Lin *et al.*, 2012). The fact that PID kinase activity can modulate the ABP1 pathway (Li *et al.*, 2011) suggests that the two pathways are likely to converge at some point. In the field of transcriptional regulation and hormonal crosstalk, a lot is still unknown. We know more or less when and where PIN proteins are expressed, but which factors exactly contribute to these expression patterns, and how their expression and subcellular distribution is regulated by environmental signals remain largely unknown. Several hormones (among which auxin itself) were not only shown to alter *PIN* transcription (Dello Ioio *et al.*, 2008; Hacham *et al.*, 2012), but also to influence the PIN abundance at the PM by modulating turnover of these auxin carriers (Crawford *et al.*, 2010; Willige *et al.*, 2011; Hacham *et al.*, 2012). A basic model starts to emerge on PIN turnover (Fig. 4) and over time this will be integrated into the model that describes the PIN endocytosis, polarity, and regulation by AGC3 kinases and ABP1/ROP/RIC (Fig. 5). Other regulators such as the GLV peptides, the MEL/NPYs and the AGC3 kinase binding proteins will most likely fit into a specific region of this model, as they are likely to function in specific developmental processes, or under specific stress conditions.

In this review, we have tried to cover the most important aspects of PIN regulation and to show the vast complexity of the regulatory

networks involved. These networks contain many feedback loops, and several mathematical models have been developed that describe PAT to help understand its complex regulation, and its function and dynamics in developmental processes such as vascular development, lateral root initiation, and phyllotaxis (van Berkel *et al.*, 2013). PIN-driven PAT is at the basis of plant developmental plasticity, and future models describing the control of these regulatory networks by different internal and external signals will allow the optimization of the development of crop plants to the growers' needs by tweaking their growth conditions.

Thesis outline

The review presented in this chapter provides the scientific basis for the other chapters in this thesis. Not only gives it the reader a solid background in understanding the experimental chapters, but it also shows that knowledge presented in this chapter is subject for new and somewhat controversial scientific insights. The best example for this can be found in **chapter 2**, where newly created *null abp1* lines show no embryo lethality, as observed in the original *abp1* mutant. We give an overview of the APB1 research until this finding and possible reasons for the observed discrepancies. **Chapter 3** describes that PDK1-mediated phosphorylation of PID causes its relocalization to the MT in protoplasts and that this effect can be copied or inhibited by creating mutant PID versions. These mutations can overcome to some degree the *pid wag1 wag2* embryo and adult phenotypes *in planta*, but we did not observe MT localization of the mutant proteins with confocal microscopy. **Chapter 4** shows a cellular mechanism that is responsible for the observed MT localization of PID after phosphorylation by PDK1. The family of BTB and TAZ domain scaffold (BT) proteins bind to PID and inhibit its phosphorylation function. Cotransfections of BT1 and PID result in a nuclear localized PID in protoplasts. The BT proteins also provide a bridge to the plant-specific At1 family of kinesins that add MT-binding capabilities to PID. **Chapter 5** provides an *in silico* phylogenetic analysis of the At1 kinesin family and investigates the conservation of the NPK1 binding and activation domain in the family members. T-DNA insert lines for the BT-interacting kinesins were obtained and examined for phenotypes in higher order mutant lines. The quadruple mutant did not give any strong phenotypes and RT-PCR showed that two of the four genes were not *null*

mutations, because residual expression could be detected. The expression domains of the kinesins and their response to external stimuli were tested with promoter-GUS constructs. In protoplasts the kinesins showed MT localization, however *in planta* the proteins were targetted for degradation by the 26S proteasome. Even after preventing this degradation, no MT localization could be observed.

Acknowledgements

M.E.J.H. was supported by NWO-CW TOP 700.58.301 grant to R.O. from the Chemical Sciences Division with financial support from the Netherlands Organisation for Scientific Research (NWO).

Bibliography

Abas, L., Benjamins, R., Malenica, N., Paciorek, T., Wiśniewska, J., Moulinier-Anzola, J. C., Sieberer, T., Friml, J. & Luschnig, C. (2006). Intracellular trafficking and proteolysis of the *Arabidopsis* auxin-efflux facilitator PIN2 are involved in root gravitropism. Nature Cell Biology **8**, 249–256.

Akiyama, K., Matsuzaki, K.-i. & Hayashi, H. (2005). Plant sesquiterpenes induce hyphal branching in arbuscular mycorrhizal fungi. Nature **435**, 824–827.

Al-Bassam, J. & Chang, F. (2011). Regulation of microtubule dynamics by TOG-domain proteins XMAP215/Dis1 and CLASP. Trends in Cell Biology **21**, 604–614.

Ambrose, C., Ruan, Y., Gardiner, J., Tamblyn, L. M., Catching, A., Kirik, V., Marc, J., Overall, R. & Wasteneys, G. O. (2013). CLASP interacts with Sorting Nexin 1 to link microtubules and auxin transport via PIN2 recycling in *Arabidopsis thaliana*. Developmental Cell **24**, 649–659.

Ballesteros, I., Domínguez, T., Sauer, M., Paredes, P., Duprat, A., Rojo, E., Sanmartín, M. & Sánchez-Serrano, J. J. (2013). Specialized functions of the PP2A subfamily II catalytic subunits PP2A-C3 and PP2A-C4 in the distribution of auxin fluxes and development in arabidopsis. Plant Journal **73**, 862–872.

Band, L. R., Wells, D. M., Larrieu, A., Sun, J., Middleton, A. M., French, A. P., Brunoud, G., Sato, E. M., Wilson, M. H., Péret, B., Oliva, M., Swarup, R., Sairanen, I., Parry, G., Ljung, K., Beeckman, T., Garibaldi, J. M., Estelle, M., Owen, M. R., Vissenberg, K., Hodgman, T. C., Pridmore, T. P., King, J. R., Vernoux, T. & Bennett, M. J. (2012). Root gravitropism is regulated by a transient lateral auxin gradient controlled by a tipping-point mechanism. Proceedings of the National Academy of Sciences of the United States of America **109**, 4668–4673.

Barbez, E., Kubeš, M., Rolčík, J., Béziat, C., Pěnčík, A., Wang, B., Ruiz Rosquete, M., Zhu, J., Dobrev, P. I., Lee, Y., Zažímalová, E., Petrášek, J., Geisler, M., Friml, J.

& Kleine-Vehn, J. (2012). A novel putative auxin carrier family regulates intracellular auxin homeostasis in plants. Nature **485**, 119–122.

Bartel, B. & Fink, G. R. (1995). ILR1, an amidohydrolase that releases active indole-3-acetic acid from conjugates. Science **268**, 1745–1748.

Baster, P., Robert, S., Kleine-Vehn, J., Vanneste, S., Kania, U., Grunewald, W., De Rybel, B., Beeckman, T. & Friml, J. (2013). SCFTIR1/AFB-auxin signalling regulates PIN vacuolar trafficking and auxin fluxes during root gravitropism. EMBO Journal **32**, 260–274.

Benjamins, R., Galván-Ampudia, C. S., Hooykaas, P. J. J. & Offringa, R. (2003). PINOID-mediated signaling involves calcium-binding proteins. Plant Physiology **132**, 1623–1630.

Benjamins, R., Quint, A., Weijers, D., Hooykaas, P. J. J. & Offringa, R. (2001). The PINOID protein kinase regulates organ development in *arabidopsis* by enhancing polar auxin transport. Development **128**, 4057–4067.

Benková, E., Michniewicz, M., Sauer, M., Teichmann, T., Seifertová, D., Jürgens, G. & Friml, J. (2003). Local, efflux-dependent auxin gradients as a common module for plant organ formation. Cell **115**, 591–602.

Bennett, M. J., Marchant, A., Green, H. G., May, S. T., Ward, S. P., Millner, P. A., Walker, A. R., Schulz, B. & Feldmann, K. A. (1996). *Arabidopsis AUX1* gene: A permease-like regulator of root gravitropism. Science **273**, 948–950.

Bennett, T., Sieberer, T., Willett, B., Booker, J., Luschnig, C. & Leyser, O. (2006). The *Arabidopsis* MAX pathway controls shoot branching by regulating auxin transport. Current Biology **16**, 553–563.

Blakeslee, J. J., Bandyopadhyay, A., Lee, O. R., Mravec, J., Titapiwatanakun, B., Sauer, M., Makam, S. N., Cheng, Y., Bouchard, R., Adamec, J., Geisler, M., Nagashima, A., Sakai, T., Martinoia, E., Friml, J., Peer, W. A. & Murphy, A. S.

(2007). Interactions among PIN-FORMED and P-Glycoprotein auxin transporters in *Arabidopsis*. Plant Cell **19**, 131–147.

Blilou, I., Xu, J., Wildwater, M., Willemsen, V., Paponov, I., Friml, J., Heidstra, R., Aida, M., Palme, K. & Scheres, B. (2005). The PIN auxin efflux facilitator network controls growth and patterning in *Arabidopsis* roots. Nature **433**, 39–44.

Boer, D. R., Freire-Rios, A., Van den Berg, W. A., Saaki, T., Manfield, I. W., Kepinski, S., López-Vidrieo, I., Franco-Zorrilla, J. M., De Vries, S. C., Solano, R., Weijers, D. & Coll, M. (2014). Structural basis for DNA binding specificity by the auxin-dependent ARF transcription factors. Cell **156**, 577–589.

Bögre, L., Ökrész, L., Henriques, R. & Anthony, R. G. (2003). Growth signalling pathways in *Arabidopsis* and the AGC protein kinases. Trends in Plant Science **8**, 424–431.

Boutilier, K., Offringa, R., Sharma, V. K., Kieft, H., Ouellet, T., Zhang, L., Hattori, J., Liu, C.-M., van Lammeren, A. A. M., Miki, B. L. A., Custers, J. B. M. & van Lookeren Campagne, M. M. (2002). Ectopic expression of BABY BOOM triggers a conversion from vegetative to embryonic growth. Plant Cell **14**, 1737–1749.

Braun, N., de Saint Germain, A., Pillot, J.-P., Boutet-Mercey, S., Dalmais, M., Antoniadi, I., Li, X., Maia-Grondard, A., Le Signor, C., Bouteiller, N., Luo, D., Bendahmane, A., Turnbull, C. & Rameau, C. (2012). The pea TCP transcription factor PsBRC1 acts downstream of strigolactones to control shoot branching. Plant Physiology **158**, 225–238.

Braun, N., Wyrzykowska, J., Muller, P., David, K., Couch, D., Perrot-Rechenmann, C. & Fleming, A. J. (2008). Conditional repression of AUXIN BINDING PROTEIN1 reveals that it coordinates cell division and cell expansion during postembryonic shoot development in *Arabidopsis* and tobacco. Plant Cell **20**, 2746–2762.

Brewer, P. B., Dun, E. A., Ferguson, B. J., Rameau, C. & Beveridge, C. A. (2009). Strigolactone acts downstream of auxin to

regulate bud outgrowth in pea and Arabidopsis. Plant Physiology **150**, 482–493.

Calderón Villalobos, L. I. A., Lee, S., De Oliveira, C., Ivetac, A., Brandt, W., Armitage, L., Sheard, L. B., Tan, X., Parry, G., Mao, H., Zheng, N., Napier, R., Kepinski, S. & Estelle, M. (2012). A combinatorial TIR1/AFB–Aux/IAA co-receptor system for differential sensing of auxin. Nature Chemical Biology **8**, 477–485.

Causier, B., Ashworth, M., Guo, W. & Davies, B. (2012). The TOPLESS interactome: A framework for gene repression in Arabidopsis. Plant Physiology **158**, 423–438.

Chen, J.-G., Ullah, H., Young, J. C., Sussman, M. R. & Jones, A. M. (2001). ABP1 is required for organized cell elongation and division in *Arabidopsis* embryogenesis. Genes & Development **15**, 902–911.

Chen, X., Naramoto, S., Robert, S., Tejos, R., Löfke, C., Lin, D., Yang, Z. & Friml, J. (2012). ABP1 and ROP6 GTPase signaling regulate clathrin-mediated endocytosis in *Arabidopsis* roots. Current Biology **22**, 1326–1332.

Cheng, Y., Qin, G., Dai, X. & Zhao, Y. (2008). NPY genes and AGC kinases define two key steps in auxin-mediated organogenesis in Arabidopsis. Proceedings of the National Academy of Sciences of the United States of America **105**, 21017–21022.

Christensen, S. K., Dagenais, N., Chory, J. & Weigel, D. (2000). Regulation of auxin response by the protein kinase PINOID. Cell **100**, 469–478.

Cook, C. E., Whichard, L. P., Turner, B., Wall, M. E. & Egley, G. H. (1966). Germination of Witchweed (Striga lutea Lour.): isolation and properties of a potent stimulant. Science **154**, 1189–1190.

Čovanová, M., Sauer, M., Rychtář, J., Friml, J., Petrášek, J. & Zažímalová, E. (2013). Overexpression of the AUXIN BINDING PROTEIN1 modulates PIN-dependent auxin transport in tobacco cells. PLoS ONE **8**, e70050.

Crawford, S., Shinohara, N., Sieberer, T., Williamson, L., George, G., Hepworth, J., Müller, D., Domagalska, M. A. & Leyser, O. (2010). Strigolactones enhance competition between shoot branches by dampening auxin transport. Development **137**, 2905–2913.

Cui, Y., Li, X., Chen, Q., He, X., Yang, Q., Zhang, A., Yu, X., Chen, H., Liu, N., Xie, Q., Yang, W., Zuo, J., Palme, K. & Li, W. (2010). BLOS1, a putative BLOC-1 subunit, interacts with SNX1 and modulates root growth in *Arabidopsis*. Journal of Cell Science **123**, 3727–3733.

Dahlke, R. I., Luethen, H. & Steffens, B. (2010). ABP1: An auxin receptor for fast responses at the plasma membrane. Plant Signaling & Behavior **5**, 1–3.

Dai, M., Zhang, C., Kania, U., Chen, F., Xue, Q., Mccray, T., Li, G., Qin, G., Wakeley, M., Terzaghi, W., Wan, J., Zhao, Y., Xu, J., Friml, J., Deng, X. W. & Wang, H. (2012). A PP6-type phosphatase holoenzyme directly regulates PIN phosphorylation and auxin efflux in *Arabidopsis*. Plant Cell **24**, 2497–2514.

Dal Bosco, C., Dovzhenko, A., Liu, X., Woerner, N., Rensch, T., Eismann, M., Eimer, S., Hegermann, J., Paponov, I. A., Ruperti, B., Heberle-Bors, E., Touraev, A., Cohen, J. D. & Palme, K. (2012). The endoplasmic reticulum localized PIN8 is a pollen-specific auxin carrier involved in intracellular auxin homeostasis. Plant Journal **71**, 860–870.

Darwin, C. R. & Darwin, F. (1880). The power of movement in plants. John Murray, London, UK.

David, K. M., Couch, D., Braun, N., Brown, S., Grosclaude, J. & Perrot-Rechenmann, C. (2007). The auxin-binding protein 1 is essential for the control of cell cycle. Plant Journal **50**, 197–206.

Delbarre, A., Muller, P. & Guern, J. (1998). Short-lived and phosphorylated proteins contribute to carrier-mediated efflux, but not to influx, of auxin in suspension-cultured tobacco cells. Plant Physiology **116**, 833–844.

Dello Ioio, R., Nakamura, K., Moubayidin, L., Perilli, S., Taniguchi, M., Morita, M. T., Aoyama, T., Costantino, P. &

Sabatini, S. (2008). A genetic framework for the control of cell division and differentiation in the root meristem. Science **322**, 1380–1384.

Dharmasiri, N., Dharmasiri, S. & Estelle, M. (2005a). The F-box protein TIR1 is an auxin receptor. Nature **435**, 441–445.

Dharmasiri, N., Dharmasiri, S., Weijers, D., Lechner, E., Yamada, M., Hobbie, L., Ehrismann, J. S., Jürgens, G. & Estelle, M. (2005b). Plant development is regulated by a family of Auxin receptor F Box Proteins. Developmental Cell **9**, 109–119.

Dhonukshe, P., Aniento, F., Hwang, I., Robinson, D. G., Mravec, J., Stierhof, Y.-D. & Friml, J. (2007). Clathrin-mediated constitutive endocytosis of PIN auxin efflux carriers in *Arabidopsis*. Current Biology **17**, 520–527.

Dhonukshe, P., Huang, F., Galván-Ampudia, C. S., Mähönen, A. P., Kleine-Vehn, J., Xu, J., Quint, A., Prasad, K., Friml, J., Scheres, B. & Offringa, R. (2010). Plasma membrane-bound AGC3 kinases phosphorylate PIN auxin carriers at TPRXS(N/S) motifs to direct apical PIN recycling. Development **137**, 3245–3255.

Dhonukshe, P., Tanaka, H., Goh, T., Ebine, K., Mähönen, A. P., Prasad, K., Blilou, I., Geldner, N., Xu, J., Uemura, T., Chory, J., Ueda, T., Nakano, A., Scheres, B. & Friml, J. (2008). Generation of cell polarity in plants links endocytosis, auxin distribution and cell fate decisions. Nature **456**, 962–966.

Ding, Z., Galván-Ampudia, C. S., Demarsy, E., Łangowski, Ł., Kleine-Vehn, J., Fan, Y., Morita, M. T., Tasaka, M., Fankhauser, C., Offringa, R. & Friml, J. (2011). Light-mediated polarization of the PIN3 auxin transporter for the phototropic response in *Arabidopsis*. Nature Cell Biology **13**, 447–452.

Ding, Z., Wang, B., Moreno, I., Dupláková, N., Simon, S., Carraro, N., Reemmer, J., Pěnčík, A., Chen, X., Tejos, R., Skůpa, P., Pollmann, S., Mravec, J., Petrášek, J., Zažímalová, E., Honys, D., Rolčík, J., Murphy, A., Orellana, A., Geisler, M. & Friml, J. (2012). ER-localized auxin transporter PIN8 regulates auxin homeostasis and male gametophyte development in *Arabidopsis*. Nature Communications **3**, 941.

Dos Santos Maraschin, F., Memelink, J. & Offringa, R. (2009). Auxin-induced, SCFTIR1-mediated poly-ubiquitination marks Aux/IAA proteins for degradation. Plant Journal **59**, 100–109.

Dun, E. A., de Saint Germain, A., Rameau, C. & Beveridge, C. A. (2013). Dynamics of strigolactone function and shoot branching responses in *Pisum sativum*. Molecular Plant **6**, 128–140.

Feldwisch, J., Zettl, R., Hesse, F., Schell, J. & Palme, K. (1992). An auxin-binding protein is localized to the plasma membrane of maize coleoptile cells: identification by photoaffinity labeling and purification of a 23-kda polypeptide. Proceedings of the National Academy of Sciences of the United States of America **89**, 475–479.

Feraru, E., Feraru, M. I., Kleine-Vehn, J., Martinière, A., Mouille, G., Vanneste, S., Vernhettes, S., Runions, J. & Friml, J. (2011). PIN polarity maintenance by the cell wall in *Arabidopsis*. Current Biology **21**, 338–343.

Feraru, E., Vosolsobě, S., Feraru, M. I., Petrášek, J. & Kleine-Vehn, J. (2012). Evolution and structural diversification of PILS putative auxin carriers in plants. Frontiers in Plant Science **3**, 227.

Fernandez, A., Drozdzecki, A., Hoogewijs, K., Nguyen, A., Beeckman, T., Madder, A. & Hilson, P. (2013). Transcriptional and functional classification of the GOLVEN/ROOT GROWTH FACTOR/CLE-Like signaling peptides reveals their role in lateral root and hair formation. Plant Physiology **161**, 954–970.

Friml, J., Benková, E., Blilou, I., Wiśniewska, J., Hamann, T., Ljung, K., Woody, S., Sandberg, G., Scheres, B., Jürgens, G. & Palme, K. (2002a). AtPIN4 mediates sink-driven auxin gradients and root patterning in *Arabidopsis*. Cell **108**, 661–673.

Friml, J., Vieten, A., Sauer, M., Weijers, D., Schwarz, H., Hamann, T., Offringa, R. & Jürgens, G. (2003). Efflux-dependent auxin gradients establish the apical-basal axis of *Arabidopsis*. Nature **426**, 147–153.

Friml, J., Wiśniewska, J., Benková, E., Mendgen, K. & Palme, K. (2002b). Lateral relocation of auxin efflux regulator PIN3 mediates tropism in *Arabidopsis*. Nature **415**, 806–809.

Friml, J., Yang, X., Michniewicz, M., Weijers, D., Quint, A., Tietz, O., Benjamins, R., Ouwerkerk, P. B. F., Ljung, K., Sandberg, G., Hooykaas, P. J. J., Palme, K. & Offringa, R. (2004). A PINOID-dependent binary switch in apical-basal PIN polar targeting directs auxin efflux. Science **306**, 862–865.

Fu, X. & Harberd, N. P. (2003). Auxin promotes *Arabidopsis* root growth by modulating gibberellin response. Nature **421**, 740–743.

Fu, Y., Gu, Y., Zheng, Z., Wasteneys, G. & Yang, Z. (2005). Arabidopsis interdigitating cell growth requires two antagonistic pathways with opposing action on cell morphogenesis. Cell **120**, 687–700.

Fu, Y., Li, H. & Yang, Z. (2002). The ROP2 GTPase controls the formation of cortical fine F-Actin and the early phase of directional cell expansion during Arabidopsis organogenesis. Plant Cell **14**, 777–794.

Furutani, M., Sakamoto, N., Yoshida, S., Kajiwara, T., Robert, H. S., Friml, J. & Tasaka, M. (2011). Polar-localized NPH3-like proteins regulate polarity and endocytosis of PIN-FORMED auxin efflux carriers. Development **138**, 2069–2078.

Galinha, C., Hofhuis, H., Luijten, M., Willemsen, V., Blilou, I., Heidstra, R. & Scheres, B. (2007). PLETHORA proteins as dose-dependent master regulators of *Arabidopsis* root development. Nature **449**, 1053–1057.

Galván-Ampudia, C. S. & Offringa, R. (2007). Plant evolution: AGC kinases tell the auxin tale. Trends in Plant Science **12**, 541–547.

Gälweiler, L., Guan, C., Müller, A., Wisman, E., Mendgen, K., Yephremov, A. & Palme, K. (1998). Regulation of polar auxin transport by AtPIN1 in *Arabidopsis* vascular tissue. Science **282**, 2226–2230.

Ganguly, A., Lee, S. H., Cho, M., Lee, O. R., Yoo, H. & Cho, H.-T. (2010). Differential auxin-transporting activities of

PIN-FORMED proteins in Arabidopsis root hair cells. Plant Physiology **153**, 1046–1061.

Ganguly, A., Park, M., Kesawat, M. S. & Cho, H.-T. (2014). Functional analysis of the hydrophilic loop in intracellular trafficking of *Arabidopsis* PIN-FORMED proteins. Plant Cell **26**.

Garbers, C., DeLong, A., Deruére, J., Bernasconi, P. & Söll, D. (1996). A mutation in protein phosphatase 2A regulatory subunit A affects auxin transport in *Arabidopsis*. EMBO Journal **15**, 2115–2124.

Garrett, J., Meents, M., Blackshaw, M., Blackshaw, L., Hou, H., Styranko, D., Kohalmi, S. & Schultz, E. (2012). A novel, semi-dominant allele of *MONOPTEROS* provides insight into leaf initiation and vein pattern formation. Planta **236**, 297–312.

Geisler, M., Blakeslee, J. J., Bouchard, R., Lee, O. R., Vincenzetti, V., Bandyopadhyay, A., Titapiwatanakun, B., Peer, W. A., Bailly, A., Richards, E. L., Ejendal, K. F. K., Smith, A. P., Baroux, C., Grossniklaus, U., Müller, A., Hrycyna, C. A., Dudler, R., Murphy, A. S. & Martinoia, E. (2005). Cellular efflux of auxin catalyzed by the Arabidopsis MDR/PGP transporter AtPGP1. Plant Journal **44**, 179–194.

Geldner, N., Anders, N., Wolters, H., Keicher, J., Kornberger, W., Muller, P., Delbarre, A., Ueda, T., Nakano, A. & Jürgens, G. (2003). The *Arabidopsis* GNOM ARF-GEF mediates endosomal recycling, auxin transport, and auxin-dependent plant growth. Cell **112**, 219–230.

Geldner, N., Friml, J., Stierhof, Y.-D., Jürgens, G. & Palme, K. (2001). Auxin transport inhibitors block PIN1 cycling and vesicle trafficking. Nature **413**, 425–428.

Gomez-Roldan, V., Fermas, S., Brewer, P. B., Puech-Pagès, V., Dun, E. A., Pillot, J.-P., Letisse, F., Matusova, R., Danoun, S., Portais, J.-C., Bouwmeester, H., Becard, G., Beveridge, C. A., Rameau, C. & Rochange, S. F. (2008). Strigolactone inhibition of shoot branching. Nature **455**, 189–194.

Guenot, B., Bayer, E., Kierzkowski, D., Smith, R. S., Mandel, T., Žádníková, P., Benková, E. & Kuhlemeier, C. (2012).

PIN1-independent leaf initiation in Arabidopsis. Plant Physiology **159**, 1501–1510.

Hacham, Y., Sela, A., Friedlander, L. & Savaldi-Goldstein, S. (2012). BRI1 activity in the root meristem involves post-transcriptional regulation of PIN auxin efflux carriers. Plant Signaling & Behavior **7**, 68–70.

Hamann, T., Benková, E., Bäurle, I., Kientz, M. & Jürgens, G. (2002). The *Arabidopsis BODENLOS* gene encodes an auxin response protein inhibiting MONOPTEROS-mediated embryo patterning. Genes & Development **16**, 1610–1615.

Hertel, R., Thomson, K.-S. & Russo, V. E. A. (1972). *In-vitro* auxin binding to particulate cell fractions from corn coleoptiles. Planta **107**, 325–340.

Huang, F., Kemel Zago, M., Abas, L., van Marion, A., Galván-Ampudia, C. S. & Offringa, R. (2010). Phosphorylation of conserved PIN motifs directs *arabidopsis* PIN1 polarity and auxin transport. Plant Cell **22**, 1129–1142.

Jaillais, Y., Fobis-Loisy, I., Miège, C., Rollin, C. & Gaude, T. (2006). AtSNX1 defines an endosome for auxin-carrier trafficking in *Arabidopsis*. Nature **443**, 106–109.

Jaillais, Y., Santambrogio, M., Rozier, F., Fobis-Loisy, I., Miège, C. & Gaude, T. (2007). The retromer protein VPS29 links cell polarity and organ initiation in plants. Cell **130**, 1057–1070.

Jones, A. M. & Herman, E. M. (1993). KDEL-containing auxin-binding protein is secreted to the plasma membrane and cell wall. Plant Physiology **101**, 595–606.

Kaneda, M., Schuetz, M., Lin, B. S. P., Chanis, C., Hamberger, B., Western, T. L., Ehlting, J. & Samuels, A. L. (2011). ABC transporters coordinately expressed during lignification of *Arabidopsis* stems include a set of ABCBs associated with auxin transport. Journal of Experimental Botany **62**, 2063–2077.

Kepinski, S. & Leyser, O. (2005). The *Arabidopsis* F-box protein TIR1 is an auxin receptor. Nature **435**, 446–451.

Kitakura, S., Vanneste, S., Robert, S., Löfke, C., Teichmann, T., Tanaka, H. & Friml, J. (2011). Clathrin mediates endocytosis and polar distribution of PIN auxin transporters in *Arabidopsis*. Plant Cell **23**, 1920–1931.

Kleine-Vehn, J., Dhonukshe, P., Sauer, M., Brewer, P. B., Wiśniewska, J., Paciorek, T., Benková, E. & Friml, J. (2008a). ARF GEF-dependent transcytosis and polar delivery of PIN auxin carriers in *Arabidopsis*. Current Biology **18**, 526–531.

Kleine-Vehn, J., Ding, Z., Jones, A. R., Tasaka, M., Morita, M. T. & Friml, J. (2010). Gravity-induced PIN transcytosis for polarization of auxin fluxes in gravity-sensing root cells. Proceedings of the National Academy of Sciences of the United States of America **107**, 22344–22349.

Kleine-Vehn, J., Huang, F., Naramoto, S., Zhang, J., Michniewicz, M., Offringa, R. & Friml, J. (2009). PIN auxin efflux carrier polarity is regulated by PINOID kinase-mediated recruitment into GNOM-independent trafficking in *Arabidopsis*. Plant Cell **21**, 3839–3849.

Kleine-Vehn, J., Leitner, J., Zwiewka, M., Sauer, M., Abas, L., Luschnig, C. & Friml, J. (2008b). Differential degradation of PIN2 auxin efflux carrier by retromer-dependent vacuolar targeting. Proceedings of the National Academy of Sciences of the United States of America **105**, 17812–17817.

Kleine-Vehn, J., Wabnik, K., Martinière, A., Łangowski, Ł., Willig, K., Naramoto, S., Leitner, J., Tanaka, H., Jakobs, S., Robert, S., Luschnig, C., Govaerts, W., W Hell, S., Runions, J. & Friml, J. (2011). Recycling, clustering, and endocytosis jointly maintain PIN auxin carrier polarity at the plasma membrane. Molecular Systems Biology **7**, 540.

Kögl, F. & Haagen-Smit, A. J. (1931). Über die chemie des wuchsstoffs. Koninklijke Akademie van Wetenschappen Amsterdam Proceedings of the Section of Sciences **34**, 1411–1416.

Korbei, B. & Luschnig, C. (2013). Plasma membrane protein ubiquitylation and degradation as determinants of positional growth in plants. Journal of Integrative Plant Biology **55**, 809–823.

Kubeš, M., Yang, H., Richter, G. L., Cheng, Y., Młodzińska, E., Wang, X., Blakeslee, J. J., Carraro, N., Petrášek, J., Zažímalová, E., Hoyerová, K., Peer, W. A. & Murphy, A. S. (2012). The Arabidopsis concentration-dependent influx/efflux transporter ABCB4 regulates cellular auxin levels in the root epidermis. The Plant Journal **69**, 640–654.

Křeček, P., Skůpa, P., Libus, J., Naramoto, S., Tejos, R., Friml, J. & Zažímalová, E. (2009). The PIN-FORMED (PIN) protein family of auxin transporters. Genome Biology **10**, 249.

Laxmi, A., Pan, J., Morsy, M. & Chen, R. (2008). Light plays an essential role in intracellular distribution of auxin efflux carrier PIN2 in *Arabidopsis thaliana*. PLoS ONE **3**, e1510.

Leitner, J., Petrášek, J., Tomanov, K., Retzer, K., Pařezová, M., Korbei, B., Bachmair, A., Zažímalová, E. & Luschnig, C. (2012). Lysine63-linked ubiquitylation of PIN2 auxin carrier protein governs hormonally controlled adaptation of Arabidopsis root growth. Proceedings of the National Academy of Sciences of the United States of America **109**, 8322–8327.

Li, H., Lin, D., Dhonukshe, P., Nagawa, S., Chen, D., Friml, J., Scheres, B., Guo, H. & Yang, Z. (2011). Phosphorylation switch modulates the interdigitated pattern of PIN1 localization and cell expansion in *Arabidopsis* leaf epidermis. Cell Research **21**, 970–978.

Lin, D., Nagawa, S., Chen, J., Cao, L., Chen, X., Xu, T., Li, H., Dhonukshe, P., Yamamuro, C., Friml, J., Scheres, B., Fu, Y. & Yang, Z. (2012). A ROP GTPase-dependent auxin signaling pathway regulates the subcellular distribution of PIN2 in *Arabidopsis* roots. Current Biology **22**, 1319–1325.

Liscum, E. & Reed, J. W. (2002). Genetics of Aux/IAA and ARF action in plant growth and development. Plant Molecular Biology **49**, 387–400.

Löfke, C., Zwiewka, M., Heilmann, I., Van Montagu, M. C. E., Teichmann, T. & Friml, J. (2013). Asymmetric gibberellin signaling regulates vacuolar trafficking of PIN auxin transporters during root gravitropism. Proceedings of the National Academy of Sciences of the United States of America **110**, 3627–3632.

Luschnig, C., Gaxiola, R. A., Grisafi, P. & Fink, G. R. (1998). EIR1, a root-specific protein involved in auxin transport, is required for gravitropism in *Arabidopsis thaliana*. Genes & Development **12**, 2175–2187.

Marhavý, P., Bielach, A., Abas, L., Abuzeineh, A., Duclercq, J., Tanaka, H., Pařezová, M., Petrášek, J., Friml, J., Kleine-Vehn, J. & Benková, E. (2011). Cytokinin modulates endocytic trafficking of PIN1 auxin efflux carrier to control plant organogenesis. Developmental Cell **21**, 796–804.

Matusova, R., Rani, K., Verstappen, F. W. A., Franssen, M. C. R., Beale, M. H. & Bouwmeester, H. J. (2005). The strigolactone germination stimulants of the plant-parasitic *Striga* and *Orobanche* spp. are derived from the carotenoid pathway. Plant Physiology **139**, 920–934.

Michniewicz, M., Zago, M. K., Abas, L., Weijers, D., Schweighofer, A., Meskiene, I., Heisler, M. G., Ohno, C., Zhang, J., Huang, F., Schwab, R., Weigel, D., Meyerowitz, E. M., Luschnig, C., Offringa, R. & Friml, J. (2007). Antagonistic regulation of PIN phosphorylation by PP2A and PINOID directs auxin flux. Cell **130**, 1044–1056.

Mravec, J., Kubeš, M., Bielach, A., Gaykova, V., Petrášek, J., Skůpa, P., Chand, S., Benková, E., Zažímalová, E. & Friml, J. (2008). Interaction of PIN and PGP transport mechanisms in auxin distribution-dependent development. Development **135**, 3345–3354.

Mravec, J., Skůpa, P., Bailly, A., Hoyerová, K., Křeček, P., Bielach, A., Petrášek, J., Zhang, J., Gaykova, V., Stierhof, Y.-D., Dobrev, P. I., Schwarzerova, K., Rolčík, J., Seifertova, D., Luschnig, C., Benková, E., Zažímalová, E., Geisler, M. & Friml, J. (2009). Subcellular homeostasis of phytohormone auxin

is mediated by the ER-localized PIN5 transporter. Nature **459**, 1136–1140.

Müller, A., Guan, C., Gälweiler, L., Tänzler, P., Huijser, P., Marchant, A., Parry, G., Bennett, M., Wisman, E. & Palme, K. (1998). *AtPIN2* defines a locus of *Arabidopsis* for root gravitropism control. EMBO Journal **17**, 6903–6911.

Nagawa, S., Xu, T., Lin, D., Dhonukshe, P., Zhang, X., Friml, J., Scheres, B., Fu, Y. & Yang, Z. (2012). ROP GTPase-dependent actin microfilaments promote PIN1 polarization by localized inhibition of clathrin-dependent endocytosis. PLoS Biology **10**, e1001299.

Nodzyński, T., Feraru, M. I., Hirsch, S., De Rycke, R., Niculaes, C., Boerjan, W., Van Leene, J., De Jaeger, G., Vanneste, S. & Friml, J. (2013). Retromer subunits VPS35A and VPS29 mediate prevacuolar compartment (PVC) function in *Arabidopsis*. Molecular Plant **6**, 1849–1862.

Noh, B., Murphy, A. S. & Spalding, E. P. (2001). *multidrug resistance*–like genes of arabidopsis required for auxin transport and auxin-mediated development. Plant Cell **13**, 2441–2454.

Offringa, R. & Huang, F. (2013). Phosphorylation-dependent trafficking of plasma membrane proteins in animal and plant cells. Journal of Integrative Plant Biology **55**, 789–808.

Okushima, Y., Overvoorde, P. J., Arima, K., Alonso, J. M., Chan, A., Chang, C., Ecker, J. R., Hughes, B., Lui, A., Nguyen, D., Onodera, C., Quach, H., Smith, A., Yu, G. & Theologis, A. (2005). Functional genomic analysis of the *AUXIN RESPONSE FACTOR* gene family members in *Arabidopsis thaliana*: unique and overlapping functions of *ARF7* and *ARF19*. Plant Cell **17**, 444–463.

Paciorek, T., Zažímalová, E., Ruthardt, N., Petrášek, J., Stierhof, Y.-D., Kleine-Vehn, J., Morris, D. A., Emans, N., Jürgens, G., Geldner, N. & Friml, J. (2005). Auxin inhibits endocytosis and promotes its own efflux from cells. Nature **435**, 1251–1256.

Perrot-Rechenmann, C. (2010). Cellular responses to auxin: division versus expansion. Cold Spring Harbor Perspectives in Biology **2**, a001446.

Petrášek, J., Mravec, J., Bouchard, R., Blakeslee, J. J., Abas, M., Seifertová, D., Wiśniewska, J., Tadele, Z., Kubeš, M., Čovanová, M., Dhonukshe, P., Skůpa, P., Benková, E., Perry, L., Křeček, P., Lee, O. R., Fink, G. R., Geisler, M., Murphy, A. S., Luschnig, C., Zažímalová, E. & Friml, J. (2006). PIN proteins perform a rate-limiting function in cellular auxin efflux. Science **312**, 914–918.

Pinon, V., Prasad, K., Grigg, S. P., Sanchez-Perez, G. F. & Scheres, B. (2013). Local auxin biosynthesis regulation by PLETHORA transcription factors controls phyllotaxis in Arabidopsis. Proceedings of the National Academy of Sciences of the United States of America **110**, 1107–1112.

Prasad, K., Grigg, S. P., Barkoulas, M., Yadav, R. K., Sanchez-Perez, G. F., Pinon, V., Blilou, I., Hofhuis, H., Dhonukshe, P., Galinha, C., Mähönen, A. P., Muller, W. H., Raman, S., Verkleij, A. J., Snel, B., Reddy, G. V., Tsiantis, M. & Scheres, B. (2011). *Arabidopsis* plethora transcription factors control phyllotaxis. Current Biology **21**, 1123–1128.

Raven, J. A. (1975). Transport of indoleacetic acid in plant cells in relation to pH and electrical potential gradients, and its significance for polar IAA transport. New Phytologist **74**, 163–172.

Ray, P. M. (1977). Auxin-binding sites of Maize coleoptiles are localized on membranes of the endoplasmic reticulum. Plant Physiology **59**, 594–599.

Remington, D. L., Vision, T. J., Guilfoyle, T. J. & Reed, J. W. (2004). Contrasting modes of diversification in the *Aux/IAA* and *ARF* gene families. Plant Physiology **135**, 1738–1752.

Rigas, S., Ditengou, F. A., Ljung, K., Daras, G., Tietz, O., Palme, K. & Hatzopoulos, P. (2013). Root gravitropism and root hair development constitute coupled developmental responses regulated

by auxin homeostasis in the *Arabidopsis* root apex. New Phytologist **197**, 1130–1141.

Rigó, G., Ayaydin, F., Tietz, O., Zsigmond, L., Kovács, H., Páy, A., Salchert, K., Darula, Z., Medzihradszky, K. F., Szabados, L., Palme, K., Koncz, C. & Cséplő, Á. (2013). Inactivation of plasma membrane–localized CDPK-RELATED KINASE5 decelerates PIN2 exocytosis and root gravitropic response in *Arabidopsis*. Plant Cell **25**, 1592–1608.

Robert, S., Kleine-Vehn, J., Barbez, E., Sauer, M., Paciorek, T., Baster, P., Vanneste, S., Zhang, J., Simon, S., Čovanová, M., Hayashi, K., Dhonukshe, P., Yang, Z., Bednarek, S. Y., Jones, A. M., Luschnig, C., Aniento, F., Zažímalová, E. & Friml, J. (2010). ABP1 mediates auxin inhibition of clathrin-dependent endocytosis in *Arabidopsis*. Cell **143**, 111–121.

Rubery, P. H. & Sheldrake, A. R. (1974). Carrier-mediated auxin transport. Planta **118**, 101–121.

Rück, A., Palme, K., Venis, M. A., Napier, R. M. & Felle, H. H. (1993). Patch-clamp analysis establishes a role for an auxin binding protein in the auxin stimulation of plasma membrane current in *Zea mays* protoplasts. The Plant Journal **4**, 41–46.

Ruegger, M., Dewey, E., Gray, W. M., Hobbie, L., Turner, J. & Estelle, M. (1998). The TIR1 protein of *Arabidopsis* functions in auxin response and is related to human SKP2 and yeast Grr1p. Genes & Development **12**, 198–207.

Ruiz Rosquete, M., Barbez, E. & Kleine-Vehn, J. (2012). Cellular auxin homeostasis: gatekeeping is housekeeping. Molecular Plant **5**, 772–786.

Ruyter-Spira, C., Kohlen, W., Charnikhova, T., van Zeijl, A., van Bezouwen, L., de Ruijter, N., Cardoso, C., Lopez-Raez, J. A., Matusova, R., Bours, R., Verstappen, F. & Bouwmeester, H. (2011). Physiological effects of the synthetic strigolactone analog GR24 on root system architecture in Arabidopsis: another belowground role for strigolactones? Plant Physiology **155**, 721–734.

Růžička, K., Ljung, K., Vanneste, S., Podhorská, R., Beeckman, T., Friml, J. & Benková, E. (2007). Ethylene regulates root growth through effects on auxin biosynthesis and transport-dependent auxin distribution. Plant Cell **19**, 2197–2212.

Růžička, K., Šimášková, M., Duclercq, J., Petrášek, J., Zažímalová, E., Simon, S., Friml, J., Van Montagu, M. C. E. & Benková, E. (2009). Cytokinin regulates root meristem activity via modulation of the polar auxin transport. Proceedings of the National Academy of Sciences of the United States of America **106**, 4284–4289.

Santner, A. A. & Watson, J. C. (2006). The WAG1 and WAG2 protein kinases negatively regulate root waving in Arabidopsis. Plant Journal **45**, 752–764.

Sassi, M., Lu, Y., Zhang, Y., Wang, J., Dhonukshe, P., Blilou, I., Dai, M., Li, J., Gong, X., Jaillais, Y., Yu, X., Traas, J., Ruberti, I., Wang, H., Scheres, B., Vernoux, T. & Xu, J. (2012). COP1 mediates the coordination of root and shoot growth by light through modulation of PIN1- and PIN2-dependent auxin transport in *Arabidopsis*. Development **139**, 3402–3412.

Sauer, M., Balla, J., Luschnig, C., Wiśniewska, J., Reinöhl, V., Friml, J. & Benková, E. (2006). Canalization of auxin flow by Aux/IAA-ARF-dependent feedback regulation of PIN polarity. Genes & Development **20**, 2902–2911.

Sawchuk, M. G., Edgar, A. & Scarpella, E. (2013). Patterning of leaf vein networks by convergent auxin transport pathways. PLoS Genetics **9**, e1003294.

Scarpella, E., Marcos, D., Friml, J. & Berleth, T. (2006). Control of leaf vascular patterning by polar auxin transport. Genes & Development **20**, 1015–1027.

Setty, S. R. G., Tenza, D., Truschel, S. T., Chou, E., Sviderskaya, E. V., Theos, A. C., Lamoreux, M. L., Di Pietro, S. M., Starcevic, M., Bennett, D. C., Dell'Angelica, E. C., Raposo, G. & Marks, M. S. (2007). BLOC-1 is required for cargo-specific sorting from vacuolar early endosomes toward lysosome-related organelles. Molecular Biology of the Cell **18**, 768–780.

Shinohara, N., Taylor, C. & Leyser, O. (2013). Strigolactone can promote or inhibit shoot branching by triggering rapid depletion of the auxin efflux protein PIN1 from the plasma membrane. PLoS Biology **11**, e1001474.

Sorefan, K., Girin, T., Liljegren, S. J., Ljung, K., Robles, P., Galván-Ampudia, C. S., Offringa, R., Friml, J., Yanofsky, M. F. & Ostergaard, L. (2009). A regulated auxin minimum is required for seed dispersal in *Arabidopsis*. Nature **459**, 583–586.

Spitzer, C., Reyes, F. C., Buono, R., Sliwinski, M. K., Haas, T. J. & Otegui, M. S. (2009). The ESCRT-related CHMP1A and B proteins mediate multivesicular body sorting of auxin carriers in *Arabidopsis* and are required for plant development. Plant Cell **21**, 749–766.

Steffens, B., Feckler, C., Palme, K., Christian, M., Böttger, M. & Lüthen, H. (2001). The auxin signal for protoplast swelling is perceived by extracellular ABP1. Plant Journal **27**, 591–599.

Swarup, R. & Péret, B. (2012). AUX/LAX family of auxin influx carriers-an overview. Frontiers in Plant Science **3**, 225.

Szemenyei, H., Hannon, M. & Long, J. A. (2008). TOPLESS mediates auxin-dependent transcriptional repression during *Arabidopsis* embryogenesis. Science **319**, 1384–1386.

Tamura, K., Shimada, T., Ono, E., Tanaka, Y., Nagatani, A., Higashi, S.-i., Watanabe, M., Nishimura, M. & Hara-Nishimura, I. (2003). Why green fluorescent fusion proteins have not been observed in the vacuoles of higher plants. Plant Journal **35**, 545–555.

Tan, X., Calderon-Villalobos, L. I. A., Sharon, M., Zheng, C., Robinson, C. V., Estelle, M. & Zheng, N. (2007). Mechanism of auxin perception by the TIR1 ubiquitin ligase. Nature **446**, 640–645.

Tanaka, H., Dhonukshe, P., Brewer, P. B. & Friml, J. (2006). Spatiotemporal asymmetric auxin distribution: a means to coordinate plant development. Cellular and Molecular Life Sciences **63**, 2738–2754.

Tian, H., Klämbt, D. & Jones, A. M. (1995). Auxin-binding protein 1 does not bind auxin within the endoplasmic reticulum despite this

being the predominant subcellular location for this hormone receptor. Journal of Biological Chemistry **270**, 26962–26969.

Titapiwatanakun, B., Blakeslee, J. J., Bandyopadhyay, A., Yang, H., Mravec, J., Sauer, M., Cheng, Y., Adamec, J., Nagashima, A., Geisler, M., Sakai, T., Friml, J., Peer, W. A. & Murphy, A. S. (2009). ABCB19/PGP19 stabilises PIN1 in membrane microdomains in Arabidopsis. Plant Journal **57**, 27–44.

Tiwari, S. B., Hagen, G. & Guilfoyle, T. (2003). The roles of Auxin Response Factor domains in auxin-responsive transcription. Plant Cell **15**, 533–543.

Tiwari, S. B., Hagen, G. & Guilfoyle, T. J. (2004). Aux/IAA Proteins contain a potent transcriptional repression domain. Plant Cell **16**, 533–543.

Ulmasov, T., Hagen, G. & Guilfoyle, T. J. (1997). ARF1, a transcription factor that binds to auxin response elements. Science **276**, 1865–1868.

Ulmasov, T., Hagen, G. & Guilfoyle, T. J. (1999a). Activation and repression of transcription by auxin-response factors. Proceedings of the National Academy of Sciences of the United States of America **96**, 5844–5849.

Ulmasov, T., Hagen, G. & Guilfoyle, T. J. (1999b). Dimerization and DNA binding of auxin response factors. Plant Journal **19**, 309–319.

Ulmasov, T., Liu, Z. B., Hagen, G. & Guilfoyle, T. J. (1995). Composite structure of auxin response elements. Plant Cell **7**, 1611–1623.

Umehara, M., Hanada, A., Yoshida, S., Akiyama, K., Arite, T., Takeda-Kamiya, N., Magome, H., Kamiya, Y., Shirasu, K., Yoneyama, K., Kyozuka, J. & Yamaguchi, S. (2008). Inhibition of shoot branching by new terpenoid plant hormones. Nature **455**, 195–200.

van Berkel, K., de Boer, R. J., Scheres, B. & ten Tusscher, K. (2013). Polar auxin transport: models and mechanisms. Development **140**, 2253–2268.

Vanstraelen, M. & Benková, E. (2012). Hormonal interactions in the regulation of plant development. Annual Review of Cell and Developmental Biology **28**, 463–487.

Vernoux, T., Besnard, F. & Traas, J. (2010). Auxin at the shoot apical meristem. Cold Spring Harbor Perspectives in Biology **2**, a001487.

Viaene, T., Delwiche, C. F., Rensing, S. A. & Friml, J. (2013). Origin and evolution of PIN auxin transporters in the green lineage. Trends in Plant Science **18**, 5–10.

Vieten, A., Vanneste, S., Wiśniewska, J., Benková, E., Benjamins, R., Beeckman, T., Luschnig, C. & Friml, J. (2005). Functional redundancy of PIN proteins is accompanied by auxin-dependent cross-regulation of PIN expression. Development **132**, 4521–4531.

Wabnik, K., Kleine-Vehn, J., Govaerts, W. & Friml, J. (2011). Prototype cell-to-cell auxin transport mechanism by intracellular auxin compartmentalization. Trends in Plant Science **16**, 468–475.

Wang, C., Yan, X., Chen, Q., Jiang, N., Fu, W., Ma, B., Liu, J., Li, C., Bednarek, S. Y. & Pan, J. (2013). Clathrin light chains regulate clathrin-mediated trafficking, auxin signaling, and development in *Arabidopsis*. Plant Cell **25**, 499–516.

Went, F. W. (1926). On growth-accelerating substances in the coleoptile of Avena sativa. Proceedings of the Koninklijke Akademie van Wetenschappen **30**, 10–19.

Wenzel, C. L., Schuetz, M., Yu, Q. & Mattsson, J. (2007). Dynamics of *MONOPTEROS* and PIN-FORMED1 expression during leaf vein pattern formation in *Arabidopsis thaliana*. Plant Journal **49**, 387–398.

Whitford, R., Fernandez, A., Tejos, R., Pérez, A. C., Kleine-Vehn, J., Vanneste, S., Drozdzecki, A., Leitner, J., Abas, L., Aerts, M., Hoogewijs, K., Baster, P., De Groodt, R., Lin, Y.-C., Storme, V., Van de Peer, Y., Beeckman, T., Madder, A., Devreese, B., Luschnig, C., Friml, J. & Hilson,

P. (2012). GOLVEN secretory peptides regulate auxin carrier turnover during plant gravitropic responses. Developmental Cell **22**, 678–685.

Willige, B. C., Isono, E., Richter, R., Zourelidou, M. & Schwechheimer, C. (2011). Gibberellin regulates PIN-FORMED abundance and is required for Auxin transport–dependent growth and development in *Arabidopsis thaliana*. Plant Cell **23**, 2184–2195.

Wiśniewska, J., Xu, J., Seifertová, D., Brewer, P. B., Růžička, K., Blilou, I., Rouquié, D., Benková, E., Scheres, B. & Friml, J. (2006). Polar PIN localization directs auxin flow in plants. Science **312**, 883.

Woodward, A. W. & Bartel, B. (2005). Auxin: regulation, action, and interaction. Annals of Botany **95**, 707–735.

Xu, J., Hofhuis, H., Heidstra, R., Sauer, M., Friml, J. & Scheres, B. (2006). A molecular framework for plant regeneration. Science **311**, 385–388.

Xu, T., Dai, N., Chen, J., Nagawa, S., Cao, M., Li, H., Zhou, Z., Chen, X., De Rycke, R., Rakusová, H., Wang, W., Jones, A. M., Friml, J., Patterson, S. E., Bleecker, A. B. & Yang, Z. (2014). Cell surface ABP1-TMK auxin-sensing complex activates ROP GTPase signaling. Science **343**, 1025–1028.

Xu, T., Wen, M., Nagawa, S., Fu, Y., Chen, J.-G., Wu, M.-J., Perrot-Rechenmann, C., Friml, J., Jones, A. M. & Yang, Z. (2010). Cell surface- and Rho GTPase-based auxin signaling controls cellular interdigitation in *Arabidopsis*. Cell **143**, 99–110.

Žádníková, P., Petrášek, J., Marhavý, P., Raz, V., Vandenbussche, F., Ding, Z., Schwarzerová, K., Morita, M. T., Tasaka, M., Hejátko, J., Van Der Straeten, D., Friml, J. & Benková, E. (2010). Role of PIN-mediated auxin efflux in apical hook development of *Arabidopsis thaliana*. Development **137**, 607–617.

Zažímalová, E., Křeček, P., Skůpa, P., Hoyerová, K. & Petrášek, J. (2007). Polar transport of the plant hormone auxin – the role of PIN-FORMED (PIN) proteins. Cellular and Molecular Life Sciences **64**, 1621–1637.

Zegzouti, H., Anthony, R. G., Jahchan, N., Bögre, L. & Christensen, S. K. (2006a). Phosphorylation and activation of PINOID by the phospholipid signaling kinase 3-phosphoinositide-dependent protein kinase 1 (PDK1) in arabidopsis. Proceedings of the National Academy of Sciences of the United States of America **103**, 6404–6409.

Zegzouti, H., Li, W., Lorenz, T. C., Xie, M., Payne, C. T., Smith, K., Glenny, S., Payne, G. S. & Christensen, S. K. (2006b). Structural and functional insights into the regulation of arabidopsis AGC VIIIa kinases. Journal of Biological Chemistry **281**, 35520–35530.

Zhang, J., Nodzyński, T., Pěnčík, A., Rolčík, J. & Friml, J. (2010). PIN phosphorylation is sufficient to mediate PIN polarity and direct auxin transport. Proceedings of the National Academy of Sciences of the United States of America **107**, 918–922.

Zheng, X., Miller, N. D., Lewis, D. R., Christians, M. J., Lee, K.-H., Muday, G. K., Spalding, E. P. & Vierstra, R. D. (2011). AUXIN UP-REGULATED F-BOX PROTEIN1 regulates the cross talk between auxin transport and cytokinin signaling during plant root growth. Plant Physiology **156**, 1878–1893.

Zourelidou, M., Müller, I., Willige, B. C., Nill, C., Jikumaru, Y., Li, H. & Schwechheimer, C. (2009). The polarly localized D6 PROTEIN KINASE is required for efficient auxin transport in *Arabidopsis thaliana*. Development **136**, 627–636.

TWO

AUXIN BINDING PROTEIN 1: A RED HERRING AFTER ALL?

Myckel E.J. Habets[1] and Remko Offringa[1]

[1] Institute of Biology Leiden / Leiden University, Sylviusweg 72, 2333 BE Leiden, The Netherlands

Published in Molecular Plant 8: 1131-1134, 2015,
doi:10.1016/j.molp.2015.04.010

The natural auxin indole-3-acetic acid is the first hormone identified in plants, and since it plays such a central role in plant growth and development, auxin has been the subject of intensive studies. A central question has been how the auxin signal is perceived by plant cells. The earliest experiments showed the presence of auxin binding particles at the plasma membrane (PM) and in the endoplasmic reticulum (ER) (Hertel *et al.*, 1972). Screens for PM-localized auxin binding activities have led to the photo-affinity labeling and purification of Auxin Binding Protein 1 (ABP1) from maize coleoptile cells (Löbler & Klämbt, 1985). Despite observations in different laboratories that ABP1 localized to the PM where it seemed to mediate rapid electrophysiological and cell physiological responses to auxin, the auxin community remained skeptical about the role of ABP1 as auxin receptor for a long time, in part because of its predominant localization in the ER (reviewed by Napier *et al.*, 2002). At some point, ABP1 was even jokingly referred to as a potential red herring in the search for the auxin receptor (Venis, 1995). However, after the first *Arabidopsis abp1-1* loss-of-function allele pointed to a key role for ABP1 in cell elongation and division, the auxin community has adopted this abundantly expressed 22-kDa protein as extracellular auxin receptor (reviewed by Napier *et al.*, 2002). Especially in recent years, the role of ABP1 in development has become more firmly established, in part as modulator of clathrin-mediated endocytosis and microtubule orientation through its action on the Rho of Plants (ROP) family of GTPases (Robert *et al.*, 2010; Chen *et al.*, 2012, 2014) but also as regulator of auxin-responsive gene expression (Tromas *et al.*, 2013). Recent evidence that auxin-bound ABP1 docks on the extracellular domain of the TRANSMEMBRANE KINASE1 (TMK1) finally linked its apoplastic localization to signaling by the PM-associated ROPs. TMK1 belongs to a small subfamily of four leucine-rich-repeat receptor-like kinases and the quadruple *tmk1234* loss-of-function mutant shows several auxin-related phenotypes (Dai *et al.*, 2013; Xu *et al.*, 2014). In addition, auxin-mediated activation of ROP2 and ROP6 and the down-stream effects on the actin and microtubule cytoskeleton, respectively, are largely abolished in this mutant (Xu *et al.*, 2014; Grones & Friml, 2015).

ARABIDOPSIS ABP1: A CENTRAL PLAYER IN DEVELOPMENT OR NOT?

The strong defects observed for the *Arabidopsis abp1-1 null* allele, which were seemingly confirmed by the later identified *abp1-1s* allele (Table 1), have considerably hampered ABP1 research. In the homozygous state, *abp1-1* causes arrest of cell division, thereby blocking embryogenesis at the globular stage (Chen *et al.*, 2001). In the heterozygous state, various weaker auxin-related defects have been reported, such as altered gravitropic and phototropic responses, changes in hypocotyl length, and changes in expression of early auxin-induced genes (Effendi *et al.*, 2011). The strong phenotype of the *abp1-1* allele has triggered the isolation of a weaker allele (*abp1-5*) with a point mutation in the auxin binding pocket, and the generation of knockdown lines by the inducible expression of either antisense *ABP1* RNA or antibodies directed against ABP1 (Table 1). In a recent publication, ABP1 mutant versions with amino acid substitutions in the auxin binding pocket were expressed in the *abp1-1* background (Effendi *et al.*, 2015). A central aspect of all these mutant lines is that they show a weak reduction in auxin sensitivity similar to heterozygous *abp1-1* mutant plants (Effendi *et al.*, 2011). Interestingly, overexpression of an ABP1 deletion version lacking the KDEL ER-retention signal also led to auxin-related phenotypes but frequently also to more severe phenotypes such as seedling lethality or sterile development (Robert *et al.*, 2010).

In an attempt to study the role of ABP1 in flower development, Gao *et al.* (2015) designed an elegant CRISPR-CAS-based strategy to obtain mutant lines that become homozygous for an *abp1 null* mutation at the onset of flower development. For this purpose, the *ABP1* gene-specific guide RNA was expressed under the constitutive *35S* promoter and the CAS9 endonuclease was expressed under the *APETALA 1* promoter. To their surprise, the authors did not obtain T1 plants with mutant phenotypes, and when they recovered a T2 plant homozygous for a 5 base pair (bp) deletion in the first exon (named *abp1-c1*), this plant also showed a wild-type appearance. Sequencing of RT-PCR-derived *ABP1* cDNA from this plant line confirmed that the 5 bp deletion is present in mRNA transcripts and causes a frame shift generating a premature stop codon. Western blot analysis using anti-ABP1 antibodies showed that the ABP1 protein is not detectably expressed and that *abp1-c1* is likely a *null* allele. To confirm their results, the authors obtained a T-DNA insertion line

from the *Arabidopsis* stock center. RT–PCR and Western blot analysis indicated that this mutant allele (*abp1-TD*) is also a *null* mutant with the same wild-type appearance as the *abp1-c1* allele. This led the authors to conclude that ABP1 is not required in plant development, at least not under the growth conditions tested.

HOW SHOULD THE AUXIN COMMUNITY DEAL WITH THESE CONFLICTING DATA SETS?

The article by Gao *et al.* (2015) presents the auxin community with a dilemma. Do we trust the data accumulated by many different laboratories during 40 years of ABP1 research or do we accept the rather convincing evidence presented by Gao *et al.* (2015) that *ABP1* is not important for plant development? There are several aspects that should be considered before drawing a final conclusion.

First, the analysis performed by Gao *et al.* (2015) makes it very likely that the new mutants represent *null* alleles but it does not fully exclude that the mutant alleles produce a low level of functional ABP1, undetectable on Western blot, but sufficient to obtain a wild-type phenotype. The 5 bp deletion in the *abp1-c1* allele is close to the first intron and a small part of the mutant transcripts could be rescued by alternative splicing, which has been shown to occur for the *ABP1* gene (Wang & Brendel, 2006), e.g. by using a possible cryptic splice acceptor site a few base pairs upstream of the mutation (AGGA). It would therefore be interesting to know if more T2 lines with larger deletions in the *ABP1* gene were rescued from the CRISPR-CAS approach. Moreover, the *abp1-TD* allele has an activation tag T-DNA, containing four tandem *35S* promoters on the right border (Robinson *et al.*, 2009), inserted close to the translation start of the *ABP1* gene. While RT–PCR and Western blot analysis exclude that ABP1 is detectably produced in this line, it is still possible that a truncated transcript is produced that leads to low-level expression of a functional ABP1 protein. For both new alleles, the mutation is located in the region coding for the signal peptide, which does not require strong conservation (Martoglio & Dobberstein, 1998; Napier *et al.*, 2002). Mutant ABP1 versions with a few amino acid deletions or substitutions in their signal peptide are therefore likely to be functional. We have to note here that this is an extremely unlikely scenario. However, if this scenario is true, this would still imply that the phenotypes observed for the *ABP1AS*

Table 1. *abp1* loss-of-function alleles and *ABP1* overexpression or inducible knockdown lines.

Allele	Type	Description	Phenotypes	Reference
abp1-c1	5 bp deletion	CRISPR/CAS generated 5 bp deletion 107 bp downstream from ATG	Wild-type	(Gao *et al.*, 2015)
abp1-TD1	T-DNA insert	T-DNA insert 27 bp downstream from ATG	Wild-type	(Gao *et al.*, 2015)
abp1-1	T-DNA insert	T-DNA insert 51 bp downstream from ATG	Embryo lethal	(Chen *et al.*, 2001)
abp1-s1	T-DNA insert	T-DNA insert in the 5' UTR of *BSM/RUG2*	Embryo lethal	(Tzafrir *et al.*, 2004)
abp1-5	Point mutation	TILLING selected point mutant: substitution in the auxin binding pocket	Pavement cell (PC) defects, auxin insensitive	(Xu *et al.*, 2010)
SS12S	Knockdown	Inducible antibody against tobacco ABP1	Cotyledon defects, growth delay/arrest, sterility	(Braun *et al.*, 2008; Tromas *et al.*, 2009)
SS12K	Knockdown	Inducible antibody against tobacco ABP1	Cotyledon defects, growth delay/arrest, sterility, reduced auxin sensitivity	(Braun *et al.*, 2008; Tromas *et al.*, 2009, 2013)
ABP1AS	Knockdown	Inducible *ABP1* antisense RNA	Cotyledon defects, growth delay/arrest, PC defects, auxin insensitivity	(Braun *et al.*, 2008; Tromas *et al.*, 2009; Xu *et al.*, 2010)
$ABP1^{\Delta KDEL}$*-GFP*	Overexpression	Overexpression of ABP1-GFP fusion lacking the KDEL domain	Reduced auxin sensitivity, seedling lethality, sterility	(Robert *et al.*, 2010)
XVE » ABP1 OE	Overexpression	Estradiol-inducible overexpression of ABP1-GFP	Enhanced auxin-induced microtubule re-orientation	(Chen *et al.*, 2014)
abp1-8	Overexpression	*abp1-1* overexpressing tagged ABP1 with substitution in auxin binding pocket	Reduced auxin sensitivity, PC defects	(Effendi *et al.*, 2015)

Table 1. (cont.) *abp1* loss-of-function alleles and *ABP1* overexpression or inducible knockdown lines.

Allele	Type	Description	Phenotypes	Reference
abp1-9	Overexpression	*abp1-1* overexpressing tagged ABP1 with substitution in auxin binding pocket	Reduced auxin sensitivity, PC defects, reduced auxin transport	(Effendi *et al.*, 2015)
abp1-10	Overexpression	*abp1-1* overexpressing tagged ABP1 with substitution in auxin binding pocket	Reduced auxin sensitivity, PC defects, reduced auxin transport	(Effendi *et al.*, 2015)
abp1-11	Overexpression	*abp1-1* overexpressing tagged ABP1	Near wild-type phenotypes, reduced auxin transport	(Effendi *et al.*, 2015)

antisense line (Braun *et al.*, 2008; Tromas *et al.*, 2009; Xu *et al.*, 2010) are not caused by the reduced, but still detectable, *ABP1* expression.
Second, it would be good to analyze the different *abp1* mutant alleles (including *abp1-5* and *abp1-1* and *abp1-1S*) by genome sequencing to know the exact nature of the mutations and to exclude the occurrence of gene duplications or second site mutations.
In the most likely situation that the *abp1-c1* and *abp1-TD* alleles are true *null* mutants, the strong phenotypes of the *abp1-1* and *abp1-1s* alleles could be explained by a second site mutation in another gene. In fact, the T-DNA insertion in the embryo lethal *abp1-1s* allele is located in the 5' untranslated region of the inversely oriented *BELAYA SMERT/RUGOSA2* (*BSM/RUG2*) gene located upstream of *ABP1* (Babiychuk *et al.*, 2011; Quesada *et al.*, 2011). Interestingly, the *bsm* mutant allele shows embryo arrest at the late globular stage (Babiychuk *et al.*, 2011) and the fact that the *BSM/RUG2* promoter region partly overlaps with the *ABP1* coding region suggests that the embryo lethality observed for *abp1-1* and *abp1-1s* might be caused by disruption of the *BSM/RUG2* promoter function, which for the *abp1-TD* allele might be overcome by the presence of the *35S* enhancer sequences on the activation tag T-DNA. In any case, it will be essential to reevaluate the *abp1-1* complementation experiments presented in previous publications (Chen *et al.*, 2001; Effendi *et al.*, 2015).
For the phenotypes observed in the *ABP1* antisense or antibody lines Gao *et al.* (2015) suggested that they could be caused by off target knockdown of other genes. It is important to note here that these off target genes could still encode redundantly acting, yet unidentified auxin receptors that may compensate for the loss of ABP1 in the *abp1-c* and *abp1-TD* alleles.

PERSPECTIVE

The publication by Gao *et al.* (2015) provides food for thought. Can plant life proceed without a PM-localized auxin receptor? If not ABP1, are there other (ABP1-related) auxin binding proteins at the PM that (by interacting with the TMKs) mediate the previously observed rapid cellular responses to auxin, such as elevated cytosolic calcium levels, changes in pH, or ROP-dependent changes in cytoskeleton localization or orientation (Napier *et al.*, 2002; Shishova & Lindberg, 2010; Monshausen *et al.*, 2011; Chen *et al.*, 2014; Xu *et al.*, 2014)? It is still too early to rewrite the text books, as one can be sure that several laboratories are

currently investigating whether ABP1 has been a red herring after all or not. It has been suggested to "re-examine previous data, down to the lab bench level" (Liu, 2015). In our opinion, the most important issue is to unequivocally determine which of the reported *abp1* alleles are true *nulls* and whether there are undetected off-site mutations or unexpected effects of the known mutations that explain the observed differences between the earlier "reference" alleles and the new *abp1* alleles that show wild-type phenotypes.

FUNDING

M.E.J.H. was supported by the Chemical Sciences Division of the Netherlands Organization for Scientific Research (NWO-CW TOP 700.58.301 to R.O.).

ACKNOWLEDGMENTS

We thank the reviewers for their useful suggestions. No conflict of interest declared.

Bibliography

Babiychuk, E., Vandepoele, K., Wissing, J., Garcia-Diaz, M., De Rycke, R., Akbari, H., Joubès, J., Beeckman, T., Jänsch, L., Frentzen, M., Van Montagu, M. C. E. & Kushnir, S. (2011). Plastid gene expression and plant development require a plastidic protein of the mitochondrial transcription termination factor family. Proceedings of the National Academy of Sciences of the United States of America **108**, 6674–6679.

Braun, N., Wyrzykowska, J., Muller, P., David, K., Couch, D., Perrot-Rechenmann, C. & Fleming, A. J. (2008). Conditional repression of AUXIN BINDING PROTEIN1 reveals that it coordinates cell division and cell expansion during postembryonic shoot development in *Arabidopsis* and tobacco. Plant Cell **20**, 2746–2762.

Chen, J.-G., Ullah, H., Young, J. C., Sussman, M. R. & Jones, A. M. (2001). ABP1 is required for organized cell elongation and division in *Arabidopsis* embryogenesis. Genes & Development **15**, 902–911.

Chen, X., Grandont, L., Li, H., Hauschild, R., Paque, S., Abuzeineh, A., Rakusova, H., Benkova, E., Perrot-Rechenmann, C. & Friml, J. (2014). Inhibition of cell expansion by rapid ABP1-mediated auxin effect on microtubules. Nature **516**, 90–93.

Chen, X., Naramoto, S., Robert, S., Tejos, R., Löfke, C., Lin, D., Yang, Z. & Friml, J. (2012). ABP1 and ROP6 GTPase signaling regulate clathrin-mediated endocytosis in *Arabidopsis* roots. Current Biology **22**, 1326–1332.

Dai, N., Wang, W., Patterson, S. E. & Bleecker, A. B. (2013). The TMK subfamily of receptor-like kinases in *Arabidopsis* display an essential role in growth and a reduced sensitivity to auxin. PLoS ONE **8**, e60990.

Effendi, Y., Ferro, N., Labusch, C., Geisler, M. & Scherer, G. F. E. (2015). Complementation of the embryo-lethal T-DNA insertion mutant of AUXIN-BINDING-PROTEIN 1 (ABP1) with *abp1* point mutated versions reveals crosstalk of ABP1 and phytochromes. Journal of Experimental Botany **66**, 403–418.

Effendi, Y., Rietz, S., Fischer, U. & Scherer, G. F. E. (2011). The heterozygous *abp1/ABP1* insertional mutant has defects in functions requiring polar auxin transport and in regulation of early auxin-regulated genes. Plant Journal **65**, 282–294.

Gao, Y., Zhang, Y., Zhang, D., Dai, X., Estelle, M. & Zhao, Y. (2015). Auxin binding protein 1 (ABP1) is not required for either auxin signaling or *Arabidopsis* development. Proceedings of the National Academy of Sciences of the United States of America **112**, 2275–2280.

Grones, P. & Friml, J. (2015). Auxin transporters and binding proteins at a glance. Journal of Cell Science **128**, 1–7.

Hertel, R., Thomson, K.-S. & Russo, V. E. A. (1972). *In-vitro* auxin binding to particulate cell fractions from corn coleoptiles. Planta **107**, 325–340.

Liu, C.-M. (2015). Auxin Binding Protein 1 (ABP1): a matter of fact. Journal of Integrative Plant Biology **57**, 234–235.

Löbler, M. & Klämbt, D. (1985). Auxin-binding protein from coleoptile membranes of corn (*Zea mays L.*). I. Purification by immunological methods and characterization. Journal of Biological Chemistry **260**, 9848–9853.

Martoglio, B. & Dobberstein, B. (1998). Signal sequences: more than just greasy peptides. Trends in Cell Biology **8**, 410–415.

Monshausen, G. B., Miller, N. D., Murphy, A. S. & Gilroy, S. (2011). Dynamics of auxin-dependent Ca2+ and pH signaling in root growth revealed by integrating high-resolution imaging with automated computer vision-based analysis. The Plant Journal **65**, 309–318.

Napier, R., David, K. & Perrot-Rechenmann, C. (2002). A short history of auxin-binding proteins. Plant Molecular Biology **49**, 339–348.

Quesada, V., Sarmiento-Mañús, R., González-Bayón, R., Hricová, A., Pérez-Marcos, R., Graciá-Martínez, E., Medina-Ruiz, L., Leyva-Díaz, E., Ponce, M. R. & Micol, J. L. (2011). *Arabidopsis* RUGOSA2 encodes an mTERF family member required for mitochondrion, chloroplast and leaf development. The Plant Journal **68**, 738–753.

Robert, S., Kleine-Vehn, J., Barbez, E., Sauer, M., Paciorek, T., Baster, P., Vanneste, S., Zhang, J., Simon, S., Čovanová, M., Hayashi, K., Dhonukshe, P., Yang, Z., Bednarek, S. Y., Jones, A. M., Luschnig, C., Aniento, F., Zažímalová, E. & Friml, J. (2010). ABP1 mediates auxin inhibition of clathrin-dependent endocytosis in *Arabidopsis*. Cell **143**, 111–121.

Robinson, S. J., Tang, L. H., Mooney, B. A. G., McKay, S. J., Clarke, W. E., Links, M. G., Karcz, S., Regan, S., Wu, Y.-Y., Gruber, M. Y., Cui, D., Yu, M. & Parkin, I. A. P. (2009). An archived activation tagged population of *Arabidopsis thaliana* to facilitate forward genetics approaches. BMC Plant Biology **9**, 101.

Shishova, M. & Lindberg, S. (2010). A new perspective on auxin perception. Journal of Plant Physiology **167**, 417–422.

Tromas, A., Braun, N., Muller, P., Khodus, T., Paponov, I. A., Palme, K., Ljung, K., Lee, J.-Y., Benfey, P., Murray, J. A. H., Scheres, B. & Perrot-Rechenmann, C. (2009). The AUXIN BINDING PROTEIN 1 is required for differential auxin responses mediating root growth. PLoS ONE **4**, e6648.

Tromas, A., Paque, S., Stierlé, V., Quettier, A.-L., Muller, P., Lechner, E., Genschik, P. & Perrot-Rechenmann, C. (2013). Auxin-Binding Protein 1 is a negative regulator of the $SCF^{TIR1/AFB}$ pathway. Nature Communications **4**, 2496.

Tzafrir, I., Pena-Muralla, R., Dickerman, A., Berg, M., Rogers, R., Hutchens, S., Sweeney, T. C., McElver, J., Aux, G., Patton, D. & Meinke, D. (2004). Identification of genes required for embryo development in *Arabidopsis*. Plant Physiology **135**, 1206–1220.

Venis, M. A. (1995). Auxin binding protein 1 is a red herring? Oh no it isn't! Journal of Experimental Botany **46**, 463–465.

Wang, B.-B. & Brendel, V. (2006). Genomewide comparative analysis of alternative splicing in plants. Proceedings of the National Academy of Sciences of the United States of America **103**, 7175–7180.

Xu, T., Dai, N., Chen, J., Nagawa, S., Cao, M., Li, H., Zhou, Z., Chen, X., De Rycke, R., Rakusová, H., Wang, W., Jones,

A. M., Friml, J., Patterson, S. E., Bleecker, A. B. & Yang, Z. (2014). Cell surface ABP1-TMK auxin-sensing complex activates ROP GTPase signaling. Science **343**, 1025–1028.

Xu, T., Wen, M., Nagawa, S., Fu, Y., Chen, J.-G., Wu, M.-J., Perrot-Rechenmann, C., Friml, J., Jones, A. M. & Yang, Z. (2010). Cell surface- and Rho GTPase-based auxin signaling controls cellular interdigitation in *Arabidopsis*. Cell **143**, 99–110.

THREE

DYNAMIC PDK1-MEDIATED ACTIVATION OF PINOID IS IMPORTANT DURING *ARABIDOPSIS THALIANA* EMBRYO AND INFLORESCENCE DEVELOPMENT.

Myckel E.J. Habets[1,4], Carlos S. Galván-Ampudia[2,4], Christa Testerink[3] and Remko Offringa[1]

[1] Institute of Biology Leiden / Leiden University, Sylviusweg 72, 2333BE Leiden, The Netherlands
[2] Laboratoire Reproduction et Développement des Plantes, Ecole Normale Supérieure de Lyon, 46, allée d'Italie, 69364 LYON cedex 07, France
[3] Laboratory of Plant Physiology / Wageningen University and Research, Droevendaalsesteeg 1, 6708PB Wageningen, The Netherlands
[4] These authors contributed equally.

Summary

The arabidopsis PINOID AGC protein serine/threonine kinase (PID) is a key determinant in the polar distribution of PIN auxin efflux carriers at the plasma membrane. It determines the direction of polar auxin transport, and thus the position where auxin maxima and minima instructive for plant development are generated. PID co-localizes with long PIN proteins at the plasma membrane (PM), and phosphorylates serines in three conserved TPRXS motifs in the large hydrophilic loop of these long PINs. How exactly this phosphorylation affects the polar subcellular localization of PIN proteins and which factors act upstream of PID to regulate its localization and activity is still largely unexplored. One of the identified upstream regulators of PID, the 3-phosphoinositide-dependent protein kinase 1 (PDK1), was shown to enhance its kinase activity by phosphorylating the activation loop of PID *in vitro*. Here we show in arabidopsis protoplasts that PDK1 phosphorylation induces a switch in PID subcellular localization from the plasma membrane to endomembrane compartments and the microtubule cytoskeleton. Removal of the PDK1 phosphorylation sites prevented PID microtubule recruitment, and a phospho-mimic PID version localized to the microtubules in the absence of PDK1. PID promoter controlled expression of wild-type, loss-of-phosphorylation or phospho-mimic versions of PID in the *pid wag1 wag2* triple loss-of-function mutant background showed that PDK1-mediated enhancement of PID activity is essential during embryo and inflorescence development. Although comparison of the subcellular localization of wild-type and mutant PID versions in root epidermis cells did not corroborate a role for PDK1 in relocalizing PID to endomembranes and microtubules, our results do reveal a new role for PDK1 in plant development.

Introduction

During the initial phase of development, the basic body plan of a plant is laid down in the embryo, comprising a shoot apical meristem (SAM), one or more embryonic leaves or cotyledons, a hypocotyl and an embryonic root. Following germination of the seedling, new organs and tissues develop from the SAM and the embryonic root, and the final adult shape of a plant is determined by the impact of both internal and environmental cues on this post-embryonic development. The plant

hormone auxin plays an important role in both the establishment of the basic body plan during embryogenesis and in directing the formation and growth of new organs during post-embryonic development. Auxin steers these developmental processes through instructive maxima and minima that are generated by polar cell-to-cell transport of this signaling molecule (Tanaka *et al.*, 2006; Sorefan *et al.*, 2009; Benková *et al.*, 2003; Reinhardt *et al.*, 2000). The rate-limiting drivers of polar auxin transport (PAT) are the PIN-FORMED (PIN) auxin efflux carriers (Wiśniewska *et al.*, 2006). The *Arabidopsis thaliana* (arabidopsis) genome encodes a family of 8 PIN proteins that can be subdivided into 5 "long" PIN proteins, which are characterized by two sets of five transmembrane domains interrupted by a large hydrophilic loop and localize to the plasmamembrane (PM), and 3 "short" PIN proteins that have a shorter or non-existing hydrophilic loop and localize to the endoplasmic reticulum (Mravec *et al.*, 2009).
The long PINs direct PAT through their polar localization at the PM (Petrášek *et al.*, 2006). Initially, the biosynthetic secretion of PIN proteins to the PM was thought to be apolar, after which polar localization was established by clathrin-mediated endocytosis and recycling to the PM (Dhonukshe *et al.*, 2008; Kitakura *et al.*, 2011; Dhonukshe *et al.*, 2007). However, recent data suggest that the ARF-GEFs GNOM and GNOM-LIKE mediate basal (rootward) polar secretion of PIN1 in root stele cells (Doyle *et al.*, 2015). Long term treatment with the fungal toxin brefeldin A (BFA) that inhibits GNOM results in a basal to apical (shootward) shift of PIN polarity, indicating that GNOM specifically acts in the basal targeting of PINs (Geldner *et al.*, 2001, 2003; Kleine-Vehn *et al.*, 2009). Moreover, the plasma membrane (PM) associated AGC-type protein serine/threonine kinases PINOID (PID), WAG1 and WAG2 were found to induce the same switch in PIN polarity by phosphorylating serines in conserved TPRXSN motifs in the hydrophilic loop of long PINs (Friml *et al.*, 2004; Huang *et al.*, 2010; Dhonukshe *et al.*, 2010). They were found to act antagonistic to PP2A/PP6 phosphatases in triggering GNOM-independent PIN recycling, thereby directing PAT to allow proper cotyledon development during embryogenesis, organ development in the shoot apical meristem and inflorescence, and directional plant growth in response to abiotic signals (Kleine-Vehn *et al.*, 2009; Huang *et al.*, 2010; Dhonukshe *et al.*, 2010; Michniewicz *et al.*, 2007; Ding *et al.*, 2011). As PIN polarity determinants, PID, WAG1 and WAG2 are excellent targets for developmental or environmental cues to establish these changes in

polarity. This would be established most likely through the action of upstream regulators. One of the known upstream regulators of PID is the 3-phosphoinositide-dependent protein kinase 1 (PDK1; Zegzouti *et al.*, 2006a). PDK1 was initially identified in mammalian cells as activator of Protein Kinase B (Alessi *et al.*, 1997), but has also been found to be conserved in other eukaryotes, including lower and higher plants (Devarenne *et al.*, 2006; Dittrich & Devarenne, 2012; Matsui *et al.*, 2010; Deak *et al.*, 1999). In animals, PDK1 seems to be essential, because *pdk1* knock out mice are embryo lethal (Lawlor *et al.*, 2002), while in plants the effect of knocking out *PDK1* differs per species. Arabidopsis double T-DNA insertion mutants for both *PDK1* homologues only show mild growth defects, whereas virus-induced gene silencing (VIGS) of *PDK1* in tomato results in plant death (Devarenne *et al.*, 2006; Camehl *et al.*, 2011). *PDK1* knock down in rice results in dwarfism (Matsui *et al.*, 2010), whereas *Physcomitrella patens pdk1* loss-of-function mutants are impaired in growth and resistance to abiotic stresses (Dittrich & Devarenne, 2012). At least for arabidopsis the weak phenotypes might be explained by the fact that no proper T-DNA insertion alleles have been obtained in the coding region of the *PDK1.1* gene (Salk Institute Genomic Analysis Laboratory: `http://signal.salk.edu`), suggesting that such mutants might confer lethality. PDK1 contains a plekstrin homology (PH) domain that in animals allows it to bind PtdIns(3,4)P_2 and PtdIns(3,4,5)P_3 and to become recruited to the plasma membrane and activated *in vitro* (Alessi *et al.*, 1997). The PH domain of plant PDK1 associates with various phospholipids in cell membranes (Deak *et al.*, 1999), but PDK1 activation has only been confirmed for PtdIns(3,4,5)P_3, which is not present in plants, PA and PI(4,5)P_2 (Deak *et al.*, 1999; Anthony *et al.*, 2004). The primary targets of PDK1 are the AGC kinases, and for several arabidopsis AGC kinases phosphorylation by PDK1 has been reported (Zegzouti *et al.*, 2006b). One of these targets is OXI1, which also responds to reactive oxygen species and elicitors and activates Mitogen Activated Protein Kinases 3 and 6 (MAPK3 and 6), indicating a role for PDK1 in defense responses (Camehl *et al.*, 2011; Anthony *et al.*, 2004; Rentel *et al.*, 2004). PDK1 has also been found to phosphorylate S288 and S290 in the activation segment of PID, resulting in an enhancement of its kinase activity (Zegzouti *et al.*, 2006a). However, a role for this activation in plant growth and development has not yet been reported. Here we have analyzed the effect of PDK1 activation of PID on its function in plant

development. To our surprise, PDK1-mediated phosphorylation of PID in protoplasts led to its relocalization to the microtubule cytoskeleton (MT), an observation that we could not reproduce *in planta*. We could, however, show that PDK1-mediated activation of PID is essential for its function during embryo and inflorescence development, providing the first evidence for a non-stress related role of PDK1 in plants.

Results

PDK1 induces PID relocalization to the microtubule cytoskeleton in protoplasts.

To investigate the effect of PDK1-dependent PID phosphorylation at the cellular level, we expressed translational fusions of these proteins to respectively cyan and yellow fluorescent protein (CFP and YFP) in arabidopsis protoplasts. As previously reported, PID-YFP localized to the PM (Figure 1A, Benjamins *et al.*, 2001), whereas protoplasts expressing only PDK1-CFP showed labelling of the entire cytoplasm with particular accumulation at endomembrane-like structures (Figure 1B). Co-expression of PDK1-CFP and PID-YFP strikingly led to PID relocalization from the PM to endomembrane-like structures (Figure 1C). In a subpopulation of protoplasts, PID was found in filamentous cytoskeleton-like structures, while PDK1 subcellular localization was unchanged (Figure 1D). Co-expression of PID-CFP and PDK1-mRFP with the MT marker YFP-CLIP170$^{1\text{-}1240}$ (Dhonukshe & Gadella, 2003) corroborated that PID is recruited to the MT network, as we found clear co-localization of PID and CLIP170$^{1\text{-}1240}$ (Figure 1D). PDK1-mRFP retained its cytosolic localization with foci in endomembrane-like structures, and did show no or only partial co-localisation with PID at the MT (Figure 1D). No co-localization was observed when CLIP170$^{1\text{-}1240}$ and PID were co-expressed in the absence of PDK1 (Figure 1E), indicating that PID MT localization is dependent on PDK1. Our findings suggest that PDK1 acts as a switch to regulate PID subcellular translocation from the PM into endomembrane- and cytoskeleton-like structures in arabidopsis protoplasts.

The PID phosphorylation status causes its MT relocalization.

The PDK1 induced translocation of PID could be caused by two possible mechanisms. On the one hand, PDK1 has been suggested to

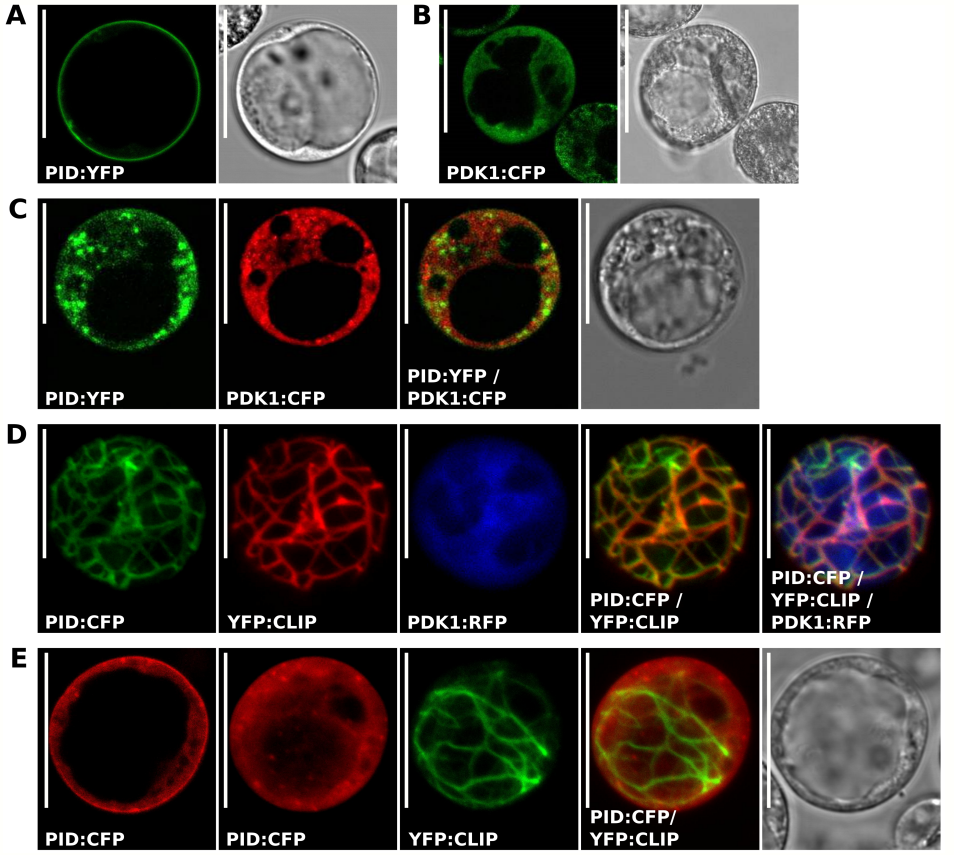

Figure 1: PDK1-dependent endomembrane and microtubule localization of PID in arabidopsis protoplasts.
(A) Arabidopsis protoplast transfected with *35S::PID-YFP*. Image of the YFP channel (left panel, green) and transmitted light channel (right panel) are shown.
(B) Arabidopsis protoplast transfected with *35S::PDK1-CFP*. Image of the CFP channel (left panel, green) and transmitted light channel (right panel) are shown.
(C) Arabidopsis protoplast co-transfected with *35S::PID-YFP* and *35S::PDK1-CFP*. Shown are from left to right images of the YFP channel (green), the CFP channel (red), a merge between the YFP and CFP channel, and the transmitted light image.
(D) Protoplast co-expressing PID-CFP, YFP-CLIP170$^{1\text{-}1240}$ and PDK1-mRFP1. Shown are from left to right confocal images of the CFP channel (green), YFP channel (red), RFP channel (blue), and a merge between the CFP and YFP channel, or between the CFP, YFP and RFP channel.
(E) Protoplast co-expressing PID-CFP and YFP-CLIP170$^{1\text{-}1240}$. Shown are from left to right confocal images of the median and top section (red) of the CFP channel, top section of the YFP channel (green), and a merge between the top sections of the CFP and YFP channel. Scale bar = 10µm.

bind to the PIF domain of PID (Zegzouti *et al.*, 2006a), and this

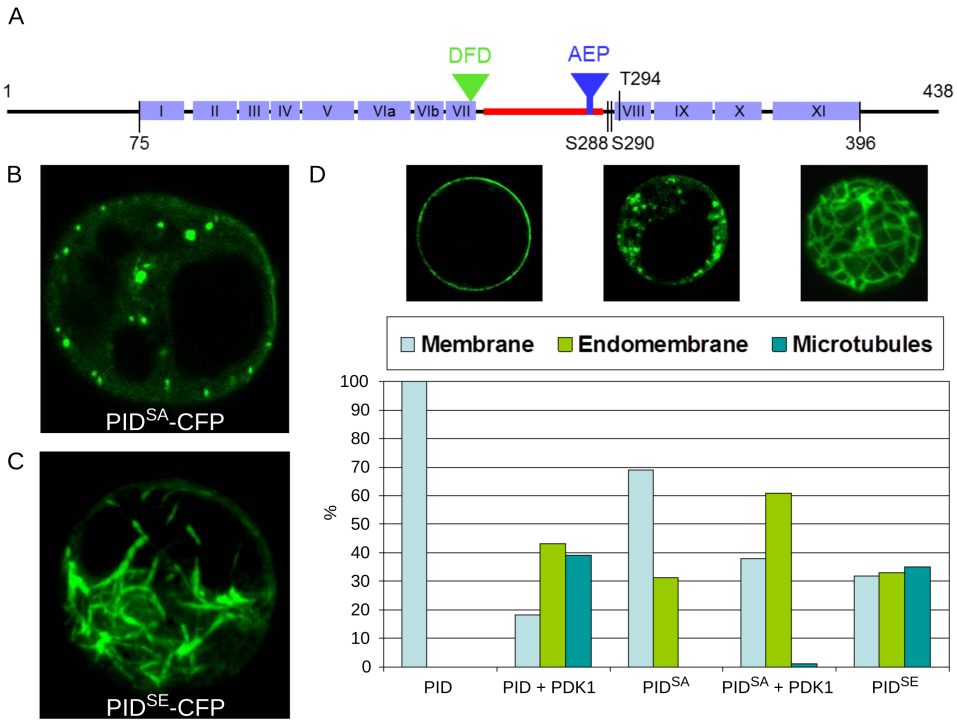

Figure 2: Subcellular localization of PID is dependent on its PDK1-dependent phosphorylation state.
(A) Schematic representation of the functional sub-domains in PID. The eleven conserved subdomains of the serine/threonine protein kinase domain (75-396 aa) are depicted with purple boxes. The insertion in the activation loop typical for the plant specific AGCVIII kinases is shown in red. The conserved Asp-Phe-Asp (DFD) and Ala-Glu-Pro (AEP) motif in the activation loop are depicted in green and blue, respectively. The positions of the PDK1 phosphorylation sites (S288, S290), and the auto-phosphorylation site (T294) in the activation loop of PID are indicated.
(B) Endomembrane internalization of the loss-of-phosphorylation PID^{S288,S290A}-CFP (PID^{SA}) version.
(C) PDK1-independent microtubule localization of the phosphomimic PID^{S288,S290E}-CFP (PID^{SE}) version.
(D) Quantitative analysis of PDK1-dependent PID translocation in arabidopsis protoplasts. Transfected protoplasts were counted and categorized according to the subcellular localization of PID-CFP: membrane localization (upper left panel), endomembrane localization (upper middle panel) or microtubule localization (upper right panel). Percentage of the transfected protoplasts with the indicated constructs (lower panel). Number of protoplasts scored per transfection: PID (n=83), PID+PDK1 (n=142), PID^{SA} (n=173), PID^{SA}+PDK1 (n=97) and PID^{SE} (n=40).

interaction itself could cause PID relocalization. On the other hand, PDK1 was reported to activate PID by phosphorylation at serine residues S288 and S290 (Zegzouti *et al.*, 2006a), and this modification could cause

its translocation. To be able to distinguish between those options, we constructed mutant versions of the PID-CFP fusion protein in which the two serines were either replaced by non-phosphorylatable alanines (PID^{SA}), or by phospho-mimicking glutamic acids (PID^{SE}) (Figure 2A). The wild-type and mutant PID-CFP versions were expressed either alone or together with PDK1-YFP. As observed in previous protoplast transfections (Figure 1), PID-CFP either localized at the plasma membrane, at endomembranes or at MT (Figure 2D), and mixed localization patterns in the same protoplast were not observed. This allowed to quantify the data by categorizing the localization for at least 40 individual protoplasts per transfection (Figure 2D). PID-CFP expressed alone only showed PM localization, and co-transfection with PDK1-YFP resulted in endomembrane and MT localization in 43% and 39% of the protoplasts, respectively (Figure 2D). In a similar way, the phosphomimic version PID^{SE}-CFP localized to either microtubules or endomembranes (33% and 35%, respectively), even in the absence of PDK1-YFP co-expression (Figure 2C), indicating that the PID phosphorylation status itself and not its interaction with PDK1 determined the subcellular localisation of PID. Interestingly, when the non-phosphorylatable PID^{SA}-CFP fusion protein was expressed alone, we only observed PM localization or internalization to endomembrane-like structures (31% of the expressing protoplasts, Figure 2B and D) and this percentage was enhanced up to 61% when PDK1 was cotransfected (χ^2-test, $p<0.05$, $n=97$, Figure 2D). These results show that phosphorylation of PID by PDK1 acts as a trigger not only to activate (Zegzouti *et al.*, 2006a), but also to translocate PID to different subcellular compartments. Phosphorylation of S288 and S290 seems to be essential for MT localization of PID, but is not required for the PDK1-induced PID localization at endomembrane structures. Possibly, the latter is mediated by the interaction between PDK1 and PID.

PDK1 activation of PID is required for inflorescence development.

To gain more insight into the biological significance of this phosphorylation and MT-relocalization of PID, we expressed the wild-type, loss-of-phosphorylation and gain-of-phosphorylation PID versions fused to 3xVENUS under control of the PID promoter in the *pid wag1 wag2* triple loss-of-function mutant background. The *pid wag1 wag2* triple mutant has a much stronger adult phenotype compared to the *pid* single mutant, in that all mutant embryos do not develop cotyledons (Dhonukshe *et al.*,

Table 1: Complementation analysis of the arabidopsis *pid wag1 wag2* triple mutant with wild-type and mutant versions of the *PID::PID-3xVENUS* construct.

Construct	Phenotypes T1 lines[a]			Genotypes T3 parent[b]		Phenotype frequency T4[c]	
	WT	*pid*-like	Total	*pid wag1 wag2*	construct	WT	*pid*-like
PID-3xVENUS	47	1	48	-/-	+/+	1.0	0.0
PID^{SA}-3xVENUS	33	13	46	-/-	+/-	0.0	1.0
PID^{SE}-3xVENUS	35	2	37	-/-	+/+	0.9	0.1

[a] Plants used for floral dipping were heterozygous for the pid-14 allele (*pid/+ wag1 wag2*), and therefore only 25% of the selected T1 plants were homozygous this allele. WT = wild-type phenotype; pid-like = as shown in figure 3A.
[b] Genotype as determined by PCR analysis for the *pid* allele, and by segregation for PPT15 resistance in T4 progeny for the construct.
[c] T4 plants obtained from the genotyped T3 parent. *PID^{SA}-3xVENUS* T4 plants used were genotyped and frequency reflects lines which were homozygous for the insert. n=69, 43 and 70 for *PID-3xVENUS*, *PID^{SA}-3xVENUS* and *PID^{SE}-3xVENUS*, respectively. WT = wild-type phenotype as shown in figure 3C or 3H; *pid*-like = as shown in figure 3F.

2010), and that the adult plant only develops a few curled darker leaves and a single short pin-formed inflorescence (Figure 3A).
The T1 generation showed that wild-type *PID::PID-3xVENUS* was able to fully complement the strong adult phenotype of the triple mutant. No pin-like inflorescences were observed (Table 1, Figure 3C,D).
To our surprise, most of the *PID::PID-3xVENUS* lines showed additional phenotypes, which in the following generations were observed in all lines. The plants were much smaller than wild-type arabidopsis plants, had shorter siliques (Figure 3E) and the internodes between the siliques were much shorter, resulting in a bushy appearance (Figure 3C and 3D). Since this phenotype was linked to the *PID::PID-3xVENUS* insert, independent of the *pid* loss-of-function mutation, and not observed in the *PID::PID^{SE}-3xVENUS* phospho-mimic lines, we concluded that it relates to a dominant negative effect of the C-terminally fused 3xVENUS tag on the PID kinases activity, which can probably be overcome by the higher activity of the PID^{SE} protein.
The *PID::PID^{SA}-3xVENUS* loss-of-phosphorylation construct only partially complemented the *pid wag1 wag2* adult phenotype, resulting in plants with larger rosettes and multiple pin-formed inflorescences that formed flowers resembling those of the strong *pid* mutant alleles (Table 1). Some of the loss-of-phosphorylation lines showing stronger PID^{SA}-VENUS expression developed flowers with weak *pid* phenotypes, characterized by more than four petals and a trumpet shaped pistil (Benjamins *et al.*, 2001; Figure 3B). Some of these flowers were fertile and set a small amount of seed,

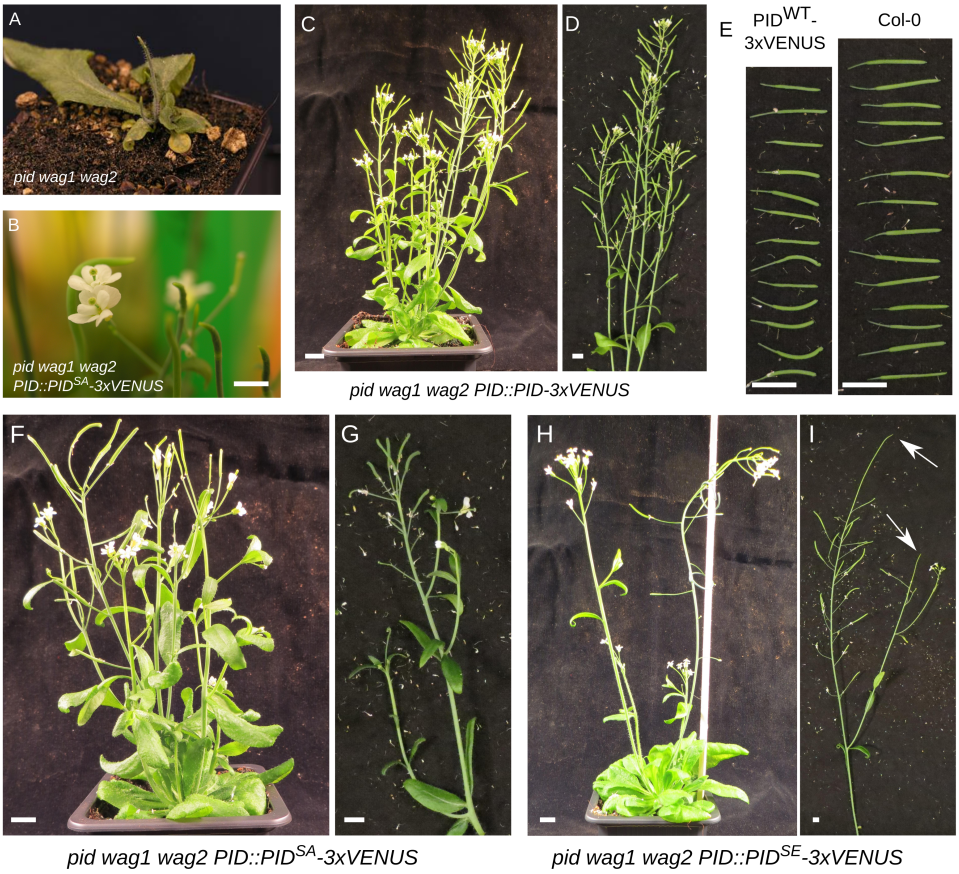

Figure 3: Phenotypic appearances of *pid wag1 wag2* mutant plants transgenic for the *PID::PID$^{SA/SE}$-3xVENUS* constructs.
(A) A 4 week old flowering *pid wag1 wag2* plant.
(B) Flower and pin-formed inflorescence phenotype of a 4 week old *pid wag1 wag2 PID::PID^{SA}-3xVENUS* plant.
(C-D) A 4 week old *pid wag1 wag2 PID::PID-3xVENUS* plant. The inflorescence image was taken one week later.
(E) Shorter siliques observed in *pid wag1 wag2 PID::PID-3xVENUS* plants compared to wild-type (Col-0) plants.
(F-G) A 4 week old *pid wag1 wag2 PID::PID^{SA}-3xVENUS* plant. The inflorescence image was taken one week later.
(H-I) A 4 week old *pid wag1 wag2 PID::PID^{SE}-3xVENUS* plant. The inflorescence image was taken one week later. The arrows in image I indicate the transition of normal inflorescences into pin-formed inflorescences.
Size bars indicate 1cm.

allowing us to obtain lines homozygous for the *pid* locus (Table 1, Figure 3F and 3G). In conclusion, these results show that PID phosphorylation by PDK1 contributes to the activity that is required to obtain phenotypically

wild-type plants, but that the non-phosphorylatable PID^{SA} version is sufficiently active to diminish the severe developmental defects of the *pid wag1 wag2* triple mutant to that of a weak *pid* allele, depending on the expression level of the mutant protein.
The *PID::PID^{SE}-3xVENUS* phospho-mimic lines mostly produced wild-type looking plants with respect to inflorescence height, rosette formation and flower development (Figure 3H), but eventually organ development ceased and all inflorescences developed pin-formed structures at their tips (Figure 3I, white arrows). This phenotype is reminiscent to what was observed previously for the *pin1 PIN1::PIN1^{S1,2,3E}-GFP* lines, where the three target serines for PID were substituted by phosphomimic residues (Huang *et al.*, 2010), suggesting that for proper inflorescence development the dynamics of PIN1 phosphorylation is important, and that either loss-of-phosphorylation, constitutive phosphomimic or constitutively high PID activity (as is the case for PID^{SE}) can disrupt the formation of auxin maxima in the inflorescence meristem that are required for organ initiation.

Dynamic PDK1-mediated PID phosphorylation positions cotyledon primordia during embryogenesis.

Next we checked whether the lack of cotyledon development in *pid wag1 wag2* mutant embryos could be rescued by the different *PID-3xVENUS* constructs. Seeds of three different homozygous lines per construct were germinated and the different cotyledon phenotypes (0-, 1-, 2-, 3- and 4-cotyledons) were scored for about 100 seedlings per line, and expressed as percentage of seedlings belonging to a phenotypic class. The results show that all three constructs were able to complement the no-cotyledon phenotype of the triple mutant (Dhonukshe *et al.*, 2010), resulting in seedlings with mostly 2 or 3 cotyledons (Figure 4). Interestingly, complementation with the wild-type construct (*PID-3xVENUS*) resulted in almost complete restoration of the 2-cotyledon phenotype (85%), whereas for both the loss-of-phosphorylation and phospho-mimic mutant constructs only 50-60% of the seedlings developed 2 cotyledons, whereas around 40-45% of the seedlings showed the 3-cotyledon phenotype that is characteristic for the *pid* loss-of-function mutant. A minority of the seedlings developed no or four cotyledons (Figure 4). In contrast to inflorescence development, loss-of-phosphorylation and phospho-mimic resulted in more or less the same phenotypes, suggesting that especially during embryogenesis, the dynamic regulation of PID activity by PDK1

is important for proper and reproducible positioning of the cotyledon primordia.

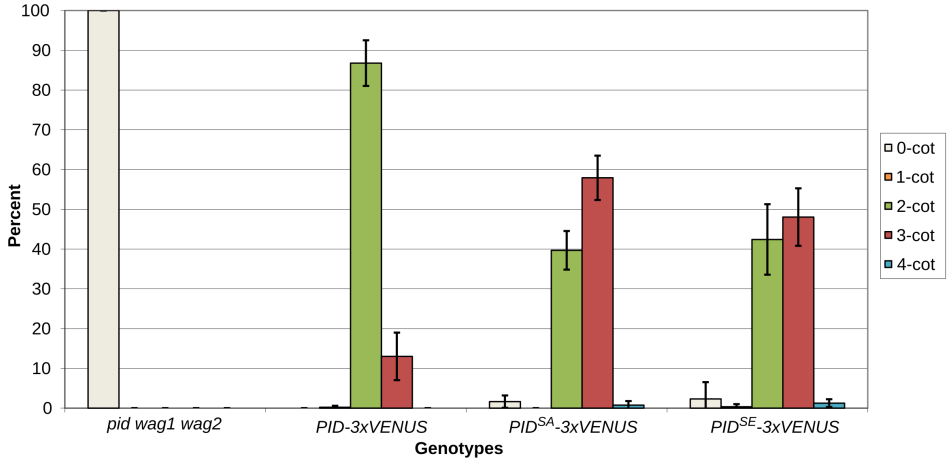

Figure 4: Phenotypic characterization of the *pid wag1 wag2 pPID::PID*$^{WT/SA/SE}$*-3xVENUS* seedlings.
Cotyledon phenotypes of 5 day old homozygous *pid wag1 wag2* (n=100, n=100, n=100), *pid wag1 wag2 pPID::PID-3xVENUS* (n=150, n=212, n=152), *pid wag1 wag2 pPID::PID*^{SA}*-3xVENUS* (n=73, n=93, n=48, n=63, n=58), and *pid wag1 wag2 pPID::PID*^{SE}*-3xVENUS* (n=81, n=107, n=241) seedlings. Error bars indicate standard error of the mean.

PINOID activation by PDK1 shows a small suppressing role in root gravitropism.

The *pid wag1 wag2* triple mutant is clearly defective in root gravitropic growth (Dhonukshe *et al.*, 2010), and therefore we tested whether the different PID-3xVENUS versions could rescue the gravitropic response, using respectively 'Columbia' (Col-0) wild-type, *wag1 wag2* and *pid wag1 wag2* as controls. Besides the *pid wag1 wag2* triple mutant root, which was strongly agravitropic, also the *wag1 wag2* double mutant showed a significant delay in the root gravitropic response after 3 hours of gravity stimulation compared to wild type (Figure 5). The gravitropic response of the mutant complementation lines positions itself between the controls (Figure 5). The large standard deviation makes it difficult to determine if there is a significant complementation of the *pid wag1 wag2* gravitropic defects. *PID*^{SA}*-3xVENUS* remains grouped to *wag1 wag2* at all time points, while *PID-3xVENUS* can be classified in to the *pid wag1 wag2* group at all time points. The difference between

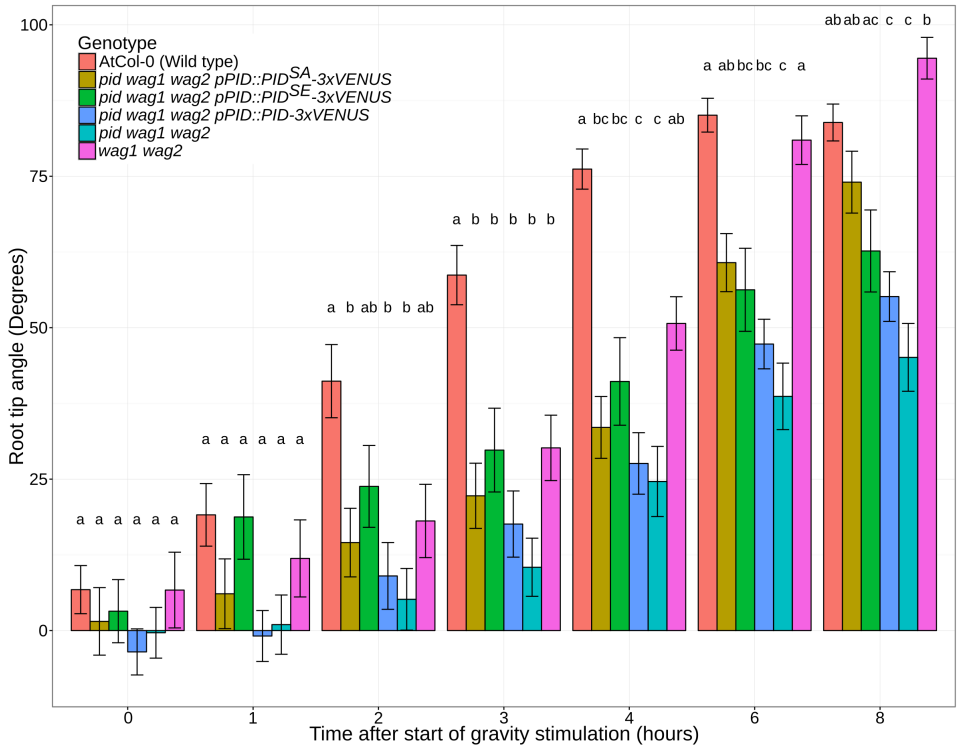

Figure 5: Phenotypic characterization of the *pid wag1 wag2 pPID::PID*$^{WT/SA/SE}$*-3xVENUS* seedlings.
Gravitropic response of 5 day old *pid wag1 wag2 pPID::PID-3xVENUS* (n=80), *pid wag1 wag2 pPID::PID*^{SA}*-3xVENUS* (n=73), and *pid wag1 wag2 pPID::PID*^{SE}*-3xVENUS* (n=80) seedlings lines compared to the Col-0 (n=21), *wag1 wag2* (n=60) and *pid wag1 wag2* (n=60) background.
Statistical testing of the gravitropic response was done with a Kruskal-Wallis H test for each time point and a 95% confidence interval. Error bars indicate standard error of the mean.

the three complementation construct lines is relative small and the only significant difference can be observed after 8 hours of gravity stimulation between the *PID*^{SA}*-3xVENUS* and *PID-3xVENUS* constructs, suggesting that phosphorylation plays a small suppressive role on the root gravitropic response.

PDK1 phosphomimic mutations do not affect PID relocalization to MT in root cells.

Based on our experiments in protoplasts we expected the mutant PID proteins to show a different localization compared to wild-type PID,

which normally shows predominant PM localization (Michniewicz *et al.*, 2007). The loss-of-phosphorylation PID^{SA} version was expected to localize to the PM and the endosomes, whereas we expected the phospho-mimic PID^{SE} version to predominantly localize to the microtubule cytoskeleton. Unexpectedly, however, the signal in all *PID-3xVENUS* complementation lines was weaker compared to the original *PID-VENUS* line (Michniewicz *et al.*, 2007), more sensitive to photobleaching, and root epidermis cells showed relatively more intracellular signal (Figure 6A versus 6C, right panel). Nonetheless, the stronger apical/basal plasma membrane signal that is characteristic for PID could be observed in all the three lines in at least part of the cells (Figure 6A). Unfortunately, the abundant intracellular signal observed in these lines did not allow us to distinguish MT or endosomal localization.

The lack of evidence for PID localization on MT in root cells made us wonder whether possibly PID localization on MT could be very transient, and therefore difficult to detect using standard confocal microscopy. However, even imaging PID-VENUS and the PID-3xVENUS versions on a more sensitive spinning disc confocal microscope did not provide evidence for its co-localization with the cortical MT in root epidermis cells (data not shown). Next we tried short-term treatment with the MT depolymerizing agent oryzalin. Twenty-five minutes treatment of 5 day old seedlings of the mCherry-5TUA MT reporter line with 10 µM oryzalin was sufficient to disrupt the MT cytoskeleton (Figure 6B). However, treatment of *PID-VENUS* seedlings for 1 hour with 10 µM of oryzalin did not result in obvious changes in PID-VENUS localization (Figure 6C). Even quantification of the apical to lateral ratio of the PID-VENUS signal at the plasma membrane did not detect a significant difference between the oryzalin and control treatment (Figure 6D). Finally, we treated 5 day old seedlings for 5 days with a lower oryzalin concentration (100nM), to test the possibility that the effect of MT disruption on PID localization would only be visible after a longer period. However, also in this experiment we did not observe a significant change in PID localization (Figure 6E) compared to the short term DMSO treatment control and earlier reported PID-VENUS localization (Michniewicz *et al.*, 2007; Figure 6C, right panel). Based on our results we concluded that in root epidermis cells, under the conditions examined, the MT cytoskeleton does not play a major role in the PDK1-dependent regulation of PID localization or activity.

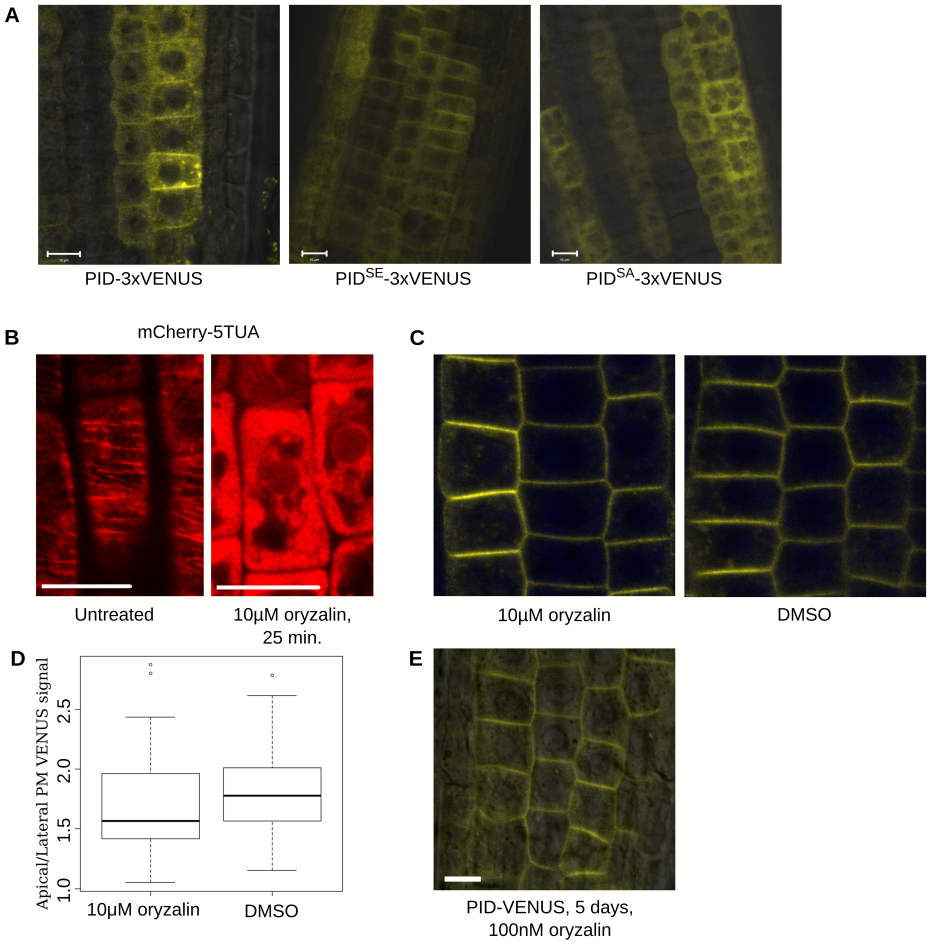

Figure 6: Subcellular localization of PID, PID^{SA} and PID^{SE} in root epidermis cells.
(A) Localization of wild-type PID-3xVENUS and the mutant versions PID^{SA}-3xVENUS and PID^{SE}-3xVENUS in root epidermis cells.
(B) Confocal images of mCherry-5TUA root epidermis cells untreated (left panel) and after treatment with 10µM oryzalin for 25 minutes (right panel).
(C) Confocal images of PID-VENUS after 1 hour treatment with 10µM oryzalin (left panel) or DMSO (right panel).
(D) Apical-to-lateral plasma membrane VENUS signal ratio, measured per cell, using images as presented in B, (n=50, 5 images). Statistical testing was done with the Welch's t-test with a 95% confidence interval.
(E) Effect of long term exposure to 0.1µM oryzalin on PID-VENUS localization in root epidermis cells. Scale bars = 10µm.

Discussion

PDK1 has been presented as master regulator of AGC protein serine/threonine kinases in the animal system, and research in plants has

until now implied a role for PDK1 in oxidative stress or defense related responses, and in root hair growth (Camehl *et al.*, 2011; Anthony *et al.*, 2004; Zegzouti *et al.*, 2006b; Anthony *et al.*, 2006).

Previously, Zegzouti and coworkers showed that the *in vitro* activity of the key developmental regulator PID is enhanced by phosphorylation of serines 288 and 290 in its activation loop by PDK1 (Zegzouti *et al.*, 2006a). Here we analysed the role of PDK1-dependent PID activation in addition to the well-established function of this kinase as PIN polarity regulator.

Our first analysis in protoplasts resulted in the interesting observation that PDK1-mediated phosphorylation of PID leads to its relocalisation to the MT cytoskeleton, and that PDK1 is also capable to cause relocalisation of PID to endosomal compartments in a phosphorylation-independent manner. The latter could be mediated by interaction with PDK1 via the PIF domain, because PDK1 itself seems localized to endosomal compartments. It is however important to note that the colocalisation of both proteins is only partial at best. The relocalisation to MT is dependent on phosphorylation, and could be caused by the change in charge. PID predominantly localizes to the PM, and this PM association has been shown to be mediated by the insertion domain (Zegzouti *et al.*, 2006b). Recently, Simon and coworkers provided evidence that a stretch of positive amino acids in the insertion domain promotes interaction with phospholipids (Simon *et al.*, 2016). Possibly the negative charge by phosphorylation close to the insertion domain decreases its affinity with the PM, and possibly at the same time enhances its affinity for factors that recruit the kinase to the MT cytoskeleton.

Unfortunately, we have not been able to find evidence for this localization in the PID mutant versions in root epidermis cells. A possible reason might be that the factors required for MT localization are not present in root epidermis cells, and are only present in cells of the shoot or inflorescence meristem.

We did, in fact, notice a small difference in gravitropic response between the non-phosphorylatable PID^{SA} mutant on one side and the phosphomimic PID^{SE} and wildtype PID complementation on the other side, where PID phosphorylation seems to suppress the gravitropic response. This finding is in line with the protoplast observations where phosphorylated PID would be less PM bound, resulting in reduced PIN polarity and thus in a slower root gravitropic response.

The presence of the triple VENUS tag at the C-terminal end of the

kinase was chosen in an attempt to enhance the visualization of the fusion protein, but our results suggest that the relatively large tag fails to improve the signal compared to the existing PID-VENUS line. In fact, the triple VENUS tag seems to have an effect in PID function. The enhanced activation of PID^{SE} mutation seems to partially overcome this effect, suggesting that more active PM-associated PID is needed when the protein has reduced PM localization.

Assuming that the pathways resulting in PID MT relocalisation are still present *in planta* and the conditions for PID MT relocalisation are met, what could it be its function? First, knowing that the phospholipid composition of the PM is part of PDK1-mediated signaling (Anthony *et al.*, 2004), it could be a possible feedback mechanism, where PDK1-mediated PID hyperactivation is followed by its subsequent removal from the vicinity of the PID targets at the PM. A second function could be active relocalisation via the MT to sites where PINs need to be recruited for apical recycling. Previously it was reported that PIN polarity in inflorescence meristem cells is established at the PM, orthogonal to the direction of the cortical MT (Heisler *et al.*, 2010). This would imply that MT would recruit PID to the lateral side where PIN phosphorylation would lead to their endocytosis and recruitment into the apical recycling pathway. PID itself has no known domains that would allow it to localize to the MT cytoskeleton, so the most likely way of relocalizing to the MT would be through a complex of interacting proteins that enable PID MT localization. Current research in our group is targeted to finding these possible interactors and examining their complex dynamics.

Even though we have not been able to confirm the PDK1-triggered relocalisation of PID *in planta*, our results show that the lack of PDK1 activation of PID yields a similar phenotype in the seedling and adult stage as if PID would be knocked out. PID^{SA} can to a large extend overcome the defects of the *pid wag wag2* triple mutant, but it has insufficient activity to properly position cotyledon development during embryogenesis or for wild-type organ initiation during inflorescence development. On the other hand, in both seedling and adult stages it was clear that the phosphorylation dynamics, the process of phorphorylation and dephosphorylation regulatory events, are important for proper development. At the adult stage this results in the ability of the shoot apical meristem to generate organs, as leaves and flowers. In each phosphomimic mutant line that we have observed we noticed that at

some point in the inflorescence development the organ formation stopped and development continued as a PIN inflorescence. The dependence on phosphorylation dynamics in inflorescence development has been observed before in the downstream target of PID, the PIN1 protein (Huang *et al.*, 2010). Also during embryo development we noticed a significant shift to seedlings with 3-cotyledons when phosphorylation dynamics was restricted in the PID protein. This is in strong contrast with the earlier reported phosphorylation dynamics restricted PIN1-mutants (Huang *et al.*, 2010), where there is a shift to 0- or 1-cotyledon embryos (the phosphomimic PIN1 mutant), or reduced germination (the loss-of-phosphorylation PIN1 mutant), suggesting that other proteins than PID act on the phosphorylation dynamics of PIN1. In conclusion, our results implicate a novel developmental role for PDK1 as enhancer of PID activity during embryogenesis and inflorescence development. Strikingly, this role is not reflected by the reported mild phenotypes of the *pdk1-1 pdk1-2* double loss-of-function mutant (Camehl *et al.*, 2011). By looking at the alleles used in more detail we noticed that the *pdk1-1* allele has an insertion in the promoter region, and that for the *PDK1* gene no other alleles with insertion in the coding region are available. We therefore suspect that the *pdk1-1* allele is not a loss-of-function allele, and that true loss of function might lead to more severe (lethal) phenotypes as described in other plant species or organisms (Devarenne *et al.*, 2006).

Acknowledgments

We would like to thank Dr. Lazlo Bögre from Royal Holloway, University of London for the *pAS PDK1* plasmid, Pankaj Dhonukshe for the *pSK YFP-CLIP70* plasmid, and Dr. Tijs Ketelaar from Wageningen University and Research Centre for the *35S::mCherry-TUA5* plant line and for help with the spinning disc confocal microscopy. M.E.J.H. was financially supported by the Netherlands Organization for Scientific Research (NWO) through the NWO-Chemical Sciences TOP grant 700.58.301 to R.O., and C.G-A. was supported by the Netherlands Organization for Scientific Research (NWO) through a grant from the Research Council for Earth and Life Sciences (ALW 813.06.004) to R.O., and by grants from the NWO-Chemical Sciences (VIDI grant 700.56.429) and from the Netherlands Organization for Health Research and Development (ZON 050-71-023) to C.T.

Material and Methods

Molecular cloning and DNA constructs

The *pART7-PID-CFP*, *pART7-PID-YFP*, *pART7-PDK1-CFP*, *pART7-PDK1-mRFP*, and *pART7-YFP-CLIP170*$^{1\text{-}1240}$ fusion constructs were made using Gateway Technology (Life Technologies Corporation, USA). Genes of interest were amplified by PCR with primers containing attB recombination sites (see Table 2) from *Arabidopsis thaliana* 'Columbia' (Col-0) cDNA from siliques using primer set PID attB1 F - PID attB2 R for *PID*, from *pAS PDK1* using the primer set PDK1 attB1F - PDK1 attB2 R for *PDK1*, and from *pSK YFP-CLIP170* (Dhonukshe & Gadella, 2003) using primer set YFP attB1 F – CLIP170$^{1\text{-}1240}$ attB2 R for the *YFP-CLIP170* (amino acids 1-1240) fused coding regions. BP reactions were performed with *pDONR207* (Life Technologies Corporation, USA) and the resulting plasmids were transformed to *E. coli* strain DH5α.

To generate the mutant *PID* constructs, specific base pair substitutions were introduced using the QuikChange XL Site-directed Mutagenesis kit (Agilent Technologies, USA). Reactions were performed using the *pDONR-PID* construct as a template and the primer sets PID SS288,290AA F - PID SS288,290AA R and PID SS288,290EE F - PID SS288,290EE R to generate *pDONR-PID*^{SA} and *pDONR-PID*^{SE}, respectively.

For subsequent LR reactions destination vectors were used that were constructed by introducing the Gateway recombination cassette (Life Technologies Corporation, USA) in frame with YFP, CFP, mRFP1 or, in case of YFP-CLIP170, no fluorescent tag between the *CaMV 35S* promoter and the *OCS* terminator of the *pART7* vector (Gleave, 1992).

The *pDONR-gPID*^{SA} or *pDONR-gPID*^{SE} plasmids were created by digesting the *pDONR-PID*^{SA} and *pDONR-PID*^{SE} vectors with *Bgl*II and ligating the fragment containing the PID cDNA into *pDONR-gPID* genomic clone, which was also digested with *Bgl*II. A 3.1kb fragment containing the promotor of *PID* was amplified from Col-0 genomic DNA using primer set attb4_promPID and attb1r_promPID. *pDONR-3xVENUS* was amplified from *pGreenII-3xVENUS t35* using primer set attb2r_3xvenus and attb3_t35S. To obtain the *pGreenII-pPID::PID*$^{WT/SA/SE}$*-3xVENUS* constructs we performed 3 fragment gateway reactions with the *pDONR-gPID*, *pDONR-gPID*^{SA} or *pDONR-gPID*^{SE} plasmids and the *PID* promoter and *3xVENUS* fragments according to the protocol supplied by the manufacturer (Life Technologies Corporation, USA). The resulting

pGreenII constructs were introduced into electro-competent *Agrobacterium tumefaciens* strain AGL1 (Lazo *et al.*, 1991) containing the *pSoup* helper plasmid (Hellens *et al.*, 2000) using a Bio-Rad Genepulser electroporation system in pre-chilled 0.1mm electroporation cuvettes and with a pulse of 2.5kV, 25µF and 200Ω. After electroporation the bacteria were incubated at 30°C in LC medium for 1 hour, and subsequently plated on LCA media containing selection. *A. tumefaciens* colonies containing both plasmids after selection were used to transform arabidopsis plants.

Table 2: Primers used for genotyping, cloning or site directed mutagenesis.

Name	Sequence (5'→3')
PID attB1 F	GGGGACAAGTTTGTACAAAAAAGCAGGCTTCAGCATGTTACGAGAATCAGACGGT
PID attB2 R	GGGGACCACTTTGTACAAGAAAGCTGGGTCAAAGTAATCGAACGCCGCTGG
PIDex1 F1	TCTCTTCCGCCAGGTAAAAA
PIDex1 R1	CGCAAGACTCGTTGGAAAAG
PID Downstream R1	CCCGTCGAACTACAAAGTCTAGGCG
PDK1 attB1F	GGGGACAAGTTTGTACAAAAAAGCAGGCTTAATGTTGGCAATGGAGAAAGAA
PDK1 attB2 R	GGGGACCACTTTGTACAAGAAAGCTGGGTAGCGGTTCTGAAGAGTCTCGAT
YFP attB1 F	GGGGACAAGTTTGTACAAAAAAGCAGGCTTAATGGTGAGCAAGGGCGAGGAG
CLIP170$^{1\text{-}1240}$ attB2 R	GGGGACCACTTTGTACAAGAAAGCTGGGTACTTGAGCTCGAGCTTCACCTTATCA
PID SS288,290AA F	GGTTACTGCCCCGGGCTGGTGCGTTCGTTGGTACGC
PID SS288,290AA R	GCGTACCAACGAACGCACCAGCCCGGGCAGTAACC
PID SS288,290EE F	GGTTACTGCCCGGGAAGGTGAGTTCGTTGGTACGC
PID SS288,290EE R	GCGTACCAACGAACTCACCTTCCCGGGCAGTAACC
attb4_promPID	GGGGACAACTTTGTATAGAAAAGTTGCTCCGAACCAATTCTAGCAA
attb1r_promPID	GGGGACTGCTTTTTTGTACAAACTTGCCGCCGGGAAAATCGAAGT
attb2r_3xvenus	GGGGACAGCTTTCTTGTACAAAGTGGCTATGGTGAGCAAGGGCGAG
attb3_t35S	GGGGACAACTTTGTATAATAAAGTTGCATTTAGGTGACACTATAG
LBa1	TGGTTCACGTAGTGGGCCATCG

Plant lines and transformations

Plants were grown on soil in a growth room at 21°C under 16 hours photoperiod, and 70% relative humidity. The *pPID::PID$^{WT/SA/SE}$-3xVENUS pid-14$^{+/-}$ wag1 wag2* arabidopsis lines were obtained by the floral dip method (Clough & Bent, 1998). In short, 600 ml *A. tumefaciens* AGL1 cultures containing each of the *pGreenII-pPID::PID$^{WT/SA/SE}$-3xVENUS* and *pSoup* helper plasmid were grown overnight at 28°C in LC medium containing 20µg/ml rifampicin, 70µg/ml carbenicillin and 100µg/ml kanamycin until OD_{600} was 0.8. Bacteria were harvested by centrifugation and resuspended in 250 ml non-sterile 5% sucrose solution. Siliques and open flowers were removed

from secondary inflorescences of 4 to 5 weeks old arabidopsis *pid-14*$^{+/-}$ *wag1 wag2* triple loss-of-function mutant plants (Dhonukshe *et al.*, 2010) following removal of the primary inflorescence. Per construct about 15 plants were dipped in the *A. tumefaciens* solution supplemented with 0.02% Silwet L77 (van Meeuwen Smeertechniek B.V., The Netherlands) for about 30 to 60 seconds. Dipped plants were put on a tray with sufficient water and covered with a plastic bag for one day, after which the plastic was gradually removed. Seeds were harvested after the plants completed their life cycle. Seeds were surface sterilized by incubation 10 minutes incubation in half strength commercial bleach. Seeds were washed 4 times with sterile MilliQ water, resuspended in 0.1% agarose and plated on MA medium (half strength MS macronutrients; Murashige & Skoog, 1962) supplemented with B5 micronutrients (Gamborg *et al.*, 1968), 1% sucrose, 0.1% 2-(N-morpholino)ethanesulfonic acid (MES) and 1% Daishin agar (Duchefa Biochemie B.V., The Netherlands), pH was adjusted to 5.8 with potassium hydroxide) with 15µg/ml phosphinothricin and 100µg/ml timentin. Seeds were imbibed for 3 days at 4°C, and germinated at 21°C and 16 hours photoperiod. Primary transformants were checked for homozygosity of the *pid-14* locus by PCR-based genotyping. T2 seeds were plated on MA medium with 15µg/ml phosphinothricin to determine the number of T-DNA insertions based on the segregation. Single locus T-DNA insertion lines were screened for PID-3xVENUS expression level by confocal microscopy, and per construct a few homozygous T3 lines were selected for further analysis.

Seedling phenotypic observations

Cotyledon phenotypes were scored 5 days after germination. For the *pPID::PID-3xVENUS* construct we used seeds of 3 independent homozygous lines (respectively, n=150, n=212 and n=152). For the *pPID::PID*^{SA}*-3xVENUS* construct we used seeds from 5 homozygous lines, with n=73, n=93, n=48, n=63 and n=58. These 5 lines descended from the same primary transformant. For the *pPID::PID*^{SE}*-3xVENUS* construct we used seeds from 3 independent homozygous lines (respectively, n=81, n=107, and n=241).

For the gravitropism experiments 5 day old seedlings of *pid wag1 wag2 pPID::PID-3xVENUS* (n=80), *pid wag1 wag2 pPID::PID*^{SA}*-3xVENUS* (n=73), *pid wag1 wag2 pPID::PID*^{SE}*-3xVENUS* (n=80), wild-type 'Columbia' (n=21), *wag1 wag2* (n=60) and *pid wag1 wag2* (n=60) were

transferred to fresh MA plates and allowed to adjust to the new plate for 1 hour. For the *pid wag1 wag2* line, only seedlings without cotyledons were taken. The plates were photographed and subsequently rotated 90 degrees to start the experiment. Subsequent images were taken at 1, 2, 3, 4, 6 and 8 hours after the start of the experiment. The gravitropic response was measured with Fiji (Schindelin *et al.*, 2012).
Two to 3 week old seedlings were transferred to soil and incubated at 21°C and 16 hours photoperiod. Adult plants were phenotyped and imaged at bolting and late flowering stage.

Protoplast transfections

Protoplasts were obtained from arabidopsis cell suspension cultures generated and maintained as described originally by Axelos and coworkers (Axelos *et al.*, 1992) and adapted by Schirawski (Schirawski *et al.*, 2000). A 50ml 1 day old 1:5 dilution of a week old cell suspension culture was pelleted at low speed (1000 RPM, 5 min). The supernatant was discarded and cells were resuspended in 20ml enzyme mix (0.4% Macerozyme R10 (Duchefa, The Netherlands), 2% Cellulase R10 (Duchefa, The Netherlands), 12% Sorbitol, pH 5.8) and incubated at 28°C in the dark for 2.5 hours. After incubation, the suspension was sieved through a 70µm cell sieve (Corning, USA) and protoplasts were washed 3 times with sterile protoplast medium (25mM KNO_3, 1mM $MgSO_4$, 1mM NaH_2PO_4, 1mM $(NH_4)_2SO_4$, 1.16 mM $CaCl_2$, 0.56mM myo-inositol, 10mg Thiamine-HCl, 1mg Pyridoxine-HCl, 1mg Nicotinic acid, 36.7mg FeEDTA, 48.52µM H_3BO_3, 59.17µM $MnSO_4$, 6.96µM $ZnSO_4$, 4.52µM KI, 0.75µM Na_2MoO_4, 0.1µM $CuSO_4$, 0.11µM $CoCl_2$, 0.1M Glucose, 0.25M Mannitol, 1µM NAA, pH 5.8), and gently resuspended in protoplast medium to a final concentration of $4*10^6$ cells/ml. 0.25ml protoplasts were added to 10µg plasmid (in a maximum volume of 10µl). 0.25ml polyethyleneglycol (PEG) solution (40% PEG 4000, 0.2M mannitol, 0.1M $CaCl_2$) was added drop-wise, and the protoplasts were gently mixed every time 3 drops of PEG solution were added. Following incubation for 10 minutes at room temperature, the 0.5 ml protoplast-PEG mix was transferred gently to a sterile 6-well plate (Greiner Bio-One, Germany) prefilled with 4.5ml protoplast medium and incubated overnight at 28°C in the dark.

Imaging

Plant tissue imaging was performed on a Leica MZ16FA fluorescence microscope equipped with a GFP3 filter, or on a Zeiss LSM5 Exciter/AxioImager confocal microscope equipped with 514nm (YFP) and 543nm (mCherry) laser lines (5-18% laser intensity), a Plan-Apochromat 63x/1.4 Oil DIC objective, a BP 530-600 excitation filter, and LP 650 (YFP) or LP 560 (mCherry) emission filters. For the protoplast experiments, a Leica DM IRBE confocal laser scanning microscope with a 63X water objective was used. The fluorescence was visualized with an argon-krypton laser (51% laser intensity) for excitation at 457 nm (CFP), 514 nm (YFP) and 568nm (mRFP) using 475-495nm, 520-545nm and 600-640nm BP emission filters, respectively.

Statistical analysis and figure assembly

Graphs were made in Microsoft Excel or in Rstudio (`https://www.rstudio.org/`), images were edited in Zen 2009 Light edition (Carl Zeiss MicroImaging GmbH) and Inkscape (`https://inkscape.org/`) and figures were assembled in Microsoft Powerpoint or Inkscape. Statistical analysis was performed in RStudio.

Bibliography

Alessi, D. R., James, S. R., Downes, C., Holmes, A. B., Gaffney, P. R. J., Reese, C. B. & Cohen, P. (1997). Characterization of a 3-phosphoinositide-dependent protein kinase which phosphorylates and activates protein kinase Bα. Current Biology **7**, 261–269.

Anthony, R. G., Henriques, R., Helfer, A., Mészáros, T., Rios, G., Testerink, C., Munnik, T., Deák, M., Koncz, C. & Bögre, L. (2004). A protein kinase target of a PDK1 signalling pathway is involved in root hair growth in *Arabidopsis*. The EMBO Journal **23**, 572–581.

Anthony, R. G., Khan, S., Costa, J., Pais, M. S. & Bögre, L. (2006). The *Arabidopsis* protein kinase PTI1-2 is activated by convergent phosphatidic acid and oxidative stress signaling pathways downstream of PDK1 and OXI1. Journal of Biological Chemistry **281**, 37536–37546.

Axelos, M., Curie, C., Mazzolini, L., Bardet, C. & Lescure, B. (1992). A protocol for transient gene expression in *Arabidopsis thaliana* protoplasts isolated from cell suspension cultures. Plant Physiology and Biochemistry **30**, 123–128.

Benjamins, R., Quint, A., Weijers, D., Hooykaas, P. J. J. & Offringa, R. (2001). The PINOID protein kinase regulates organ development in *arabidopsis* by enhancing polar auxin transport. Development **128**, 4057–4067.

Benková, E., Michniewicz, M., Sauer, M., Teichmann, T., Seifertová, D., Jürgens, G. & Friml, J. (2003). Local, efflux-dependent auxin gradients as a common module for plant organ formation. Cell **115**, 591–602.

Camehl, I., Drzewiecki, C., Vadassery, J., Shahollari, B., Sherameti, I., Forzani, C., Munnik, T., Hirt, H. & Oelmüller, R. (2011). The OXI1 kinase pathway mediates *Piriformospora indica*-induced growth promotion in Arabidopsis. PLoS Pathogens **7**, e1002051.

Clough, S. J. & Bent, A. F. (1998). Floral dip: a simplified method for *Agrobacterium*-mediated transformation of *Arabidopsis thaliana*. The Plant Journal **16**, 735–743.

Deak, M., Casamayor, A., Currie, R. A., Peter Downes, C. & Alessi, D. R. (1999). Characterisation of a plant 3-phosphoinositide-dependent protein kinase-1 homologue which contains a pleckstrin homology domain. FEBS Letters **451**, 220–226.

Devarenne, T. P., Ekengren, S. K., Pedley, K. F. & Martin, G. B. (2006). Adi3 is a Pdk1-interacting AGC kinase that negatively regulates plant cell death. The EMBO Journal **25**, 255–265.

Dhonukshe, P., Aniento, F., Hwang, I., Robinson, D. G., Mravec, J., Stierhof, Y.-D. & Friml, J. (2007). Clathrin-mediated constitutive endocytosis of PIN auxin efflux carriers in *Arabidopsis*. Current Biology **17**, 520–527.

Dhonukshe, P. & Gadella, T. W. J. (2003). Alteration of microtubule dynamic instability during preprophase band formation revealed by yellow fluorescent protein–CLIP170 microtubule plus-end labeling. Plant Cell **15**, 597–611.

Dhonukshe, P., Huang, F., Galván-Ampudia, C. S., Mähönen, A. P., Kleine-Vehn, J., Xu, J., Quint, A., Prasad, K., Friml, J., Scheres, B. & Offringa, R. (2010). Plasma membrane-bound AGC3 kinases phosphorylate PIN auxin carriers at TPRXS(N/S) motifs to direct apical PIN recycling. Development **137**, 3245–3255.

Dhonukshe, P., Tanaka, H., Goh, T., Ebine, K., Mähönen, A. P., Prasad, K., Blilou, I., Geldner, N., Xu, J., Uemura, T., Chory, J., Ueda, T., Nakano, A., Scheres, B. & Friml, J. (2008). Generation of cell polarity in plants links endocytosis, auxin distribution and cell fate decisions. Nature **456**, 962–966.

Ding, Z., Galván-Ampudia, C. S., Demarsy, E., Łangowski, Ł., Kleine-Vehn, J., Fan, Y., Morita, M. T., Tasaka, M., Fankhauser, C., Offringa, R. & Friml, J. (2011). Light-mediated polarization of the PIN3 auxin transporter for the phototropic response in *Arabidopsis*. Nature Cell Biology **13**, 447–452.

Dittrich, A. C. N. & Devarenne, T. P. (2012). Characterization of a PDK1 Homologue from the moss *Physcomitrella patens*. Plant Physiology **158**, 1018–1033.

Doyle, S. M., Haeger, A., Vain, T., Rigal, A., Viotti, C., Łangowska, M., Ma, Q., Friml, J., Raikhel, N. V., Hicks, G. R. & Robert, S. (2015). An early secretory pathway mediated by GNOM-LIKE 1 and GNOM is essential for basal polarity establishment in *Arabidopsis thaliana*. Proceedings of the National Academy of Sciences of the United States of America **112**, E806–E815.

Friml, J., Yang, X., Michniewicz, M., Weijers, D., Quint, A., Tietz, O., Benjamins, R., Ouwerkerk, P. B. F., Ljung, K., Sandberg, G., Hooykaas, P. J. J., Palme, K. & Offringa, R. (2004). A PINOID-dependent binary switch in apical-basal PIN polar targeting directs auxin efflux. Science **306**, 862–865.

Gamborg, O. L., Miller, R. a. & Ojima, K. (1968). Nutrient requirements of suspension cultures of soybean root cells. Experimental cell research **50**, 151–158.

Geldner, N., Anders, N., Wolters, H., Keicher, J., Kornberger, W., Muller, P., Delbarre, A., Ueda, T., Nakano, A. & Jürgens, G. (2003). The *Arabidopsis* GNOM ARF-GEF mediates endosomal recycling, auxin transport, and auxin-dependent plant growth. Cell **112**, 219–230.

Geldner, N., Friml, J., Stierhof, Y.-D., Jürgens, G. & Palme, K. (2001). Auxin transport inhibitors block PIN1 cycling and vesicle trafficking. Nature **413**, 425–428.

Gleave, A. (1992). A versatile binary vector system with a T-DNA organisational structure conducive to efficient integration of cloned DNA into the plant genome. Plant Molecular Biology **20**, 1203–1207.

Heisler, M. G., Hamant, O., Krupinski, P., Uyttewaal, M., Ohno, C., Jönsson, H., Traas, J. & Meyerowitz, E. M. (2010). Alignment between PIN1 polarity and microtubule orientation in the shoot apical meristem reveals a tight coupling between morphogenesis and auxin transport. PLoS Biology **8**, e1000516.

Hellens, R. P., Edwards, E. A., Leyland, N. R., Bean, S. & Mullineaux, P. M. (2000). pGreen: a versatile and flexible binary Ti vector for *Agrobacterium*-mediated plant transformation. Plant Molecular Biology **42**, 819–832.

Huang, F., Kemel Zago, M., Abas, L., van Marion, A., Galván-Ampudia, C. S. & Offringa, R. (2010). Phosphorylation of conserved PIN motifs directs *arabidopsis* PIN1 polarity and auxin transport. Plant Cell **22**, 1129–1142.

Kitakura, S., Vanneste, S., Robert, S., Löfke, C., Teichmann, T., Tanaka, H. & Friml, J. (2011). Clathrin mediates endocytosis and polar distribution of PIN auxin transporters in *Arabidopsis*. Plant Cell **23**, 1920–1931.

Kleine-Vehn, J., Huang, F., Naramoto, S., Zhang, J., Michniewicz, M., Offringa, R. & Friml, J. (2009). PIN auxin efflux carrier polarity is regulated by PINOID kinase-mediated recruitment into GNOM-independent trafficking in *Arabidopsis*. Plant Cell **21**, 3839–3849.

Lawlor, M. A., Mora, A., Ashby, P. R., Williams, M. R., Murray-Tait, V., Malone, L., Prescott, A. R., Lucocq, J. M. & Alessi, D. R. (2002). Essential role of PDK1 in regulating cell size and development in mice. The EMBO Journal **21**, 3728–3738.

Lazo, G. R., Stein, P. A. & Ludwig, R. A. (1991). A DNA transformation-competent *Arabidopsis* genomic library in *Agrobacterium*. Biotechnology (N Y) **9**, 963–967.

Matsui, H., Miyao, A., Takahashi, A. & Hirochika, H. (2010). Pdk1 kinase regulates basal disease resistance through the OsOxi1–OsPti1a phosphorylation cascade in rice. Plant and Cell Physiology **51**, 2082–2091.

Michniewicz, M., Zago, M. K., Abas, L., Weijers, D., Schweighofer, A., Meskiene, I., Heisler, M. G., Ohno, C., Zhang, J., Huang, F., Schwab, R., Weigel, D., Meyerowitz, E. M., Luschnig, C., Offringa, R. & Friml, J. (2007). Antagonistic regulation of PIN phosphorylation by PP2A and PINOID directs auxin flux. Cell **130**, 1044–1056.

Mravec, J., Skůpa, P., Bailly, A., Hoyerová, K., Křeček, P., Bielach, A., Petrášek, J., Zhang, J., Gaykova, V., Stierhof, Y.-D., Dobrev, P. I., Schwarzerova, K., Rolčík, J., Seifertova, D., Luschnig, C., Benková, E., Zažímalová, E., Geisler, M. & Friml, J. (2009). Subcellular homeostasis of phytohormone auxin is mediated by the ER-localized PIN5 transporter. Nature **459**, 1136–1140.

Murashige, T. & Skoog, F. (1962). A revised medium for rapid growth and bioassays with tobacco tissue cultures. Physiologia plantarum **15**, 473–497.

Petrášek, J., Mravec, J., Bouchard, R., Blakeslee, J. J., Abas, M., Seifertová, D., Wiśniewska, J., Tadele, Z., Kubeš, M., Čovanová, M., Dhonukshe, P., Skůpa, P., Benková, E., Perry, L., Křeček, P., Lee, O. R., Fink, G. R., Geisler, M., Murphy, A. S., Luschnig, C., Zažímalová, E. & Friml, J. (2006). PIN proteins perform a rate-limiting function in cellular auxin efflux. Science **312**, 914–918.

Reinhardt, D., Mandel, T. & Kuhlemeier, C. (2000). Auxin regulates the initiation and radial position of plant lateral organs. Plant Cell **12**, 507–518.

Rentel, M. C., Lecourieux, D., Ouaked, F., Usher, S. L., Petersen, L., Okamoto, H., Knight, H., Peck, S. C., Grierson, C. S., Hirt, H. & Knight, M. R. (2004). OXI1 kinase is necessary for oxidative burst-mediated signalling in *Arabidopsis*. Nature **427**, 858–861.

Schindelin, J., Arganda-Carreras, I., Frise, E., Kaynig, V., Longair, M., Pietzsch, T., Preibisch, S., Rueden, C., Saalfeld, S., Schmid, B., Tinevez, J.-Y., White, D. J., Hartenstein, V., Eliceiri, K., Tomancak, P. & Cardona, A. (2012). Fiji: an open-source platform for biological-image analysis. Nature Methods **9**, 676–682.

Schirawski, J., Planchais, S. & Haenni, A.-L. (2000). An improved protocol for the preparation of protoplasts from an established *Arabidopsis thaliana* cell suspension culture and infection with RNA of

turnip yellow mosaic tymovirus: a simple and reliable method. Journal of Virological Methods **86**, 85–94.

Simon, M. L. A., Platre, M. P., Marquès-Bueno, M. M., Armengot, L., Stanislas, T., Bayle, V., Caillaud, M.-C. & Jaillais, Y. (2016). A PtdIns(4)P-driven electrostatic field controls cell membrane identity and signalling in plants. Nature Plants **2**, 16089.

Sorefan, K., Girin, T., Liljegren, S. J., Ljung, K., Robles, P., Galván-Ampudia, C. S., Offringa, R., Friml, J., Yanofsky, M. F. & Ostergaard, L. (2009). A regulated auxin minimum is required for seed dispersal in *Arabidopsis*. Nature **459**, 583–586.

Tanaka, H., Dhonukshe, P., Brewer, P. B. & Friml, J. (2006). Spatiotemporal asymmetric auxin distribution: a means to coordinate plant development. Cellular and Molecular Life Sciences **63**, 2738–2754.

Wiśniewska, J., Xu, J., Seifertová, D., Brewer, P. B., Růžička, K., Blilou, I., Rouquié, D., Benková, E., Scheres, B. & Friml, J. (2006). Polar PIN localization directs auxin flow in plants. Science **312**, 883.

Zegzouti, H., Anthony, R. G., Jahchan, N., Bögre, L. & Christensen, S. K. (2006a). Phosphorylation and activation of PINOID by the phospholipid signaling kinase 3-phosphoinositide-dependent protein kinase 1 (PDK1) in arabidopsis. Proceedings of the National Academy of Sciences of the United States of America **103**, 6404–6409.

Zegzouti, H., Li, W., Lorenz, T. C., Xie, M., Payne, C. T., Smith, K., Glenny, S., Payne, G. S. & Christensen, S. K. (2006b). Structural and functional insights into the regulation of arabidopsis AGC VIIIa kinases. Journal of Biological Chemistry **281**, 35520–35530.

FOUR

BT SCAFFOLD PROTEINS RECRUIT THE PINOID KINASE TO THE NUCLEUS OR TO KINESINS ON MICROTUBULES.

Myckel Habets[1,7], Hélène S. Robert[1,2,7], Marcelo K. Zago[1], René Benjamins[1,3], Yang Xiong[1,4], Carlos Galván-Ampudia[1,5], Panagiota Giardoglou [1], Willemijn van Mossevelde[1], Eike Rademacher [1,6], Ab Quint[1], Remko Offringa[1]

[1] Institute of Biology Leiden / Leiden University, Sylviusweg 72, 2333 BE Leiden, The Netherlands

[2] Current affiliation: Mendel Centre for Genomics and Proteomics of Plants Systems, CEITEC MU - Central European Institute of Technology, Masaryk University, 625 00 Brno, Czech Republic

[3] Current affiliation: Syngenta Seeds B.V., Westeinde 62, 1601 BK Enkhuizen, The Netherlands

[4] Current affiliation: College of Life Sciences, Peking University, Beijing 100871, China

[5] Current affiliation: Laboratoire de Reproduction et Développement des plantes, CNRS, INRA, ENS Lyon, UCBL, Université de Lyon, Lyon, France

[6] Current affiliation: Rijk Zwaan Zaadteelt en Zaadhandel B.V., Burgemeester Crezeelaan 40, 2678 KX De Lier, The Netherlands

[7] These authors contributed equally to this chapter.

Summary

Polar transport of the plant hormone auxin directs plant development by producing dynamic gradients through the concerted action of asymmetrically localized PIN-FORMED (PIN) auxin efflux carriers. The PINOID (PID) protein serine/threonine kinase determines the direction of this transport by regulating the polar subcellular targeting of PIN proteins through their direct phosphorylation. In our search for upstream regulators of this kinase we identified *Arabidopsis thaliana* BTB and TAZ domain protein 1 (BT1) as a PID binding protein. The *BT1* gene belongs to a five-member gene family in arabidopsis, encoding proteins with a land plant-specific domain structure consisting of an amino-terminal BTB domain, a TAZ domain and a carboxy-terminal calmodulin binding domain. At least four of the five BT proteins interacted with PID through their BTB domain. *In vitro* phosphorylation assays indicated that BT1 is not a phosphorylation target of PID, but that BT1 binding reduces the activity of the kinase. BT1 localized in the nucleus and the cytoplasm, and upon co-expression with PID, BT1 was found at the plasma membrane whereas PID localization became partially nuclear. Overexpression of BT1 reduced *PID* overexpression seedling phenotypes and enhanced *pid* loss-of-function embryo phenotypes. In contrast, *bt* loss-of-function enhanced adult phenotypes of *PID* overexpression plants. A subsequent yeast two-hybrid screen for BT1 interacting proteins yielded two At1-family kinesins that were found to induce BT1-dependent relocalization of PID and its closest family members WAG1, WAG2 and AGC3-4 to the microtubule cytoskeleton in arabidopsis protoplasts. Together these data suggest that BT1 acts as signaling scaffold that regulates AGC3 kinase activity in part by relocating PID to the nucleus or, for all the kinases, to the microtubule cytoskeleton.

Introduction

The phytohormone auxin plays a crucial role in plant developmental processes such as embryogenesis, phyllotaxis and root meristem maintenance (Sabatini *et al.*, 1999; Reinhardt *et al.*, 2003; Benková *et al.*, 2003). Characteristic for auxin action is its polar transport, which generates maxima and minima that are instrumental in directing cell division, -elongation and -differentiation (Perrot-Rechenmann, 2010). Auxin transport can be chemically inhibited, resulting in inflorescence

meristems that lose the capacity to produce leaves and flowers and therefore form pin-like structures (Okada *et al.*, 1991). The *Arabidopsis thaliana* (arabidopsis) *pin-formed1* and the *pinoid* loss-of-function mutants phenocopy plants that have been treated with polar auxin transport inhibitors (Okada *et al.*, 1991; Bennett *et al.*, 1995). The *PIN-FORMED1* (*PIN1*) gene is part of a family of eight genes in arabidopsis that encode integral membrane proteins characterized by two groups of five conserved transmembrane domains separated by a short or long hydrophilic loop (Adamowski & Friml, 2015; Armengot *et al.*, 2016). PIN proteins with the long hydrophilic loop (long PIN proteins) were shown to be the rate limiting factors in auxin efflux, and to determine the direction of polar auxin transport through their asymmetric subcellular localization at the plasma membrane (PM) (Petrášek *et al.*, 2006; Wiśniewska *et al.*, 2006). The *PINOID* (*PID*) gene encodes a plant specific protein serine/threonine kinase that has been implied as a regulator of polar auxin transport, and was shown to induce the subcellular targeting of long PIN proteins to the apical (shoot apex facing) PM by phosphorylating serines in three conserved TPRSX/N motifs in the long hydrophilic loop (Christensen *et al.*, 2000; Benjamins *et al.*, 2001; Friml *et al.*, 2004; Michniewicz *et al.*, 2007; Huang *et al.*, 2010; Dhonukshe *et al.*, 2010).

The PID kinase has also been shown to be a target for regulation. While PID is able to activate itself by autophosphorylation, phosphorylation by the 3-phosphoinositide-dependent kinase 1 (PDK1) was shown to result in a significant enhancement of the activity of this kinase *in vitro* (Zegzouti *et al.*, 2006a). In Chapter 3 of this thesis we report the phosphorylation-dependent relocalization of PINOID to the microtubule cytoskeleton (MT) following cotransfection with PDK1 in arabidopsis protoplasts. In addition, we show that phosphorylation of PID by PDK1 is essential for its function during vegetative and reproductive shoot development. In order to identify candidate proteins that could be involved in recruiting PID to the cytoskeleton, we used PID as bait in a yeast two-hybrid screen for PID BINDING PROTEINs (PBPs). Two of these PBPs are the calcium-binding proteins TOUCH3 (TCH3) and PBP1 that regulate PID kinase activity in response to changes in the cytosolic calcium concentration (Benjamins *et al.*, 2003; Fan, 2014). Here we analyzed the function of a third PBP and its interaction with PID, a Broad-Complex, Tramtrack, Bric-à-Brac (BTB) domain protein that was previously identified as the potato calmodulin interactor BT1 (Du &

Poovaiah, 2004). BTB domain proteins are known to act as scaffold- or linker-proteins that organize protein complexes (Albagli *et al.*, 1995). The arabidopsis genome encodes eighty BTB domain proteins that can be grouped in ten subfamilies (Gingerich *et al.*, 2005), based on the presence of other conserved protein domains that specify their function (Motchoulski & Liscum, 1999; Sakai *et al.*, 2000; Wang *et al.*, 2004; Weber *et al.*, 2005; Dieterle *et al.*, 2005). Besides the amino-terminal BTB domain, BT1 contains two additional protein-protein interaction domains: a TAZ domain (Transcriptional Adaptor Zinc finger; Ponting *et al.*, 1996) and a carboxy-terminal calmodulin binding domain (Du & Poovaiah, 2004).
Here we show that PID interacts with the BTB domain containing part of BT1, and that BT1 is not a phosphorylation target of PID but a repressor of its kinase activity. Overexpression of *BT1* reduced *PID* overexpression phenotypes and enhanced *pid* loss-of-function phenotypes. When fluorescent protein-tagged versions of PID and BT1 were co-expressed, the proteins sequestered each other to their individual locations, being the PM and the nucleus, respectively. Nuclear localization of PID was only observed in the presence of BT1, and our data suggests that BT proteins might be responsible for the nuclear localization of the other three AGC-3 kinases WAG1, WAG2 and AGC3-4 (Galván-Ampudia & Offringa, 2007). Apart from BT1, also other members of the BT protein family were found to interact with PID, and multiple *bt* knock-out adult phenotypes were enhanced by *PID* overexpression, suggesting that despite being multifunctional scaffolds, their role as regulator of PID is conserved for all BT proteins. Interestingly, BT1 was found to co-localize with the PDK1 phospho-mimic version of PID at the MT. A second yeast two-hybrid screen for BT1-binding proteins identified two plant specific kinesins, and further analysis showed that the BT1-kinesin complex most likely recruits PID to the MT after PDK1-mediated phosphorylation (see also Chapter 3 of this thesis).

Results

PINOID interacts with BT proteins through their BTB domain.

Previously, two arabidopsis yeast two-hybrid cDNA libraries were screened for proteins that interact with the PID protein serine/threonine kinase (Benjamins, 2003). One of the identified PBPs was BT1, a protein containing an amino-terminal BTB domain that is well-known

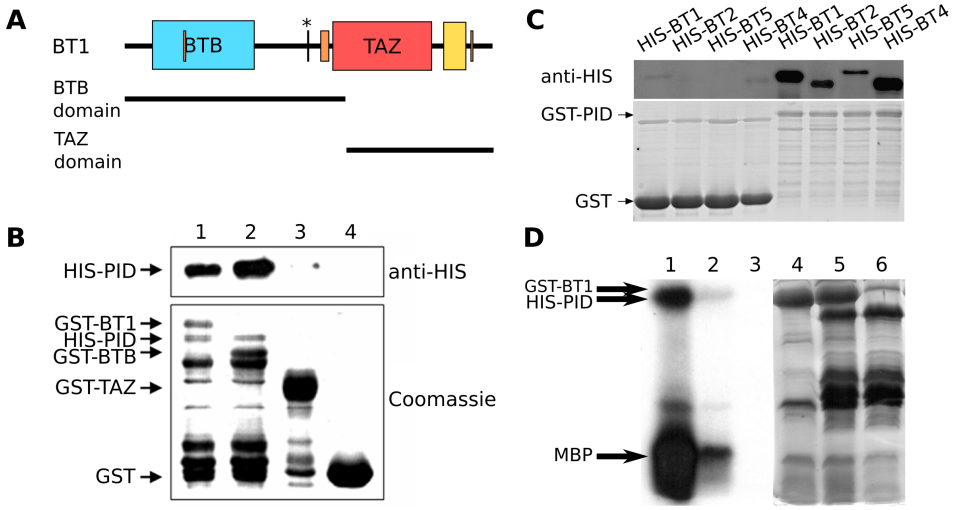

Figure 1: Binding of PID to the BTB domain of BT1 represses its kinase activity *in vitro*.
(A) Schematic representation of BT1 (365 aa) and the two deletion versions comprising either the BTB (aa 1–219) or the TAZ (aa 220-365) domains. The orange box (aa 193-203) and the vertical bars (aa 57-60 and aa 342-345) indicate the positions of predicted nuclear localization signals and a nuclear export signal is indicated by the vertical line with asterisk (aa 181-183). The yellow box (aa 316-339) indicates the calmodulin binding site.
(B) Western-blot analysis (top panel) with anti-His antibodies detects His-tagged PID after pull-down with GST-BT1 (lane 1) or the GST-tagged BTB domain (lane 2), but not with the GST-tagged TAZ domain (lane 3) or GST alone (lane 4), from the soluble fraction of *E. coli* protein extracts. The bottom panel shows the Coomassie stained gel of the pull-down reactions, with the positions of the different proteins indicated.
(C) Western blot with the anti-His antibody (top panel) showing specific pull-down of His-tagged BT1, -BT2, -BT5 and -BT4 by GST-tagged PID (right), and only background levels when GST is used in the pull-down assay (left). The bottom panel represents a Coomassie stained gel of the same experiment showing the presence of the GST and the GST-tagged PID.
(D) Autoradiograph (lanes 1, 2 and 3) and Coomassie stained gel (lanes 4, 5 and 6) of a phosphorylation assay containing PID and MBP (lanes 1 and 4), PID, BT1 and MBP (lanes 2 and 5), or BT1 and MBP (lanes 3 and 6).

to mediate both homo- and hetero-dimerization of proteins (Bardwell & Treisman, 1994; Weber *et al.*, 2005; Figueroa *et al.*, 2005), a TAZ domain that also mediates protein-protein interactions (Ponting *et al.*, 1996) and a carboxy-terminal domain that was found to interact with the potato calmodulin 6 (Du & Poovaiah, 2004; Figure 1A). *In vitro* pull down of His-tagged PID with GST-tagged full length BT1, or the GST-tagged BTB or TAZ domains alone (Figure 1A) showed that PID efficiently binds

the BTB domain containing amino-terminus part but not the TAZ domain containing carboxy-terminus part of BT1 (Figure 1B).
BT1 is part of a small protein family comprising five members in arabidopsis that share the same domain structure (Robert *et al.*, 2009), and of which BT1, BT2 and BT4 were found to interact with bromodomain transcription factors (Du & Poovaiah, 2004). *In vitro* pull-down assays showed that His-tagged BT1, -BT2, -BT4 and -BT5 were efficiently pulled down from a crude *E. coli* extract by GST-tagged PID, but not by the GST tag alone (Figure 1C). Although we were not able to test His-BT3 due to unavailability of the full length *BT3* cDNA, our results suggest that PID is a conserved interaction partner for all five arabidopsis BT proteins. Previous genetic and expression analyses of the *BT* family already indicated that there is functional redundancy between the *BT* genes (Robert *et al.*, 2009), and our results suggest that the BT proteins may also act redundantly in the PID pathway.

_BT1_ expression overlaps with that of _PINOID_.

For PID and BT1 to interact *in planta*, it is crucial that their spatio-temporal expression patterns overlap. To investigate this, Northern blot analysis was performed and the results were compared with the available Genevestigator micro-array data (Zimmermann *et al.*, 2004) and the previously published *PID* expression pattern (Christensen *et al.*, 2000; Benjamins *et al.*, 2001). *PID* expression is most abundant in roots, young developing flowers and siliques, and the gene is expressed at relatively low levels in seedling- and plant shoots (Figure S1A). In these tissues, *PID* is expressed in the young vascular tissues and around organ primordia (both in root and shoot; Benjamins *et al.*, 2001). *BT1* mRNA is particularly abundant in seedling shoots, but can also be detected in seedling roots, and in stems and flower buds (Figure S1B). Furthermore, the expression of both *PID* and *BT1* is auxin inducible (Benjamins *et al.*, 2001; Robert *et al.*, 2009; Figure S1C). These data indicate that *PID* and *BT1* expression patterns partially overlap, which corroborates a possible *in vivo* interaction between the two proteins.

BT1 binding to the amino-terminus of PID causes its relocation to the nucleus.

Previous experiments indicated that PID is a PM-associated protein (Lee & Cho, 2006; Michniewicz *et al.*, 2007), whereas BT1 is

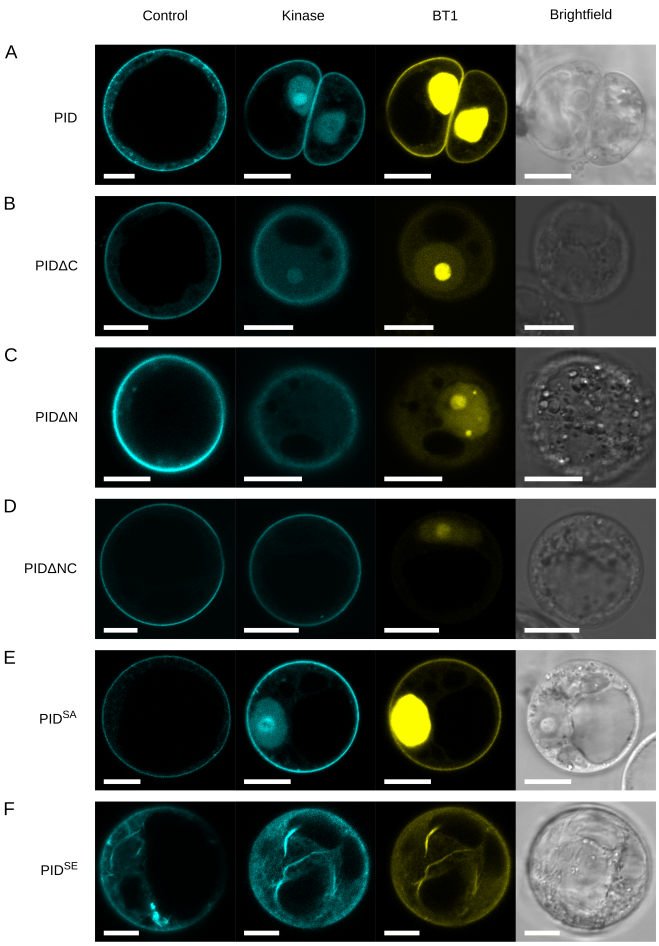

Figure 2: Interaction between co-expressed PID and BT1 in arabidopsis protoplasts leads to mutual relocalization.
(A) Arabidopsis protoplasts co-expressing PID-CFP and BT1-YFP.
(B) Arabidopsis protoplasts co-expressing PIDΔC and BT1-YFP.
(c) Arabidopsis protoplasts co-expressing PIDΔN-CFP and BT1-YFP.
(D) Arabidopsis protoplasts co-expressing PIDΔNC and BT1-YFP.
(E) Arabidopsis protoplasts co-expressing PID^{SA}-CFP and BT1-YFP.
(F) Arabidopsis protoplasts co-expressing PID^{SE}-CFP and BT1-YFP (F).
Left panel: control (kinase-CFP), middle-left panel: CFP (kinase) channel, middle-right panel: YPF (BT1) channel, right panel: bright field image. Size bars indicate 10µm.

predominantly nuclear localized in *35S::BT1-GFP* transfected protoplasts or in *35S::BT1-GFP* plant lines (Robert *et al.*, 2009). Both proteins also show partial localization in the cytosol (Figure 2C; Figure S2; Michniewicz *et al.*, 2007; Robert *et al.*, 2009), indicating that this is where PID and BT1 can meet to form a complex.

Co-expression of PID-CFP and BT1-YFP in arabidopsis protoplasts showed re-localization of both PID-CFP and BT1-YFP (Figure 2A). Besides at the PM, the PID-CFP signal could also be detected in the nucleus, and vice versa the BT1-YFP signal was observed both in the nucleus and at the PM (Figure 2A). This mutual relocalization suggested that the proteins are able to recruit each other to their predominant

location. Based on these results we concluded that PID and the BT proteins can interact both *in vitro* and *in vivo* and that the *in vivo* interaction can result in their subsequent mutual relocalization.
The PID protein has short amino- and carboxy-terminal domains linked to its conserved catalytic kinase core. Co-expression of PID-CFP versions, lacking the amino-terminus, the carboxy-terminus, or both the carboxy- and amino-terminus with BT1-YFP indicated that BT1 binds to the amino-terminus of the PID kinase, since only the versions were this part was deleted did not co-localize with BT1 in the nucleus and did not recruit BT1 to the PM (Figure 2B, C and D).

BT1 represses PID kinase activity.

PID is a protein serine/threonine kinase that can autophosphorylate and activate itself and trans-phosphorylate other proteins (Christensen *et al.*, 2000; Benjamins *et al.*, 2003; Figure 1D, lane 1). However, in *in vitro* reactions no phosphorylation of BT1 was observed. Instead the presence of BT1 in the reaction mixture resulted in a significant reduction of the PID kinase activity, as indicated by the reduced levels of PID autophosphorylation and Myelin Basic Protein (MBP) trans-phosphorylation (Figure 1D). These results suggested that BT1 is not a target of PID phosphorylation, but that it rather functions as a negative regulator of PID activity.
To obtain more *in vivo* confirmation on the possible role of BT1 as negative regulator of PID activity, we generated *35S::BT1* overexpression lines and selected two lines showing significantly increased *BT1* transcript levels for further analysis (Figure 3A). Neither of these lines showed mutant phenotypes, but when we introduced the *BT1* overexpression loci into the intermediately strong *pid-14* loss-of-function mutant background, the penetrance of the tricotyledon phenotype that is typical for *pid* mutant seedlings (Bennett *et al.*, 1995; Figure 3B) was significantly increased from 40% in *pid-14* to 58% in *pid-14 35S::BT1* (Figure 3F). In addition, seedlings with more severe cotyledon phenotypes were observed, such as no-cotyledons (1%, Figure 3C), monocotyledons (2%, Figure 3D) and even tetracotyledons (1% for the combination *pid-14 35S::BT1-2*, Figure 3E), phenotypes that were never observed for *pid-14* mutant seedlings (Figure 3F). These severe phenotypes are observed in some strong *pid* alleles (Bennett *et al.*, 1995), indicating that *BT1* overexpression enhances the mutant phenotypes of the *pid-14* allele during embryo development, which

fits with a role of BT1 as negative regulator of PID. At the adult plant stage, however, *BT1* overexpression did not enhance the typical pin-shaped inflorescence phenotype of the *pid-14* mutant allele.
PID overexpression leads to a significantly reduced auxin accumulation at the root meristem due to a polarity switch in the subcellular localization of PIN auxin efflux carriers (Friml *et al.*, 2004). This results in agravitropic root growth and in the differentiation of root meristem initials, leading to the collapse of the main root meristem (Benjamins *et al.*, 2001). *35S::PID-21*-induced root meristem collapse is observed in 17% of the seedlings at 3.5 days after germination (dag) and in 91% of the seedlings at 5.5 dag (Figure 3G). When the selected *35S::BT1-1* and *-2* overexpression lines were combined with the strong *35S::PID-21* overexpression line, this resulted in a significant reduction of the *35S::PID-21* induced root collapse between 3.5 dag (3% and 7% for *35S::PID-21 BT1-1* and *-2* respectively) and 5.5 dag (71% and 80% for *35S::PID-21 BT1-1* and *-2*, respectively) (Figure 3G). Since the level of PID overexpression in *35S::PID-21 35S::BT1-2* did not significantly differ from that in the parental *35S::PID-21* line (Figure 3A), these results corroborate our previous conclusion that BT1 is a negative regulator of PID activity. Similar to the single overexpression lines, no striking phenotypic changes could be observed in adult *35S::PID-21 35S::BT1* plants.

BT proteins dampen the effect of PID overexpression in adult plants.

Previously, we have shown that PID is required for the correct asymmetric subcellular localization of PIN proteins, and that above-threshold levels of PID expression causes the apicalization of the PIN proteins (Friml *et al.*, 2004; Michniewicz *et al.*, 2007). To investigate whether the observed negative effect of BT1 on PID activity results in changes in PIN polar targeting, we immunolocalized PIN1 and PIN2 in wild-type, *35S::PID-21*, *35S::BT1-1* and *35S::PID-21 35S::BT1-1* seedlings. As expected, in wild-type roots, PIN1 localized at the basal (root tip facing) membrane in endodermis and stele cells (Figure S3A), whereas PIN2 localized basally in the epidermis and apically (shoot apex facing) in the cortex (Figure S3B). In *35S::PID-21* seedlings roots, PIN1 and PIN2 localized to the apical PM in the cells where they are expressed. No significant changes in PIN1 or PIN2 localization were observed in root tips of *35S::BT1-1* or *35S::PID-21 35S::BT1-1* seedlings as compared to

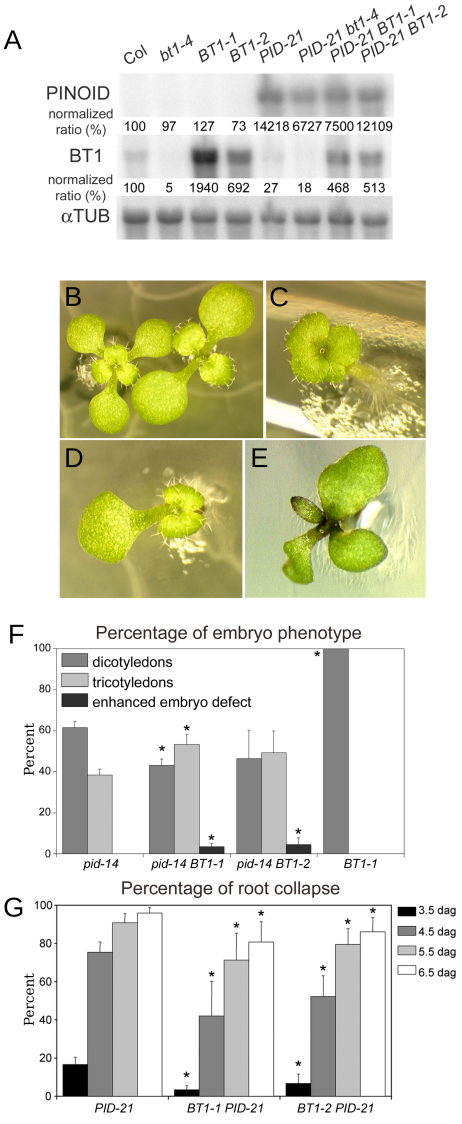

Figure 3: Overexpression of BT1 enhances *pid-14* embryo phenotypes and inhibits *35S::PID-21* root meristem collapse.
A) Northern blot analysis showing *PID* (top), *BT1* (middle) and *α-Tubulin* (bottom) expression in seedlings of *Arabidopsis thaliana* 'Columbia' wild-type, *bt1-4*, the *35S::BT1* overexpression lines -1 and -2, *35S::PID-21* and in seedlings of the crosses *35S::PID-21 bt1-4*, *35S::PID-21 35S::BT1-1* and *35S::PID-21 35S::BT1-2*. The expression levels were quantified using ImageQuant, corrected for loading differences using *α-Tubulin* as a reference and normalized to the expression level in wild type.
(B) Cotyledon phenotypes observed in the *pid-14* mutant line, with the tricotyledon phenotype (left) indicative for seedlings homozygous for the *pid-14* allele.
(C-E) The enhanced cotyledon phenotypes observed in the *pid-14 35S::BT1* line range from no cotyledon (C) and monocotyledon (D) to tetracotyledon (E) seedlings.
(F) Graph showing the proportion of tri- and di-cotyledons seedlings and seedlings with enhanced embryo phenotype (no-, mono- or tetracotyledons) in *pid-14* (n = 290, 424, 298), *pid-14 35S::BT1-1* (n = 372, 658, 367), *pid-14 35S::BT1-2* (n = 302, 688, 408) and *35S::BT1-1* (n = 191, 193). Stars (*) indicated that the values are significantly higher compared to *pid-14* (Student's t-test, $p < 0.05$).
(G) Graph showing the percentage of root collapse at 3.5, 4.5, 5.5 and 6.5 days after germination (dag) in *35S::PID-21* (n = 199, 186, 275), *35S::PID-21 35S::BT1-1* (n = 233, 321, 344), *35S::PID-21 35S::BT1-2* (n = 214, 315, 348). For each time point the values of the *35S::PID-21 35S::BT1* lines were significantly lower than those of *35S::PID-21* (Stars (*), Student's t-test, $p < 0.01$).

wild type or *35S::PID-21*, respectively (Figure S3). These observations indicate that *BT1* overexpression does not result in a clear reversal of the effect of *PID* overexpression on the subcellular PIN1 and PIN2 localization in root tips, and suggest that BT1 is involved in suppressing rather than completely inhibiting PID kinase activity.

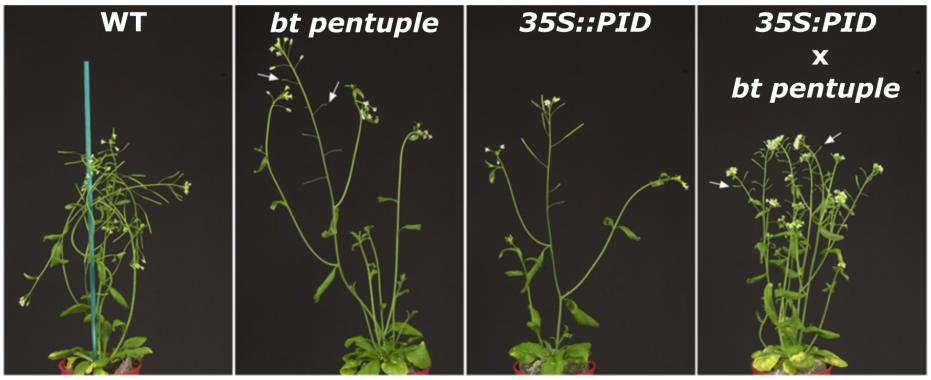

Figure 4: The pentuple *bt1 bt2/+ bt3/+ bt4 bt5* loss-of-function mutant and the *35S::PID* line synergistically enhance each other's phenotypes.

Since our analysis of the arabidopsis BT family indicated that there is considerable functional redundancy among the *BT* genes (Robert *et al.*, 2009), and we showed that at least four of the five arabidopsis BT proteins interact with PID (Figure 1C), we introduced the *PID* overexpression locus of line *35S::PID-21* in the *bt* quintuple loss-of-function mutant background. Flowering *bt1 bt2/+ bt3/+ bt4 bt5* plants showed a mildly reduced apical dominance, similar to what was observed for *35S::PID* plants (Benjamins *et al.*, 2001), but developed shorter siliques compared to wild-type or *35S::PID* plants (Table 1, Figure 4). The latter phenotype was most likely caused by the gametophytic lethality of the *bt* quintuple mutant (Robert *et al.*, 2009). Interestingly, flowering *35S::PID-21 bt1 bt2/+ bt3/+ bt4 bt5* plants were more bushy with short inflorescences and developed even shorter siliques than *bt1 bt2/+ bt3/+ bt4 bt5*, (Table 1 and Figure 4). The synergistic effect of the *bt* quintuple mutant on the relatively mild *PID* overexpression phenotypes in adult plants is in line with the role of BT proteins in suppressing PID kinase activity.

Table 1: *bt* loss of function and *PID* overexpression synergistically reduce silique length.

	silique length[a]	n[b]
Wild type	15.0 ± 1.3	5
bt1 bt2/+ bt3/+ bt4 bt5	8.7 ± 1.6[*]	7
35S::PID-21	14.4 ± 1.0	5
35S::PID-21 bt1 bt2/+ bt3/+ bt4 bt5	5.3 ± 0.6[*] [†] [#]	6

[a] in mm ± standard deviation.
[b] number of siliques measured.
[*] Significantly different from 'Columbia' wild type (Student's t-test, $p < 0.01$).
[†] Significantly different from *35S::PID-21* (Student's t-test, $p < 0.01$).
[#] Significantly different from *bt1 bt2/+ bt3/+ bt4 bt5* (Student's t-test, $p < 0.01$).

The TAZ domain of BT1 interacts with kinesins.

The initial analysis in arabidopsis protoplasts indicated that BT1 is predominantly nuclear and cytosolic localized (Figure 2C, D). However, when onion cells were bombarded with the *35S::BT1-GFP* construct, we observed string-like structures reminiscent of cortical microtubules (Figure S4). Since PID localized to microtubules following phosphorylation by PDK1 (Chapter 3), we co-expressed BT1-YFP with mutant PID-CFP versions where the PDK1 phosphorlyation sites were substituted by alanine (PID^{SA}: loss-of-phosphorylation) or by glutamic acid (PID^{SE}: phospho-mimic) in arabidopsis protoplasts. Like wild-type PID, PID^{SA} co-localized with BT1 in the nucleus and at the PM. In contrast, PID^{SE} and BT1 predominantly co-localized on thread-like structures in the cytosol and no clear nuclear or PM localization was observed (Figure 2F). This result suggested that BT1 might be the scaffold protein that recruits PID to the microtubule cytoskeleton upon PDK1 phosphorylation. Interestingly, a yeast two-hybrid screen for BT1 interacting proteins identified the paralogous PBP2/BT1 Binding Kinesin 1 and 2 (PBK1 and PBK2) belonging to the large family of sixty-one microtubule motor proteins in arabidopsis. The six cDNA clones that were picked up in the yeast two-hybrid screen, two for *PBK1* (*At4g38950*) and four for *PBK2* (*At2g21300*), were all partials encoding only the carboxy-terminal portions PBK1CT and PBK2CT, respectively. These results indicate that the carboxy-terminal portion of the kinesins interacts with BT1 (Figure 5A). *In vitro* protein pull down experiments using affinity-purified histidine-tagged PBK2CT and GST-tagged BT1 confirmed this interaction

(Figure 5B). Additional *in vitro* protein pull down experiments with histidine-tagged PBK2CT and GST-tagged versions of the BTB domain- or the TAZ domain-containing portion of BT1, showed that PBK2CT preferentially interacts with the TAZ domain part of BT1 (Figure 5B). Earlier, we showed that PID interacts with the BTB domain containing portion of BT1 (Figure 1B), and our current finding builds to the model that BT1 may act as a scaffold protein that is involved in relocating PID to the MT after its activation by PDK1, by forming a protein complex using its TAZ and BTB interaction domains to bind PBK1/2 and PID.

The PBK kinesins are family members of the AtNACK kinesins.

Alignment of the PBK1 and PBK2 amino acid sequences showed that these proteins are very similar, sharing an overall amino acid identity of 81.6% (Figure 5A). Protein domain analysis using ScanProsite software identified their motor domains to be located at the amino-terminus, suggesting a minus to plus-end motility on MT strands (Wade & Kozielski, 2000). Separate analysis of the different parts of the PBK proteins indicated that they share respectively 91% and 75.4% amino acid identity in their motor- and carboxy-terminal BT1-interacting domains (Figure 5A). Alignment of the full length amino acid sequences of the arabidopsis kinesins (Figure 5C) confirmed a previous large scale comparison of kinesins, indicating that PBK1 and PBK2 belong to a plant-specific clade that includes proteins encoded by the genes *At3g51150*, *At4g24170*, *At5g42490* and *At5g66310*, and the well-characterized kinesins AtNACK1/HINKEL and STUD/TETRASPORE/AtNACK2. The latter two are involved in cell plate expansion during gametophytic cytokinesis (Nishihama *et al.*, 2002; Yang *et al.*, 2003; Tanaka *et al.*, 2004; Oh *et al.*, 2008). The eight clade members share four highly conserved domains: an amino-terminal motor domain, a single coiled-coil domain and two domains of unknown function in the carboxy-terminal region (Figure 5A). The proposed binding site for the arabidopsis MAPKKK-ortholog AtNPK1 (Nishihama *et al.*, 2002) that is present in the carboxy-terminus of AtNACK1 and 2, could not be identified in other members of the clade, suggesting that AtNPK1 acts specifically on the AtNACKs and not on the other kinesins of this clade.

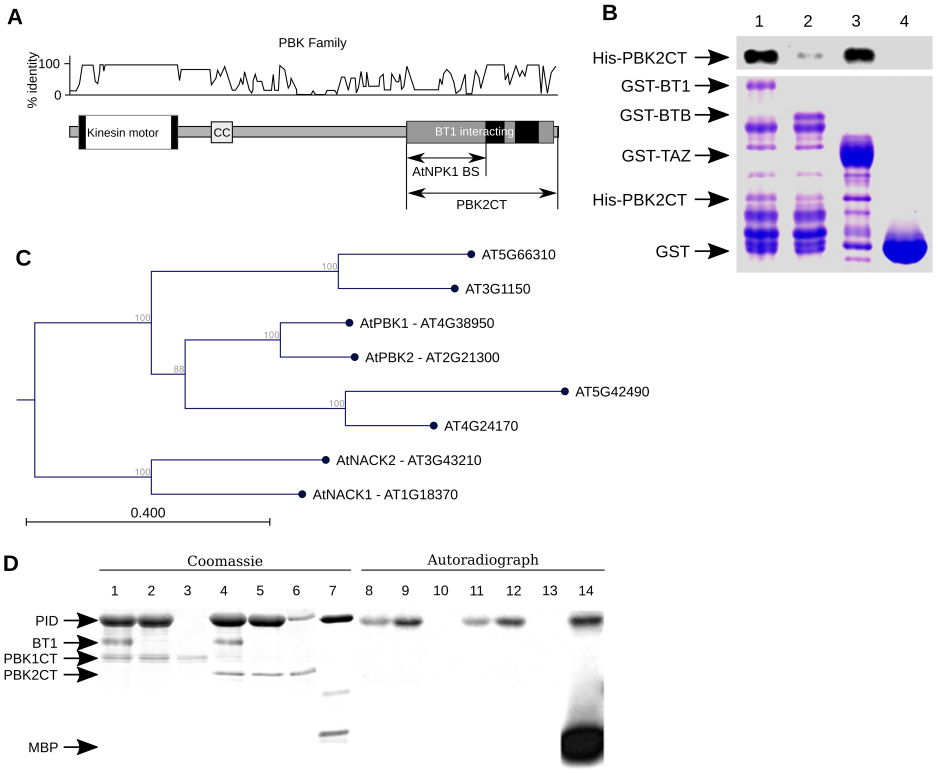

Figure 5: The plant specific kinesins PBK1 and PBK2 interact with BT1, but are not phosphorylated by PID *in vitro*.
(A) Graph showing the percentage of identity between the eight PBK clade members (upper part) in relation to their different conserved domains (lower part). Indicated are the kinesin motor domain, the coiled-coil domain (CC), the arabidopsis NPK1-ortholog binding site (AtNPK1 BS) in AtNACK1/2, and the two PBK clade-specific PFam signatures (black boxes). The PBK clade-specific domains are present in the region corresponding with the 258 amino acid BT1-interacting carboxy-terminal portion of PBK2 (PBK2CT) that was picked up in the yeast two-hybrid screen and subsequently used in the *in vitro* pull down.
(B) Immuno-detection (top, anti-HIS) and coomassie stained gel (bottom) of an *in vitro* pull down assay using his-tagged PBK2CT together with GST-tagged BT1 (lane 1), GST-tagged BTB (lane 2) or TAZ domain containing portion (lane 3) of BT1 or the GST protein alone (lane 4).
(C) Phylogenetic tree showing the PBKs and their plant-specific relatives. Bootstrap values, based on 100 repeats, are indicated.
(D) Coomassie stained gel (lanes 1 to 7) and autoradiograph (lanes 8 to 14) of an *in vitro* phosphorylation assay using PID (lanes 1, 2, 4, 5, 7, 8, 9, 11, 12 and 14), BT1 (lanes 1, 4, 8 and 11), PBK1CT (lanes 1 to 3 and 8 to 10), PBK2CT (lanes 4 to 6 and 11 to 13) and MBP (lanes 7 and 14).

The carboxy-terminus of PBK kinesins is not phosphorylated by PID.

BT1-dependent recruitment of PID to PBK1 and PBK2 could function to alter their functionality through phosphorylation, as has been reported for cyclin-dependent kinases (CDKs), where phosphorylation of the carboxy-terminus both NACK1 and NPK1 prevents their interaction and stalls mitotic progression (Sasabe *et al.*, 2011). To test this possibility, we performed *in vitro* phosphorylation assays using PID and PBK2CT or PBK1CT with or without BT1 in separate reactions. The general phosphorylation substrate Myelin Basic Protein (MBP) was used as a positive control. While strong phosphorylation of MBP could be detected, no significant PID-dependent phosphorylation of PBK1CT or PBK2CT was observed in these experiments, even in the presence of BT1 (Figure 5D), indicating that carboxy-terminal domains of the kinesins are not targets for phosphorylation by PID. This observation, however, does not exclude the possibility that PID phosphorylates residues in the amino-terminus part of PBK1/2. Interestingly, the presence of BT1 reproducibly reduced the autophosphorylation activity of PID, which is in line with the proposed function of BT1 in suppressing PID activity.

The PBKs cause BT1-dependent MT localization of PID.

The identification of kinesins as BT1 interacting proteins made us hypothesize that the previously observed PDK1-induced PID relocalization to the MT could be mediated by the BT-PBK complex. While we already showed that the interaction between PID and BT1 in protoplasts caused relocalization of PID to the nucleus, cotransfection of PID with PBK1 resulted in a relocalization of PID to thread-like structures in the cytosol (Figure 6A). Treatment of protoplasts with the MT depolymerizing agent oryzalin dissolved these thread-like structures, confirming that PID colocalizes with PBK1-YFP on the MT (Figure 6B). Interestingly, in these cotransfections, PID localized to the MT, even without PDK1 induction. This suggested that phosphorylation of PID causes a conformational change in the protein that decreases its affinity for the PM, and enhances its affinity for the BT-PBK complex. The fact that enhanced expression of PBK1 in the cell also resulted in MT recruitment of PID (Figure 6B) suggested that the PBK component was rate-limiting for PID-BT-PBK complex formation. Cotransfection of the PID^{SA} loss-of-phosphorylation mutant with PBK1-YFP also resulted in its translocation to the MT

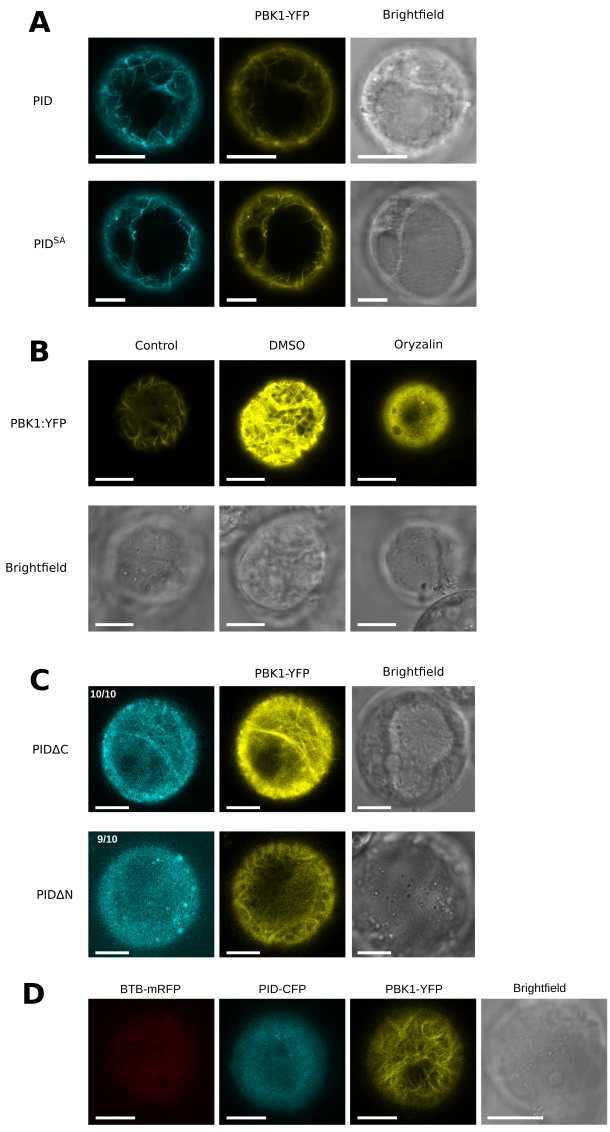

Figure 6: BT-dependent PID relocalization to MT by PBK does not require phosphorylation by PDK1.
(A) Arabidopsis protoplasts co-expressing PID-CFP and PBK1-YFP (upper panels), and PID^{SA}-CFP and PBK1-YFP (lower panels). Left panels: CFP (kinase) channel, middle panels: YPF (PBK1) channel, right panels: bright field image.
(B) Confocal YFP channel images showing PBK1-YFP localization in untreated, DMSO treated and Oryzalin treated arabidopsis protoplasts, respectively (upper panels) and bright field images of the same cells (lower panels).
(C) Arabidopsis protoplast co-expressing PIDΔC-CFP and PBK1-YFP (upper panels), and PIDΔN-CFP and PBK1-YFP (lower panels). Left panels: CFP (kinase) channel, middle panels: YPF (PBK1) channel, right panels: bright field image.
(D) Arabidopsis protoplast co-expressing BTB-mRFP (left), CFP-tagged PID, (middle, 2^{nd}) and PBK1-YFP (middle, 3^{rd}). Bright field image is in the right panel.
Size bars indicate 10µm.

(Figure 6A), confirming that PBK1 levels are rate-limiting, and that enhanced PBK levels are sufficient to recruit PID to the MT, independent of PDK1-mediated phosphorylation of PID.

In our model PID links to the PBKs through the BT proteins, and we have shown before that PID binds to the BT proteins through the amino-terminus. To show that BT1 is required as scaffold to recruit PID and the PBKs and cause MT localization of the kinase, we cotransfected PID-CFP versions lacking the amino- or carboxy-terminus

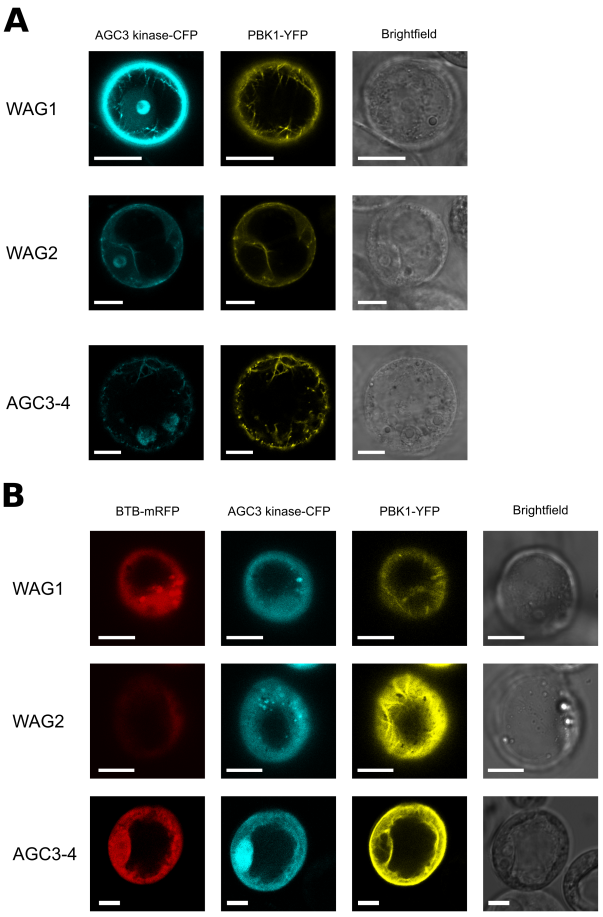

Figure 7: The AGC3 kinases WAG1, WAG2 and AGC3-4 are also recruited to the MT by the BT-PBK complex.
(A) Arabidopsis protoplasts co-expressing CFP-tagged WAG1, WAG2, or AGC3-4 (left) with PBK1-YFP (middle). Bright field image of the same protoplasts are in the right panel.
(B) Arabidopsis protoplasts co-expressing BTB-mRFP (left), PBK1-YFP (middle, 3rd) with CFP-tagged WAG1, WAG2 or AGC3-4 (middle, 2nd) Bright field image of the same protoplasts are in the right panel.
Size bars indicate 10µm.

with PBK1-YFP. The PID version lacking the amino-terminus did not localize to the MT in 9 out of 10 observed protoplasts, while the PID version without the carboxy-terminus did localize to the MT cytoskeleton in 10 out of 10 observed protoplasts (Figure 6C). Co-expression of PID-CFP with PBK1-YFP and the BTB domain-containing part of BT1 fused to mRFP (BTB-mRFP) resulted in cytosolic localization of PID-CFP and BTB-mRFP, whereas PBK1-YFP was found at the MT (Figure 6D). These results not only confirm the involvement of BT1 in MT localization of PID, but also suggest that the BTB domain alone is quite effective in recruiting the kinase from the PM to the cytosol. Moreover, the results suggest that the predicted nuclear localization signal (NLS) in the BTB domain (Robert *et al.*, 2009) is not sufficient to confer nuclear localization of BT1. Co-expression of CFP fusions of the other three AGC3 kinases

with PBK1-YFP, or with BTB-mRFP and PBK1-YFP showed that PBK1 can also relocalize these kinases to the MT (Figure 7A), and that this relocalization is dependent on the full length BT1 protein (Figure 7B). Based on these results we conclude that MT recruitment by the BT-PBK complex is conserved among the AGC3 kinases. For PID this recruitment can be enhanced by PDK1-dependent phosphorylation, but for the other three AGC3 kinases no MT localization was observed when they were co-expressed with PDK1 (Figure S5). For WAG1 and WAG2 it has been shown that they are not PDK1 targets (Zegzouti *et al.*, 2006b), and it is more likely that these kinases are recruited when the levels of the BT-PBK components in the cell are not rate-limiting.

Discussion

An important characteristic of the plant hormone auxin is its polar transport, which generates gradients and maxima that are instructive for cell division and growth during plant development. PIN proteins have been identified as auxin efflux carriers that determine the direction of transport through their asymmetric subcellular localization (Gälweiler *et al.*, 1998; Petrášek *et al.*, 2006; Wiśniewska *et al.*, 2006). Previously, we reported that the protein kinase PID controls the direction of the auxin flux by regulating the subcellular localization of the PIN proteins by phosphorylating conserved serine residues in their hydrophilic loop (Friml *et al.*, 2004; Huang *et al.*, 2010; Dhonukshe *et al.*, 2010). In this process, PID acts antagonistic to specific PP2A/PP6-type phosphatases (Garbers *et al.*, 1996; Michniewicz *et al.*, 2007; Dai *et al.*, 2012; Ballesteros *et al.*, 2013), and its PM association was shown to be important for efficient (maintenance of) PIN protein phosphorylation (Dhonukshe *et al.*, 2010). The PM association of PID is regulated either by changes in the composition of the PM (Dhonukshe *et al.*, 2010; Simon *et al.*, 2016), or by PBPs that trigger PID relocalization. A previous yeast two-hybrid screen identified several PID interacting proteins, of which the two calcium binding proteins TCH3 and PBP1 were shown to bind PID in calcium-responsive manner (Benjamins *et al.*, 2003; Fan, 2014). For TCH3 it was shown that it sequesters PID from the PM, displacing the kinase from the vicinity of its PIN phosphorylation targets, in response to elevated cytosolic calcium levels. This interaction was shown to play a role in enhancing the root gravitropic response (Fan, 2014). Here we show

that the plant specific BTB and TAZ domain protein1 (BT1) binds PID, and that this protein, like TCH3, is not phosphorylated by the kinase, but instead inhibits PID kinase activity. Unlike TCH3, however, BT1 does not bind the PID catalytic core but rather the amino-terminal part of PID, suggesting that the primary function of this interaction is not inhibition but rather modulation and fine tuning of PID activity. In line with this, *BT1* overexpression delayed the root meristem collapse in *PID* overexpressing arabidopsis seedlings without having a significant effect on the *PID* overexpression-induced basal-to-apical (root- to shootward) switch in PIN polarity.

As predicted from its domain structure, BT1 is likely to serve as a scaffold protein that recruits PID to the appropriate signaling complex and/or subcellular localization. Indeed, BT1 was shown to induce nuclear or microtubule localization of PID in arabidopsis protoplasts, the latter because it links PID to the kinesins PBK1 and PBK2. While this subcellular localization for PID has only been observed in protoplasts and not *in planta*, the maize PID ortholog BARREN INFLORESCENCE 2 (BIF2) was shown to be nuclear localized and to phosphorylate the nuclear bHLH transcription factor (McSteen *et al.*, 2007; Skirpan *et al.*, 2008). Interestingly, the other three arabidopsis AGC3 kinases WAG1, WAG2 and AGC3-4 do show nuclear localization (Galván-Ampudia & Offringa, 2007), suggesting that also in arabidopsis these kinases have a role in the nucleus. The fact that in protoplasts all three kinases can be recruited by PBK1/2 to the microtubule cytoskeleton in a BT1-dependent manner suggests that the interaction between these kinases and BT1 is possible *in vivo*. Whether the nuclear localization of these kinases is dependent on BT proteins remains to be determined.

The observation that all four AGC3 kinases form a complex with BT-PBK in protoplasts was quite surprising, since WAG1, WAG2 and AGC3-4 are not phosphorylated by PDK1 (Zegzouti *et al.*, 2006b). In fact, co-expression of WAG1, WAG2 and AGC3-4 with PDK1 in protoplasts did not result in MT relocalization. We therefore conclude that recruitment of AGC3 kinases to the MT can occur via two mechanisms: 1) for PID by PDK1-mediated phosphorylation, which enhances the affinity of the kinase for the BT-PBK complex and allows its recruitment to the MT, or 2) for all four kinases by enhanced expression of one of the PBKs, which drives the abundance of the BT-PBK complex and thus allows recruitment of the kinase at low affinity conditions.

The enhanced cotyledon phenotypes observed for *pid-14 35S::BT1-1* seedlings are reminiscent of phenotypes observed for *pid14 wag1* or *pid14 wag2* double mutant seedlings (Dhonukshe *et al.*, 2010), suggesting that the higher BT1 levels repress the activity of the redundantly acting WAG1 and WAG2 kinases. In contrast, however, *BT1* overexpression did not enhance the inflorescence phenotype of the *pid-14* allele. It is unlikely that this is caused by the use of the *35S* promoter, since this promoter is known to be active in floral meristems and in flowers (Bossinger & Smyth, 1996; Meister *et al.*, 2005), and overexpression of other genes, e.g. *MADS-box* genes, using this promoter has led to clear flower/inflorescence phenotypes (Robles & Pelaz, 2005). Previously, we have shown that BT1 is an unstable protein that is a target for degradation by the 26S proteasome, and that the instability might be linked to the BTB domain (Robert *et al.*, 2009). The absence of the effect of *BT1* overexpression may be due to instability of the BT1 protein in these tissues. It would be interesting to test whether BT1 is involved in PID turn-over as part of its own degradation process. In this respect it has always been peculiar why *PID* overexpression only leads to strong phenotypes at the young seedling stage, and that at later developmental stages *35S::PID* plants only show a few minor defects. The enhanced phenotypes at the adult plant stage, such as dwarf, bushy stature and short siliques, when the *35S::PID-21* construct was introduced into the quintuple *bt* mutant background, are in line with a model where BT proteins reduce PID activity, by inhibiting, relocating and/or by causing degradation of the kinase. Another class of BTB domain containing proteins for which a genetic interaction with PID has been established is formed by the MACCHI-BOU 4/ENHANCER OF PINOID-Like/NAKED PINS IN YUC MUTANTS (MAB/MEL/NPY) proteins (Treml *et al.*, 2005; Furutani *et al.*, 2007; Cheng *et al.*, 2007). In contrast to BT proteins, the MAB/MEL/NPY proteins seem to act in concert with PID to enhance PIN polarity during embryogenesis and inflorescence development. As a result, *npy* loss-of-function mutations enhance *pid* phenotypes and affect PIN1 localization and expression in the embryo and inflorescence meristems. It could be that the NPY proteins bind to PID as well and that as a result BT proteins compete with the NPY proteins for PID interaction and regulation.

In conclusion, here we show that the PID kinase and its close homologs interact with BT scaffold proteins, which in turn interact with the MT motor proteins PBK1 and PBK2 (Figure 8). In the absence of the PBKs,

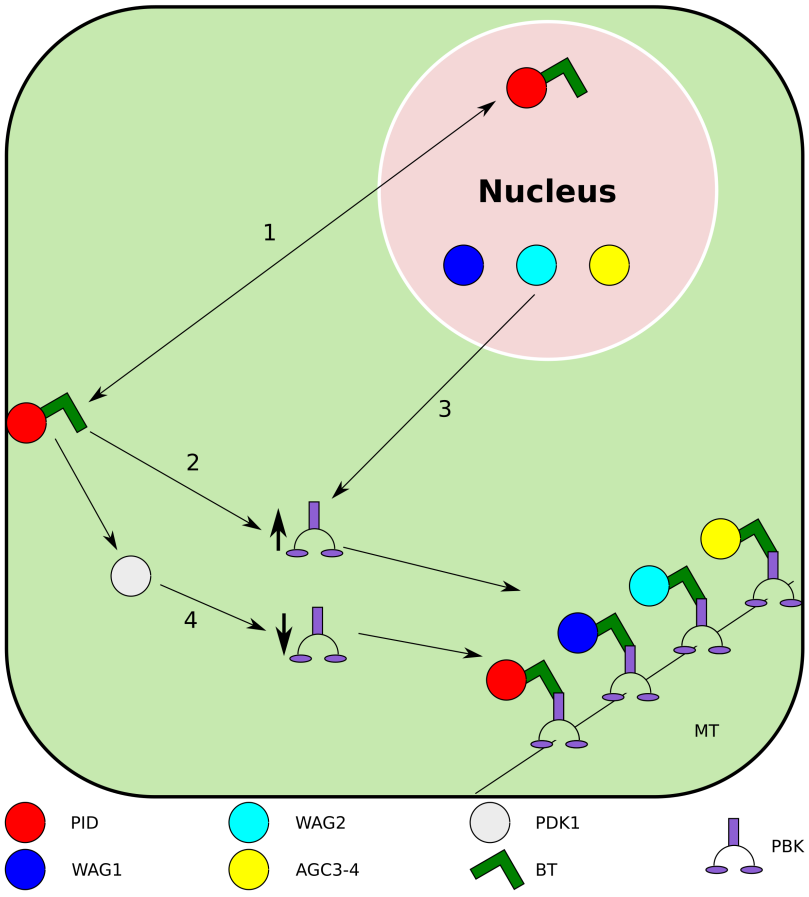

Figure 8: Model describing the regulation of AGC3 kinase activity by the BT/PBK complex. AGC3 kinases are PM-associated proteins, of which PID is recruited to the nucleus by the scaffold protein BT1 (1). The other three kinases show clear nuclear localisation, but it is unclear whether BT1 plays a role in this. Based on what is known from the PID ortholog in maize, the nuclear kinases probably regulate gene transcription by phosphorylation of specific transcription factors. All four kinases can also be recruited to the MT cytoskeleton by forming a complex with PBK1 or PBK2 through BT proteins. If PBK levels in the cell are high, kinase phosphorylation by PDK1 is not required for the recruitment of the AGC3 kinases (2,3). When PBK levels in the cell are low only PID can be recruited to the MT cytoskeleton following phosphorylation by PDK1 (4). The MT localized AGC kinases might be stored in an inactive state, transported to specific subcellular locations, or the kinases might be involved in MT reorganisation.

this interaction allows the predominantly PM-associated PID kinase (and possibly also WAG1, WAG2 and AGC3-4) to relocalize to the nucleus, were the kinase, in analogy to the maize BIF2, possibly affects gene expression

by phosphorylating specific transcription factors. Sufficient expression of the PBKs stabilizes the BT1-PBK complex, which subsequently recruits the kinase to the MT cytoskeleton. However, when PBK levels in the cell are low, the formation of the kinase-BT1-PBK complex requires activation of the kinase by PDK1-dependent phosphorylation. This latter route is only used by PID, since the other kinases are not phosphorylated by PDK1. Possible roles for the MT localization of PID (and the other kinases) might be 1) to alter the structure or polarity of the MT cytoskeleton, 2) to transiently store the kinase at a distance from its phosphorylation targets (feed-back), or 3) to directionally transport the kinase via the MT cytoskeleton to new phosphorylation targets (at the PM). Further research is required to show that AGC3 kinases actually localize to the MT cytoskeleton *in planta*, and what role this has in the regulation of polar auxin transport during plant development.

Acknowledgments

We would like to thank Ward Winter, Douwe Doevedans, Niels Wattel, and Daan Brand for technical assistance, Gerda Lamers for helpful advice concerning microscopy, Jiří Friml and Christian Luschnig for providing respectively PIN1 and PIN2 antibodies. This work was financially supported by the Brazilian Funding Agency for Post-Graduation Education-CAPES (M.K.Z.). C. G.-A. was supported by the Earth and Life Sciences Division (ALW 813.06.004 to R.O.), and M.E.J.H. and E.R. were supported by the Chemical Sciences Division (CW TOP 700.58.301 to R.O), both with financial support from the Netherlands Organisation for Scientific Research (NWO). Y.X. was supported by the Royal Dutch Academy of Sciences (CEP project 10CD016)

Material and Methods

Molecular cloning and constructs

Molecular cloning was performed following standard procedures (Sambrook *et al.*, 1989), using primers listed in Table 2. The complete coding region of PID, excluding the start codon, was amplified using primers PID-*Sal*I-F1 and PID-*Xba*I-R1 and cloned into *pBluescriptSK+* to create *pBS-PID* (pSDM6005). The cDNA of *PID* was then amino-terminally fused (*Xmn*I-*Sal*I) to the His-tag (10x His) present in *pET16H* (Klenow blunted *BamH*I-*Xho*I), a derivative of *pET16B* (J. Memelink, unpublished results). The construct *pGEX-PID* (pSDM6004) has been described before (Benjamins *et al.*, 2003). The *35S::PID-GFP* construct was generated by amplifying the *PID* cDNA using the primers PID cDNA F and PID cDNA R and the *eGFP* coding region using the primers eGFP F and eGFP R. Both PCR products were used in a fusion PCR with outer primers, and the amplified *PID-GFP* fragment was cloned into *pUC28* digested with *Nco*I and *Hinc*II, and excised again with *EcoR*I and *Stu*I (blunted) for ligation into *EcoR*I-*Sma*I digested *pART7* (Gleave, 1992). The *35S::PID-CFP* construct was made using the Gateway Technology (Invitrogen). The *PID* cDNA was PCR amplified from *pGEX-PID* with primers PID attB1 F and PID –Stop attB R and a BP reaction was performed into *pDONOR207* according to manufacturer's instructions (Invitrogen, USA). Recombinant plasmid was isolated and sequenced. LR reaction was performed into a *pART7*-derived plasmid containing the CFP fluorescent markers in frame with the gateway recombinant cassette (Dhonukshe *et al.*, 2010).

The plasmids *pBS-BT1* (pSDM6014), *pUC28-BT2* (pSDM6069), *pC1300-BT1* (pSDM6086), *pUC28-BT4* (pSDM6092), *pART7-BT1-YFP* (pSDM6099) and *pDONOR207-BT5* (pSDM6309) were previously described (Robert *et al.*, 2009). The cDNA of BT1 (*Xho*I-*Sma*I digested from *pBS-BT1*), excluding the start codon, was cloned into *pGEX-KG* (Guan & Dixon, 1991) to obtain *pGEX-BT1* encoding an amino-terminal GST-BT1 fusion. The plasmid *pGEX-BTB*, encoding the GST-tagged BT1 BTB/POZ domain, was generated by digesting *pGEX-BT1* with *Nde*I and filling in with Klenow. The plasmid *pGEX-TAZ*, encoding the GST-tagged BT1 TAZ domain, was constructed by deleting the *Nco*I fragment from *pGEX-BT1*. For the amino-terminal His-BT1 fusion used within the *in vitro* pull-down and the *in vitro* phosphorylation assay experiments, the *BT1*

Table 2: Primers list. Underlined bases are restriction sites.

Name	Sequence (5'→3')
PID attB1 F	GGGGACAAGTTTGTACAAAAAAGCAGGCTTCAGCATGTTACGAGAATCAGACGGT
PID –Stop attB R	GGGGACCACTTTGTACAAGAAAGCTGGGTCAAAGTAATCGAACGCCGCTGG
PID cDNA F	TTAATATGACTCACTATAGG
PID cDNA R	GCTCACCATAAAGTAATCGAACGC
eGFP F	GATTACTTTATGGTGAGCAAGGGC
eGFP R	TCAATCTGAGTACTTGTACAG
AT2 attB F	GGGACAAGTTTGTACAAAAAAGCAGGCTTCAGCATGGCTAATTCTAGTATCTTT
AT2 -Stop attB R	GGGGACCACTTTGTACAAGAAAGCTGGGTCAAAATAATCAAAATAATTAGA
WAG1 attB F	GGGGACAAGTTTGTACAAAAAAGCAGGCTTCAGCATGGAAGACGACGGTTATTAC
WAG1 –Stop attB R	GGGGACCACTTTGTACAAGAAAGCTGGGTCTAGCTTTTTACCCACATAATG
WAG2 attB F	GGGGACAAGTTTGTACAAAAAAGCAGGCTTCAGCATGGAACAAGAAGATTTCTAT
WAG2 –Stop attB R	GGGGACCACTTTGTACAAGAAAGCTGGGTCAACGCGTTTGCGACTCGCGTA
BT1 cDNA Sal1	CCGTCGACGCTATAAACCGCCACTCA
BT1 cDNA Pst1	CCGGAACAAGTTAATGTGACTGCAGAA
BT1 attB F	GGGGACAAGTTTGTACAAAAAAGCAGGCTTAATGGCTATAACCGCCACT
BT1 -Stop attB R	GGGGACCACTTTGTACAAGAAAGCTGGGTACATTAACTTGTTCCGGAT
PID -N-tail S attB1	GGGGACAAGTTTGTACAAAAAAGCAGGCTTCATGTTTCGCCTCATGCGTCGTATCG
PID -C-tail AS attB2	GGGGACCACTTTGTACAAGAAAGCTGGGTCGAGCGCAAAGTTTAGACC
attB PBK1 F	GGGGACAAGTTTGTACAAAAAAGCAGGCTTAATGGAGAAGACACAGATGCCTGTAGC
attB -STOP PBK1 R	GGGGACCACTTTGTACAAGAAAGCTGGGTTGAAAAGTGCAGGCATGCTTTTTCTCCAACTATG
attB1-BTB	GGGGACAAGTTTGTACAAAAAAGCAGGCTTTATGGAAACTGATGTTGAGATCATCACCTCCGG
attB2-BTB	GGGGACCACTTTGTACAAGAAAGCTGGGTCCATCTCATTCTCCGTGACACTCGG
PID-SalI-F1	GGGTCGACTTACGAGAATCAGACGGTGAG
PID-XbaI-R1	CCTCTAGACCGTAGAAAACGTTCAAAAGT
BT1 probe F	CATCCCAAACATTACAAAGGGC
BT1 probe R	TTCTCCGAGGTTCGTCTTTC
PID probe F	AGGCACGTGACAACGTCTC
PID probe R	CGCAAGACTCGTTGGAAAAG
TUB probe F	CGGAATTCATGAGAGAGATCCTTCATATC
TUB probe R	CCCTCGAGTTAAGTCTCGTACTCCTCTTC

coding region which excluded the start codon was cloned as a *Xho*I-*Sma*I fragment into *pET16H*. The *BT2* cDNA was cloned (*Eco*RI-*Bam*HI from *pUC28-BT2*) in frame with a His-tag in *pET16H* to obtain *pET16H-BT2*. The *BT4* cDNA was cloned (*Eco*RI-*Bam*HI from *pUC28-BT4*) in frame with the His-tag in *pET16H* to obtain *pET16H-BT4*. The translational fusion between *BT5* cDNA (from *pDONR207-BT5*) and the His-tag was generated into the *pET16H* derived destination vector, creating *pET16H-BT5* (C. Galván-Ampudia, unpublished data) using the Gateway technology (Invitrogen, USA). Histidine-tagged PBK1CT and PBK2CT expression vectors were created by excising PBK1CT and PBK2CT from the *pACT2-PBK1CT* and *pACT2-PBK2CT* yeast two-hybrid clones with *Nde*I/*Xho*I and cloning these fragments into the corresponding restriction sites in *pET16B* (Novagen, Germany).

The *35S::GFP-BT1* construct used in the onion epidermis cell particle bombardment experiment was generated by fusing the coding sequence of BT1 to the carboxy-terminus of the GFP in *pTH2* (Chiu *et al.*, 1996) as an *Xho*I-*Sma*I fragment. To generate the fluorescent fusions for the protoplast experiments, Gateway technology was used. For PID and AGC3-4 the coding regions were amplified from *Arabidopsis thaliana* 'Columbia' cDNA using the primer sets PID attB F with PID - Stop attB R, and AT2 attB F with AT2 -Stop attB R, respectively. For WAG1 and WAG2 *Arabidopsis thaliana* 'Columbia' genomic DNA was used in combination with the primer sets WAG1 attB F with WAG1 -Stop attB R, and WAG2 attB F with WAG2 –Stop attB R, respectively. For the BTB fragment the *pART7-BT1-YFP* construct was used in combination with primers attB1-BTB and attB2-BTB. Resulting PCR products were recombined into *pDONR207* to generate entry clones for the AGC kinases and the BTB domain.
The *pDONR-PID* entry clone was used in PCR reactions with primer combinations PID -N-tail S attB1 and PID –Stop attB R, or with PID attB1 F and PID -C-tail AS attB2, and the resulting fragments were BP recombined in *pDONR207* resulting in *pDONR-PIDΔN* and *pDONR-PIDΔC*, respectively.
The yeast two-hybrid bait plasmid *pAS2-BT1* was obtained by cloning a BT1 *Pst*I/*Sal*I fragment derived from *pBS-BT1* into *pAS2* digested with *Pst*I/*Xma*I.

Yeast two-hybrid screens

The yeast two hybrid screens were performed using the Matchmaker (PID) and Matchmaker II (BT1) system (Clontech, USA) and the *Saccharomyces cerevisiae* strain PJ69-4A (James *et al.*, 1996; Clontech, USA). For each screen PID or BT1 were fused to the GAL4 DNA binding domain as bait. The cDNA libraries used were constructed from *Arabidopsis thaliana* 'Columbia' mRNA samples isolated from a mix of untreated and 24 hour 1µM 1-naphthaleneacetic acid (1-NAA) treated root cultures (1:1 ratio; PID and BT1) and mRNA isolated from green tissue of 6 week old flowering *Arabidopsis thaliana* 'Columbia' plants (PID). The used cDNA libraries were fused to the GAL4 activation domain. The yeast two-hybrid screens were performed at 20°C (PID and BT1) and 30°C (PID), as described previously (Benjamins *et al.*, 2003).

Arabidopsis lines and plant growth

The *35S::PID-21* line (Benjamins *et al.*, 2001), the *pid-14* allele (Dhonukshe *et al.*, 2010; SALK_049736) and the quintuple mutant *bt1 bt2/+ bt3/+ bt4 bt5* (Robert *et al.*, 2009) have been described previously. Arabidopsis seeds were surfaced-sterilized by incubation for 15 minutes in 50% commercial bleach solution, rinsed four times with sterile water and resuspended in 0.1% agarose for plating. Seeds were vernalized for 2 to 4 days before germination (21°C, 16-hour photoperiod and 3000 lux) on solid MA medium (Masson & Paszkowski, 1992) supplemented with antibiotics when required. Two to three week old plants were transferred to soil and grown at 21°C with a 16-hour photoperiod of 10000 lux and at 70% relative humidity.
Arabidopsis thaliana 'Columbia' was transformed by floral dipping method as described (Clough & Bent, 1998) using *Agrobacterium tumefaciens* strain LBA1115. The binary construct *35S::BT1* was transformed into *Arabidopsis thaliana* 'Columbia' plants. Primary transformants were selected on medium supplemented with 20 µg/ml hygromycin for the 35S constructs and 100 µg/ml timentin to inhibit *A. tumefaciens* growth. For further analysis, single locus insertion lines were selected by segregation on 10 µg/ml hygromycin and analyzed for expression by Northern blot analysis.

Particle bombardment of onion epidermal cells

Gold particles with a 1.0 and 1.6 µm diameter (mixed in 1:1 ratio) were coated with 10µg plasmid for expressing GFP-BT1 by precipitation (Varagona *et al.*, 1992). Onion epidermal cells were bombarded using a helium gun (Biolistic Particle Delivery Systems, BioRad, USA). After incubation at 28°C in the dark for 12 to 36 hours, the cells were stained with 0.1mM propidium iodine (PI) solution and imaged using a confocal microscope.

Protoplast transfection

Protoplasts were made from *Arabidopsis thaliana* cell suspensions generated and maintained as described originally by Axelos and coworkers (Axelos *et al.*, 1992) and adapted by Schirawski and coworkers (Schirawski *et al.*, 2000). For protoplast isolation, a 50ml 1-day old 1:5 dilution of a week old cell suspension was pelleted at low speed (1000 RPM,

5 min). The supernatant was discarded and replaced by 20ml enzyme mix (0.4% Macerozyme R10, 2% Cellulase R10, 12% Sorbitol, pH set to 5.8 by KOH) and incubated at 28°C in dark for 2.5 hours. After incubation the protoplasts were sieved by a 70µm cell sieve and washed 3 times with sterile protoplast medium (25mM KNO_3, 1mM $MgSO_4$, 1mM NaH_2PO_4, 1mM $(NH_4)_2SO_4$, 1.16 mM $CaCl_2$, 0.56mM myo-inositol, 10mg Thiamine-HCl, 1mg Pyridoxine-HCl, 1mg Nicotinic acid, 36.7mg FeEDTA, 48.52µM H_3BO_3, 59.17µM $MnSO_4$, 6.96µM $ZnSO_4$, 4.52µM KI, 0.75µM Na_2MoO_4, 0.1µM $CuSO_4$, 0.11µM $CoCl_2$, 0.1M Glucose, 0.25M Mannitol, 1µM NAA, pH set to 5.8 with KOH). Protoplasts were taken up in protoplast medium to a final concentration of $4*10^6$ cells/ml. 250µl protoplasts were added to 10µg plasmid (maximum of 10µl volume). 250µl PEG solution (40% polyethylene glycol 4000, 0.2M mannitol, 0.1M $CaCl_2$) was added dropwise with gently mixing the protoplasts every time after adding 3 drops of PEG solution. After all PEG had been added, the protoplasts were left to incubate for 10 minutes. After incubation the protoplasts were put in a sterile 6-well plate (Greiner Bio-One, Germany, No. 657185) with 4.5ml protoplast medium. The whole plate was wrapped in aluminum foil and incubated overnight at 28°C in dark.

***In vitro* pull down experiments**

The constructs *pGEX-KG*, *pGEX-PID* (pSDM6004), *pET16H-BT1* (pSDM6006), *pET16H-BT2* (pSDM6078), *pET16H-BT4* (pSDM6093) and *pET16H-BT5* (pSDM6310) were transformed to *Escherichia coli* strain Rosetta (Novagen, Germany) and the constructs *pET16H-PID*, *pGEX-BT1*, *pGEX-BTB*, *pGEX-TAZ* and *pGEX-KG* were transformed to *E. coli* strain BL21-DE03. The *E. coli* strains containing the respective constructs were grown in 50ml LC containing antibiotics at 37°C. When OD_{600} reached 0.8, the cultures were induced with 1mM IPTG for 4 hours at 30°C, after which the cells were pelleted and resuspended in 2ml extraction buffer (1x PBS, 2 mM EDTA, 2 mM DTT (Dithiothreitol)) supplemented with 0.1 mM PMSF (Phenylmethanesulfonyl Fluoride), 0.1 mM leupeptin and 0.1 mM aprotinin for the GST-tagged proteins or in 2 ml binding buffer (50 mM Tris-HCl pH 6.8, 100 mM NaCl, 10 mM $CaCl_2$) supplemented with 0.1 mM PMSF, 0.1 mM leupeptin and 0.1 mM aprotinin for the His-tagged proteins. The suspensions were sonicated on ice for two minutes and kept at 4°C for the rest of the experiment. The sonicated cells were centrifuged at 14000RPM for 20 minutes in Eppendorf tubes and the supernatant was

transferred to a fresh Eppendorf tube.
Glutathione Sepharose 4B resin (Amersham-Pharmacia, USA/UK) was pre-equilibrated with three washes of 10 resin volumes of 1x PBS followed by three washes of 10 resin volumes of 1x extraction buffer at 500 x g for 5 min. From this equilibrated resin 100µl was added to the tubes containing the GST-fusion proteins and incubated for 1 hour with gentle agitation. After incubation, the tubes were centrifuged at 500 x g for 3 minutes and the resin was washed three times with 20 resin volumes of extraction buffer. Next, 2ml of the supernatant containing his-tagged proteins was added to the GST-fusion protein containing resins and the mixture was incubated for 1 hour with gentle agitation. After incubation the resins were centrifuged again at 500 x g for 3 minutes and the supernatant was discarded. The resins were washed three times with 20 resin volumes of extraction buffer. Protein loading buffer was added to the resin, samples were boiled for 5 minutes and subsequently run on a 10% (BT proteins pull-down assay) or 12% (domain pull-down assay) polyacrylamide gel prior to transfer to an Immobilon-P PVDF (Millipore, USA) membrane. Western blots were hybridized using a horse radish peroxidase (HRP)-conjugated anti-penta Histidine antibody (Qiagen, The Netherlands) and detection according to the protocol supplied for the Phototope-HRP Western Blot Detection Kit (New England Biolabs, USA). For a loading control, a second gel was run, stained with Coomassie Brilliant Blue (BioRad, USA) and dried in cellophane sheets (Sigma-Aldrich, USA).

In vitro phosphorylation assays

All proteins used in *in vitro* phosphorylation assays were produced as described for the *in vitro* pull down experiments. Five pellets from 50ml cultures were resuspended in 2ml lysis buffer (25 mM Tris-HCl pH 8.0, 500 mM NaCl, 20 mM Imidazol, 0.1% Tween-20) supplemented with 0.1 mM PMSF, 0.1 mM Leupeptin and 0.1 mM Aprotinin and sonicated for 2 min on ice and subsequent steps were performed at 4°C for the rest of the experiment. The sonicated cells were centrifuged at 14000 RPM for 20 minutes and the supernatants collected in 15ml tubes. 100µl of Ni-NTA resin (Qiagen, The Netherlands) was equilibrated with 3 washes of 10 resin volumes of lysis buffer, with 5 minutes centrifuging at 500 x g between each washing step. The equilibrated Ni-NTA resin was added to the 15ml tubes, mixed and incubated for 1 hour with gentle agitation. After incubation the tube was centrifuged at 500 x g for 3

minutes. The resin was then washed three times with 20 resin volumes of lysis buffer, once with 20 resin volumes of wash buffer 1 (25 mM Tris-HCl pH 8.0, 500 mM NaCl, 40 mM Imidazol, 0.05% Tween-20) and once with 20 resin volumes of wash buffer 2 (25 mM Tris-HCl pH 8.0, 600 mM NaCl, 80 mM Imidazol). Next, the resin was incubated in 20 volumes of elution buffer (25 mM Tris-HCl pH 8.0, 500 mM NaCl, 500 mM Imidazol) for 15 min with gentle agitation. After incubation, the tube was centrifuged for 3 minutes at 500 x g, and the supernatant containing the isolated protein was diluted a 1000-fold in Tris buffer (25 mM Tris-HCl pH 7.5, 1mM DTT). The diluted sample was then concentrated to a workable volume using Vivaspin microconcentrators (10 kDa cut off, Vivascience, Germany). Glycerol was added to a final concentration of 10% and the sample was stored at -80°C until further use. Myelin Basic Protein (MBP, Sigma-Aldrich, USA) was used as generic phosphosubstrate. Approximately 1µg of each required protein was added to individual 20µl kinase reaction mixes containing 1x kinase buffer (25 mM Tris-HCl pH 7.5, 1mM DTT, 5mM $MgCl_2$) and 1 x ATP solution (100µM $MgCl_2$, 100µM ATP-Na_2, 1µCi ^{32}P-γ-ATP). Reactions were incubated at 30°C for 30 minutes. After incubation 5µl of 5x protein loading buffer (310mM Tris-HCl pH 6.8, 10% SDS, 50% glycerol, 750mM β-mercaptoethanol, 0.125% bromophenol blue) was added to the reactions and the samples were boiled for 5 minutes. The samples were loaded and run on 12.5% acrylamide gels, and the gels were washed three times for 30 min with kinase gel wash buffer (5% trichloroacetic acid, 1% $Na_2H_2P_2O_7$), stained with Coomassie Brilliant Blue (BioRad, USA) and dried in cellophane sheets (Sigma, USA). Autoradiography was performed for 24 to 48 hours at -80°C using Fuji Super RX X-ray films and intensifier screens.

RNA extraction and Northern blots

RNA extraction and Northern blots were performed as described (Robert *et al.*, 2009). Probes were PCR amplified and column purified (Qiagen, USA): primers BT1 probe F and BT1 probe R were used to amplify the *BT1* cDNA from *pET16H-BT1*, primers PID probe F and PID probe R for *PID* from *Arabidopsis thaliana* 'Columbia' genomic DNA and primers TUB probe F and TUB probe R for *α-Tubulin* from *Arabidopsis thaliana* 'Columbia' genomic DNA. Probes were radioactively labeled using ^{32}P-α-ATP (Amerscham, UK) and a Prime-a-gene kit (Promega, USA).

Immunolocalization

Whole-mount immunolocalizations were performed on 3-day old seedlings fixed in 4% paraformaldehyde in MTSB buffer as described previously (Friml *et al.*, 2003) using the medium size basket format in an InSituPro robot (INTAVIS, Germany). Rabbit anti-PIN1 and anti-PIN2 primary antibodies (1/400, obtained from respectively Jiří Friml and Christian Luschnig) and Alexa 488-conjugated anti-rabbit secondary antibodies (1/200, Molecular Probes, USA) were used for detection. Samples were observed using confocal laser scanning microscopy.

Biological assays

For the root meristem collapse assay, about 200 seedlings per line were grown in triplicate on vertical plates on MA medium, while the development of the seedling root was monitored and scored each day during eight days for the collapse of the primary root meristem. For the phenotypic analysis of *35S::BT1 pid-14* seedlings, about 300 seeds from a *35S::BT1 pid-14/+* plant or 200 from a wild-type or *35S::BT1-1* plant were plated in triplicate on MA medium and germinated for one week. The number of dicotyledonous seedlings and seedlings with specific cotyledon defects were counted. The penetrance of the specific phenotypes were calculated based on a 1:3 segregation ratio for homozygous *pid-14* seedlings.

Confocal Laser Scanning Microscopy

The GFP-BT1 expressing onion epidermis cells were imaged on a Leica confocal microscope equipped with an Argon/Krypton laser (Biorad) with 488nm and 568nm band pass excitation and 522nm band pass and 605nm long pass emission filters for GFP and PI, respectively.
Immunolocalizations were observed using 40x dry and oil objectives on a ZEISS Axioplan microscope equipped with a confocal laser scanning unit (MRC1024ES, BIO-RAD, USA). Protoplasts were imaged on a Zeiss AxioObserver equiped with a Zeiss LSM5 Exciter using Argon/Krypton laser lines 458 nm (CFP), 514 nm (YFP) and 543nm (mRFP). When required, different fluorescent proteins were imaged in separate tracks. A HFT 405/488/543/633 beam splitter was used for laser lines 488 and 543, and HFT 458/514 for laser line 514. Band-pass filters 475-525 nm and 530-600 nm were used to detect CFP and YFP signals, respectively.

The RFP signal was separated from the YFP signal with a 560 nm long-pass filter. The protoplast cells were observed in a 6-chamber slide using a C-Apochromat 63x/1.20 W Korr UV-VIS-IR M27 objective. Laser intensities ranged from 15-40% for 458nm, 2-18% for 514nm and 15-20% for 543nm depending on the amount of signal received of the cell. The images were processed in ImageJ (`http://rsb.info.nih.gov/ij/`) and assembled in Adobe Photoshop 7.0 or Inkscape (`https://inkscape.org`).

Accession numbers

The Arabidopsis Genome Initiative locus identifiers for the genes mentioned in this chapter are as follows: *BT1* (*At5g63160*), *BT2* (*At3g48360*), *BT3* (*At1g05690*), *BT4* (*At5g67480*), *BT5* (*At4g37610*), *PBK1* (*At4g38950*), *PBK2* (*At2g21300*), *PID* (*At2g34650*), *WAG1* (*At1g53700*), *WAG2* (*At3g14370*), *AGC3-4* (*At2g26700*), *PIN1* (*At1g73590*), *PIN2* (*At5g57090*) and α-*TUBULIN* (*At5g44340*).

Bibliography

Adamowski, M. & Friml, J. (2015). PIN-dependent auxin transport: action, regulation, and evolution. The Plant Cell **27**, 20–32.

Albagli, O., Dhordain, P., Deweindt, C., Lecocq, G. & Leprince, D. (1995). The BTB/POZ domain: a new protein-protein interaction motif common to DNA- and actin-binding proteins. Cell Growth & Differentiation **6**, 1193–1198.

Armengot, L., Marquès-Bueno, M. M. & Jaillais, Y. (2016). Regulation of polar auxin transport by protein and lipid kinases. Journal of Experimental Botany **67**, 4015–4037.

Axelos, M., Curie, C., Mazzolini, L., Bardet, C. & Lescure, B. (1992). A protocol for transient gene expression in *Arabidopsis thaliana* protoplasts isolated from cell suspension cultures. Plant Physiology and Biochemistry **30**, 123–128.

Ballesteros, I., Domínguez, T., Sauer, M., Paredes, P., Duprat, A., Rojo, E., Sanmartín, M. & Sánchez-Serrano, J. J. (2013). Specialized functions of the PP2A subfamily II catalytic subunits PP2A-C3 and PP2A-C4 in the distribution of auxin fluxes and development in arabidopsis. Plant Journal **73**, 862–872.

Bardwell, V. J. & Treisman, R. (1994). The POZ domain: a conserved protein-protein interaction motif. Genes & Development **8**, 1664–1677.

Benjamins, R. (2003). Functional analysis of the PINOID protein kinase in *Arabidopsis thaliana*. PhD thesis, Leiden University.

Benjamins, R., Galván-Ampudia, C. S., Hooykaas, P. J. J. & Offringa, R. (2003). PINOID-mediated signaling involves calcium-binding proteins. Plant Physiology **132**, 1623–1630.

Benjamins, R., Quint, A., Weijers, D., Hooykaas, P. J. J. & Offringa, R. (2001). The PINOID protein kinase regulates organ development in *arabidopsis* by enhancing polar auxin transport. Development **128**, 4057–4067.

Benková, E., Michniewicz, M., Sauer, M., Teichmann, T., Seifertová, D., Jürgens, G. & Friml, J. (2003). Local,

efflux-dependent auxin gradients as a common module for plant organ formation. Cell **115**, 591–602.

Bennett, S. R. M., Alvarez, J., Bossinger, G. & Smyth, D. R. (1995). Morphogenesis in *pinoid* mutants of *Arabidopsis thaliana*. The Plant Journal **8**, 505–520.

Bossinger, G. & Smyth, D. R. (1996). Initiation patterns of flower and floral organ development in *Arabidopsis thaliana*. Development **122**, 1093–1102.

Cheng, Y., Qin, G., Dai, X. & Zhao, Y. (2007). NPY1, a BTB-NPH3-like protein, plays a critical role in auxin-regulated organogenesis in arabidopsis. Proceedings of the National Academy of Sciences of the United States of America **104**, 18825–18829.

Chiu, W.-l., Niwa, Y., Zeng, W., Hirano, T., Kobayashi, H. & Sheen, J. (1996). Engineered GFP as a vital reporter in plants. Current Biology **6**, 325–330.

Christensen, S. K., Dagenais, N., Chory, J. & Weigel, D. (2000). Regulation of auxin response by the protein kinase PINOID. Cell **100**, 469–478.

Clough, S. J. & Bent, A. F. (1998). Floral dip: a simplified method for *Agrobacterium*-mediated transformation of *Arabidopsis thaliana*. The Plant Journal **16**, 735–743.

Dai, M., Zhang, C., Kania, U., Chen, F., Xue, Q., Mccray, T., Li, G., Qin, G., Wakeley, M., Terzaghi, W., Wan, J., Zhao, Y., Xu, J., Friml, J., Deng, X. W. & Wang, H. (2012). A PP6-type phosphatase holoenzyme directly regulates PIN phosphorylation and auxin efflux in *Arabidopsis*. Plant Cell **24**, 2497–2514.

Dhonukshe, P., Huang, F., Galván-Ampudia, C. S., Mähönen, A. P., Kleine-Vehn, J., Xu, J., Quint, A., Prasad, K., Friml, J., Scheres, B. & Offringa, R. (2010). Plasma membrane-bound AGC3 kinases phosphorylate PIN auxin carriers at TPRXS(N/S) motifs to direct apical PIN recycling. Development **137**, 3245–3255.

Dieterle, M., Thomann, A., Renou, J.-P., Parmentier, Y., Cognat, V., Lemonnier, G., Müller, R., Shen, W.-H., Kretsch,

T. & Genschik, P. (2005). Molecular and functional characterization of *Arabidopsis* Cullin 3A. The Plant Journal **41**, 386–399.

Du, L. & Poovaiah, B. W. (2004). A novel family of Ca2+/calmodulin-binding proteins involved in transcriptional regulation: interaction with fsh/ring3 class transcription activators. Plant Molecular Biology **54**, 549–569.

Fan, Y. (2014). The role of AGC3 kinases and calmodulins in plant growth responses to abiotic signals. PhD thesis, Leiden University.

Figueroa, P., Gusmaroli, G., Serino, G., Habashi, J., Ma, L., Shen, Y., Feng, S., Bostick, M., Callis, J., Hellmann, H. & Deng, X. W. (2005). *Arabidopsis* has two redundant cullin3 proteins that are essential for embryo development and that interact with RBX1 and BTB proteins to form multisubunit E3 ubiquitin ligase complexes *in vivo*. The Plant Cell **17**, 1180–1195.

Friml, J., Benková, E., Mayer, U., Palme, K. & Muster, G. (2003). Automated whole mount localisation techniques for plant seedlings. The Plant Journal **34**, 115–124.

Friml, J., Yang, X., Michniewicz, M., Weijers, D., Quint, A., Tietz, O., Benjamins, R., Ouwerkerk, P. B. F., Ljung, K., Sandberg, G., Hooykaas, P. J. J., Palme, K. & Offringa, R. (2004). A PINOID-dependent binary switch in apical-basal PIN polar targeting directs auxin efflux. Science **306**, 862–865.

Furutani, M., Kajiwara, T., Kato, T., Treml, B. S., Stockum, C., Torres-Ruiz, R. A. & Tasaka, M. (2007). The gene *MACCHI-BOU 4/ENHANCER OF PINOID* encodes a NPH3-like protein and reveals similarities between organogenesis and phototropism at the molecular level. Development **134**, 3849–3859.

Galván-Ampudia, C. S. & Offringa, R. (2007). Plant evolution: AGC kinases tell the auxin tale. Trends in Plant Science **12**, 541–547.

Gälweiler, L., Guan, C., Müller, A., Wisman, E., Mendgen, K., Yephremov, A. & Palme, K. (1998). Regulation of polar auxin transport by AtPIN1 in *Arabidopsis* vascular tissue. Science **282**, 2226–2230.

Garbers, C., DeLong, A., Deruére, J., Bernasconi, P. & Söll, D. (1996). A mutation in protein phosphatase 2A regulatory subunit A affects auxin transport in *Arabidopsis*. EMBO Journal **15**, 2115–2124.

Gingerich, D. J., Gagne, J. M., Salter, D. W., Hellmann, H., Estelle, M., Ma, L. & Vierstra, R. D. (2005). Cullins 3a and 3b assemble with members of the broad complex/tramtrack/bric-a-brac (BTB) protein family to form essential ubiquitin-protein ligases (E3s) in *Arabidopsis*. Journal of Biological Chemistry **280**, 18810–18821.

Gleave, A. (1992). A versatile binary vector system with a T-DNA organisational structure conducive to efficient integration of cloned DNA into the plant genome. Plant Molecular Biology **20**, 1203–1207.

Guan, K. & Dixon, J. E. (1991). Eukaryotic proteins expressed in *Escherichia coli*: An improved thrombin cleavage and purification procedure of fusion proteins with glutathione S-transferase. Analytical Biochemistry **192**, 262–267.

Huang, F., Kemel Zago, M., Abas, L., van Marion, A., Galván-Ampudia, C. S. & Offringa, R. (2010). Phosphorylation of conserved PIN motifs directs *arabidopsis* PIN1 polarity and auxin transport. Plant Cell **22**, 1129–1142.

James, P., Halladay, J. & Craig, E. A. (1996). Genomic libraries and a host strain designed for highly efficient two-hybrid selection in yeast. Genetics **144**, 1425–1436.

Lee, S. H. & Cho, H.-T. (2006). PINOID positively regulates auxin efflux in arabidopsis root hair cells and tobacco cells. The Plant Cell **18**, 1604–1616.

Masson, J. & Paszkowski, J. (1992). The culture response of *Arabidopsis thaliana* protoplasts is determined by the growth conditions of donor plants. Plant Journal **2**, 829–833.

McSteen, P., Malcomber, S., Skirpan, A., Lunde, C., Wu, X., Kellogg, E. & Hake, S. (2007). *barren inflorescence2* encodes a co-ortholog of the PINOID serine/threonine kinase and is required for organogenesis during inflorescence and vegetative development in maize. Plant Physiology **144**, 1000–1011.

Meister, R. J., Oldenhof, H., Bowman, J. L. & Gasser, C. S. (2005). Multiple protein regions contribute to differential activities of YABBY proteins in reproductive development. Plant Physiology **137**, 651–662.

Michniewicz, M., Zago, M. K., Abas, L., Weijers, D., Schweighofer, A., Meskiene, I., Heisler, M. G., Ohno, C., Zhang, J., Huang, F., Schwab, R., Weigel, D., Meyerowitz, E. M., Luschnig, C., Offringa, R. & Friml, J. (2007). Antagonistic regulation of PIN phosphorylation by PP2A and PINOID directs auxin flux. Cell **130**, 1044–1056.

Motchoulski, A. & Liscum, E. (1999). Arabidopsis NPH3: A NPH1 photoreceptor-interacting protein essential for phototropism. Science **286**, 961–964.

Nishihama, R., Soyano, T., Ishikawa, M., Araki, S., Tanaka, H., Asada, T., Irie, K., Ito, M., Terada, M., Banno, H., Yamazaki, Y. & Machida, Y. (2002). Expansion of the cell plate in plant cytokinesis requires a kinesin-like protein/MAPKKK complex. Cell **109**, 87–99.

Oh, S.-A., Bourdon, V., Das 'Pal, M., Dickinson, H. & Twell, D. (2008). *Arabidopsis* kinesins HINKEL and TETRASPORE act redundantly to control cell plate expansion during cytokinesis in the male gametophyte. Molecular Plant **1**, 794–799.

Okada, K., Ueda, J., Komaki, M. K., Bell, C. J. & Shimura, Y. (1991). Requirement of the auxin polar transport system in early stages of arabidopsis floral bud formation. The Plant Cell **3**, 677–684.

Perrot-Rechenmann, C. (2010). Cellular responses to auxin: division versus expansion. Cold Spring Harbor Perspectives in Biology **2**, a001446.

Petrášek, J., Mravec, J., Bouchard, R., Blakeslee, J. J., Abas, M., Seifertová, D., Wiśniewska, J., Tadele, Z., Kubeš, M., Čovanová, M., Dhonukshe, P., Skůpa, P., Benková, E., Perry, L., Křeček, P., Lee, O. R., Fink, G. R., Geisler, M., Murphy, A. S., Luschnig, C., Zažímalová, E. & Friml, J. (2006). PIN

proteins perform a rate-limiting function in cellular auxin efflux. Science **312**, 914–918.

Ponting, C. P., Blake, D. J., Davies, K. E., Kendrick-Jones, J. & Winder, S. J. (1996). ZZ and TAZ: new putative zinc fingers in dystrophin and other proteins. Trends in Biochemical Sciences **21**, 11–13.

Reinhardt, D., Pesce, E.-R., Stieger, P., Mandel, T., Baltensperger, K., Bennett, M., Traas, J., Friml, J. & Kuhlemeier, C. (2003). Regulation of phyllotaxis by polar auxin transport. Nature **426**, 255–260.

Robert, H. S., Quint, A., Brand, D., Vivian-Smith, A. & Offringa, R. (2009). BTB and TAZ domain scaffold proteins perform a crucial function in arabidopsis development. Plant Journal **58**, 109–121.

Robles, P. & Pelaz, S. (2005). Flower and fruit development in *Arabidopsis thaliana*. International Journal of Developmental Biology **49**, 633–643.

Sabatini, S., Beis, D., Wolkenfelt, H., Murfett, J., Guilfoyle, T., Malamy, J., Benfey, P., Leyser, O., Bechtold, N., Weisbeek, P. & Scheres, B. (1999). An auxin-dependent distal organizer of pattern and polarity in the arabidopsis root. Cell **99**, 463–472.

Sakai, T., Wada, T., Ishiguro, S. & Okada, K. (2000). RPT2: A signal transducer of the phototropic response in arabidopsis. The Plant Cell **12**, 225–236.

Sambrook, J., Fritsch, E. F. & Maniatis, T. (1989). Molecular Cloning: A Laboratory Manual. Cold Spring Harbor Laboratory Press, New York.

Sasabe, M., Boudolf, V., De Veylder, L., Inzé, D., Genschik, P. & Machida, Y. (2011). Phosphorylation of a mitotic kinesin-like protein and a MAPKKK by cyclin-dependent kinases (CDKs) is involved in the transition to cytokinesis in plants. Proceedings of the National Academy of Sciences of the United States of America **108**, 17844–17849.

Schirawski, J., Planchais, S. & Haenni, A.-L. (2000). An improved protocol for the preparation of protoplasts from an established

Arabidopsis thaliana cell suspension culture and infection with RNA of turnip yellow mosaic tymovirus: a simple and reliable method. Journal of Virological Methods **86**, 85–94.

Simon, M. L. A., Platre, M. P., Marquès-Bueno, M. M., Armengot, L., Stanislas, T., Bayle, V., Caillaud, M.-C. & Jaillais, Y. (2016). A PtdIns(4)P-driven electrostatic field controls cell membrane identity and signalling in plants. Nature Plants **2**, 16089.

Skirpan, A., Wu, X. & McSteen, P. (2008). Genetic and physical interaction suggest that *BARREN STALK1* is a target of BARREN INFLORESCENCE2 in maize inflorescence development. Plant Journal **55**, 787–797.

Tanaka, H., Ishikawa, M., Kitamura, S., Takahashi, Y., Soyano, T., Machida, C. & Machida, Y. (2004). The AtNACK1/HINKEL and STUD/TETRASPORE/AtNACK2 genes, which encode functionally redundant kinesins, are essential for cytokinesis in arabidopsis. Genes to Cells **9**, 1199–1211.

Treml, B. S., Winderl, S., Radykewicz, R., Herz, M., Schweizer, G., Hutzler, P., Glawischnig, E. & Ruiz, R. A. T. (2005). The gene *ENHANCER OF PINOID* controls cotyledon development in the arabidopsis embryo. Development **132**, 4063–4074.

Varagona, M. J., Schmidt, R. J. & Raikhel, N. V. (1992). Nuclear localization signal(s) required for nuclear targeting of the maize regulatory protein Opaque-2. The Plant Cell **4**, 1213–1227.

Wade, R. H. & Kozielski, F. (2000). Structural links to kinesin directionality and movement. Nature Structural & Molecular Biology **7**, 456–460.

Wang, K. L.-C., Yoshida, H., Lurin, C. & Ecker, J. R. (2004). Regulation of ethylene gas biosynthesis by the arabidopsis ETO1 protein. Nature **428**, 945–950.

Weber, H., Bernhardt, A., Dieterle, M., Hano, P., Mutlu, A., Estelle, M., Genschik, P. & Hellmann, H. (2005). Arabidopsis AtCUL3a and AtCUL3b form complexes with members of the BTB/POZ-MATH protein family. Plant Physiology **137**, 83–93.

Wiśniewska, J., Xu, J., Seifertová, D., Brewer, P. B., Růžička, K., Blilou, I., Rouquié, D., Benková, E., Scheres, B. & Friml, J. (2006). Polar PIN localization directs auxin flow in plants. Science **312**, 883.

Yang, C.-Y., Spielman, M., Coles, J. P., Li, Y., Ghelani, S., Bourdon, V., Brown, R. C., Lemmon, B. E., Scott, R. J. & Dickinson, H. G. (2003). TETRASPORE encodes a kinesin required for male meiotic cytokinesis in arabidopsis. Plant Journal **34**, 229–240.

Zegzouti, H., Anthony, R. G., Jahchan, N., Bögre, L. & Christensen, S. K. (2006a). Phosphorylation and activation of PINOID by the phospholipid signaling kinase 3-phosphoinositide-dependent protein kinase 1 (PDK1) in arabidopsis. Proceedings of the National Academy of Sciences of the United States of America **103**, 6404–6409.

Zegzouti, H., Li, W., Lorenz, T. C., Xie, M., Payne, C. T., Smith, K., Glenny, S., Payne, G. S. & Christensen, S. K. (2006b). Structural and functional insights into the regulation of arabidopsis AGC VIIIa kinases. Journal of Biological Chemistry **281**, 35520–35530.

Zimmermann, P., Hirsch-Hoffmann, M., Hennig, L. & Gruissem, W. (2004). GENEVESTIGATOR. Arabidopsis microarray database and analysis toolbox. Plant Physiology **136**, 2621–2632.

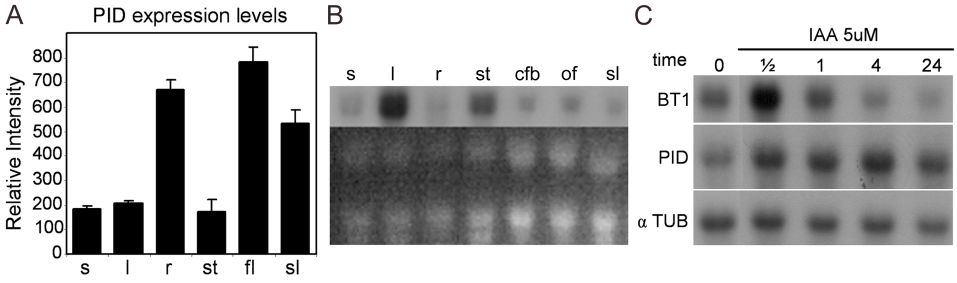

Figure S1: The auxin responsive *BT1* gene is co-expressed with *PID*.
(A) The Genevestigator micro-array data show that *PID* expression is higher in roots (r), flowers (fl) and siliques (sl), and lower in seedlings (s), leaves (l) and stems (st).
(B) Northern blot analysis showing the expression of *BT1* mRNA in wild-type *Arabidopsis thaliana* 'Columbia' tissues. Leaf (l) and root (r) tissues are from 2-week old seedlings (s). Stems (st), closed flower buds (cfb), opened flowers (of) and siliques (sl) are from 6-week old plants.
(C) Northern blot analysis showing that *BT1* (upper panel) and *PID* (middle panel) expression are induced in 8-day old seedlings as soon as 30 minutes after auxin treatment (5µM IAA). The expression of *α-Tubulin* (lower panel) was used as loading control. Indicated time in hours.

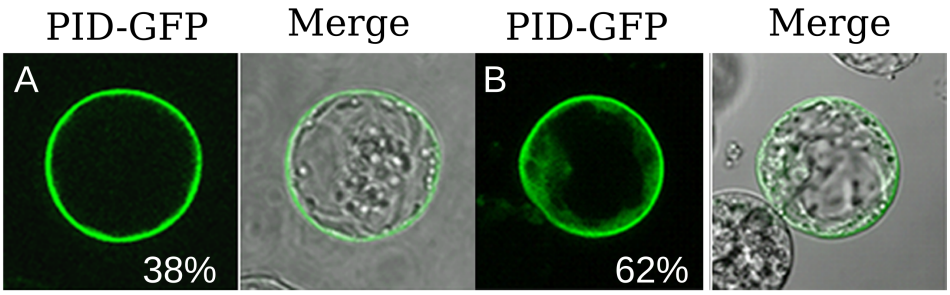

Figure S2: Arabidopsis protoplasts expressing PID-GFP show either pure PM localization (A) or PM and cytoplasmic signal (B).

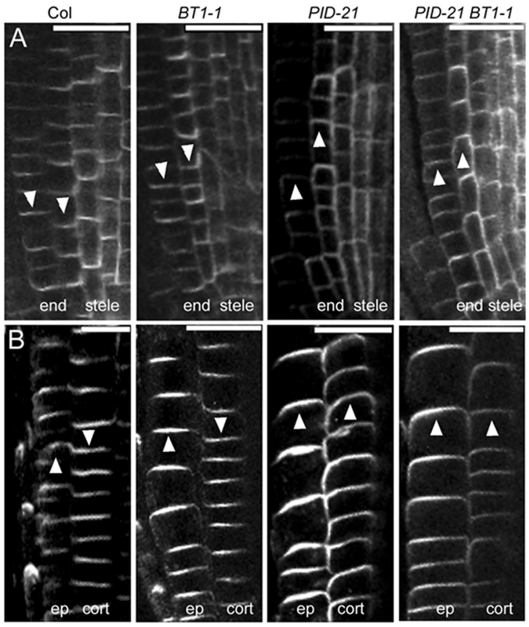

Figure S3: PIN1 and PIN2 polar targeting is not significantly changed by *BT1* overexpression.
(A,B) Confocal images of *Arabidopsis thaliana* 'Columbia' wild type, *35S::BT1-1*, *35S::PID-21* and *35S::PID-21 35S::BT1-1* roots following immunolocalization of PIN1 in endodermis (end) and stele (A) and PIN2 in epidermis (ep) and cortex (cort) (B). White arrowheads indicate the PIN polarity.
Size bars indicate 50µm.

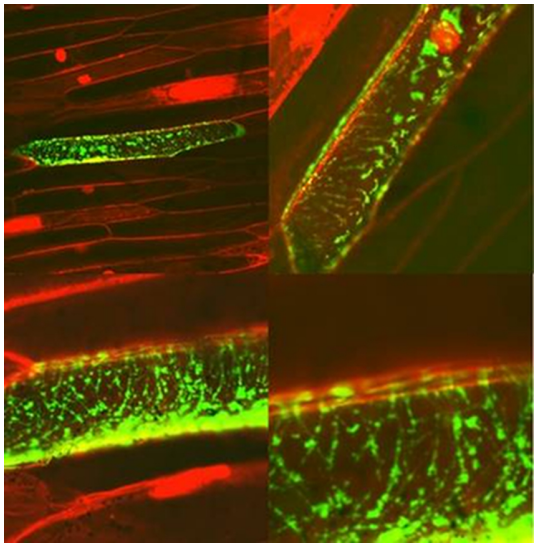

Figure S4: BT1-GFP localizes to thread-like structures in onion cells following particle bombardment with *35S::BT1-GFP*.

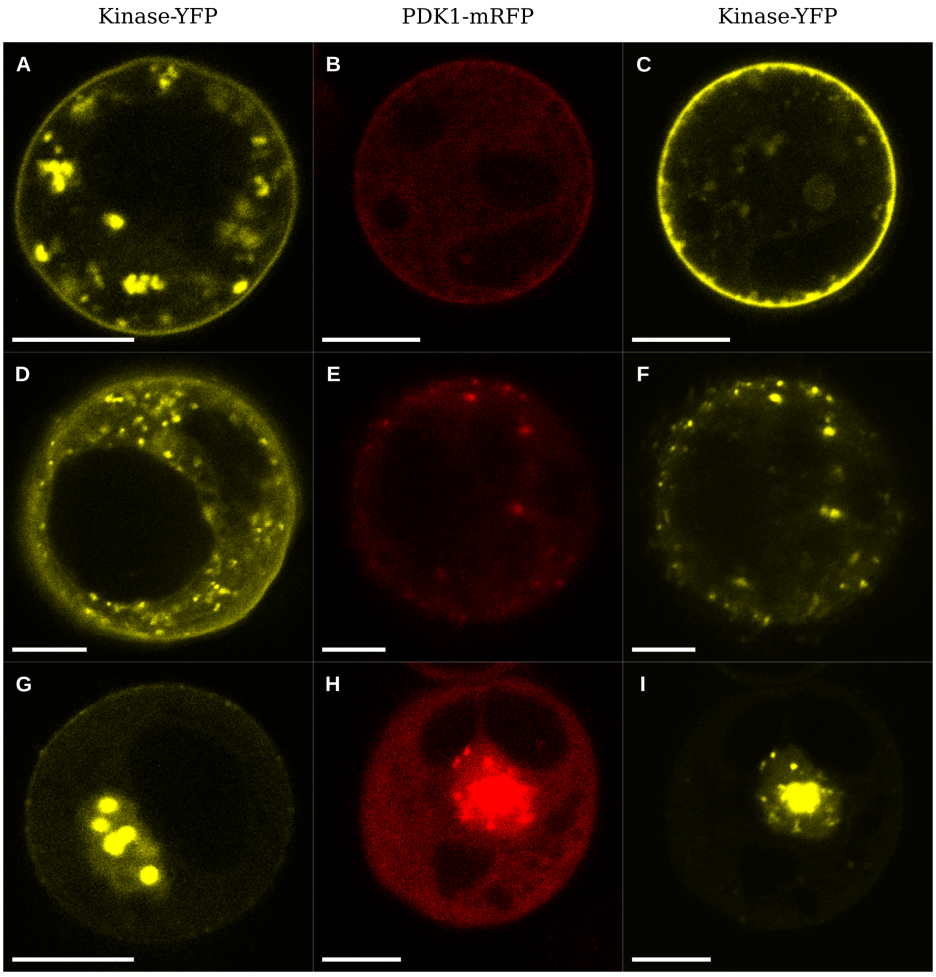

Figure S5: Co-expression of WAG1, WAG2 or AGC3-4 with PDK1 in arabidopsis protoplasts does not result in MT relocalization of the kinases.
(A) Arabidopsis protoplast expressing WAG1-YFP.
(B-C) Arabidopsis protoplast co-expressing PDK1-mRFP (B) and WAG1-YFP (C).
(D) Arabidopsis protoplast expressing WAG2-YFP.
(E-F) Arabidopsis protoplast co-expressing PDK1-mRFP (E) and WAG2-YFP (F).
(G) Arabidopsis protoplast expressing AGC3-4-YFP.
(H-I) Arabidopsis protoplast co-expressing PDK1-mRFP (H) and AGC3-4-YFP (I).
Size bars indicate 10µm.

FIVE

CHARACTERIZATION OF ARABIDOPSIS PBP2/BT1 BINDING KINESINS 1 AND 2.

Myckel Habets[1,], Leriesha Badrie, Sander Baart, Remko Offringa[1]

[1] Plant Developmental Genetics, Institute of Biology Leiden, Leiden University, Sylviusweg 72, 2333 BE Leiden, The Netherlands.

Summary

3-Phosphoinositide-dependent protein kinase 1 (PDK1)-mediated phosphorylation of the polar auxin transport regulator PINOID (PID) triggers relocalization of PID to the microtubule cytoskeleton in *Arabidopsis thaliana* (arabidopsis) protoplasts. The complex responsible for this relocalization consists of the PINOID BINDING PROTEIN 2 (PBP2)/BTB AND TAZ DOMAIN 1 (BT1) scaffold protein and PBP2/BT1 BINDING KINESIN 1 or 2 (PBK1 or PBK2) that mediate microtubule binding. In this chapter we investigated the function of PBK1 and PBK2 and other members of the plant specific At1 kinesin family in more detail. We were able to identify and classify At1 family members in almost all plant species of which the genome has been sequenced to date, with the exception of the unicellular Chlorophyte algae. We obtained arabidopsis T-DNA insertion lines for *PBK1* and *PBK2* and the two closest paralogues (*PBKH1* and *PBKH2*), but were unable to find convincing mutant phenotypes, even in the quadruple mutant. This suggests that other members of the At1 gene family still act redundantly. Expression analysis of the *PBK* and *PBKH* genes using *promoter::GUS* reporter lines showed that the expression domains of the genes overlapped, with strong expression in meristems and young tissues. The expression of the genes was not altered by changes in temperature or light or by external auxin application. Expression of kinesin-YFP fusions in arabidopsis protoplasts showed cortical microtubule localization. However, *in planta* these fusion proteins appeared to be targets for proteasome-mediated degradation, and no clear microtubule localization could be observed. Based on the known function of the related NACK kinesins, it is tempting to speculate that the BT1-PBK complex is involved in relocating PID to the phragmoplast during cell division. However, further research is needed to confirm this hypothesis.

Introduction

In eukaryotic cells, the actin and microtubule cytoskeleton are important structural components that determine cell shape, and mediate cell division and intracellular transport. In animal cells, cell shape and also cell migration is directly determined by the microtubule cytoskeleton (MT), whereas plant cell movement and shape is restricted by the external cell wall matrix. However, since in plant cells the MT plays an important role in cell wall synthesis, it is indirectly involved in cell shape

establishment (Ishida *et al.*, 2007; Szymanski & Cosgrove, 2009; Sotiriou *et al.*, 2016).

In plants, the actin cytoskeleton is composed of subunit members from the ACT family (McDowell *et al.*, 1996). Actin and their filaments can be found in two main forms, G-actin (globular actin), which is the common name for monomeric actin, and F-actin (filamentous actin), which contains long actin bundles. Fine F-actin can be found in growth tips of root hairs and pollen tubes, and its presence there correlates with high levels of exocytosis and accumulation of the cytoplasm at the growth tip (Hussey *et al.*, 2006; Ketelaar, 2013). Besides tip growth, the actin cytoskeleton has also been shown to play a key role in cytoplasmic streaming (Kachar & Reese, 1988; Gutierrez *et al.*, 2009; Tominaga *et al.*, 2017), in supporting the MT in positioning the cell plate during cytokinesis (Hoshino *et al.*, 2003; Sano *et al.*, 2005), and in positioning intracellular compartments, including mitochondria (Zheng *et al.*, 2009) and the nucleus (Ketelaar *et al.*, 2002), in the cytoplasm.

The MT is made up of α- and β-tubulin subunits (Bryan & Wilson, 1971; Olmsted *et al.*, 1971; Erickson, 1974; Kopczak *et al.*, 1992; Snustad *et al.*, 1992; Mizuno, 1993; Liu *et al.*, 1993; Qin *et al.*, 1997; Yoshikawa *et al.*, 2003) and sometimes includes the γ-tubulin subunit (Liu *et al.*, 1993, 1994). The MT is best known for its function during mitosis (Pickett-Heaps & Northcote, 1966; Gunning & Wick, 1985; Hasezawa *et al.*, 2000), but another important role for the MT is guiding the movement of cellulose synthase complexes in the plasma membrane (PM). By doing so, these cortical microtubules regulate cell shape (for in depth review see Bashline *et al.*, 2014), as has been shown for the lobe and neck pattern in pavement cells (Fu *et al.*, 2005; Armour *et al.*, 2015).

While the actin and MT provide structural cell components, they also provide a scaffold for many cytoskeleton-associated proteins that are involved in altering the cytoskeleton, or that have functions in the processes described above. Kinesins are motor proteins that associate with the MT to transport cargoes along the strands, or to move MT strands in opposite directions, e.g. for chromosome segregation during mitosis or meiosis. Structurally, kinesins contain an ATPase motor domain (the 'head'), which interacts with the MT, often on one side of the protein, a 'stalk', which contains a coiled-coil domain for dimerization, and a tail region that interacts with the cargo on the other side of the protein (Kamal & Goldstein, 2002). The protein dimerizes to form the functional

motor protein, where the two ATPase domains form the 'feet' that allow a 'walk'-like movement along the MT (Rice *et al.*, 1999).

Eukaryotic kinesins have been classified into fourteen families (Lawrence *et al.*, 2004), of which the Kinesin-7 family contains a plant-specific subfamily II that is also referred to as the At1 subfamily of kinesins (Dagenbach & Endow, 2004; Richardson *et al.*, 2006; Shen *et al.*, 2012). Until now, only two members of this subfamily, NACK1/HINKEL (Strompen *et al.*, 2002; Nishihama *et al.*, 2002; Tanaka *et al.*, 2004) and NACK2/TETRASPORE (Spielman *et al.*, 1997; Yang *et al.*, 2003), have been investigated in detail in tobacco BY2 cells and in *Arabidopsis thaliana* (arabidopsis).

The NACK kinesins are part of the NACK-PQR mitogen-activated protein kinase (MAPK) pathway, which regulates cytokinesis in plants (Takahashi *et al.*, 2010). After the separation of the chromosomes, a structure is formed, called the phragmoplast, that determines the position of the new cell wall. Some components of this NACK-PQR MAPK pathway were found to be recruited to the phragmoplast (Nishihama *et al.*, 2002; Takahashi *et al.*, 2010; Naito & Goshima, 2015), while others were not (Soyano *et al.*, 2003). To build the growing plasma membrane and cell wall (the cell plate), the phragmoplast has to expand outwards. This process is repressed by the high activity of the cyclin-dependent protein kinases (CDKs), which phosphorylate the NACKs and the MAPKKKs NtNPK1/AtANP1/AtANP2/AtANP3 to prevent their interaction (Sasabe *et al.*, 2011). When all cell cycle checkpoints have been passed and cytokinesis can start, the CDK activity drops, and the NACKs and the MAPKKKs become dephosphorylated (Sasabe *et al.*, 2011). The NACKs and MAPKKKs can then interact and the MAPKKKs become activated, triggering MAPK cascade-mediated phosphorylation of microtubule-associating protein 65 (MAP65; Soyano *et al.*, 2003; Sasabe *et al.*, 2006; Takahashi *et al.*, 2010). The phosphorylated MAP65 causes depolymerization of the MT at the inner part of the phragmoplast (Sasabe *et al.*, 2006), and the released tubulin is then available for outward growth of the MT scaffold at the outside of the phragmoplast (Yasuhara *et al.*, 1993). This allows the phragmoplast to expand radially with continued destabilization on the inner side and stabilization of the MT at the outer side of the phragmoplast.

During cytokinesis, membrane proteins have to be targeted to the two newly formed PMs. An interesting group of PM-localized proteins in this

respect comprises the PIN-FORMED (PIN) auxin efflux carriers, since they determine the direction of cell-to-cell polar auxin transport through their asymmetric localization at the cell's PM (Chapter 1). Following cell division, where PINs are deposited at both newly formed PMs, PIN polar distribution needs to be re-established through clathrin-mediated endocytosis, and it has been shown that this requires the activity of the MT (Geldner *et al.*, 2001; Dhonukshe *et al.*, 2007). The MT is not directly involved in PIN trafficking, but provides positional information within the tissue to the PIN trafficking machinery (Boutté *et al.*, 2006). PIN polarity has also been shown to be determined by the PINOID (PID) protein serine/threonine kinase, which was found to trigger relocalization of PINs from the rootward (basal) to the shootward (apical) PM of the cell by phosphorylating the hydrophilic loop of these auxin transporters (Friml *et al.*, 2004). By regulating the kinase activity, the auxin transport direction can be changed, e.g. in response to internal developmental or external environmental signals (Habets & Offringa, 2014). The 3-phosphoinositide-dependent protein kinase 1 (PDK1) has been identified as one of the upstream regulators of PID (Zegzouti *et al.*, 2006). Although PID is an auto-activating kinase, PDK1 was shown to upregulate its activity by phosphorylating serine 288 and serine 290 in the activation loop of PID (Zegzouti *et al.*, 2006). After PDK1 phosphorylation, PID was found to relocalize to the MT in arabidopsis protoplasts (Chapter 3). PINOID BINDING PROTEIN 2 (PBP2)/BTB AND TAZ DOMAIN 1 (BT1) was found to interact with PID and expression of BT1 in onion cells showed a MT-like localization (Chapter 4). Further research confirmed that BT1 forms a complex with two homologous kinesins of the At1 subfamily, which we named PBP2/BT1 BINDING KINESIN 1 and 2 (PBK1 and PBK2), and that this complex is required for MT localization of PID (Chapter 4).

Here we further characterized these two kinesins and their paralogs, which we named PBKH1 and PBKH2, in more detail. Phylogenetic analysis of the At1 family showed that family members are present in all Embryophytes, however, no sequences linked to this family could be identified in the unicellular Chlorophytes. In Angiosperms, the At1 subfamily splits into a conservative NACK branch and a diverse branch containing the PBK homologs (PBK-HLs). Analysis of arabidopsis T-DNA insertion lines for *PBK1*, *PBK2*, *PBKH1* and *PBKH2* showed wild-type appearing plants in the quadruple mutant and subsequent RT-PCR

analysis in this mutant indicated that this might be caused by residual expression of PBK1 and PBKH2. Expression analysis of the *PBK* and *PBKH* genes using *promoter::GUS* constructs indicated that these kinesins are highly expressed in young, developing tissues, and that their expression is not affected by changes in temperature, light or auxin concentration. Finally, we examined the localization of PBK1 and PBK2 in arabidopsis protoplasts, where clear MT localization could be observed, and *in planta*, where we noticed high turn-over of the proteins, but could not observe MT localization as in protoplasts. The role of this plant-specific group of kinesins therefore remains elusive, despite our analysis.

Results

Phylogenetic analysis of the At1 kinesin subfamily.

Arabidopsis PBK1 and PBK2 have been identified as proteins interacting with BT1 (Chapter 4, this thesis). They belong to the plant-specific At1 subfamily of kinesins, which in arabidopsis beside the PBKs includes two closely related PBK paralogs (PBKH1 and PKH2), two PBK-likes (PBKL1 and PBKL2) and the NACKs (NACK1 and NACK2). To identify homologs in other plant species and analyze the evolutionary origin of this subfamily within the kinesin family, we performed a phylogenetic analysis using the arabidopsis protein sequences of the PBKs, PBKHs, PBKLs and NACKs as a starting point (Figure 1). We were able to identify family members in Embryophytes, but not in Chlorophyte species, indicating that this protein family is land plant specific (Figure 1, Table S1). The first diversification of the At1 kinesins occurred in Angiosperms, where we found a clear split of the At1 kinesins into a NACK branch and a PBK homolog (PBK-HL) branch (Figure 1). The subsequent evolution of the NACK branch is relative simple compared to that of the PBK-HL branch. The number of gene duplications is limited, and the variation between the genes is low. The only major event in this branch is the gene duplication event during the formation of the eudicots giving rise to the NACK1 and NACK2 branch (Figure 1). Remarkably, further gene duplications mainly occurred in the NACK1 branch, and as a result most plant species only have a single *NACK2* gene copy (Table 1). In contrast, the evolution of the PBK-HL branch appeared to be far more complex, with two major diversification events, various gene duplication events and much more variation between the proteins in different species.

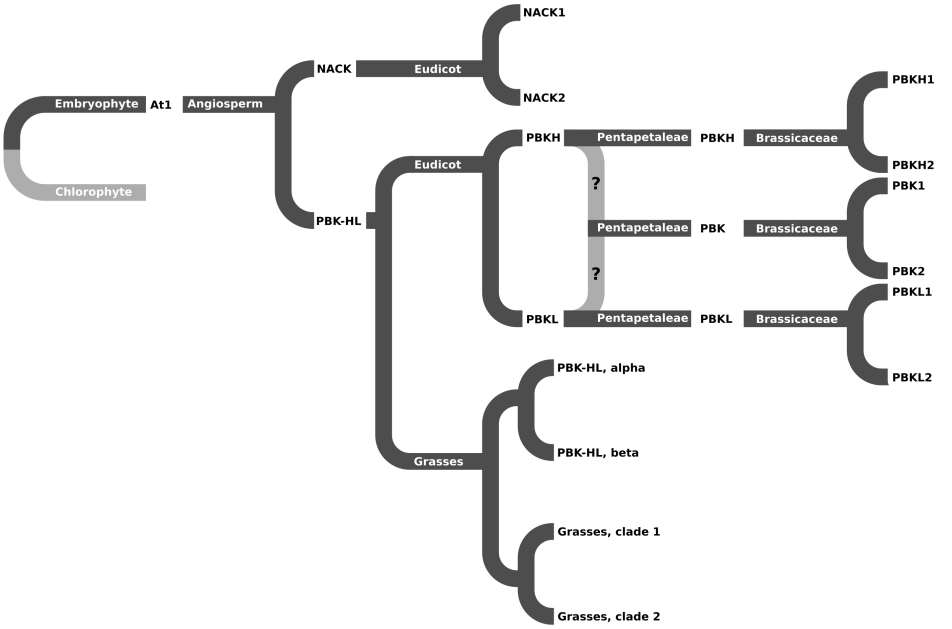

Figure 1: Schematic representation of the At1 kinesin subfamily phylogeny. Plant clade names are indicated as white text on a dark background. Protein classification is indicated as dark text on white background. No At1 subfamily members could be identified in the chlorophyte clade. The origin of the PBKs (whether derived from PBKH or from PBKL) remains to be determined.

Specifically in grasses we found that the PBK-HL branch splits into four clades, two of which are closely related to the ancestral PBK-HL, which we named PBK-HL alpha and PBK-HL beta, and two clades that diverged from PBK-HL. We decided not to name these branches, but to designate them as the "Grasses" clades (Figure 1). In Eudicots, the PBK-HL branch splits into two clades, the PBKLs and the PBKHs. The PBKs could only be identified first in the Pentapetaleae clade. However, because the sequence resolution in early members of this clade is low, we could not determine if the PBKs are derived from the PBKLs or from the PBKHs. Finally, we found that gene duplications occurred in all three PBK-HL branches in 5 of the 9 Brassicaceae species, suggesting that this most likely occurred during the *At-α* whole genome duplication (WGD) event that is specific for the Brassicaceae family (Bowers *et al.*, 2003).

Table 1: Overview of species containing At1 kinesin subfamily sequences, the clade they belong to, their common English name, their common Dutch name and the number of sequences identified, sorted by At1, NACK, PBK-HL, or Grasses origin.

Latin name	**Clade**	**English common name**	**Dutch common name**	**Number of sequences**			
				At1	**Nack**	**PBK-HL**	**Grasses**
Marchantia polymorpha	Embryophyte	Common liverwort	Paraplluutjesmos	1			
Physcomitrella patens	Embryophyte	Spreading-leaved earth moss		3			
Sphagnum fallax	Embryophyte	Flat-top Bogmoss	Fraai veenmos	2			
Selaginella moellendorffii	Tracheophyte	Gemniferous Spikemoss		1			
Ananas comosus	Angiosperm	Pineapple	Ananas		2	3	
Amborella trichopoda	Angiosperm	Amborella			1	1	
Musa acuminata	Angiosperm	Banana	Banaan		2	5	
Spirodela polyrhiza	Angiosperm	Common duckweed	Veelwortelig kroos		1	2	
Zostera marina	Angiosperm	Common eel-grass	Groot zeegras		2	2	
Brachypodium distachyon	Grasses	False brone			3	2	2
Brachypodium stacei	Grasses				3	2	2
Oryza sativa	Grasses	Rice	Rijst		1	3	2
Oropetium thomaeum	Grasses				1	1	1
Panicum hallii	Grasses	Hall's panicgrass			1	2	2
Panicum virgatum	Grasses	Old Switch Panicgrass			2	4	4
Setaria italica	Grasses	Foxtail millet	Trosgierst		1	2	2
Setaria viridis	Grasses	Green bristlegrass	Groene naaldaar		1	2	2
Sorghum bicolor	Grasses	Sorghum	Kafferkoren		1	2	2
Zea mays	Grasses	Maize	Mais		1	3	2
Aquilegia coerulea	Eudicot	Colorado Blue Columbine			1+1 (2)†	0+1+1 (2)§	
Amaranthus hypochondriacus	Pentapetalae	Prince-of-Wales feather	Kattenstaartamarant		1+1 (2)†	1+1+2 (4)§	
Kalanchoe fedtschenkoi	Pentapetalae	Lavender scallops			1+1 (2)†	2+3+1 (6)§	
Kalanchoe laxiflora	Pentapetalae	Milky widow's thrill			2+1 (3)†	4+2+2 (8)§	
Daucus carota	Astrid	Wild carrot	Wilde peen		2+1 (3)†	2+2+1 (5)§	
Mimulus guttatus	Astrid	Seep monkeyflower	Gele maskerbloem		1+1 (2)†	2+1+2 (5)§	
Solanum lycopersicum	Astrid	Tomato	Tomaat		1+1 (2)†	1+1+2 (4)§	
Solanum tuberosum	Astrid	Potato	Aardappel		1+1 (2)†	1+1+0 (2)§	
Eucalyptus grandis	Rosid	Flooded gum			1+1 (2)†	1+0+1 (2)§	
Vitis vinifera	Rosid	Common grape vine	Wijnstok		1+1 (2)†	1+1+1 (3)§	
Cucumis sativus	Fabidae	Cucumber	Komkommer		1+1 (2)†	1+1+1 (3)§	

† Amount of NACK sequences identified in the format: NACK1 + NACK2 (total NACK).

§ Amount of PBK-HL sequences identified in the format: PBK + PBKH + PBKL (total PBK-HL).

Table 1 (cont.): Overview of species containing At1 kinesin subfamily sequences, the clade they belong to, their common English name, their common Dutch name and the number of sequences identified, sorted by At1, NACK, PBK-HL, or Grasses origin.

Latin name	Clade	English common name	Dutch common name	Number of sequences			
				At1	Nack	PBK-HL	Grasses
Fragaria vesca	Fabidae	Woodland strawberry	Bosaardbei		1+1 (2)†	1+0+1 (2) §	
Glycine max	Fabidae	Soybean	Soyaboon		2+2 (4)†	4+2+4 (10) §	
Malus domestica	Fabidae	Apple	Appel		2+1 (3)†	2+0+1 (3)§	
Medicago truncatula	Fabidae	Barrelclover			1+1 (2)†	1+1+2 (4)§	
Phaseolus vulgaris	Fabidae	Common bean	Gewone boon		1+1 (2)†	2+1+2 (5)§	
Prunus persica	Fabidae	Peach	Perzik		1+1 (2)†	1+1+1 (3)§	
Trifolium pratense	Fabidae	Red clover	Rode klaver		1+1 (2)†	1+1+2 (4)§	
Linum usitatissimum	Malpighiales	Flax	Vlas		2+1 (3)†	1+0+1 (2)§	
Manihot esculenta	Malpighiales	Cassava	Cassave		2+1 (3)†	2+2+1 (5)§	
Populus trichocarpa	Malpighiales	Western balsam poplar	West-Amerikaanse balsempopulier		2+1 (3)†	2+1+2 (5)§	
Ricinus communis	Malpighiales	Castor bean	Wonderboom		0+1 (1)†	1+1+1 (3)§	
Salix purpurea	Malpighiales	Purple willow	Bittere Wilg		3+1 (4)†	2+1+3 (6)§	
Citrus clementina	Citrus	Clementine	Clementine		1+1 (2)†	1+1+1 (3)§	
Citrus sinensis	Citrus	Sweet orange	Sinasappel		1+1 (2)†	1+1+1 (3)§	
Carica papaya	Brassicales-Malvales	Papaya	Papaja		1+0 (1)†	1+1+1 (3)§	
Gossypium raimondii	Brassicales-Malvales	Cotton plant	Katoenplant		2+1 (3)†	2+2+2 (6)§	
Theobroma cacao	Brassicales-Malvales	Cacao tree	Cacaoboom		1+1 (2)†	1+1+1 (3)§	
Arabidopsis halleri	Brassicaceae		Kruipende steenkers		1+1 (2)†	2+2+2 (6)§	
Arabidopsis lyrata	Brassicaceae	Lyrate rockcress			1+1 (2)†	2+2+2 (6)§	
Arabidopsis thaliana	Brassicaceae	Thale cress	Zandraket		1+1 (2)†	2+2+2 (6)§	
Boechera stricta	Brassicaceae	Drummond's rockcress			1+0 (1)†	2+2+2 (6)§	
Brassica oleracea Capitata Gp	Brassicaceae	Cabbage	Kool		2+1 (3)†	2+0+2 (4)§	
Brassica rapa	Brassicaceae	Turnip mustard	Raapzaad		1+1 (2)†	2+1+3 (6)§	
Capsella grandiflora	Brassicaceae				1+1 (2)†	2+1+2 (5)§	
Capsella rubella	Brassicaceae	Pink shepherd's-purse	Rood herderstasje		1+1 (2)†	2+1+2 (5)§	

† Amount of NACK sequences identified in the format: NACK1 + NACK2 (total NACK).

§ Amount of PBK-HL sequences identified in the format: PBK + PBKH + PBKL (total PBK-HL).

A search for the NPK1 binding (Nishihama *et al.*, 2002; Ishikawa *et al.*, 2002) and activating domains (Finn *et al.*, 2017; IPR021881) that are characteristic for the NACK kinesins in the other At1 kinesin family members, using protein sequences of three conserved regions present in arabidopsis NACK1 and NACK2 (Table 2), showed that all three regions were present in the ancestral At1 and the NACK classified proteins, but that region 1 was lost in proteins of the PBK-HL branch. Region 2 could be identified in all PBK-HL members, whereas region 3 was present in all PBK and PBKH members but was lost in some members of the PBKL branch. These data suggest that the PBK-HL proteins would still be able to activate NPK1 to some degree, but unable to associate with it.

Table 2: Conserved regions in the arabidopsis NPK1 binding and activating domain, used to determine their presence in the At1 sequences.

Region number	Sequence	Putative functionality
1	SIRAYVTELKERVAKLQYQKQLLVCQVLELE	Binding region
2	VSIIHRTQFYLLFKGDPADQIYMEVELRRTWL	Activation region
3	KEMFELNFA	Activation region

The *pbk1 pbk2 pbkh1 pbkh2* quadruple mutant has a wild-type phenotype.

To examine the possible function of PBK1 and PBK2 in plant development, we obtained T-DNA insertion alleles for the corresponding genes. For PBK1 we obtained an allele (*pbk1-1*) with an insertion in exon 9, and for PBK2 an allele (*pbk2-1*) with an insertion in intron 2. Insertion positions were confirmed by PCR, and we noticed that the *pbk2-1* allele had a double inverted T-DNA insert (Figure 2A). Both mutant alleles produced wild-type looking plants, and also the *pbk1 pbk2* double mutant had a wild-type appearance. Seedlings were tested for root length and root gravitropic response, but no significant difference with wild-type seedlings was observed (not shown). Since the lack of phenotypes could be caused by redundancy with other PBK-HL clade members, we also obtained T-DNA insertion lines for the *PBKH1* and *PBKH2* genes, which were identified as closest homologues in an initial comparison of the arabidopsis At1 family members. Again, T-DNA insertions were confirmed by PCR in the 6th exon for *pbkh1-1*, and in the 9th exon for *pbkh2* (Figure 2A). These alleles were combined with the *pbk1 pbk2* double mutant. The resulting

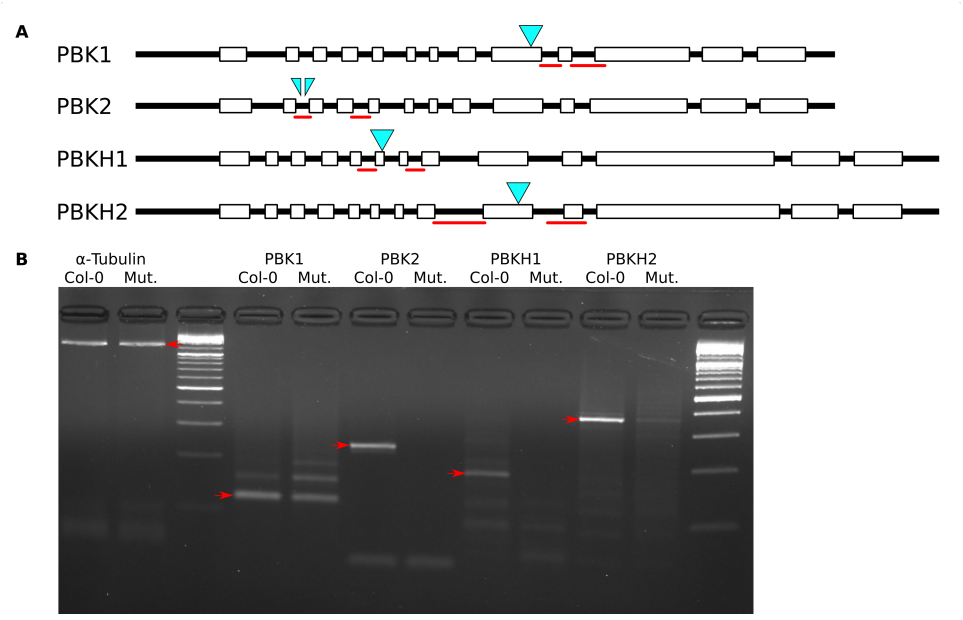

Figure 2: Structure of the *PBK* and *PBKH* genes and the loss-of-function confirmation in the *pbk1 pbk2 pbkh1 pbkh2* quadruple T-DNA insertion mutant.
(A) Structure of the *PBK* and *PBKH* genes. Exons are indicated with open blocks, upstream and downstream sequences and intervening introns with a black line, positions of T-DNA insertions are indicated with blue triangles, the position of exon specific RT-PCR primer binding sites overlapping with splice sites are indicated with red lines (intron sequences are not included, preventing recognition of genomic DNA). *PBK2* has a double inverted T-DNA insertion.
(B) Agarose gel of the RT-PCR reactions on *A. thaliana* 'Columbia' wild-type and the *pbk1 pbk2 pbkh1 pbkh2* quadruple mutant. The *α-Tubulin* gene was used as a positive control. The positions in the gel where the expected product bands should appear are indicated with a red arrow head.

quadruple mutant plants also showed a wild-type appearance, and seedlings did not show deviating root phenotypes. RT-PCR analysis on the *pbk1 pbk2 pbkh1 pbkh2* quadruple mutant line showed that the *pbk2* and *pbkh1* alleles are true loss-of-function alleles, whereas wild-type transcript levels could still be detected for the *PBK1* gene and significantly reduced levels for the *PBKH2* gene (Figure 2B). Although the T-DNA insertions in these genes are in an exon in the middle of the gene, and should thus lead to loss-of-function, we cannot exclude that the lack of mutant phenotypes of the quadruple mutant is caused by restoration of gene function by e.g. alternative gene splicing. Our results do suggest, however, that the PBKs and PBKHs act functionally redundant with other PBK-HL kinesin family

members.

The PBKs are expressed ubiquitously in young, developmentally active tissues.

To investigate the expression of the *PBK* and *PBKH* genes, we introduced (∼2.5-3.0kpb) *promoter::GUS-GFP* constructs for each of the four *PBK* and *PBKH* genes into arabidopsis and selected several single copy lines showing reproducible expression patterns per construct (Figure 3). Generally, all four *promoter::GUS-GFP* fusions showed strong expression throughout the seedling, with the highest activity observed in the shoot and root meristem (Figure 3A). The *PBK1* promoter consistently did not show activity in the hypocotyl, whereas the *PBKH1* promoter showed limited expression in the root (Figure 3A-D).
Exposure of seedlings of the *promoter::GUS-GFP* lines to heat (37°C, 6 hours), darkness (6 hours), or 100µM IAA did not induce a significant change in the expression level or pattern (Figure 3B-D). In flowering plants, strong expression could be observed in the young flower buds, flowers, bracts, early stage siliques and the upper two internode stem segments (Figure 3E).
In conclusion, the *promoter::GUS-GFP* fusions indicated that all four genes show an overlapping more or less constitutive expression pattern that is not very responsive to hormonal or external signals, with highest expression in meristems and young developing tissues. The results suggest that the kinesins might play a role during cell division.

The PBKs localize to the microtubules in protoplasts, but not *in planta*.

To observe PBK localization in protoplasts and *in planta*, we generated *35S::PBK/PBKH-YFP* constructs, containing the genomic clones translationally fused to YFP. Transfection of arabidopsis suspension-based protoplasts with these constructs showed that all four PBKs localized to string-like structures (Figure 4A). Treatment of *35S::PBK1-YFP* expressing protoplasts with microtubule depolymerizing agents oryzalin or colchicine resulted in an evenly diffused YFP signal as a result of the catastrophe of the MT, whereas the DMSO control showed the same string-like structures as the untreated cells (Figure 4B). These results show that in protoplasts the PBKs indeed localize to the MT.

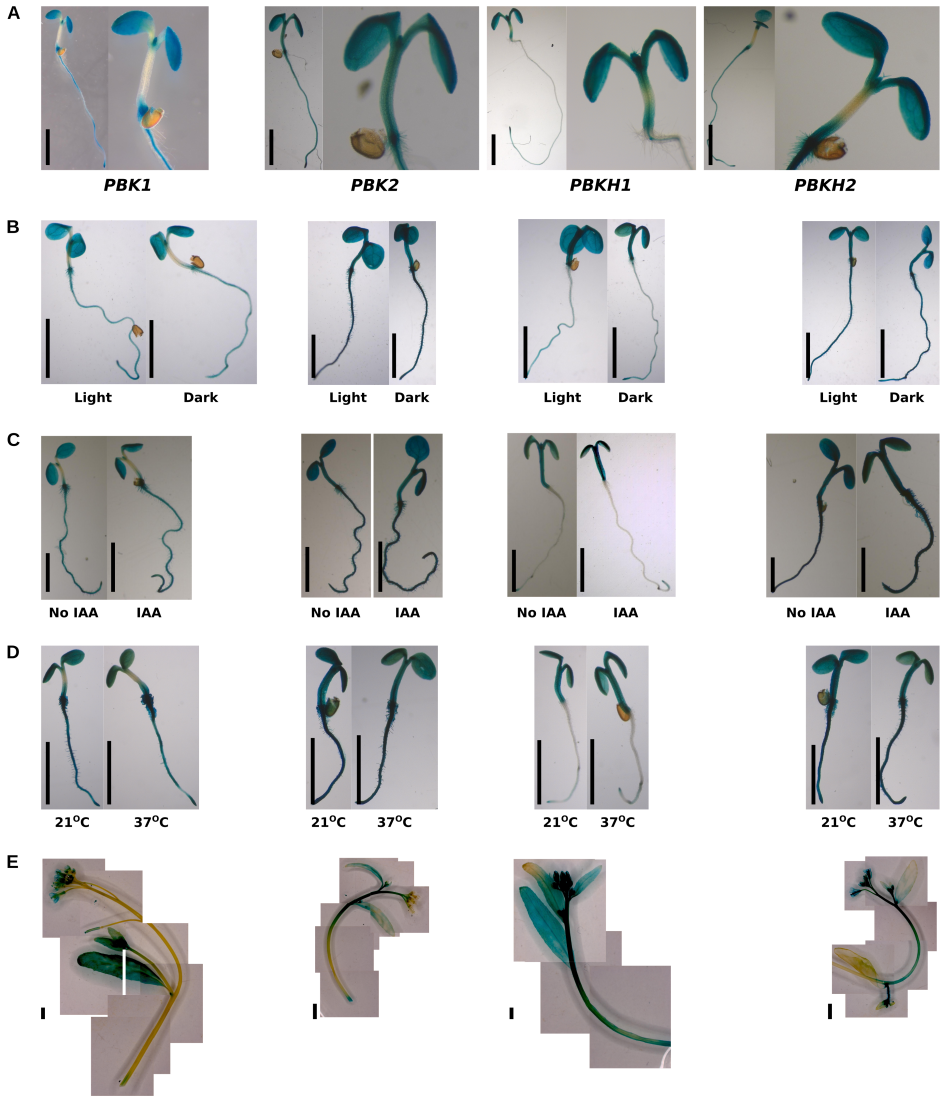

Figure 3: Expression pattern of respectively *PBK1*, *PBK2*, *PBKH1* and *PBKH2* (from left to right) as indicated by their *promoter::GUS-GFP* reporter. (A-D) Expression pattern as indicated by GUS stained 3 day-old seedlings. Untreated seedlings (A), or seedlings incubated for 6 hours at 21°C in medium in light or dark (B), without or with 100µM IAA (C), or at 21°C or at 37°C (D), (E) Expression pattern indicated by GUS stained young inflorescences. Size bar indicates 1 cm.

To confirm this localization *in planta*, we generated transgenic arabidopsis lines carrying a *pUBI::PBK1-YFP* or a *pUBI::PBK2-YFP* construct. The *pUBI10* promoter is known to drive homogeneous expression at moderate

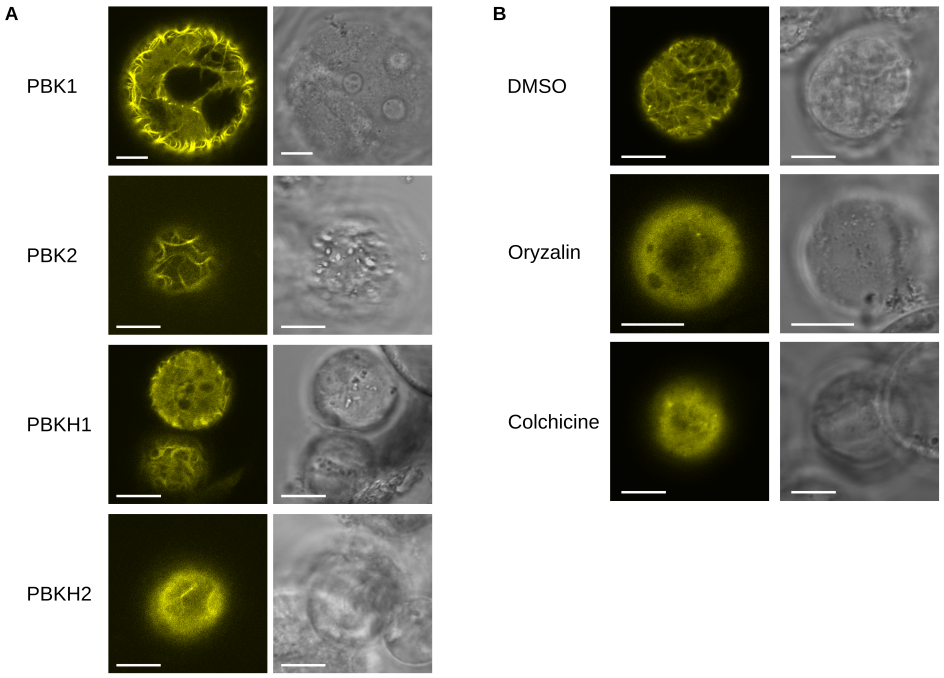

Figure 4: PBK(H)-YFP fusions localize to the MT in arabidopsis protoplasts. Confocal microscopy images (left: YFP channel; right: transmitted light channel) of arabidopsis protoplasts expressing respectively (from top to bottom) the PBK1-YFP, PBK2-YFP, PBKH1-YFP or PBKH2-YFP fusion (A) or of arabidopsis protoplasts expressing the PBK1-YFP fusion following treatment with respectively (from top to bottom) DMSO (control), or with the MT depolymerizating agents oryzalin (50µM) or colchicine (323.3µM) (B). Size bar indicates 10µm.

levels in all cell types (Norris *et al.*, 1993; Geldner *et al.*, 2009), but even in the stronger expressing lines, the YFP signal was only barely visible. Treatment of the seedlings with the proteasome inhibitor MG132 resulted in a strong constitutive signal (Figure 5), suggesting that both kinesins are subject to targeted degradation by the 26S proteasome. To our surprise, the stabilized kinesins localized mainly to the periphery of the cell, and only weak internal signals could be observed, that occasionally were reminiscent of the thread-like structures observed in protoplasts. By using a RFP-labelled TUBULIN ALPHA-5 marker line (*35S::TUA5-RFP*), we could clearly visualize the cortical MT in root epidermis cells (Figure 5; bottom), but similar structures were not observed in *pUBI::PBK1-YFP* or *pUBI::PBK2-YFP* root epidermis cells, even when focusing on the cell cortex (Figure 5; stars in detail panel in upper and middle images). These

results suggest the PBKs do localize to the MT, but that their localization to MT *in planta* is very transient and difficult to detect, due to their high proteasomal degradation.

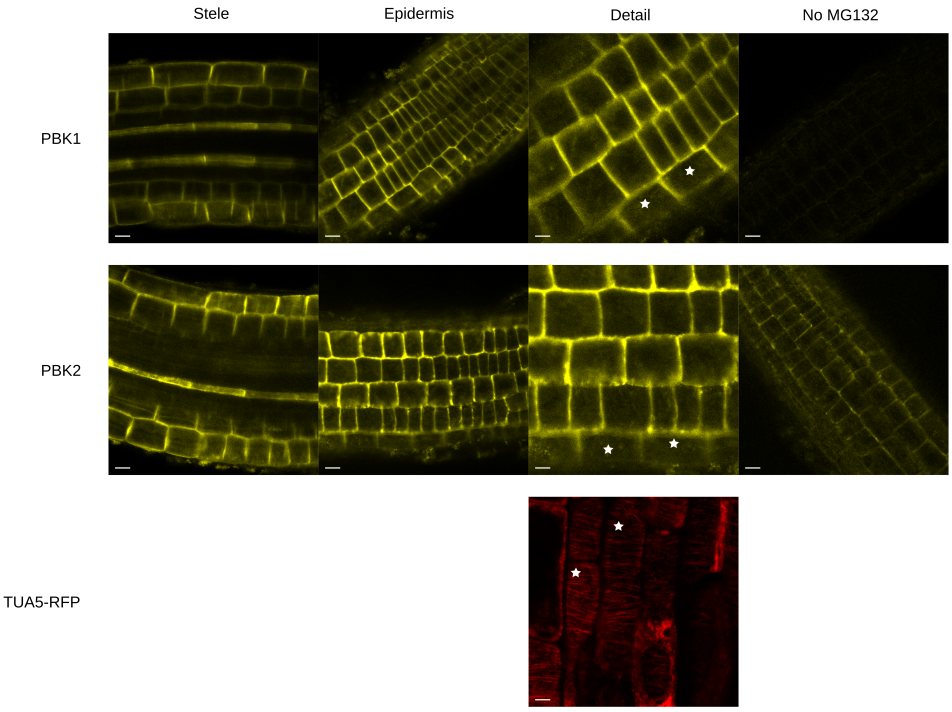

Figure 5: Localization of PBK-YFP fusion proteins in arabidopsis seedling roots. Confocal images of roots of 5 days old *pUBI::PBK1-YFP* (upper), *pUBI::PBK2-YFP* (middle) or *35S::TUA5-RFP* (bottom, untreated) seedlings after treatment with 50µM MG132. Images show longitudinal cross sections through the stele (left), epidermis (middle-left), close up detail of the epidermis (middle-right), and without MG132 treatment (right). Detail images (middle-right) show at least a few cells (indicated with an asterisk) where the optical section is at the cell cortex. Size bars indicate 10µm.

Discussion

The arabidopsis AGC protein serine/threonine kinase PID plays an important role as regulator of polar auxin transport. The kinase determines the polar distribution of PIN proteins in plant cells by phosphorylating the cytosolic loop of these auxin efflux carriers. Previous research indicated that PDK1 is an important upstream regulator of PID, as it enhances the kinase activity of PID by phosphorylating residues in its activation loop. In Chapter 3 of this thesis we show that this activation in protoplasts

promotes microtubule localization of PID. Furthermore, in chapter 4 we show that the previously identified PID binding protein BT1, and the homologous kinesins PBK1 and PBK2 make up the complex that is responsible for this MT localization of PID in protoplasts. Unfortunately, however, we have not been able to find evidence for the MT localization of PID *in planta* (Chapter 4). In this chapter, we therefore performed a more detailed functional analysis of the PBKs to find more clues for a possible role of these kinesins in PID function.

Phylogenetic analysis indicated that the PBKs belong to the At1 family of kinesins to which also the NACK kinesins belong (Dagenbach & Endow, 2004; Richardson *et al.*, 2006), and that the PBK branch arose in the Pentapetalae branch, by gene duplication resulting in two gene copies in the Brassicaceae. At1 kinesins seem land plant specific, since they were not found in Chlorophytes, but since we did not check Charophyte genomes, we cannot be absolutely sure about this. At least it seems that the evolution of At1 kinesins co-occurred with the evolution of the AGC3 kinases and the PIN transporters during the transition of plants from water to land (Galván-Ampudia & Offringa, 2007).

When looking at the conservation of the NPK1 binding and activation domains that are characteristic for the NACK kinesins, it is unlikely that the PBK-HL members are able to bind NPK1. It would be interesting, however, to see if the retained activating domains in PBKs would be able to activate the AGC3 kinases. The fact that the quadruple mutant does not show a phenotype suggests that there is further functional redundancy among the PBK-HL members and possibly with the NACK members of the At1 family in arabidopsis. However, the PBK-HL branch shows more gene duplications, increasing the total amount of genes per species in this branch, compared with the NACK branch (Table 1). This suggests that there is more genetic and, possibly, functional drift of the kinesins in the PBK-HL branch, which makes it more difficult to put a specific function to these kinesins within multiple species.

Analysis of the *promoter::GUS* lines indicated that the *PBK* and *PBKH* genes are quite abundantly expressed, especially in young and meristematic tissues, but do not seems to be directly regulated by auxin or environmental triggers. In line with the function of the NACK kinesins and the PQR MAPK pathway in plant cytokinesis, these expression data suggest a role for the PBKs in cell division. Where the NACKs cooperate with the PQR MAPK cascade to progress the outgrowth of

the phragmoplast, the PBKs (and PBKHs) could function in a MT associated signaling pathway that includes the BT1 protein, PID and the upstream regulator PDK1. PDK1-mediated phosphorylation of PID leads to recruitment of this kinase to the MT by the BT1-PBK complex in protoplasts. The fact that MT localization of neither PID nor BT1 or PBK could be observed *in planta* is probably caused by the efficient proteasome-mediated degradation of the latter two components, as shown previously for BT1 (Robert *et al.*, 2009) and here for the PBKs. Plants expressing either the loss-of-phosphorylation or the phospho-mimic PID version showed problems with cotyledon positioning in embryos and with organ formation at the inflorescence and flower meristems (Chapter 3). This indicates that dynamic phosphorylation of PID by PDK1 is essential for these processes, as was previously shown for phosphorylation of PIN proteins by PID (Huang *et al.*, 2010). A possible and logical function for the PID-BT1-PBK complex could be that during cell division this complex guides PID to the phragmoplast via the MT. In dividing cells, PIN proteins are preferentially secreted in a MT-dependent manner to the phragmoplast, but by the time the new daughter cells are formed they have assumed their correct polar position (Geldner *et al.*, 2001; Boutté *et al.*, 2006; Mravec *et al.*, 2011). PID could thus be involved in establishing the correct PIN polarity by phosphorylating these auxin carriers at the growing cell plate.

Acknowledgments

We would like to thank Maurijn van der Zee for his feedback regarding the section about evolutionary and phylogenetic analysis. M.E.J.H. was financially supported by the Netherlands Organization for Scientific Research (NWO) through the NWO-Chemical Sciences TOP grant 700.58.301 to R.O.

Material and Methods

Plant lines, accessions and genes

All plant lines used in this chapter are in the *Arabidopsis thaliana* 'Columbia' background.

The SALK T-DNA insertion lines (`http://signal.salk.edu/`) *pbk1* (Salk: SALK_006264, NASC: N506264), *pbk2* (Salk: SALK_008956, NASC: N508956), *pbkh1* (Salk: SALK_105051, NASC: N605051) and *pbkh2* (Salk: SALK_068539, NASC: N568539) were obtained from the Arabidopsis stock centre.

The *pbk1 pbk2 pbkh1 pbkh2* quadruple T-DNA insert line was generated from the single T-DNA insert lines by crossing. After each cross, the resulting plants were genotyped for homo- or heterozygosity for the T-DNA insertions by PCR using 3 primers (two gene specific primers and LBA1a for the T-DNA insert) in one reaction. The gene specific primer pairs for *PBK1*, *PBK2*, *PBKH1* and *PBKH2* were respectively PBK1 LP and PBK1 RP, PBK2A LP and PBK2A RP, PBKH1 LP and PBKH1 RP, and PBKH2 LP and PBKH2 RP (Table 3).

Plasmids, molecular cloning and arabidopsis transformation

For the generation of the *PBK promoter::GUS-GFP* reporter lines we used plasmid *R4L1pGWB532* (Nakamura *et al.*, 2009). Promoter sequences of *PBK1* (3088bp), *PBK2* (3052bp), *PBKH1* (2540bp) and *PBKH2* (2724bp) were amplified from genomic *Arabidopsis thaliana* 'Columbia' DNA by PCR using respectively primer combinations PBK1-B1 and PBK1-B4, PBK2-B1 and PBK2-B4, PBKH1-B1 and PBKH1-B4 and PBKH2-B1 and PBKH2-B4 (Table 3). The amplified PCR products were cleaned from primer dimers, BP recombined into entry vector *pDONR-P4-P1R*, and subsequently LR recombined into the *R4L1pGWB532* destination vector, all according to the Gateway system manual (Thermo Fisher Scientific, USA).

For the protoplast experiments, the coding regions of *PBK1*, *PBK2*, *PBKH1* and *PBKH2* were obtained by BP recombining PCR products derived from *Arabidopsis thaliana* 'Columbia' genomic DNA using respectively primer pairs attB PBK1 F and attB –STOP PBK1 R, attB PBK2 F and attB –STOP PBK2 R, attB PBKH1 F and attB -STOP PBKH1 R and attB PBKH2 F and attB –STOP PBKH2 R (Table 3) into the *pDONR* gateway entry vector. The expression vectors for the

Table 3: List of primers used in this research.

Name	Sequence (5'→3')
PBK1-B1	GGGGACTGCTTTTTTGTACAAACTTGTCTTCTTTAGCAAGTGCTACCAATT
PBK1-B4	GGGGACAACTTTGTATAGAAAAGTTGTTCTCACTCTATTCGGAACAATGAATCTCACC
PBK2-B1	GGGGACTGCTTTTTTGTACAAACTTGTTGCTCACTGGTCAAATCACAATGATGC
PBK2-B4	GGGGACAACTTTGTATAGAAAAGTTGCAGTATTCTGAAAATGTTTCTGCGTCGGTCC
PBKH1-B1	GGGGACTGCTTTTTTGTACAAACTTGTCTTCACCCGTCACCTCCCTTCCCG
PBKH1-B4	GGGGACAACTTTGTATAGAAAAGTTGTTGGGCCAGAAATTCAAGTGTTATCTCGG
PBKH2-B1	GGGGACTGCTTTTTTGTACAAACTTGTCTTCTACCCTACCTCTACCACAAAGGAAC
PBKH2-B4	GGGGACAACTTTGTATAGAAAAGTTGATGGAGTAGAGACAAGCCAGTGTACCG
attB PBK1 F	GGGGACAAGTTTGTACAAAAAAGCAGGCTTAATGGAGAAGACACAGATGCCTGTAGC
attB -STOP PBK1 R	GGGGACCACTTTGTACAAGAAAGCTGGGTTGAAAAGTGCAGGCATGCTTTTTCTCCAACTATG
attB PBK2 F	GGGGACAAGTTTGTACAAAAAAGCAGGCTTAATGGGAGCGATTGCTGGAGAAGAGC
attB -STOP PBK2 R	GGGGACCACTTTGTACAAGAAAGCTGGGTTGAACAGTGTGGCCATGCTTTTCCTCC
attB PBKH1 F	GGGGACAAGTTTGTACAAAAAAGCAGGCTTAATGGGTATAGGAGAGGATCAGATGCAAGG
attB -STOP PBKH1 R	GGGGACCACTTTGTACAAGAAAGCTGGGTTCAAAATAGAGAGCGACAAAACGCTGCG
attB PBKH2 F	GGGGACAAGTTTGTACAAAAAAGCAGGCTTAATGACTACAGAAGATGATGATCAGATGCTAGGACC
attB -STOP PBKH2 R	GGGGACCACTTTGTACAAGAAAGCTGGGTTCAAAAAGGAGAGGGACAAAACGCTGCG
aTUB F	CGGAATTCATGAGAGAGATCCTTCATATC
aTUB R	CCCTCGAGTTAAGTCTCGTACTCCTCTTC
LBA1a	TGGTTCACGTAGTGGGCCATCG
PBK1 LP	TTCTCACCCTGACGTTCTGGC
PBK1 RP	GATTGCTGTCTTTGGCATGCTT
PBK2A LP	GCAAATCCTGAGCAAGCTCCAT
PBK2A RP	GCGATTGCTGGAGAAGAGCTG
PBKH1 LP	AACTCGCTCTCCAGTTTAGCC
PBKH1 RP	CTGAAGTTCTCAGCCATGGAG
PBKH2 LP	TGGTTCAACACTGCCTTCTTC
PBKH2 RP	TTCAACCATTCGTCGAAGATC
RT-PCR PBK1 F1	CAGATACAAAAGATGGAAAAGGAGATCGCAGAGT
RT-PCR PBK1 R1	TGGAGTTCCAGGCTTTGACGC
RT-PCR PBK2 F1	GGAATTAACTCTAGTATTTTCGCG
RT-PCR PBK2 R1	CGGCGGCCCCTTTCTCAGGGTCATCTCG
RT-PCR PBKH1 F1	GGAGCTTTTATCAATCTGTATcGCTCAACGGC
RT-PCR PBKH1 R1	CCAGCAAGATCAATGAAATTCACTGTCGCTGTG
RT-PCR PBKH2 F1	CCGTAAGCTAAGTAAAGAAAAAACTGGGC
RT-PCR PBKH2 R1	CCTCTTTCTTAgGCTTTTCAACCTCAAGG

protoplast experiments were generated by LR recombining the coding regions from *pDONR* into the *pART7*-derived Gateway-YFP destination vector (see Chapter 3), all according to the Gateway system manual (Thermo Fisher Scientific, USA).

To generate the *PBK1-YFP* and *PBK2-YFP* overexpression constructs, the respective coding regions were LR recombined from the *pDONR-PBK1* and *pDONR-PBK2* entry vectors into the *pDONR-UBC-YFP* destination vector (Grefen *et al.*, 2010), resulting in *pUBC::PBK1-YFP* and *pUBC::PBK2-YFP*.

All binary vectors were introduced into *Agrobacterium tumefaciens* strain LBA1100 by electroporation (den Dulk-Ras & Hooykaas, 1995), and transgenic *Arabidopsis thaliana* 'Columbia' plants were obtained by floral dip transformation (Clough & Bent, 1998; see also Chapter 3).

RT-PCR analysis

Total RNA was isolated from one week old *pbk1 pbk2 pbkh1 pbkh2* quadruple mutant and arabidopsis wild-type seedlings using the Nucleospin RNA Plant kit (Macherey-Nagel, Germany). Same amounts of RNA were used to generate cDNA by adding 2µl Oligo(dT), 1µl RNAsin ribonuclease inhibitor (Promega) and RNAse-free water to a final volume of 50µl. This mixture was heated to 70°C for 5 minutes and subsequently cooled on ice. Next, 5µl of 2.5mM dNTPs, 5µl of 5x reaction buffer, 1µl RNAsin and 1µl M-MLV Reverse Transcriptase (Promega) was added, and the mixture was incubated at 37°C for 1.5 hours. The generated cDNA was used as template in a PCR reaction (42 cycles and 64°C annealing temperature) using primer pairs aTUB F and aTUB R for the *α-tubulin* control, and RT-PCR PBK F1 and RT-PCR PBK1 R1, RT-PCR PBK2 F1 and RT-PCR PBK2 R1, RT-PCR PBKH1 F1 and RT-PCR PBKH1 R1, and RT-PCR PBKH2 F1 and RT-PCR PBKH2 R1 for *PBK1*, *PBK2*, *PBKH1* and *PBKH2*, respectively (Table 3).

Phylogenetic analysis

Protein sequences of At1 subfamily members (Table S1) were obtained by P-Blast using the *Arabidopsis thaliana* At1 kinesin family members, or the reconstructed common ancestors (described below) against the Phytozome database (`http://phytozome.jgi.doe.gov/pz/`). For each BLAST search an error threshold was chosen based on the results. All sequences above that threshold were imported into CLC Workbench 7 for further analysis and common ancestor reconstruction. Imported sequences were aligned to identify duplicate sequences and detect polymorphisms and splicing variants. Duplicates, polymorphisms and splicing variants within a single species were taken out of the data set.

Common ancestors were reconstructed by aligning all sequences in a clade and, if available, common ancestors of the descendant clade(s). The consensus sequence of the alignment was taken as a separate sequence. Amino acid positions that could not be assigned with an amino acid automatically, were manually corrected against the majority of the amino acid at that position, taking into consideration multiple sequences within a species, polymorphisms and common ancestor sequences of the clade(s) below. In case assigning the amino acid was still not possible, one of the amino acids at the position of the sequences were randomly chosen from one of the species sequences. Alignments were performed by the software's

slow alignment function (Settings: Gap open cost: 10.0; Gap extension cost: 1.0; End gap cost: as any other).

Confocal microscopy

Confocal images of arabidopsis roots were obtained using a Zeiss AxioImager equipped with a LSM5 Exciter and a Plan-Neofluar 40x/0.9 Imm corr or Plan-Apochromat 63x/1.4 Oil DIC objective. An Argon/Krypton laser line with excitation on 514 nm (YFP) and 543nm (RFP) was used at 15-20% intensity. We used the beam splitters HFT 458/514 and NFT 635 VIS and a band pass filter of 530-600 nm (YFP) or beam splitters HFT 543 and NFT 545 and a long pass filter of 560nm. The proteasome inhibitor MG132 was applied at a 50µM concentration during 4 hours.
Confocal images of the protoplasts were taken with a Zeiss AxioObserver equipped with a Zeiss LSM5 Exciter and a C-Apochromat 63x/1.20 W Korr UV-VIS-IR M27 objective. We used the Argon/Krypton laser line of 514nm with a HFT 405/514 beam splitter and bandpass filter of 530-600nm to visualize the YFP signal. All confocal images were further processed with the Zen 2009 light edition (Carl Zeiss MicroImaging GmbH).

Plant growth conditions

Seedlings were germinated on solid MA medium (Masson & Paszkowski, 1992) at 21°C, 16 hours photoperiod and 70% relative humidity. Seven days old seedlings were transferred to soil and grown at 21°C, 70% relative humidity, and 16 hours photoperiod. For the different treatments of the *PBK promoter::GUS-GFP* reporter lines, 3 days-old seedlings were transferred to 6-well plates filled with 2ml MA medium (Masson & Paszkowski, 1992), and plates were standardly wrapped in aluminium foil and incubated for 6 hours at 21°C, 70% relative humidity. For auxin treatment IAA dissolved in DMSO was added to a final concentration ranging from 1µM to 100µM. Control seedlings were incubated in MA medium to which the same volume of DMSO was added. For the light treatment the 6-well plate was left unwrapped. For the high temperature treatment, a wrapped plate was incubated at 37°C instead of 21°C.

GUS staining

Five day old seedlings were transferred to 6 well plates containing 3ml of ice cold acetone per well and the plates were incubated at -20°C for 20 minutes. The acetone was removed and GUS staining solution (100mM Phosphate buffer, pH 7.0; 10mM EDTA; 1mM $K_3Fe(CN)_6$; 1mM $K_4Fe(CN)_6$; 0.5mg/ml X-gluc) was added to the wells and the plates were transferred to a vacuum chamber for 20 minutes in the dark. After the vacuum infiltration, the plates were wrapped in aluminium foil and incubated at 37°C. After 24 hour incubation, the staining solution was removed, and a solution of 0.24M hydrochloric acid in 20% methanol was added and the plates were incubated at 65°C for 20 minutes. The solution was replaced by 7% NaOH in 60% ethanol and plates were incubated at room temperature for 15 minutes. After this incubation step, the seedlings were washed for 5 minutes with subsequently 70%, 40%, and 10% ethanol, and finally with 5% ethanol in 25% glycerol for 15 minutes. After washing, the seedlings were kept in 50% glycerol until imaging. For the inflorescences the same staining method was used, except that the ice cold acetone treatment was incubated at room temperature instead of at -20°C. Stained seedlings and inflorescences were imaged with a Leica MZ12 equipped with Leica DC500 digital color camera. For the inflorescences, multiple detailed images were taken that were later merged into one single image by using the Inkscape software (`https://inkscape.org/`).

Bibliography

Armour, W. J., Barton, D. A., Law, A. M. K. & Overall, R. L. (2015). Differential growth in periclinal and anticlinal walls during lobe formation in arabidopsis cotyledon pavement cells. The Plant Cell **27**, 2484–2500.

Bashline, L., Li, S. & Gu, Y. (2014). The trafficking of the cellulose synthase complex in higher plants. Annals of Botany **114**, 1059–1067.

Boutté, Y., Crosnier, M.-T., Carraro, N., Traas, J. & Satiat-Jeunemaitre, B. (2006). The plasma membrane recycling pathway and cell polarity in plants: studies on PIN proteins. Journal of Cell Science **119**, 1255 LP – 1265.

Bowers, J. E., Chapman, B. A., Rong, J. & Paterson, A. H. (2003). Unravelling angiosperm genome evolution by phylogenetic analysis of chromosomal duplication events. Nature **422**, 433–438.

Bryan, J. & Wilson, L. (1971). Are cytoplasmic microtubules heteropolymers? Proceedings of the National Academy of Sciences of the United States of America **68**, 1762–1766.

Clough, S. J. & Bent, A. F. (1998). Floral dip: a simplified method for *Agrobacterium*-mediated transformation of *Arabidopsis thaliana*. The Plant Journal **16**, 735–743.

Dagenbach, E. M. & Endow, S. A. (2004). A new kinesin tree. Journal of Cell Science **117**, 3–7.

den Dulk-Ras, A. & Hooykaas, P. J. J. (1995). Electroporation of *Agrobacterium tumefaciens*. In Plant Cell Electroporation and Electrofusion Protocols. Methods in Molecular Biology™, (Nickoloff, J. A., ed.), pp. 63–72. Springer New York Totowa, NJ.

Dhonukshe, P., Aniento, F., Hwang, I., Robinson, D. G., Mravec, J., Stierhof, Y.-D. & Friml, J. (2007). Clathrin-mediated constitutive endocytosis of PIN auxin efflux carriers in *Arabidopsis*. Current Biology **17**, 520–527.

Erickson, H. P. (1974). Microtubule surface lattice and subunit structure and observations on reassembly. The Journal of Cell Biology **60**, 153–167.

Finn, R. D., Attwood, T. K., Babbitt, P. C., Bateman, A., Bork, P., Bridge, A. J., Chang, H.-Y., Dosztányi, Z., El-Gebali, S., Fraser, M., Gough, J., Haft, D., Holliday, G. L., Huang, H., Huang, X., Letunic, I., Lopez, R., Lu, S., Marchler-Bauer, A., Mi, H., Mistry, J., Natale, D. A., Necci, M., Nuka, G., Orengo, C. A., Park, Y., Pesseat, S., Piovesan, D., Potter, S. C., Rawlings, N. D., Redaschi, N., Richardson, L., Rivoire, C., Sangrador-Vegas, A., Sigrist, C., Sillitoe, I., Smithers, B., Squizzato, S., Sutton, G., Thanki, N., Thomas, P. D., Tosatto, S., Wu, C. H., Xenarios, I., Yeh, L.-S., Young, S.-Y. & Mitchell, A. L. (2017). InterPro in 2017—beyond protein family and domain annotations. Nucleic Acids Research **45**, D190–D199.

Friml, J., Yang, X., Michniewicz, M., Weijers, D., Quint, A., Tietz, O., Benjamins, R., Ouwerkerk, P. B. F., Ljung, K., Sandberg, G., Hooykaas, P. J. J., Palme, K. & Offringa, R. (2004). A PINOID-dependent binary switch in apical-basal PIN polar targeting directs auxin efflux. Science **306**, 862–865.

Fu, Y., Gu, Y., Zheng, Z., Wasteneys, G. & Yang, Z. (2005). Arabidopsis interdigitating cell growth requires two antagonistic pathways with opposing action on cell morphogenesis. Cell **120**, 687–700.

Galván-Ampudia, C. S. & Offringa, R. (2007). Plant evolution: AGC kinases tell the auxin tale. Trends in Plant Science **12**, 541–547.

Geldner, N., Dénervaud-Tendon, V., Hyman, D. L., Mayer, U., Stierhof, Y.-D. & Chory, J. (2009). Rapid, combinatorial analysis of membrane compartments in intact plants with a multicolor marker set. Plant Journal **59**, 169–178.

Geldner, N., Friml, J., Stierhof, Y.-D., Jürgens, G. & Palme, K. (2001). Auxin transport inhibitors block PIN1 cycling and vesicle trafficking. Nature **413**, 425–428.

Grefen, C., Donald, N., Hashimoto, K., Kudla, J., Schumacher, K. & Blatt, M. R. (2010). A ubiquitin-10 promoter-based vector set for fluorescent protein tagging facilitates temporal stability and native protein distribution in transient and stable expression studies. Plant Journal **64**, 355–365.

Gunning, B. E. S. & Wick, S. M. (1985). Preprophase bands, phragmoplasts, and spatial control of cytokinesis. Journal of Cell Science **1985**, 157 LP – 179.

Gutierrez, R., Lindeboom, J. J., Paredez, A. R., Emons, A. M. C. & Ehrhardt, D. W. (2009). *Arabidopsis* cortical microtubules position cellulose synthase delivery to the plasma membrane and interact with cellulose synthase trafficking compartments. Nature Cell Biology **11**, 797–806.

Habets, M. E. J. & Offringa, R. (2014). PIN-driven polar auxin transport in plant developmental plasticity: A key target for environmental and endogenous signals. New Phytologist **203**, 362–377.

Hasezawa, S., Ueda, K. & Kumagai, F. (2000). Time-sequence observations of microtubule dynamics throughout mitosis in living cell suspensions of stable transgenic *arabidopsis*—direct evidence for the origin of cortical microtubules at M/G1 interface—. Plant and Cell Physiology **41**, 244–250.

Hoshino, H., Yoneda, A., Kumagai, F. & Hasezawa, S. (2003). Roles of actin-depleted zone and preprophase band in determining the division site of higher-plant cells, a tobacco BY-2 cell line expressing GFP-tubulin. Protoplasma **222**, 157–165.

Huang, F., Kemel Zago, M., Abas, L., van Marion, A., Galván-Ampudia, C. S. & Offringa, R. (2010). Phosphorylation of conserved PIN motifs directs *arabidopsis* PIN1 polarity and auxin transport. Plant Cell **22**, 1129–1142.

Hussey, P. J., Ketelaar, T. & Deeks, M. J. (2006). Control of the actin cytoskeleton in plant cell growth. Annual Review of Plant Biology **57**, 109–125.

Ishida, T., Thitamadee, S. & Hashimoto, T. (2007). Twisted growth and organization of cortical microtubules. Journal of Plant Research **120**, 61–70.

Ishikawa, M., Soyano, T., Nishihama, R. & Machida, Y. (2002). The NPK1 mitogen-activated protein kinase kinase kinase contains a functional nuclear localization signal at the binding site for the NACK1 kinesin-like protein. The Plant Journal **32**, 789–798.

Kachar, B. & Reese, T. S. (1988). The mechanism of cytoplasmic streaming in characean algal cells: sliding of endoplasmic reticulum along actin filaments. The Journal of Cell Biology **106**, 1545–1552.

Kamal, A. & Goldstein, L. S. B. (2002). Principles of cargo attachment to cytoplasmic motor proteins. Current Opinion in Cell Biology **14**, 63–68.

Ketelaar, T. (2013). The actin cytoskeleton in root hairs: all is fine at the tip. Current Opinion in Plant Biology **16**, 749–756.

Ketelaar, T., Faivre-Moskalenko, C., Esseling, J. J., de Ruijter, N. C. A., Grierson, C. S., Dogterom, M. & Emons, A. M. C. (2002). Positioning of nuclei in arabidopsis root hairs: an actin-regulated process of tip growth. The Plant Cell **14**, 2941–2955.

Kopczak, S. D., Haas, N. A., Hussey, P. J., Silflow, C. D. & Snustad, D. P. (1992). The small genome of arabidopsis contains at least six expressed alpha-tubulin genes. The Plant Cell **4**, 539–547.

Lawrence, C. J., Dawe, R. K., Christie, K. R., Cleveland, D. W., Dawson, S. C., Endow, S. A., Goldstein, L. S. B., Goodson, H. V., Hirokawa, N., Howard, J., Malmberg, R. L., McIntosh, J. R., Miki, H., Mitchison, T. J., Okada, Y., Reddy, A. S. N., Saxton, W. M., Schliwa, M., Scholey, J. M., Vale, R. D., Walczak, C. E. & Wordeman, L. (2004). A standardized kinesin nomenclature. The Journal of Cell Biology **167**, 19–22.

Liu, B., Joshi, H. C., Wilson, T. J., Silflow, C. D., Palevitz, B. A. & Snustad, D. P. (1994). Gamma-tubulin in arabidopsis: gene sequence, immunoblot, and immunofluorescence studies. The Plant Cell **6**, 303–314.

Liu, B., Marc, J., Joshi, H. C. & Palevitz, B. A. (1993). A gamma-tubulin-related protein associated with the microtubule arrays of higher plants in a cell cycle-dependent manner. Journal of Cell Science **104**, 1217 LP – 1228.

Masson, J. & Paszkowski, J. (1992). The culture response of *Arabidopsis thaliana* protoplasts is determined by the growth conditions of donor plants. Plant Journal **2**, 829–833.

McDowell, J. M., Huang, S., McKinney, E. C., An, Y. Q. & Meagher, R. B. (1996). Structure and evolution of the actin gene family in *Arabidopsis thaliana*. Genetics **142**, 587–602.

Mizuno, K. (1993). Microtubule-nucleation sites on nuclei of higher plant cells. Protoplasma **173**, 77–85.

Mravec, J., Petrášek, J., Li, N., Boeren, S., Karlova, R., Kitakura, S., Pařezová, M., Naramoto, S., Nodzyński, T., Dhonukshe, P., Bednarek, S. Y., Zažímalová, E., de Vries, S. & Friml, J. (2011). Cell plate restricted association of DRP1A and PIN proteins is required for cell polarity establishment in *Arabidopsis*. Current Biology **21**, 1055–1060.

Naito, H. & Goshima, G. (2015). NACK kinesin is required for metaphase chromosome alignment and cytokinesis in the moss *Physcomitrella patens*. Cell Structure and Function **40**, 31–41.

Nakamura, S., Nakao, A., Kawamukai, M., Kimura, T., Ishiguro, S. & Nakagawa, T. (2009). Development of Gateway binary vectors, R4L1pGWBs, for promoter analysis in higher plants. Bioscience, Biotechnology, and Biochemistry **73**, 2556–2559.

Nishihama, R., Soyano, T., Ishikawa, M., Araki, S., Tanaka, H., Asada, T., Irie, K., Ito, M., Terada, M., Banno, H., Yamazaki, Y. & Machida, Y. (2002). Expansion of the cell plate in plant cytokinesis requires a kinesin-like protein/MAPKKK complex. Cell **109**, 87–99.

Norris, S. R., Meyer, S. E. & Callis, J. (1993). The intron of *Arabidopsis thaliana* polyubiquitin genes is conserved in location and is a quantitative determinant of chimeric gene expression. Plant Molecular Biology **21**, 895–906.

Olmsted, J. B., Witman, G. B., Carlson, K. & Rosenbaum, J. L. (1971). Comparison of the microtubule proteins of neuroblastoma cells, brain, and chlamydomonas flagella. Proceedings of the National Academy of Sciences of the United States of America **68**, 2273–2277.

Pickett-Heaps, J. D. & Northcote, D. H. (1966). Organization of microtubules and endoplasmic reticulum during mitosis and cytokinesis in wheat meristems. Journal of Cell Science **1**, 109 LP – 120.

Qin, X., Gianì, S. & Breviario, D. (1997). Molecular cloning of three rice α-tubulin isotypes: differential expression in tissues and during flower development. Biochimica et Biophysica Acta (BBA) - Gene Structure and Expression **1354**, 19–23.

Rice, S., Lin, A. W., Safer, D., Hart, C. L., Naber, N., Carragher, B. O., Cain, S. M., Pechatnikova, E., Wilson-Kubalek, E. M., Whittaker, M., Pate, E., Cooke, R., Taylor, E. W., Milligan, R. A. & Vale, R. D. (1999). A structural change in the kinesin motor protein that drives motility. Nature **402**, 778–784.

Richardson, D. N., Simmons, M. P. & Reddy, A. S. N. (2006). Comprehensive comparative analysis of kinesins in photosynthetic eukaryotes. BMC Genomics **7**, 18.

Robert, H. S., Quint, A., Brand, D., Vivian-Smith, A. & Offringa, R. (2009). BTB and TAZ domain scaffold proteins perform a crucial function in arabidopsis development. Plant Journal **58**, 109–121.

Sano, T., Higaki, T., Oda, Y., Hayashi, T. & Hasezawa, S. (2005). Appearance of actin microfilament 'twin peaks' in mitosis and their function in cell plate formation, as visualized in tobacco BY-2 cells expressing GFP–fimbrin. The Plant Journal **44**, 595–605.

Sasabe, M., Boudolf, V., De Veylder, L., Inzé, D., Genschik, P. & Machida, Y. (2011). Phosphorylation of a mitotic kinesin-like protein and a MAPKKK by cyclin-dependent kinases (CDKs) is involved in the transition to cytokinesis in plants. Proceedings of the National Academy of Sciences of the United States of America **108**, 17844–17849.

Sasabe, M., Soyano, T., Takahashi, Y., Sonobe, S., Igarashi, H., Itoh, T. J., Hidaka, M. & Machida, Y. (2006). Phosphorylation of NtMAP65-1 by a MAP kinase down-regulates its activity of microtubule bundling and stimulates progression of cytokinesis of tobacco cells. Genes & Development **20**, 1004–1014.

Shen, Z., Collatos, A. R., Bibeau, J. P., Furt, F. & Vidali, L. (2012). Phylogenetic analysis of the kinesin superfamily from physcomitrella. Frontiers in Plant Science **3**, 230.

Snustad, D. P., Haas, N. A., Kopczak, S. D. & Silflow, C. D. (1992). The small genome of arabidopsis contains at least nine expressed beta-tubulin genes. The Plant Cell **4**, 549–556.

Sotiriou, P., Giannoutsou, E., Panteris, E., Apostolakos, P. & Galatis, B. (2016). Cell wall matrix polysaccharide distribution and cortical microtubule organization: two factors controlling mesophyll cell morphogenesis in land plants. Annals of Botany **117**, 401–419.

Soyano, T., Nishihama, R., Morikiyo, K., Ishikawa, M. & Machida, Y. (2003). NQK1/NtMEK1 is a MAPKK that acts in the NPK1 MAPKKK-mediated MAPK cascade and is required for plant cytokinesis. Genes & Development **17**, 1055–1067.

Spielman, M., Preuss, D., Li, F. L., Browne, W. E., Scott, R. J. & Dickinson, H. G. (1997). TETRASPORE is required for male meiotic cytokinesis in *Arabidopsis thaliana*. Development **124**, 2645–2657.

Strompen, G., El Kasmi, F., Richter, S., Lukowitz, W., Assaad, F. F., Jürgens, G. & Mayer, U. (2002). The arabidopsis HINKEL gene encodes a kinesin-related protein involved in cytokinesis and is expressed in a cell cycle-dependent manner. Current Biology **12**, 153–158.

Szymanski, D. B. & Cosgrove, D. J. (2009). Dynamic coordination of cytoskeletal and cell wall systems during plant cell morphogenesis. Current Biology **19**, R800–R811.

Takahashi, Y., Soyano, T., Kosetsu, K., Sasabe, M. & Machida, Y. (2010). HINKEL kinesin, ANP MAPKKKs and MKK6/ANQ MAPKK, which phosphorylates and activates MPK4 MAPK, constitute a pathway that is required for cytokinesis in *Arabidopsis thaliana*. Plant and Cell Physiology **51**, 1766–1776.

Tanaka, H., Ishikawa, M., Kitamura, S., Takahashi, Y., Soyano, T., Machida, C. & Machida, Y. (2004). The AtNACK1/HINKEL and STUD/TETRASPORE/AtNACK2 genes, which encode functionally redundant kinesins, are essential for cytokinesis in arabidopsis. Genes to Cells **9**, 1199–1211.

Tominaga, M., Kimura, A., Yokota, E., Haraguchi, T., Shimmen, T., Yamamoto, K., Nakano, A. & Ito, K. (2017). Cytoplasmic streaming velocity as a plant size determinant. Developmental Cell **27**, 345–352.

Yang, C.-Y., Spielman, M., Coles, J. P., Li, Y., Ghelani, S., Bourdon, V., Brown, R. C., Lemmon, B. E., Scott, R. J. & Dickinson, H. G. (2003). TETRASPORE encodes a kinesin required for male meiotic cytokinesis in arabidopsis. Plant Journal **34**, 229–240.

Yasuhara, H., Sonobe, S. & Shibaoka, H. (1993). Effects of taxol on the development of the cell plate and of the phragmoplast in tobacco BY-2 cells. Plant and Cell Physiology **34**, 21–29.

Yoshikawa, M., Yang, G., Kawaguchi, K. & Komatsu, S. (2003). Expression analyses of β-tubulin isotype genes in rice. Plant and Cell Physiology **44**, 1202–1207.

Zegzouti, H., Anthony, R. G., Jahchan, N., Bögre, L. & Christensen, S. K. (2006). Phosphorylation and activation of PINOID by the phospholipid signaling kinase 3-phosphoinositide-dependent protein kinase 1 (PDK1) in arabidopsis. Proceedings of the National Academy of Sciences of the United States of America **103**, 6404–6409.

Zheng, M., Beck, M., Müller, J., Chen, T., Wang, X., Wang, F., Wang, Q., Wang, Y., Baluška, F., Logan, D. C., Šamaj, J. & Lin, J. (2009). Actin turnover is required for myosin-dependent mitochondrial movements in arabidopsis root hairs. PLoS ONE **4**, e5961.

Table S1: Identified sequences of the At1 kinesin family and the clade to which they belong used in this research.

Species	Clade	Sequence name / Locus
Marchantia polymorpha	At1	Mapoly0025s0108
Physcomitrella patens	At1	Pp3c1_18150V3
Physcomitrella patens	At1	Pp3c14_1560V3
Physcomitrella patens	At1	Pp3c2_19380V3
Sphagnum fallax	At1	Sphfalx0017s0218
Sphagnum fallax	At1	Sphfalx0087s0021
Selaginella moellendorffii	At1	126650
Ananas comosus	NACK	Aco006713
Ananas comosus	NACK	Aco23883
Ananas comosus	PBK-HL	Aco007585
Ananas comosus	PBK-HL	Aco015125
Ananas comosus	PBK-HL	Aco029105
Amborella trichopoda	NACK	evm_27.TU.AmTr_v1.0_scaffold00079.117
Amborella trichopoda	PBK-HL	evm_27.TU.AmTr_v1.0_scaffold00182.18
Musa acuminata	NACK	GSMUA_Achr1G23180
Musa acuminata	NACK	GSMUA_Achr9G18690
Musa acuminata	PBK-HL	GSMUA_Achr1G07780
Musa acuminata	PBK-HL	GSMUA_Achr2G03390
Musa acuminata	PBK-HL	GSMUA_Achr2G11920
Musa acuminata	PBK-HL	GSMUA_Achr4G24730
Musa acuminata	PBK-HL	GSMUA_Achr7G05800
Spirodela polyrhiza	NACK	Spipo8G0065000
Spirodela polyrhiza	PBK-HL	Spipo11G0024400
Spirodela polyrhiza	PBK-HL	Spipo16G0010000
Zostera marina	NACK	Zosma111g00200
Zostera marina	NACK	Zosma15g00280
Zostera marina	PBK-HL	Zosma46g00420
Zostera marina	PBK-HL	Zosma77g00270
Brachypodium distachyon	NACK	Bradi1g04397
Brachypodium distachyon	NACK	Bradi1g08010
Brachypodium distachyon	NACK	Bradi2g32300
Brachypodium distachyon	PBK-HL, beta	Bradi3g50150
Brachypodium distachyon	PBK-HL, alpha	Bradi5g17020
Brachypodium distachyon	Grasses	Bradi3g42190
Brachypodium distachyon	Grasses	Bradi4g35930
Brachypodium stacei	NACK	Brast02G314300
Brachypodium stacei	NACK	Brast02G353100
Brachypodium stacei	NACK	Brast08G174400
Brachypodium stacei	PBK-HL, beta	Brast04G122600
Brachypodium stacei	PBK-HL, alpha	Brast09G157400
Brachypodium stacei	Grasses	Brast03G299600
Brachypodium stacei	Grasses	Brast05G190400
Oryza sativa	NACK	LOC_Os01g33040
Oryza sativa	PBK-HL, beta	LOC_Os02g43050
Oryza sativa	PBK-HL, beta	LOC_Os02g43130

Table S1 (cont.): Identified sequences of the At1 kinesin family and the clade to which they belong used in this research.

Species	Clade	Sequence name / Locus
Oryza sativa	PBK-HL, alpha	LOC_Os04g45580
Oryza sativa	Grasses	LOC_Os08g43400
Oryza sativa	Grasses	LOC_Os09g35890
Oropetium thomaeum	NACK	Oropetium_20150105_05267
Oropetium thomaeum	PBK-HL, alpha	Oropetium_20150105_12229
Oropetium thomaeum	Grasses	Oropetium_20150105_14563
Panicum hallii	NACK	Pahal.E02529
Panicum hallii	PBK-HL, beta	Pahal.A02745
Panicum hallii	PBK-HL, alpha	Pahal.G01754
Panicum hallii	Grasses	Pahal.B04993
Panicum hallii	Grasses	Pahal.F00452
Panicum virgatum	NACK	Pavir.Ea01891
Panicum virgatum	NACK	Pavir.J28545
Panicum virgatum	PBK-HL, beta	Pavir.Aa01216
Panicum virgatum	PBK-HL, beta	Pavir.Ab02433
Panicum virgatum	PBK-HL, alpha	Pavir.Ga00901
Panicum virgatum	PBK-HL, alpha	Pavir.Gb00752
Panicum virgatum	Grasses	Pavir.Ba00254
Panicum virgatum	Grasses	Pavir.Bb03707
Panicum virgatum	Grasses	Pavir.Fa00217
Panicum virgatum	Grasses	Pavir.Fb02332
Setaria italica	NACK	Seita.5G179700
Setaria italica	PBK-HL, beta	Seita.1G252700
Setaria italica	PBK-HL, alpha	Seita.7G183000
Setaria italica	Grasses	Seita.2G437300
Setaria italica	Grasses	Seita.6G237500
Setaria viridis	NACK	Sevir.5G180600
Setaria viridis	PBK-HL, beta	Sevir.1G257000
Setaria viridis	PBK-HL, alpha	Sevir.7G192900
Setaria viridis	Grasses	Sevir.2G449800
Setaria viridis	Grasses	Sevir.6G243800
Sorghum bicolor	NACK	Sobic.010G008900
Sorghum bicolor	PBK-HL, beta	Sobic.004G301200
Sorghum bicolor	PBK-HL, alpha	Sobic.006G162000
Sorghum bicolor	Grasses	Sobic.002G273200
Sorghum bicolor	Grasses	Sobic.007G179400
Zea mays	NACK	GRMZM2G136838
Zea mays	PBK-HL, alpha	GRMZM2G054418
Zea mays	PBK-HL, beta	GRMZM2G129569
Zea mays	PBK-HL, alpha	GRMZM5G860469
Zea mays	Grasses	GRMZM2G015395
Zea mays	Grasses	GRMZM2G338928
Aquilegia coerulea	NACK1	Aqcoe3G026400
Aquilegia coerulea	NACK2	Aqcoe7G439100
Aquilegia coerulea	PBKH	Aqcoe6G247900

Table S1 (cont.): Identified sequences of the At1 kinesin family and the clade to which they belong used in this research.

Species	Clade	Sequence name / Locus
Aquilegia coerulea	PBKL	Aqcoe5G178000
Amaranthus hypochondriacus	NACK2	AHYPO_006714
Amaranthus hypochondriacus	NACK1	AHYPO_008264
Amaranthus hypochondriacus	PBK	AHYPO_017522
Amaranthus hypochondriacus	PBKH	AHYPO_003131
Amaranthus hypochondriacus	PBKH	AHYPO_012652
Amaranthus hypochondriacus	PBKL	AHYPO_021240
Kalanchoe fedtschenkoi	NACK1	Kaladp0040s0733
Kalanchoe fedtschenkoi	NACK2	Kaladp0085s0130
Kalanchoe fedtschenkoi	PBK	Kaladp0018s0219
Kalanchoe fedtschenkoi	PBK	Kaladp0047s0023
Kalanchoe fedtschenkoi	PBKH	Kaladp0579s0003
Kalanchoe fedtschenkoi	PBKL	Kaladp0001s0062
Kalanchoe fedtschenkoi	PBKL	Kaladp0003s0059
Kalanchoe fedtschenkoi	PBKL	Kaladp0100s0030
Kalanchoe laxiflora	NACK2	Kalax.0025s0068
Kalanchoe laxiflora	NACK1	Kalax.0085s0104
Kalanchoe laxiflora	NACK1	Kalax.0342s0030
Kalanchoe laxiflora	PBK	Kalax.0053s0104
Kalanchoe laxiflora	PBK	Kalax.0165s0058
Kalanchoe laxiflora	PBK	Kalax.0735s0021
Kalanchoe laxiflora	PBK	Kalax.1737s0002
Kalanchoe laxiflora	PBKH	Kalax.0507s0021
Kalanchoe laxiflora	PBKH	Kalax.0635s0015
Kalanchoe laxiflora	PBKL	Kalax.0204s0027
Kalanchoe laxiflora	PBKL	Kalax.0155s0029
Daucus carota	NACK1	DCAR_011365
Daucus carota	NACK1	DCAR_015153
Daucus carota	NACK2	DCAR_028529
Daucus carota	PBK	DCAR_003684
Daucus carota	PBK	DCAR_022916
Daucus carota	PBKH	DCAR_000465
Daucus carota	PBKH	DCAR_017343
Daucus carota	PBKL	DCAR_022444
Mimulus guttatus	NACK1	Migut.E01768
Mimulus guttatus	NACK2	Migut.L01595
Mimulus guttatus	PBK	Migut.B00175
Mimulus guttatus	PBK	Migut.N01276
Mimulus guttatus	PBKH	Migut.H02477
Mimulus guttatus	PBKH	Migut.L00042
Mimulus guttatus	PBKL	Migut.C00792
Solanum lycopersicum	NACK1	SoLyc03g119220
Solanum lycopersicum	NACK2	Solyc07g042560
Solanum lycopersicum	PBK	Solyc01g110380
Solanum lycopersicum	PBKH	Solyc02g062330

Table S1 (cont.): Identified sequences of the At1 kinesin family and the clade to which they belong used in this research.

Species	Clade	Sequence name / Locus
Solanum lycopersicum	PBKH	Solyc02g084390
Solanum lycopersicum	PBKL	Solyc04g081060
Solanum tuberosum	NACK1	PGSC0003DMG400005650
Solanum tuberosum	NACK2	PGSC0003DMG400013573
Solanum tuberosum	PBK	PGSC0003DMG400014213
Solanum tuberosum	PBKL	PGSC0003DMT400009519
Eucalyptus grandis	NACK2	Eucgr.C03198
Eucalyptus grandis	NACK1	Eucgr.K02233
Eucalyptus grandis	PBK	Eucgr.I01329
Eucalyptus grandis	PBKH	Eucgr.J02401
Vitis vinifera	NACK1	GSVIVG01008333001
Vitis vinifera	NACK2	GSVIVG01015015001
Vitis vinifera	PBK	GSVIVG01024172001
Vitis vinifera	PBKH	GSVIVG01018815001
Vitis vinifera	PBKL	GSVIVG01009828001
Cucumis sativus	NACK2	Cucsa.011820
Cucumis sativus	NACK1	Cucsa.121690
Cucumis sativus	PBK	Cucsa.377950
Cucumis sativus	PBKH	Cucsa.106680
Cucumis sativus	PBKL	Cucsa.159670
Fragaria vesca	NACK2	gene12943-v1.0-hybrid
Fragaria vesca	NACK1	gene25125-v1.0-hybrid
Fragaria vesca	PBK	gene15230-v1.0-hybrid
Fragaria vesca	PBKH	gene14871-v1.0-hybrid
Glycine max	NACK1	Glyma.07G096500
Glycine max	NACK1	Glyma.09G181200
Glycine max	NACK2	Glyma.13G114200
Glycine max	NACK2	Glyma.17G045600
Glycine max	PBK	Glyma.04G008200
Glycine max	PBK	Glyma.06G008000
Glycine max	PBK	Glyma.11G110800
Glycine max	PBK	Glyma.12G037100
Glycine max	PBKH	Glyma.01G168200
Glycine max	PBKH	Glyma.02G050400
Glycine max	PBKH	Glyma.11G075100
Glycine max	PBKH	Glyma.16G130500
Glycine max	PBKL	Glyma.04G026800
Glycine max	PBKL	Glyma.06G026700
Malus domestica	NACK1	MDP0000049091
Malus domestica	NACK2	MDP0000067021
Malus domestica	NACK1	MDP0000300249
Malus domestica	PBK	MDP0000169446
Malus domestica	PBK	MDP0000211096
Malus domestica	PBKH	MDP0000259935
Medicago truncatula	NACK2	Medtr4g124650

Table S1 (cont.): Identified sequences of the At1 kinesin family and the clade to which they belong used in this research.

Species	Clade	Sequence name / Locus
Medicago truncatula	NACK1	Medtr6g082470
Medicago truncatula	PBK	Medtr4g071900
Medicago truncatula	PBKH	Medtr5g021650
Medicago truncatula	PBKH	Medtr8g076190
Medicago truncatula	PBKL	Medtr3g113110
Phaseolus vulgaris	NACK2	Phvul.003G127400
Phaseolus vulgaris	NACK1	Phvul.004G154300
Phaseolus vulgaris	PBK	Phvul.009G003000
Phaseolus vulgaris	PBK	Phvul.011G038800
Phaseolus vulgaris	PBKH	Phvul.002G111200
Phaseolus vulgaris	PBKH	Phvul.003G260200
Phaseolus vulgaris	PBKL	Phvul.009G014400
Prunus persica	NACK1	Prupe.5G224200
Prunus persica	NACK2	Prupe.7G192200
Prunus persica	PBK	Prupe.8G084900
Prunus persica	PBKH	Prupe.7G166000
Prunus persica	PBKL	Prupe.1G370500
Trifolium pretense	NACK2	Tp57577_TGAC_v2_gene12717
Trifolium pretense	NACK1	Tp57577_TGAC_v2_gene29484
Trifolium pretense	PBK	Tp57577_TGAC_v2_gene22383
Trifolium pretense	PBKH	Tp57577_TGAC_v2_gene2343
Trifolium pretense	PBKH	Tp57577_TGAC_v2_gene30046
Trifolium pretense	PBKL	Tp57577_TGAC_v2_gene30290
Linum usitatissimum	NACK2	Lus10005181
Linum usitatissimum	NACK1	Lus10032452
Linum usitatissimum	NACK1	Lus10042952
Linum usitatissimum	PBK	Lus10031086
Linum usitatissimum	PBKH	Lus10014268
Manihot esculenta	NACK1	Manes.01G014700
Manihot esculenta	NACK2	Manes.03G044500
Manihot esculenta	NACK1	Manes.05G132500
Manihot esculenta	PBK	Manes.04G083600
Manihot esculenta	PBK	Manes.11G082000
Manihot esculenta	PBKH	Manes.02G101900
Manihot esculenta	PBKL	Manes.05G152000
Manihot esculenta	PBKL	Manes.18G017300
Populus trichocarpa	NACK2	Potri.006G136600
Populus trichocarpa	NACK1	Potri.012G054400
Populus trichocarpa	NACK1	Potri.015G044600
Populus trichocarpa	PBK	Potri.004G162800
Populus trichocarpa	PBK	Potri.009G124500
Populus trichocarpa	PBKH	Potri.005G116900
Populus trichocarpa	PBKH	Potri.007G014800
Populus trichocarpa	PBKL	Potri.002G027600
Ricinus communis	NACK2	29739.t000128

Table S1 (cont.): Identified sequences of the At1 kinesin family and the clade to which they belong used in this research.

Species	Clade	Sequence name / Locus
Ricinus communis	PBK	30131.t000283
Ricinus communis	PBKH	28623.t000007
Ricinus communis	PBKL	30170.t000547
Salix purpurea	NACK2	SapurV1A.0249s0060
Salix purpurea	NACK1	SapurV1A.0475s0110
Salix purpurea	NACK1	SapurV1A.0530s0110
Salix purpurea	NACK1	SapurV1A.0915s0010
Salix purpurea	PBK	SapurV1A.0091s0180
Salix purpurea	PBK	SapurV1A.0379s0200
Salix purpurea	PBKH	SapurV1A.0166s0490
Salix purpurea	PBKH	SapurV1A.0487s0240
Salix purpurea	PBKH	SapurV1A.1879s0040
Salix purpurea	PBKL	SapurV1A.0025s0760
Citrus clementina	NACK2	Ciclev10007377m
Citrus clementina	NACK1	Ciclev10018724m
Citrus clementina	PBK	Ciclev10027756m
Citrus clementina	PBKH	Ciclev10024791m
Citrus clementina	PBKL	Ciclev10000097m
Citrus sinensis	NACK1	orange1.1g002128m
Citrus sinensis	NACK2	orange1.1g003967m
Citrus sinensis	PBK	orange1.1g002137m
Citrus sinensis	PBKH	orange1.1g001693m
Citrus sinensis	PBKL	orange1.1g001305m
Carica papaya	NACK1	evm.TU.supercontig_3.468
Carica papaya	PBK	evm.TU.supercontig_150.18
Carica papaya	PBKH	evm.TU.supercontig_6.222
Carica papaya	PBKL	evm.TU.supercontig_140.22
Gossypium raimondii	NACK1	Gorai.001G075200
Gossypium raimondii	NACK1	Gorai.008G287600
Gossypium raimondii	NACK2	Gorai.013G222300
Gossypium raimondii	PBK	Gorai.002G148900
Gossypium raimondii	PBK	Gorai.005G248400
Gossypium raimondii	PBKH	Gorai.007G196800
Gossypium raimondii	PBKH	Gorai.008G063800
Gossypium raimondii	PBKL	Gorai.009G196700
Gossypium raimondii	PBKL	Gorai.010G006400
Theobroma cacao	NACK1	Thecc1EG012433
Theobroma cacao	NACK2	Thecc1EG037463
Theobroma cacao	PBK	Thecc1EG006781
Theobroma cacao	PBKH	Thecc1EG000241
Theobroma cacao	PBKL	Thecc1EG034158
Arabidopsis halleri	NACK1	Araha.3597s0004
Arabidopsis halleri	NACK2	Araha.9819s0003
Arabidopsis halleri	PBK1	Araha.16804s004
Arabidopsis halleri	PBK2	Araha.38650s001

Table S1 (cont.): Identified sequences of the At1 kinesin family and the clade to which they belong used in this research.

Species	Clade	Sequence name / Locus
Arabidopsis halleri	PBKH1	Araha.1049s0005
Arabidopsis halleri	PBKH2	Araha.1084s0025
Arabidopsis halleri	PBKL2	Araha.13048s0006
Arabidopsis halleri	PBKL1	Araha.30768s0003
Arabidopsis lyrata	NACK2	AL5G21280
Arabidopsis lyrata	NACK1	AL1G30790
Arabidopsis lyrata	PBK2	AL4G10440
Arabidopsis lyrata	PBK1	AL7G10850
Arabidopsis lyrata	PBKH1	AL5G31580
Arabidopsis lyrata	PBKH2	AL8G45210
Arabidopsis lyrata	PBKL2	AL7G29120
Arabidopsis lyrata	PBKL1	AL8G18850
Arabidopsis thaliana	NACK1	AT1G18370
Arabidopsis thaliana	NACK2	AT3G43210
Arabidopsis thaliana	PBK2	AT2G21300
Arabidopsis thaliana	PBK1	AT4G38950
Arabidopsis thaliana	PBKH1	AT3G51150
Arabidopsis thaliana	PBKH2	AT5G66310
Arabidopsis thaliana	PBKL2	AT4G24170
Arabidopsis thaliana	PBKL1	AT5G42490
Boechera stricta	NACK1	Bostr.7128s0439
Boechera stricta	PBK1	Bostr.25542s0078
Boechera stricta	PBK2	Bostr.5022s0105
Boechera stricta	PBKH2	Bostr.0568s0043
Boechera stricta	PBKH1	Bostr.6864s0130
Boechera stricta	PBKL1	Bostr.3148s0252
Boechera stricta	PBKL2	Bostr.7867s0222
Brassica oleracea Capitata Gp	NACK1	Bol009730
Brassica oleracea Capitata Gp	NACK2	Bol013827
Brassica oleracea Capitata Gp	NACK1	Bol030782
Brassica oleracea Capitata Gp	PBK1	Bol028790
Brassica oleracea Capitata Gp	PBK2	Bol045874
Brassica oleracea Capitata Gp	PBKH2	Bol027154
Brassica oleracea Capitata Gp	PBKH1	Bol035960
Brassica rapa	NACK1	Brara.F01292
Brassica rapa	NACK2	Brara.F01985
Brassica rapa	PBK1	Brara.A00020
Brassica rapa	PBK2	Brara.D01259
Brassica rapa	PBKH1	Brara.C04354
Brassica rapa	PBKH2	Brara.G01269

Table S1 (cont.): Identified sequences of the At1 kinesin family and the clade to which they belong used in this research.

Species	Clade	Sequence name / Locus
Brassica rapa	PBKH1	Brara.I03449
Brassica rapa	PBKL1	Brara.B02468
Capsella grandiflora	NACK1	Cagra.0909s0017
Capsella grandiflora	NACK2	Cagra.8415s0002
Capsella grandiflora	PBK1	Cagra.1383s0072
Capsella grandiflora	PBK2	Cagra.2961s0032
Capsella grandiflora	PBKH1	Cagra.0926s0080
Capsella grandiflora	PBKH2	Cagra.10427s0041
Capsella grandiflora	PBKL2	Cagra.1226s0082
Capsella rubella	NACK1	Carubv10008207
Capsella rubella	NACK2	Carubv10016650
Capsella rubella	PBK1	Carubv10004132
Capsella rubella	PBK2	Carubv10025517
Capsella rubella	PBKH1	Carubv10016639
Capsella rubella	PBKH2	Carubv10028003
Capsella rubella	PBKL2	Carubv10006728
Eutrema salsugineum	NACK2	Thhalv10002392
Eutrema salsugineum	NACK1	Thhalv10006702
Eutrema salsugineum	PBK2	Thhalv10000043
Eutrema salsugineum	PBK1	Thhalv10024409
Eutrema salsugineum	PBKH2	Thhalv10003607
Eutrema salsugineum	PBKH1	Thhalv10010086
Eutrema salsugineum	PBKL1	Thhalv10003349
Eutrema salsugineum	PBKL2	Thhalv10026976

SIX

SUMMARY

During their life cycle, organisms react to various external signals in order to avoid adverse environmental conditions. The ways various organisms react to these signals are diverse. Animals, for example, are generally mobile and therefore have the possibility to move to a different location to improve their living conditions. Plants, in contrast, are sessile organisms, and therefore have developed alternative strategies to adapt to changes in their environment, in part by altering their growth and development. When a signal is percieved by a receptor protein, the signal is generally transduced via one or multiple chemical or physical intermediates, which eventually results in a cellular response. During this signal transduction cells can utilize various processes including, but not limited to, protein phosphorylation, changes in membrane lipid composition, changes in metabolism and gene expression. The final result of these changes is the response that puts the cells, in case of multicellular organisms the tissues and the organism as a whole in a state to handle the signal. One of the central regulators of this adaptive plant growth and development is the plant hormone auxin or indole-3-acetic acid (IAA). Auxin is involved in directional growth responses of plant roots and shoots to signals; such as gravity, light and mechanical stress, and it also positions and regulates the outgrowth of new organs.

Auxin is transported by the PINFORMED (PIN) class of proteins. PIN proteins are plasma membrane (PM) or endoplasmatic reticulum (ER) localized proteins that transport auxin through the membrane. PM localized PIN proteins often show a polarized localization. Multiple, adjacent cells that have the same PIN polarity in a tissue show a directional transport of auxin. This Polar Auxin Transport (PAT) allows the plant to make auxin gradients and sites that contain high or low auxin concentrations, enabling it to alter developmental programs in the cells affected. The polar localization of the PIN proteins is the result of a combination of processes. Following their apolar biosynthetic secretion, PIN proteins become polarized by endocytosis and subsequent transcytosis of the PIN loaded vesicles to another PM domain, or by recycling back to the original PM domain. Once established, PIN polarity is maintained by a process of continuous endocytosis and recycling back to the same PM domain. These PM domains are largely defined by the ADP-ribosylation factor-guanine nucleotide exchange factors (ARF-GEF) that trigger exocytosis to a specific domain. For the arabidopsis ARF-GEF

GNOM it is well established that it is responsible for the PIN polarity at the rootward (basal) PM domain. Moreover, phosphorylation of PIN proteins by the plant-specific protein kinase A, cyclic GMP-dependent protein kinase, protein kinase C (AGC) kinases PINOID (PID), WAG1 and WAG2 in arabidopsis leads to their sorting to the GNOM-independent shootward (apical) sorting pathway.

Beside the transport of auxin, cells also need to sense the hormone quantitatively in order to respond to it. In **chapter 2** we discuss our view on a recent finding in this auxin perception. The Auxin Binding Protein 1 (ABP1) is encoded by a single copy gene in *Arabidopsis thaliana* (arabidopsis), and since its discovery the consensus was that *abp1* loss-of-function results in embryo lethality. A recent paper describes the creation of a new loss-of-function line that was found to be not embryo lethal, putting its status as one of the auxin receptors in jeopardy. We provide an overview of all alleles and constructs that have been used in the past 40 years of ABP1 research and give possible explanations for the observed conflicting results between the recently published paper and previous research.

In **chapter 3** we investigated the regulation of the PID kinase by phosphoinositide-dependent protein kinase 1 (PDK1), a central upstream regulator of AGC kinases. Previous research has shown that phosphorylation of PID by PDK1 on serine residues S288 and S290 in the activation loop enhances PID kinase activity *in vitro*. In chapter 3 we show in arabidopsis protoplasts that PDK1 phosphorylation induces a switch in PID subcellular localization from the plasma membrane to endomembrane compartments and the microtubule cytoskeleton (MT). Removal of the PDK1 phosphorylation sites prevented PID MT recruitment, and a phospho-mimic PID version localized to the MT in the absence of PDK1. *PID* promoter controlled expression of wild-type, loss-of-phosphorylation or phospho-mimic versions of PID in the *pid wag1 wag2* triple loss-of-function mutant background showed that PDK1-mediated enhancement of PID activity is essential during embryo and inflorescence development. Although comparison of the subcellular localization of wild-type and mutant PID versions in root epidermis cells did not corroborate a role for PDK1 in relocalizing PID to endomembranes and MT, our results suggest a new role for dynamic PDK1-mediated activation of PID in plant development.

The protein complex responsible for the MT localization of PID in protoplasts was explored in **chapter 4**. In our search for upstream

regulators of the PID kinase we identified arabidopsis BTB and TAZ domain protein1 (BT1) as a PID binding protein. The *BT1* gene belongs to a five-member gene family in arabidopsis, encoding proteins with a land plant-specific domain structure consisting of an amino-terminal BTB domain, a TAZ domain and a carboxy-terminal calmodulin binding domain. At least four of the five BT proteins interacted with PID through their BTB domain, and *in vitro* phosphorylation assays indicated that BT1 is not a phosphorylation target of PID, but that BT1 binding reduces the activity of the kinase. BT1 localized in the nucleus and the cytoplasm. Upon co-expression with PID, BT1 was found at the plasma membrane, whereas PID localization became partially nuclear. Overexpression of *BT1* led to a reduction of *PID* overexpression seedling phenotypes and enhanced *pid* loss-of-function embryo phenotypes. In contrast, *bt* loss-of-function enhanced adult phenotypes of *PID* overexpression plants. A subsequent yeast two-hybrid screen for BT1 interacting proteins yielded two At1-family kinesins (which we named PBK1 and PBK2) that were found to induce BT1-dependent relocalization of PID and its closest family members WAG1, WAG2 and AGC3-4 to the MT in arabidopsis protoplasts. Together these data suggest that BT1 acts as signaling scaffold that regulates AGC3 kinase activity in part by relocating PID to the nucleus or, for all the kinases, to the MT.

In **chapter 5** we investigated the function of PBK1 and PBK2 and other members of the plant specific At1 kinesin family in more detail. We were able to identify and classify At1 family members in almost all plant species of which the genome has been sequenced to date, with the exception of the unicellular Chlorophyte algae. We obtained arabidopsis T-DNA insertion lines for *PBK1* and *PBK2* and the two closest paralogues (*PBKH1* and *PBKH2*), but were unable to find convincing mutant phenotypes, even in the quadruple mutant. This suggests that other members of the At1 gene family still act redundantly. Expression analysis of the *PBK* and *PBKH* genes using *promoter::GUS* reporter lines showed that the expression domains of the genes overlapped, with strong expression in meristems and young tissues. The expression of the genes was not altered by changes in temperature or light or by external auxin application. Expression of kinesins-YFP fusions in arabidopsis protoplasts showed cortical MT localization. However, *in planta* these fusion proteins appeared to be targets for proteasome-mediated degradation, and no clear MT localization could be observed. Based on the known function of the related NACK

kinesins, it is tempting to speculate that the BT1-PBK complex is involved in relocating PID to the phragmoplast during cell division.
Our results reveal a regulatory complex that on the one hand links PID to a dynamic process in young tissues that requires high protein turnover and the MT. These characteristics make cytokinesis a logical candidate for a process where this complex could play a role. On the other hand, the complex is not essential for survival and allows more variability within the PBK sequences compared to the NACKs. This rather suggests a role for the PID-BT1-PBK complex in altering the dynamics, fine tuning or timing of cytokinesis, instead of being an essential part of the cytokinesis processes. A possible and logical function for the PID-BT1-PBK complex could be that during cell division this complex guides PID to the phragmoplast via the MT. In dividing cells, PIN proteins are preferentially secreted in a MT-dependent manner to the phragmoplast, but by the time the new daughter cells are formed they have assumed their correct polar position. PID could thus be involved in establishing the correct PIN polarity by phosphorylating these auxin carriers at the growing cell plate.

SEVEN

SAMENVATTING

Gedurende hun leven moeten organismen op diverse externe signalen reageren om nadelige omgevingscondities te voorkomen. De manieren waarop verschillende organismen op deze signalen reageren zijn divers. Dieren, bijvoorbeeld, zijn over het algemeen mobiel en hebben daarom de mogelijkheid om zichzelf naar een andere locatie te verplaatsen. Planten zijn daarentegen, vastgegroeide organismen en hebben daarom alternatieve strategieën ontwikkeld om hun groei en ontwikkeling, vanwege veranderingen in hun omgeving, te sturen. Als een signaal wordt waargenomen door een receptoreiwit, dan wordt deze via een of meerdere chemische of fysische tussenstappen doorgegeven om uiteindelijk te resulteren in een reactie. Voor deze signaaltransductie hebben cellen diverse processen tot hun beschikking, zoals eiwitfosforylering, veranderingen in lipide-opbouw van membranen en veranderingen in metabolisme of genexpressie. Het uiteindelijke resultaat van deze veranderingen is de reactie die de cel, weefsels en het organisme als geheel in een staat brengen om de veranderende conditie aan te kunnen. Een van de centrale regulatoren van deze aanpasbare groei en ontwikkeling is het plantenhormoon auxine of indool-3-azijnzuur (IAA). Auxine is betrokken bij directionele groei van plantenwortels en scheuten onder invloed van signalen zoals zwaartekracht, licht en mechanische stress, en het positioneert en reguleert de uitgroei van nieuwe organen.
Auxine wordt getransporteerd door de PINFORMED (PIN) eiwitfamilie. PIN-eiwitten zijn plasmamambraan- (PM) of endoplasmatisch reticulum- (ER) gelokaliseerde eiwitten die transport van auxine over het membraan faciliteren. PM-gelokaliseerde PIN-eiwitten laten vaak een asymmetrische verdeling over het celmembraan zien, die de richting van het van cel naar cel transport van auxine bepaalt. Dit polaire auxine transport (PAT) stelt de plant in staat auxinegradiënten en plekken met hoge of lage auxineconcentraties te maken, om zo de ontwikkeling in specifieke cellen aan te passen. De polaire lokalisatie van de PIN-eiwitten is het resultaat van een combinatie van processen. Navolgend van hun apolaire biosynthetische secretie, worden PIN eiwitten gepolariseerd door endocytose en vervolgens door mede van transcytose van de vesikels met PIN eiwitten naar een ander PM domein verplaatst, of door terug te recyclen naar het originele PM domein. Eenmaal gevormd, wordt de PIN polariteit behouden door een continue proces van endocytosis en terug recycling naar hetzelfde PM domein. Deze PM domeinen

worden grotendeels gedefinieerd door de ADP-ribosylation factor-guanine nucleotide exchange factors (ARF-GEF) die exocytose naar een specifiek domein reguleren. Van de arabidopsis ARF-GEF GNOM is bekend dat het de PIN polariteit naar het wortelgericht (rootward, basaal) PM domain reguleert. Daarnaast zorgt fosforylatie van PIN eiwitten door de plant-specifieke eiwitkinase A, cyclisch GMP-afhankelijk eiwitkinases en eiwitkinase C (AGC) eiwitkinases PINOID (PID), WAG1 en WAG2 in arabidopsis voor sortering naar het GNOM-onafhankelijke scheutgericht (shootward, apicale) PM domein.

Naast de transport van het hormoon, moeten cellen het ook kwantitatief kunnen waarnemen, om erop te kunnen reageren. In **hoofdstuk 2** bediscussiëren we onze visie op een recente ontdekking in deze auxineperceptie. Het Auxine Bindend Eiwit 1 (ABP1) wordt gecodeerd door een enkel-kopie-gen in *Arabidopsis thaliana* (arabidopsis), en sinds zijn ontdekking was de consensus dat de *abp1* verlies-van-functie resulteerde in embryoletaliteit. Een recent artikel beschrijft de creatie van een nieuwe verlies-van-functie lijn die echter niet embryoletaal bleek te zijn, waardoor de status van ABP1 als een van de auxinereceptoren ter discussie staat. We geven een overzicht van alle allelen en constructen die in de afgelopen 40 jaar in het ABP1 onderzoek gebruikt zijn en geven mogelijke verklaringen voor de waargenomen conflicterende resultaten tussen het recentelijk gepubliceerde onderzoek en het voorgaande onderzoek.

In **hoofdstuk 3** onderzochten we de regulatie van het PID kinase door fosfoinositide-afhankelijk eiwitkinase 1 (PDK1), een centrale upstream regulator van AGC kinases. Eerder onderzoek liet zien dat de fosforylatie van PID door PDK1 op serines S288 en S290 in de activatielus, PID kinaseactiviteit *in vitro* versterkt. In hoofdstuk 3 laten we in arabidopsis protoplasten zien dat PDK1 fosforylatie een verandering in PID subcellulaire lokalisatie van het plasmamembraan naar endomembrane compartimenten en het microtubule cytoskelet (MT) laat zien. Verwijdering van de PDK1 fosforylatieplekken voorkomt PID herlokalisatie naar het MT, en een fosfo-imitatie PID versie lokaliseerde naar het microtubule cytoskelet in afwezigheid van PDK1. Expressie van wildtype, verlies-van-fosforylatie of fosfo-imitiatie versies van PID door de *PID* promoter in de *pid wag1 wag2* drievoudige verlies-van-functie mutante achtergrond liet zien dat PDK1-versterking van PID activiteit tijdens embryo- en bloeiwijzeontwikkeling essentieel is. Ondanks vergelijking van de subcellulaire lokalisatie van wildtype en mutante PID versies in

de epidermiscellen van de wortel kon er geen rol voor PDK1 in de herlokalisatie van PID naar de endomembranen en het MT toegewezen worden, maar laten onze resultaten echter een nieuwe rol voor PDK1 in plantontwikkeling zien.

Het eiwitcomplex dat verantwoordelijk is voor de MT lokalisatie van PID werd in **hoofdstuk 4** verkend. In onze zoektocht naar upstream regulatoren van het PID kinase identificeerde we arabidopsis BTB en TAZ domein eiwit 1 (BT1) als een PID bindend eiwit. Het *BT1* gen behoort tot een vijf leden tellende genfamilie in arabidopsis, welke voor eiwitten met een landplant-specifiek domeinstructuur, bestaande uit een BTB domein op het amino-einde, een TAZ domein en een calmoduline bindend domein op het carboxy-einde. Ten minste vier van de vijf BT eiwitten interacteerde met PID via hun BTB domein, en *in vitro* fosforylatieassays gaven aan dat BT1 geen fosforylatiesubstraat van PID is, maar dat BT1 binding wel de activiteit van het kinase onderdrukt. BT1 lokaliseert in de celkern en het cytoplasma. Bij co-expressie met PID, werd BT1 aan het plasmamembraan gedetecteerd, terwijl PID lokalisatie ook gedeeltelijk in de celkern waargenomen werd. Overexpressie van *BT1* leidde tot een reductie van de *PID* overexpressie zaailingfenotypes en versterkte *pid* verlies-van-functie embryofenotypes. In contrast, *bt* verlies-van-functie versterkte de volwassenfenotypes van de *PID* overexpressie planten. Een tweede yeast two-hybrid screen voor BT1 interacterende eiwitten leverde twee At1-familie kinesines (welke PBK1 en PBK2 genoemd werden) op, welke BT1-afhankelijke herlokalisatie van PID en zijn familieleden WAG1, WAG2 en AGC3-4 naar het MT in arabidopsis protoplasten kon induceren. Samengenomen, suggereren deze gegevens dat BT1 zich als een signaleringsbrug gedraagt die gedeeltelijk AGC3 kinaseactiviteit reguleert door PID naar de celkern, of in geval van alle kinases, naar het MT herlokaliseert.

In **hoofdstuk 5** onderzochten we de functie van PBK1 en PBK2 en de andere leden van de plant-specifieke At1 kinesinefamilie in meer detail. We waren in staat om At1 familieleden te identificeren en classificeren in bijna alle plantensoorten die tot op heden gesequenced zijn, waarbij de unicellulaire Chlorophyte algen de uitzondering waren. We hebben arabidopsis T-DNA insertielijnen voor *PBK1* en *PBK2* en de twee meest gelijkende paralogen (*PBKH1* en *PBKH2*) verkregen, maar waren niet in staat om overtuigende mutante fenotypes te verkrijgen, zelfs in de viervoudige mutant. Dit suggereert dat andere leden van de At1 familie

nog steeds redundantie kunnen geven. Expressieanalyse van de *PBK* en *PBKH* genen met behulp van *promoter::GUS* reporterlijnen gaf aan dat de expressiedomeinen van de genen overlapt, met sterke expressie in de meristemen en jonge weefsels. De expressie van de genen veranderde niet bij veranderingen in temperatuur, licht of toepassing van externe auxine. Expressie van kinesine-YFP fusies in arabidopsis protoplasten gaf een corticale MT lokalisatie weer. Echter, *in planta* waren deze fusie-eiwitten doelwit voor degradatie door het proteasoom en kon geen duidelijke MT lokalisatie waargenomen worden. Gebaseerd op de bekende functie van de gerelateerde NACK kinesines, is het aantrekkelijk om te speculeren dat het BT1-PBK complex betrokken is bij de herlokalisatie van PID naar de fragmoplast tijdens celdeling.

Onze resultaten laten licht op een regulatoir complex schijnen dat aan de ene kant PID linkt aan een dynamisch proces in jonge weefsels die hoge eiwitturnover en het MT vereisen. Deze eigenschappen make cytokinese een logische kandidaat voor een proces waar dit complex een rol in kan spelen. Aan de andere kant is het complex niet essentieel voor overleving en is er meer variabiliteit in de PBK sequenties, vergeleken met de NACKs, toegestaan. Dit suggereert een rol voor het PID-BT-PBK complex in het aanpassen van de dynamiek, het fijnsturen van de tijdsplanning in cellen en/of weefsels, in plaats van een essentieel onderdeel van het cytokinese proces. Een mogelijke en logische functie voor het PID-BT1-PBK complex zou kunnen zijn dat tijdens de celdeling dit complex PID, via de MT, naar de fragmoplast leidt. In delende cellen worden PIN eiwitten voornamelijk via de MT naar de fragmoplast gestuurd, maar tegen de tijd dat de dochtercellen gevormd zijn hebben ze echter reeds de correcte polaire positie aangenomen. PID zou dus betrokken kunnen zijn in het vaststellen van de correcte PIN polariteit door fosforylatie van deze auxinetransporters op de groeiende celplaat.

EIGHT

CURRICULUM VITAE

Mickel Elisabeth Johannes Habets was born on October 25th, 1982 in Heerlen, the Netherlands. After finishing the HAVO at the Stella Maris College in Meerssen, the Netherlands in 2000, he started the study "Laboratory Sciences" at the Agricultural University of Applied Sciences Larenstein in Velp, the Netherlands. During this time he did two internships, the first at Genetwister Technologies in Wageningen, the Netherlands, where he was involved in identifying molecular markers linked to fruit ripening traits in apple (*Malus domestica*). The second internship was at Plant Research International (PRI), part of the Wageningen University and Research Centre (WUR), in the group of Dr. Kim Boutilier. Under supervision of Ing. Ronny Joosen, Myckel used Tandem Affinity Purification (TAP) tagging to identify *in planta* interactors of the AP2 domain transcription factor BABYBOOM (BBM).

After obtaining his Bachelor of Science degree in 2004, Myckel worked for a short time as quality control analyst at Rijk Zwaan in De Lier, the Netherlands. In 2006, he moved to the Protein Chemistry laboratory of Prof. dr. Gerard Canters at the Leiden Institute of Chemistry (LIC) at Leiden University, the Netherlands. Under supervision of Dr. Gregg Siegal, he investigated the N-terminal region of Replication Factor C and its involvement in the Trans-Lesion Synthesis (TLS) DNA repair pathway. In 2008, he became researcher in the Auxin group of Dr. Remko Offringa at the Institute of Biology Leiden (IBL) at Leiden University and worked under supervision of Dr. Adam Vivian-Smith on a project investigating fertilization-independent fruit set in sweet pepper (*Capsicum annuum*).

In 2010, he started his PhD studies in the same group, with Prof. dr. Remko Offringa as promotor, on the regulation of the PINOID kinase by 3-phosphoinositide-dependent kinase 1 (PDK1) and its translocation to the microtubule cytoskeleton after PDK1-mediated phosphorylation. The results of these studies are described in this thesis. Currently, Myckel is working as an independent software developer.